# Ce ba ma

# CEBAMA
## ➢ (Contract Number: 662147)

## Deliverable D 1.03

## WP1 Experimental studies – State of the art literature review (M09 - Feb 2016)

| | |
|---|---|
| Editors: | Tapio Vehmas (VTT), Erika Holt (VTT) |
| Date of issue of this report: | 22.3.2016 |
| Report number of pages: | 235 |
| Start date of project: | 01/06/2015        Duration: 48 Months |

**Abstract**

This report is an initial state-of-the-art literature review in the CEBAMA –project for work package 1. Chapters are written by the participants of CEBAMA and the chapters serve as state-of-the-art reviews for the the experimental research conducted by various partners.

The report has short an introduction to the nuclear waste repository concepts of the project's participating countries. The research methods section gives a general overview of some of the internationally used techniques in cementitious materials research for nuclear waste repositories. More details about specific experimental method boundary conditions used in CEBAMA are described in the Deliverable D1.04 (to be published April 2016). In the materials section, the historic development of low-hydration heat, low-pH concrete formulations is presented. More details about specific materials used in CEBAMA are described in the Deliverable D1.05 (to be published May 2016).

Most of this literature reviews presented in the chapters here are focused on the processes related to cementitious materials. Geochemical and physical evolution of the cementitious materials in a repository environment is described from various viewpoints.

Detailed information about the authors and affiliations is presented at the beginning of each chapter.

# 1    Introduction

This document contains a state-of-the-art review of the behaviour of cementitious materials for use in deep geological nuclear waste repositories. Chapters of the state-of-the-art report are written by the various CEBAMA–project participants. Detailed information about the authors and their affiliations is presented at the beginning of each chapter.

The safety of a nuclear waste repository is ensured by the combination of natural and engineered barriers. In deep-geological repositories, a natural barrier is provided by the surrounding bedrock and its inherent isolating properties. The engineered barrier system isolates the radionuclides from the natural barrier and further stabilizes the repository system.

Cementitious materials are largely utilised in nuclear waste repositories. Cementitious materials are used as structural components of the repository and/or as a part of the engineered barrier system. Concrete is used in the deposition tunnel end plugs, voussoirs in clay host rock repositories and other structural components. Cement-based grouts and mortars are used in shotcrete for tunnel wall rock supports, rock bolting grouts and injection grouts for fissure sealing. In the UK conceptual repository design, cementitious materials are utilised as backfill material as part of the engineered barrier system. The Netherlands also has an option to utilise cementitious backfill. Specially designed cementitious backfill material provides a chemical barrier against the release of radionuclides and is an essential component of the engineered barrier system. The alkaline nature of the cement pore water lowers the solubility of many radioactive elements and prevents the release of radionuclides to the far field. State-of-the-art review of the backfill is given in: *2.9.1 State-of-the-art review of the NRVB: A UK high pH backfill cement*.

In many repository concepts, cementitious materials do not play a significant role in the engineered barrier system. In these systems, cementitious materials are utilised for mechanical and hydrological isolation of the compartments of the repository and in the structural components. However, the cementitious materials are in direct contact with the backfill and closure materials. Physicochemical compatibility of cementitious materials with the rest of the multi-barrier system is essential for the longevity of the repository. It is assumed that cementitious materials will interact with the backfill and closure materials, but not to an extent that compromises the long-term safety of the barrier system. In nuclear waste repositories, the compatibility of cementitious materials must be evaluated up to hundred thousand's year time span.

The information in this report is presented with two objectives. In the first objective, knowledge is summarised by comparing various nuclear waste repository concepts. Information from this viewpoint is presented in Chapter 2, where nuclear waste repository concepts relevant to the CEBAMA-project are described. This chapter also includes detailed information about the Dutch Nuclear Waste Disposal concept *(2.6.1 OPERA Disposal concept)*, and more general details of nuclear waste disposal concepts from other countries participating in the project.

The second objective is to summarise the phenomena that will affect the performance of all repositories. Cementitious materials' interactions with the buffer, backfill, and closure materials are key concepts of phenomenological approaches. As bentonite is the most common buffer and backfill material, a significant amount of research is focused on the interaction between bentonite and the cementitious materials. Another important feature is the groundwater effect. Groundwater is the medium where various dissolution/precipitation reactions take place in the repository. Additionally, most of the chemical reactions of the cementitious materials occur through dissolution and precipitation mechanisms in aqueous medium. Therefore the composition of the groundwater is of utmost importance when the longevity of the engineered barrier system is evaluated. The role of

the groundwater is described in the following Chapters: *5.3 Experimental studies of hydro-mechanical behaviour of concrete fractures*, *5.4 Chemical degradation of concrete with emphasis on Ca-leaching and carbonation*, *5.5 Geochemical and physical evolution of cementitious materials in aggressive environment* and *5.7 Geochemical Interaction of the groundwater-concrete-bentonite system and its impact in the near field and EDZ*.

Materials and their properties play important roles in the long-term performance evaluation of nuclear waste repositories. The role materials play is described in detail in Chapters 4.1, 5.1, 5.2, and 5.6*. Diffusion of species through cement materials* is presented in Chapter 5.1. *Diffusion on cement materials* is presented in Chapter 5.2. The role of proper material selection and concrete mixture proportioning is presented in Chapter *4.1 Development of low-pH (low-hydration heat) concretes*. Key features of calcium-silicate-hydrates, the main binding phase of Ordinary Portland Cement is presented in Chapter 5.6: *Calcium-silicate-hydrates in low-pH concretes and deep geological nuclear waste repository environment*. A systematic approach to describe processes of chemical species is given in Chapter *5.7 Geochemical Interaction of the groundwater-concrete-bentonite system and its impact in the near field EDZ*.

The selection of appropriate research methods is important when assessing the interactions between the cementitious materials and the engineered barrier systems. Some of these methods are presented in Chapter 3. Methods to study the water-concrete interaction are presented in Chapter *3.1 Testing methods for water-concrete interaction characterization*. Determination of the permeability and the diffusivity of cementitious materials are described in Chapter *3.2 Methodologies to determine permeability and diffusivity of cementitious materials*. Utilisation of tomographic methods is summarized in Chapter *3.3 Laboratory observations of processes in heterogeneous material*.

This deliverable report serves as a basis for the experimental work to be done during CEBAMA, by understanding international best practices to-date. More details about specific experimental method boundary conditions used in CEBAMA are described in the Deliverable D1.04 (to be published April 2016). More details about specific materials used in CEBAMA are described in the Deliverable D1.05 (to be published May 2016).

# 2　Nuclear waste repository concepts relevant to CEBAMA

## 2.1　Belgium

### 2.1.1　Background on Belgian concept for geological disposal in poorly indurated clay

*N. Maes, Q.T. Phung,*

*Belgian Nuclear Research Centre (SCK•CEN), Belgium*

**Layout of the current reference repository for geological disposal in poorly indurated clay**

The envisaged repository consists of a series of rectilinear galleries, in which the waste will be disposed, situated around the middle of a clay formation. Access to the disposal galleries is provided via the centrally located access gallery, to which all disposal galleries are linked. In its turn, the access gallery is connected to the surface via at least two shafts. All galleries are lined with concrete wedge blocks (gallery liner). Because the indurated clay formations in Belgium have a high plasticity, this concrete lining is required to limit convergence of the gallery walls [1].

A sketch of the different components in the envisaged repository system is shown in Figure 2.1.1.1.
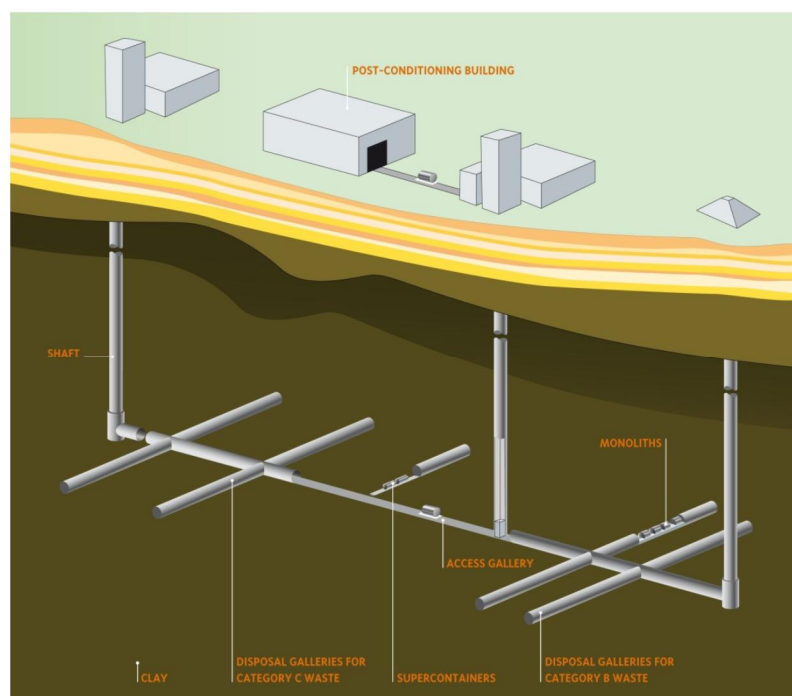


*Figure 2.1.1.1. Indicative diagram of the geological repository layout envisaged for B&C waste in poorly indurated clays.*

Separate sections are foreseen for disposal of category B (bituminized and compacted residual waste) and C waste (HLW and SF). The waste packages, supercontainers (C-waste) or monoliths (B-waste), will be emplaced horizontally one after the other (with no gaps between them) in the centre of the disposal galleries. These galleries are drifts of maximum 1 km length and depend on the waste type an inventory. The distance between disposal galleries is between 50–120 metres and depends also on the waste type. The considered backfill material, that will be used to fill the void space between waste packages and tunnel liner, is also based on cement.

**Waste packages design – concrete based supercontainer & monoliths**

The current reference design of the engineered barrier system (EBS) is often called the "supercontainer design", the name of the category C waste disposal package. It comprises specific disposal waste packages developed respectively for category C waste and category B waste [1].

The supercontainer for category C waste comprises a carbon steel overpack and a Portland cement concrete buffer with or without an outer stainless steel envelope surrounding the primary waste packages. The intention of the buffer is to act as a radiation shield and pH controller in order to create favourable conditions with regards to passivation of carbon steel.

The length varies between 4–6.2 m long and 2.1 m wide with a mass of 70 tons. The supercontainer fulfills several functions contributing to the operational and long-term safety of the man and environment: i) provide permanent shielding for safe handling, ii) provide sufficient mechanical strength and iii) containment of the radionuclides and contaminants at least during the thermal phase.

The supercontainers are constructed at the surface before being transported underground for disposal.
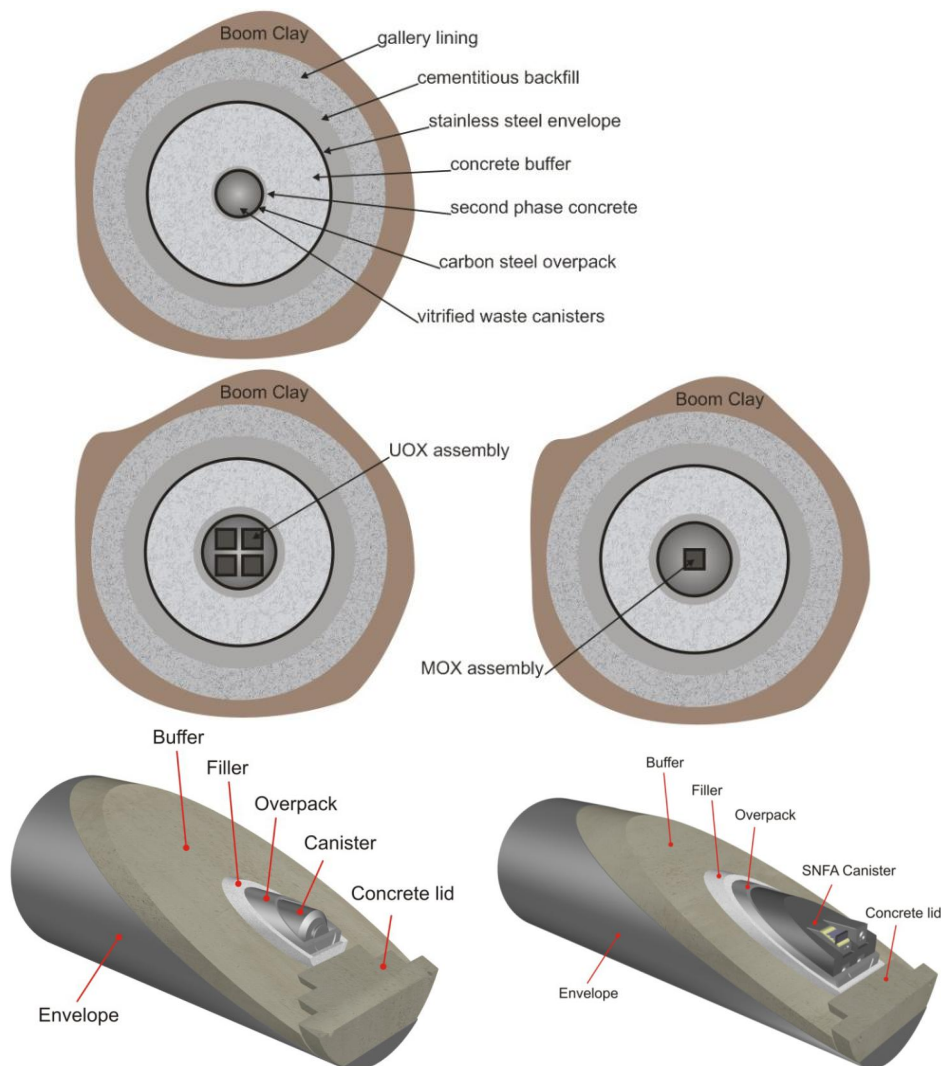


*Figure 2.1.1.2. Cross-section and 3D views of the supercontainer concept for present high-level waste types.*
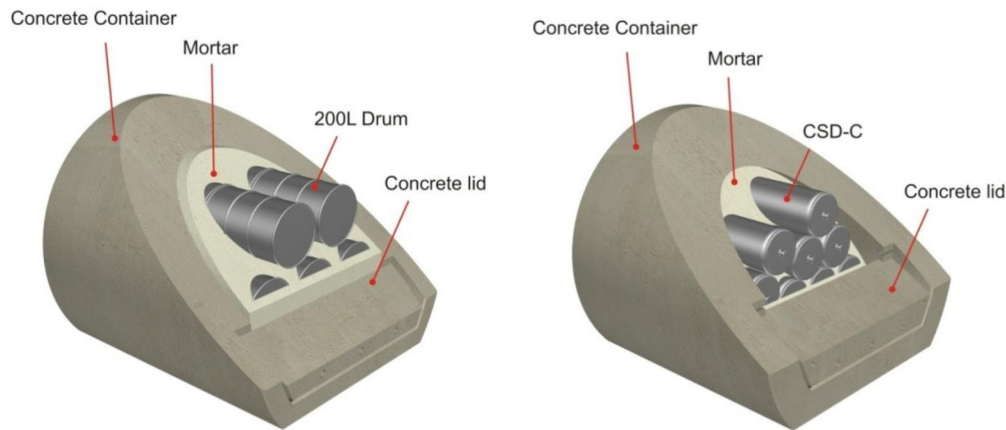
*Figure 2.1.1.3. Current design of the monolith type of containers for bituminised (Eurobitumen) (left) and compacted (CSD-C) (right) waste.*

The disposal packages for category B waste (Eurobitumen), [2] and compacted residual waste (CSD-C) are called monoliths. In the reference design, the primary packages of B-waste are immobilised in mortar in concrete caissons made of portland cement and are constructed at the surface. The length varies between 1.9–2.9 m long and 2.9 m wide with a mass ranging from 32 to 39 tons. Similar to the supercontainer, the monolith fulfils several functions: i) standardize dimensions and limiting underground works, ii) provide permanent shielding and iii) provide mechanical strength.

Following waste emplacement, all remaining voids in the disposal galleries will be backfilled with a cement-based material and, following the completion of underground operations, all access tunnels and shafts will be backfilled and sealed.

**References**

[1] ONDRAF/NIRAS. ONDRAF/NIRAS Research, Development and demonstration (RD&D) Plan for the geological disposal of high-level and/or long-lived radioactive waste including irradiated fuel if considered as waste, State-of-the-art report as of December 2012. NIROND-TR 2013-12E 2013. p. 413.

## 2.2 Czech Republic

### 2.2.1 SURAO disposal concept

*V. Havlova[1], A. Vokal[2]*

*[1]UJV Rez, a.s., Hlavni 130, Rez, 250 68 Husinec, Czech Republic*
*[2]SURAO, Dlazdena 6, Praha, Czech Republic*

The Czech deep geological repository (DGR) concept assumes that waste packages containing spent nuclear fuel (SNF) assemblies will be enclosed in steel-based canisters placed in vertical or horizontal boreholes at a depth of ~ 500m below the surface. The void between the canisters and the host crystalline rock will be backfilled with compacted bentonite which will make up the final engineered barrier (Figure 2.2.1.1). The reference SNF canister design contained is composed of two layers, an outer layer of carbon steel which will corrode very slowly under anaerobic conditions and a second inner layer of stainless steel which will corrode at an almost negligible general corrosion rate and exhibit a low tendency to local corrosion under anaerobic conditions.
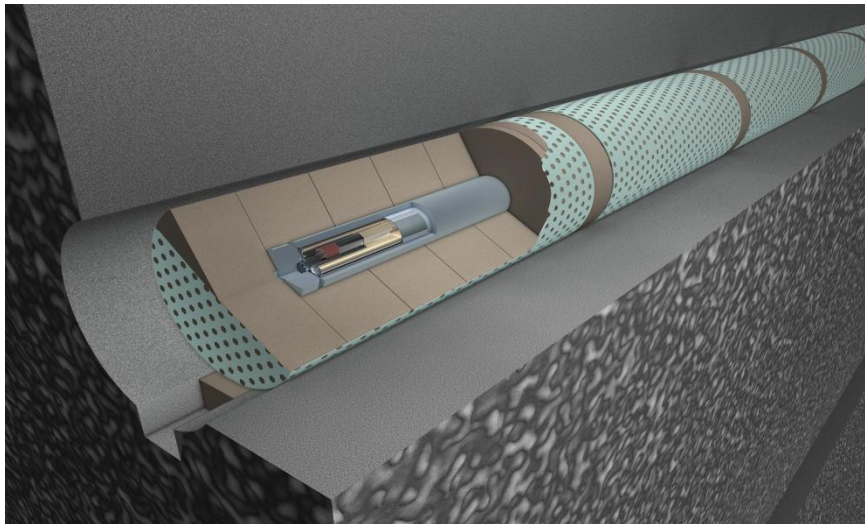


*Figure 2.2.1.1. Visualisation of the Czech DGR concept using horizontal boreholes (SURAO).*

Intermediate-level waste (ILW) with long-lived radionuclides, such as decomissioned reactor core parts or serpentinite concrete, not being allowed to be disposed of in the near-surface repositories, will be also disposed of in a future DGR. The ILW repository will be located at the same site as the one for SNF assemblies; however not in the identical repository section. The main requirement is that the repository areas for both SNF and ILW should not affect each other. A scheme for both repositories is provided in Figure 2.2.1.2. The ILW will be emplaced in concrete canisters in specially excavated chambers that will be filled with bentonite based backfill (Figure 2.2.1.3).
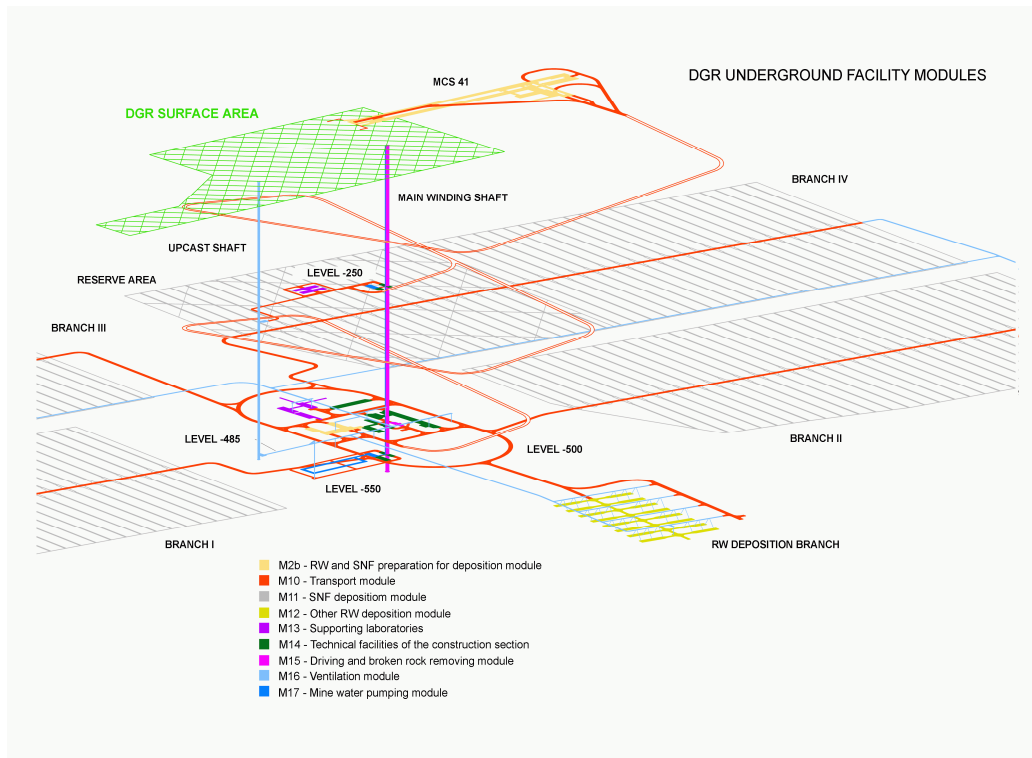
*Figure 2.2.1.2. Scheme of the future Czech DGR for spent fuel assemblies and ILW [1].*
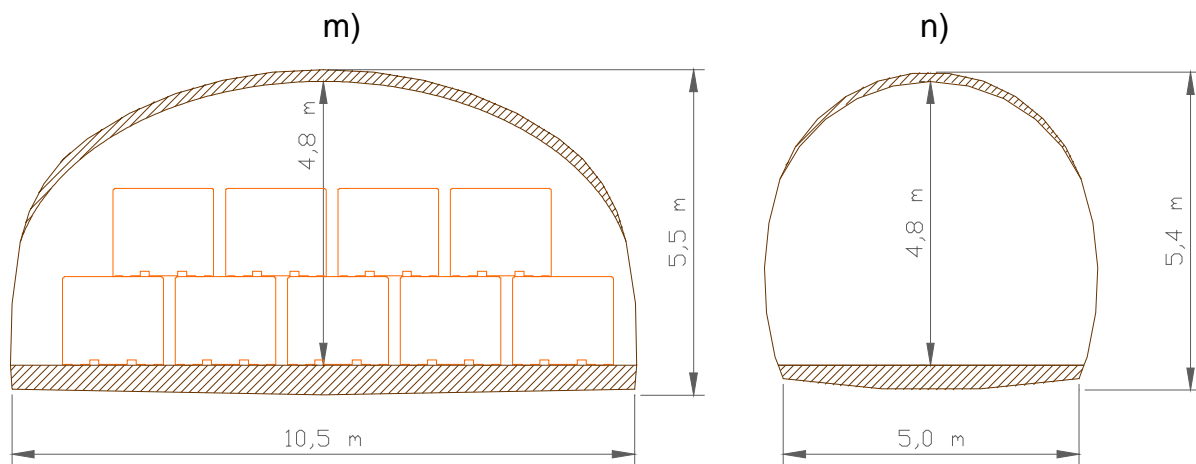


*Figure 2.2.1.3. ILW disposal chambers [1].*

It is presumed that the buffer material will originate from Czech Republic bentonite deposits. Nowadays so call Rokle bentonite is used (Ca-Mg bentonite). The primary safety function of bentonite buffer in the CZ concept is to isolate SNF or HLW and retent radionuclide migration toward environment in order to fulfil optimisation limit 0.25 mSv/year for radiation safety.

As mentioned above, concrete will be used in the repository as both barrier material and construction material. Except using fibre concrete containers for ILW, sealing and separation concrete plugs and other construction elements (floors, walls, supporting construction elements, shotcrete, grouting etc.) are considered be used. Two types of cements would be used: Ordinary Portland Cement (OPC, pH>12) and low pH cement (LPC, pH<11). However, the material types and the detailed scheme for their use have not been specified yet [1]. Eventhough LPC is expected to be used for sealing plugs as plug construction parts could be in direct contact with bentonite

buffer in the disposal corridors. It is assumed in [1] that 1 100 t of cement materials will be used in DGR each year.

LPC material is recommended in order to decrease the impact of OPC leaching in contact with groundwater. Generally, OPC degradation generates high-alkaline gradient, with pH>13, being rich in $K^+$, $Na^+$, $Ca2^+$ in the first period. In the second period pH is governed namely by portlandite transformation with pH around 12.4. The last period will be influenced by CSH with pH around 10 [2, 3, 4, 5]. The extent of alkaline reaction can be modified using different additives/alternative recepies, as mentioned above [4]. It is assumed in [1] that 1 100 t of cement materials will be used in DGR each year.

## References

[1]     Actualisation of DGR reference concept in the hyphotetic site. SURAO, 2011.
[2]     Gaucher C. E., Blanc P. (2006): Cement/clay interactions – A review: Experiments, natural analogues and modeling, Waste Management 26, 776-788 s.
[3]     Savage D. (2013): Constraints on cement-clay interaction, Proceeding Earth and Planetary Science 7, 770-773 s
[4]     Sánchez L., Cuevas J., Ramírez S., Riuiz De León D., Fernández R., Vigil Dela Villa R., Leguey S. (2006): Reaction kinetics of FEBEX bentonite in hyperalkaline conditions resembling the cement-bentonite interface, Applied Clay Science 33 (2006), 125-141 s.
[5]     Dolder F., Mäder U., Jenni A., Schwendener N. (2014): Experimental characterization of cement-bentonite interaction using core infiltration techniques and 4D computed tomography, Physics and Chemistry of the Earth 70-71, 104-113

## 2.3   Finland

### 2.3.1   Posiva's KBS-3V concept

*T. Vehmas*

*VTT Technical Research Centre of Finland Ltd, Espoo, Finland*

Posiva Oy is constructing one of the world's first long-term nuclear waste repositories in Finland.[1] The safety of the nuclear waste repository is ensured with a combination of natural and engineered barriers. Final nuclear waste disposal will take place in ONKALO, a deep underground repository in Olkiluoto bedrock at a depth of 400–450 meters underground. The natural barrier consists of the surrounding Olkiluoto bedrock and its inherent isolating properties. The engineered barrier system consists of water- and gas-tight sealed copper canisters with a cast iron insert and bentonite-based buffer and backfill. Permanent concrete structural tunnel plugs are used for closure and sealing of the deposition tunnels.[2][3] In the KBS-3V -type repository, copper canisters are placed in a vertical position into disposal holes drilled into the floor of deposition tunnels, as shown in Figure 2.3.1.1. Bentonite-based buffer is stable material with self-sealing capability. Bentonite-buffer also has good retention of potentially leaking radionuclides. Bentonite-based backfill limits the upward expansion of the buffer into deposition tunnels and prevents the development of hydraulic pathways in the deposition tunnels so that the natural water flux at the repository level is not affected. Initially heterogeneous backfill material should become homogeneous material with a low permeability as a consequence of water saturation and swelling.
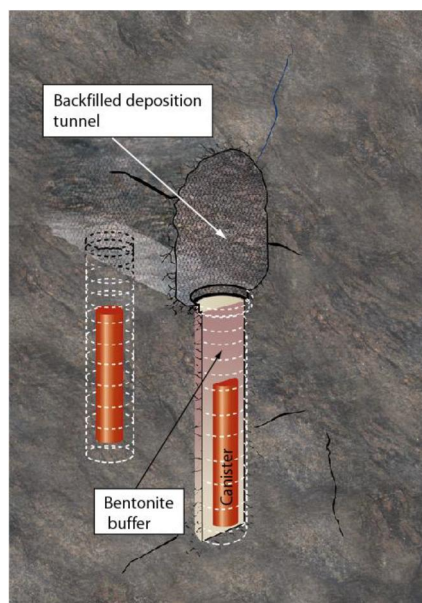


*Figure 2.3.1.1. Schematic presentation KBS-3V concept. [3]*

Concrete plugs are used for closure and sealing of the repository and the deposition tunnels. Concrete plugs are utilized to assure mechanical and hydrological isolation of the compartments of the repository. Isolation is needed because compartments have different states in terms of water saturation and pressures. Such difference could potentially induce undesired mass redistributions. Besides concrete plugs, cementitious materials are used in shotcrete for tunnel wall rock supports, rock-bolting grouts and injection grouts for fissure sealing. Only some of the cementitious materials

will remain in the repository after final closure. Shotcrete is removed before the final closure with an assumed efficiency of 95%.[4]

The amount of cementitious materials in the repository will be significant although some of the materials are removed before final closure. Approximately half of the cementitious materials that will remain in the closed repository are located in the access tunnels and consists of grouts, shotcrete remnants and concrete constructions. In deposition tunnels, cementitious materials are present in grouted fractures, rock bolt mortars and deposition tunnel end plugs.

The total amount of cementitious materials including central tunnels are assumed to be: 550 000–740 000 kg for grouts, 540 000–600 000 kg for shotcrete, 340 000–1 010 000 kg for rock bolt mortars and 16 500 kg for other constructions. The total mass of cementitious materials in access tunnels is approximately 1 446 000–2 367 000 kg. The mass of a single deposition tunnel end plug is 16 600 kg. The total mass of tunnel end plug concrete is 2 170 000 kg. [5]

Cementitious materials will be in direct contact with backfill and closure materials. It is assumed that cementitious leachates will interact with backfill and closure materials but not to extent that compromises the long-term safety of the barrier system. The bentonite buffer is not in direct contact with cementitious materials. However, the buffer may be affected due the migration of cementitious leachates through the bedrock fracture network. To meet the designed performance requirements during the lifecycle of the repository, the properties of the engineered barrier system should not alter due the presence of cementitious materials.[4]

It should be noted that the reference concept for SKB in Sweden for a high-level waste repository is very similar to Posiva's (Finland's) concept described here. The description in Chapter 2.7 for Sweden is related to the low- and medium-level waste repository.

### References

[1]    www.posiva.fi.
[2]    Palomäki, J., Ristimäki, L. (editors). 2013. Facility Description 2012: Summary Report of the Encapsulation Plant and Disposal Facility Designs. Posiva Oy, Working Report 2012-66, 148 p.
[3]    Keto, P.,Dixon, D., Jonsson, E., Börgesson, L, Hansen, J., and D. Gunnarsson. 2010. Assessment of backfill design for KBS-3V Repository. Posiva Oy, Working Report 09-115. 162 p.
[4]    Koskinen, K. 2014. Effects of Cementitious Leachates on the EBS. Posiva Oy, Working Report 2013-4, 63 p.
[5]    Karvonen, T. 2011. Foreign materials in the repository -Update of estimated Quantities. Posiva Oy, Working report 2011-32. 102p.

## 2.4 France

### 2.4.1 Andra's Nuclear Waste repository concept

*X. Bourbon*

*ANDRA - French National Agency for nuclear Waste Management, R&D Division, France*

**The origin - Definition**

Low hydration heat/Low pH cement are, since their appearance in the late '90's, developed within the nuclear waste disposal context. At the very beginning, second half of the 90's, Malcolm Gray & Bary Shenton said « For better concrete: take out some of the cement » (Gray & Shenton, 1998). What was the context and what was their purpose?

To build a concrete plug for the TSX (Tunnel Sealing eXperiment) international project, they had to design a specific concrete able to fulfill some requirements not achievable with a classical material, especially with regards to the hydration heat of the cement due to the size of the structure to build. The main goal of this experiment was to demonstrate the feasibility and to assess hydraulic performances of two seals made with swelling clay or concrete, in the AECL URL (Lac du Bonnet, MB, Canada).

To formulate such a concrete, the first requirement was to prepare a low hydration heat concrete due to the geometry of the concrete plug and the boundary conditions. Moreover, hydraulic behaviour expectation for the concrete plug led to a high performance concrete. Then they had to take into account shrinkage and cracking. This concrete has been prepared with classical devices in a surface facility and pumped at 420 m depth (after a transfer through the shaft and galleries with skips). This was the first concrete designed and used of that kind. As a consequence of the choices made to design this concrete, the chemical properties of this material were significantly different from those measured on classical concretes. The pH of the pore solution was very low compared to what was observed and that is why these materials are also called "low pH concrete".

Since then, due to the interest in the context of nuclear waste repositories, other countries worked on such materials and designed their own low hydration heat/low pH concretes.

**Concepts and present specifications**

*Seals: Concept and requirements*

Andra (the French National Agency for Nuclear Waste Management) has to design and to build a nuclear waste disposal for High and Intermediate Level radioactive Wastes (HLW and ILW) (Andra, 2015).

Cigeo is the name of the deep geological disposal facility for radioactive wastes to be built in France. It will serve as a repository for highly radioactive long-lived wastes generated by France's current fleet of nuclear power plants, from operation to dismantling, as well as from reprocessing of spent fuel from these same plants.

Located in the east of France, at about 500 m depth in the Callovo-Oxfordian layer, the (planned) facilities will cover the needs for about 75 000 $m^3$ of ILW and 10 000 $m^3$ HLW. At the end of the operating phase, galleries and access facilities will represent a length about 100 km and disposal

vaults a total length about 220 km (total underground surface ~15 km²; total surface facilities ~3 km²). The total excavated volume will be close to 9.2 million m$^3$. After the operating period, about half of the total volume will be filled with cementitious materials.

Concepts, for the different types of waste, have been designed taking into account the physical and the chemical properties of the Callovo-Oxfordian argillite as host rock. ILW will be handled in reinforced concrete waste packages and put into reinforced concrete vaults. HLW conditioned into steel canisters, will be put into small tunnels made with a steel liner. During the operating period, structures (vaults and waste packages) have to ensure safety and security of the repository (obviously preventing from any radioactive dissemination), according to the global mechanical stability of the site. With regards to the post closure and long term evolution, the clay host rock will be the main barrier to prevent from radionuclides transfer.

To seal the underground facilities, specific structures have been designed to restore the hydraulic properties of the geological medium to prevent from transfer all along and through the structures. Seals are composite structures involving swelling clay and concrete plugs. Access, galleries, vaults seals are based on the same concept.

To ensure mechanical stability of the seals and an increase of the swelling pressure during water saturation of the clay, concrete plugs:

- Must not chemically react with clays (as low as achievable), to prevent detrimental changes of the physical properties of the swelling clay;

- Have to ensure mechanical constraints during the water saturation period to make sure the swelling pressure will increase as planned;

- Have not to change the chemical behaviour of the clay materials (host rock, swelling clay, backfill) during the building period due to a thermal degradation; have not to create significant thermal gradients to avoid mechanical damages;
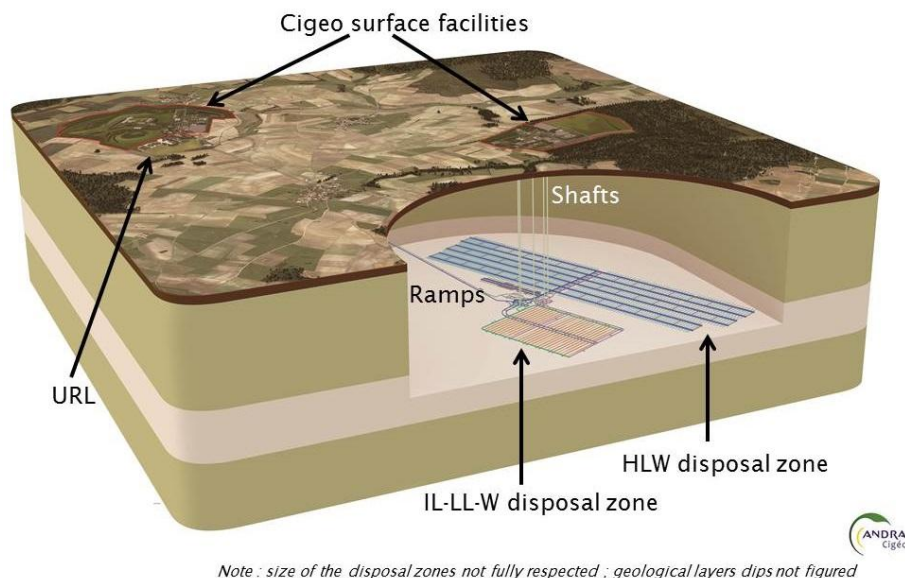


*Figure 2.4.1.1. Global lay-out of the (planned) facilities at Cigeo. © Andra.*
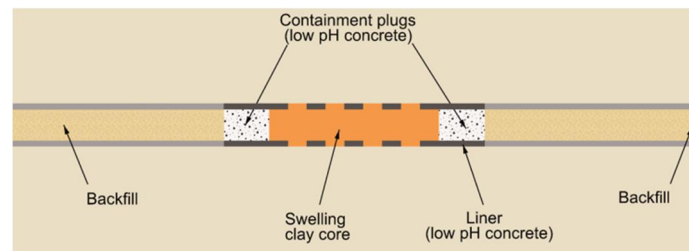
*Figure 2.4.1.2. Concrete/clay seal concept.*

The key issues for the concrete plugs are then connected to "massive structures building" (few hundreds of cubic meters each) and "chemical reactivity with clays" (direct contact with the clay host rock and the swelling clay):

- To fulfill requirements with regards to massive structures (short term expectations), the two key points are the temperature increase during the setting and the shrinkage. As a consequence, "low hydration heat cement" has to be formulated.

- Considering the mechanical stability of the seal zones (liners in the structures and plugs) over a long period of time (operating phase, closure and post closure period, up to the water saturation of the swelling clay plug), a high performance concrete is required.

- To fulfill the requirement dealing with the chemical reactivity with clays (long term expectations), this was one of the main conclusions of the ECOCLAY European project (ECOCLAY II, 2005), the pH has to be lowered. Consequently, that leads to a "low pH cement" formulation.

**Concrete specifications**

*Physical specifications*

To reduce the maximum temperature reached during setting and then to limit thermal gradients in large and/or monolithic structures, the hydration heat has to be limited. The thermal criterion is the maximum temperature reached during setting: $\Delta T < 20$ °C (measured in semi-adiabatic conditions).

To decrease the hydration heat, identified/specified cements (LHH) have to be chosen but the main key issue is to mitigate the clinker content in the blend. In the same time, due to the required physical properties to ensure the mechanical stability of the structures, a high performance concrete is needed ($Rc > 60$ MPa). This means clinker has to be replaced (and not only taken out) in the binder. High substitution level of the cement with pozzolanic or hydraulic compounds has to be considered.

To prevent from mechanical disorders, the shrinkage has to be close -or at least same order of magnitude- to those measured on classical HPC (endogenous shrinkage $< 300$ µm/m; Total shrinkage $\leq 500$ µm/m).

Technologies and means to realize these concrete plugs have to be industrially available. Formulated materials could be shotcrete, pumped/vibrated concrete or self-compacted concrete (SCC).

As these materials will be prepared in a surface facility and put in place/layered in a deep geological structure, an important workability is then required. The materials need a workability period $\geq 2$ hours.

14

*Chemical specifications*

To lower as much as possible the chemical reactivity with clays, the pH of hydrated cement pore solution has to remain below 11 after hydration (few weeks to few months). To reach that limit, significant chemical modifications are necessary in comparison with "classical" cements. Even industrial blended cements such as CEM III or CEM V have an interstitial water pH level higher than 12.5.

At first, the main alkaline hydrates (i.e. portlandite and C-S-H with the highest molar Ca/Si ratio (C/S)) have to be neutralized. The pozzolanic reaction consumes the portlandite to form some C-S-H inducing the decrease of the global C/S ratio. In the same time, the chemical evolution of the hydrated phases has to enhance the sorption of the alkali ions. The alkali sorption is enhanced (i) by the decrease of the C/S ratio of C-S-H (and consequently the decrease of pH) and (ii) by the increase of C-S-H content. These last two points are favored by the pozzolanic reaction. As a consequence, the pozzolanic reaction using a high substitution level of clinker promotes the lowering of the pH equilibrium value below 11.

*Global specification*

All raw materials have to be available at an industrial scale as well as the techniques and materials to be used.

## References

Gray M.N. & Shenton B.S. (1998) For Better Concrete, Take Out Some of the Cement. Proc. 6th ACI/CANMET Symposium on the Durability of Concrete, Bangkok, Thailand, 5-31.

Andra (2015) http://www.andra.fr/international/index.html and http://www.cigeo.com/en/.

ECOCLAY II (2005) Effect of cement on clay barrier performance. European Report EN 21921.

## 2.5 Netherlands

### 2.5.1 OPERA disposal concept

*A. Sabau, D. Bykov*

*Section Nuclear Energy and Radiation Applications, Department of Radiation Science and Technology, Delft University of Technology, Mekelweg 15, 2629 JB Delft, Netherlands*

All radioactive waste produced in the Netherlands is managed by COVRA (Centrale Organisatie Voor Radioactief Afval). Compared to other European countries (France, Finland or Belgium), the radioactive waste disposal process in the Netherlands is at an early conceptual phase.

Based on the research program CORA (Commissie Opberging Radioactief Afval/Committee on Disposal of Radioactive Waste, 1996–2001) which is focused on the technical feasibility of a retrievable deep underground repository in salt rock, as well as on the suitability of Boom Clay as a host rock.

The current policy in the Netherlands is an interim storage of all the radioactive waste for a period of at least 100 years at COVRA, to perform research preferably in an international collaborative program and eventually to dispose all radioactive waste retrievably in a deep geological facility.

The Dutch research programme OPERA (Onderzoeks Programma Eindberging Radioactief Afval, 2011–2016) is currently investigating the geological disposal of high, as well as low, level radioactive waste in one facility. The outlines of the repository concept is proposed by Verhoef et al.[1] on which this study is based. The geological conditions in the Netherlands are in principle favourable from the perspective of disposal of radioactive waste. To begin with, the generic repository is to be situated at a depth of approximately 500 m in a Boom Clay stratum of approximately 100 m thickness. Due to the small waste quantities projected for the Netherlands, all low and intermediate level waste (LILW) and high level waste (HLW) is planned to be disposed of in one facility which are depicted in Figure 2.5.1.1.
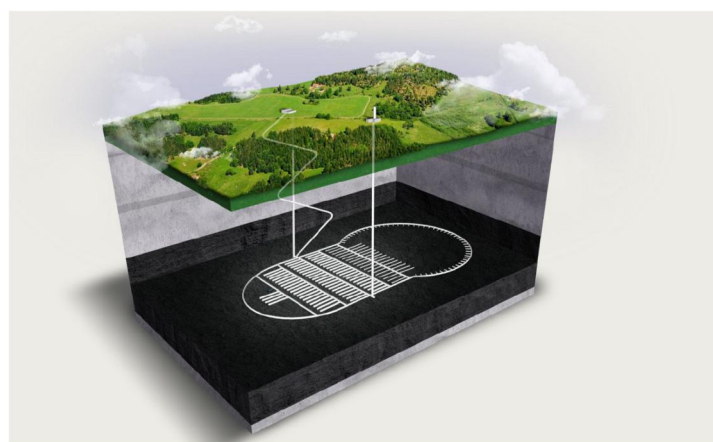


*Figure 2.5.1.1. Schematic representation of the Dutch deep geological repository in Boom Clay.*

For a clay host rock, the engineered barrier system specific for HLW is adapted from the Belgian waste management organisation; the ONDRAF/NIRAS supercontainer concept. HLW waste containers are placed in steel overpack surrounded by a concrete buffer in order to prevent the waste matrix coming into contact with (pore) water until the decay of radionuclides no longer increases

the temperature of the host rock. Concrete support is envisaged against clay convergence. To prevent cave-in when the concrete support has degraded, a backfill made with foamed concrete is investigated Verhoef et al. [2]. For a Dutch disposal facility in salt rock, no engineered barrier system with safety functions is yet defined Hart et al. [3].

The future repository life-cycle can be considered in three phases: (i) the pre-operation phase, including the conceptual development, site investigation and selection, design and construction; (ii) the operational phase, including waste emplacement, backfill disposal drifts, and any period of time prior to closure; and (iii) the post-operational phase.

Several types of cements are planned to be used as a function of their utility: mechanical support, enclosure or containment waste. The mechanical support is provided by the gallery lining during the constructional and operational phase of a geological disposal facility. The cement that is proposed to be used for mechanical support against clay convergence in the connecting galleries is the high sulphate resistant CEM II A to B-V 42.5 (concrete in reinforced concrete segments is made with Portland fly ash cement), because of the high content of sulphates in the Dutch Boom Clay, but also sulphate coming from the pyrite oxidation during excavation.

The LILW is conditioned with concrete and is expected to be suitable with no other further packaging or conditioning [1]. For the LILW the CEM III/B 42.5 LH/SR is made with blast furnace slag cement at COVRA [2]. The description and the composition are presented in Table 2.5.1.1.

*Table 2.5.1.1. Concrete composition for the disposal of compacted waste CEM III/B 42.5 LH/SR.*

| Component | Type | | |
|---|---|---|---|
| Cement | CEM III/B 42.5 LH/SR | 385 and 421 | kg m-3 |
| Water | - | 176 and 180 | kg m-3 |
| Plasticiser | TM OFT-II B84/39 CON. 35% (BT-SPL) | 5 and 6 | kg m-3 |
| Fine aggregate | Quartz sand: 0–4 mm | 864 and 860 | kg m-3 |
| Coarse aggregate | Quartz gravel: 2–8 mm | 865 and 848 | kg m-3 |

For depleted uranium, which is stored as $U_3O_8$ (TENORM), Portland cement with limestone aggregates is proposed, because sufficient Ca will react with $UF_6$ traces. The cement proposed for this type of waste is CEM I 42.5 N HS. The composition of concrete for TENORM containment is depicted in Table 2.5.1.2.

*Table 2.5.1.2. Composition concrete for containment of TENORM.*

| Component | Type | | |
|---|---|---|---|
| Cement | CEM I/42.5 N HS | 365 | kg m-3 |
| Water | - | 175 | kg m-3 |
| Plasticiser | TM OFT-II B84/39 CON. 35% (BT-SPL) | 3.3 | kg m-3 |
| Fine aggregate | U3O8: 0–4 mm | 2664 | kg m$^{-3}$ |
| Coarse aggregate | Limestone: 2–8 mm | 911 | kg m$^{-3}$ |
| w/c | Property | 0.48 | |

Enclosure of emplaced waste is provided by the backfill. Foam concrete made with Portland cement (CEM I SR 3 < 3% $C_3A$) and Blas-furnace slag based backfill are proposed (Table 2.5.1.3 and Table 2.5.1.4).

*Table 2.5.1.3. Composition enclosure emplaced waste (Portland-based backfill.).*

| Component | Receipt for 1 m$^3$ of Aercrete FC 1200 to 1600 kg m$^{-3}$ | Type for OPERA-Cebama | 1567 kg m$^{-3}$ | Wet density measured |
|---|---|---|---|---|
| Cement | 360 to 400 kg | CEM I 52.5 N SR 3 <3% C3A | 377 | kg m$^{-3}$ |
| Water | 140 to 160 kg | - | 151 | kg m$^{-3}$ |
| Fine aggregate | 750 to 1100 kg | Quartz sand: 0–4 mm | 1038 | kg m$^{-3}$ |
| Foaming agent Synthetic surfactant | 0.57 to 0.36 l | Foaming agent TM 80/23 Synthetic | 1 | kg m$^{-3}$ |

*Table 2.5.1.4. Composition enclosure emplaced waste (backfill-foamed concrete).*

| Component | Receipt for 1 m$^3$ of Aercrete FC 1200 to 1600 kg m$^{-3}$ | Type for OPERA-Cebama | 1576 kg m$^{-3}$ | Wet density measured |
|---|---|---|---|---|
| Cement | 360 to 400 kg | CEM III/B 42.5 N LH/SR | 380 | kg m$^{-3}$ |
| Water | 140 to 160 kg | - | 152 | kg m$^{-3}$ |
| Fine aggregate | 750 to 1100 kg | Quartz sand: 0–4 mm | 1044 | kg m$^{-3}$ |
| Foaming agent Synthetic surfactant | 0.57 to 0.36 l | Foaming agent TM 80/23 Synthetic | 1 | kg m$^{-3}$ |

The durability of cementitious materials is dependent on the chemical and physical evolution of the repository system. These processes have the potential to significantly change the original properties of the cement-based materials. These alterations evolve series of highly time dependent coupled physic-chemical processes. For the establishment of a geological disposal facility, The Netherlands policy does not exclude the option of international cooperation [4].

## References

[1]     Verhoef E.V., Neeft E. A. C., and Grupa J., *Outline of a disposal concept in clay*. OPERA-PG-COV008, (2011).
[2]     Verhoef E.V., et al., *Cementitious materials in OPERA disposal concept in Boom Clay*. OPERA-PG-COV020, (2014).
[3]     Hart J., et al., *Collection and analysis of current knowledge on salt based repositories*. OPERA-PU-NRG221A, (2015).
[4]     Ministry of Economic Affairs - Netherlands, *Joint Convention on the Safety of Spent Fuel Management and on the Safety of Radioactive Waste Management*. 5th National Report of the Netherlands (2015).

## 2.6 Spain

### 2.6.1 Spanish Disposal concept

*M.J. Turrero[1], P.L. Martín[1], J. Cuevas[2], M.C. Alonso[3]*

*[1]CIEMAT Research Centre for Energy, Environment and Technology, Madrid, Spain*
*[2]UAM Autonomous University of Madrid, Madrid, Spain*
*[3]CSIC High Research Council of Spain, Madrid, Spain*

The Spanish deep geological repository (DGR) concept for high level radioactive waste (HLRW) is based on the multi-barrier concept, and considers granite and clay as disposal options. The definitive disposal is planned to be accomplished in Carbon steel (S355) canisters placed along the axis of horizontal drifts excavated at a close to 250 m (clay) or 500 m (granite) and surrounded by bentonite as buffer and sealing material, the drifts being closed up with concrete plugs, as shown in Figure 2.6.1.1 [1][2]. If the host rock is clay, an additional structure made of concrete voussoirs is placed between the bentonite buffer and the gallery wall. Canister, bentonite and concrete constitute the engineered barrier system (EBS).
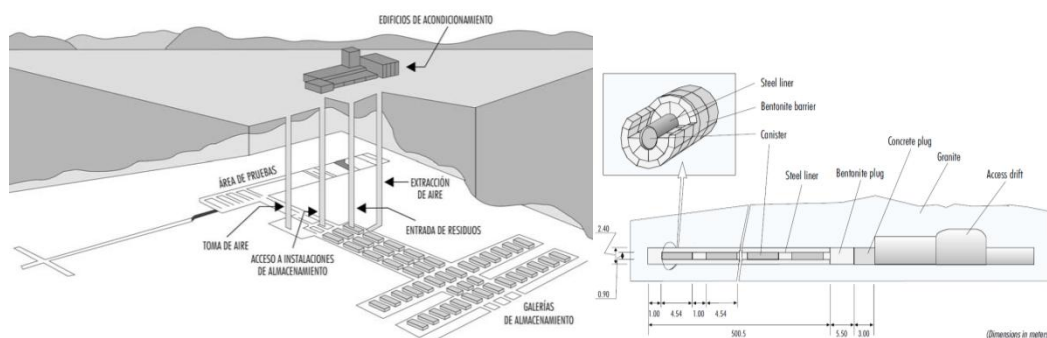


*Figure 2.6.1.1. General representation of a DGR system in granite [1][2].*

The long-term safety is provided by the joint performance of the multibarrier system. In general terms, in case of a granite host rock, the repository is located in an intact granite block without important conductive features, providing a considerable delay for the transport of any radionuclide dissolved in water. The bentonite buffer allows the transport of substances only by diffusion, a slow mechanism, and provides a strong sorption in pore spaces. In a clay formation, the clay layer has some hundreds of meters, causing a long travel time to the dissolved nuclides being transported through diffusion.

The functions attributed to the bentonite surrounding the canister are those of reducing groundwater flow around canisters and the transport of corrosive substances, establishing a suitable physico-chemical environment near the canisters and providing mechanical protection against possible movements of the rock thanks to its plasticity. Consequently, the properties to be provided by the bentonite are fundamentally low permeability and diffusivity, good thermal conductivity, a high sorption capacity and long-term stability [2]. Regarding the concrete, the main qualities as a component of the multibarrier system are its low permeability, high mechanical resistance and suitable chemical properties; the alkaline nature of cement pore water lowers the solubility of many radioactive elements.

The layer of bentonite used as seal in the disposal galleries of the DGR will have a thickness between 0.55 and 0.75 m and the temperature at the inner surface will not exceed 100 °C. The blocks will be manufactured from a clay granulate material with its hygroscopic water content, thus not being saturated at disposal time. Once in the repository environment, the bentonite will hydrate and swell becoming a continuous porous mass of very low hydraulic conductivity. This process will take place in the presence of a thermal gradient. The Spanish reference bentonite was selected by ENRESA from suitability studies performed between 1987 and 1991 and extracted from the Cortijo de Archidona deposit in the Cabo de Gata region (Almería).

To demonstrate the technical feasibility of installing the engineered barriers for a high level waste disposal facility in crystalline rock and to study their behavior ENRESA initiated in 1995 the FEBEX Project. A part of the project consisted of a full-scale *in situ* test, performed at the Grimsel underground facility (Switzerland) which includes the Spanish reference bentonite and a plug constructed by the shotcreting technique [3]. From 2008 until dismantling in 2015, the test was part of a consortium consisting of Ciemat, Nagra, SKB and Posiva [4]. In 2013 Kaeri joined the consortium. Post-mortem samples of bentonite/shotcrete interface and shotcrete itself coming from dismantling, will be studied in the context of CEBAMA to analyze if materials maintain their technical requirements as barriers.

Furthermore, a series of small-scale, long-term laboratory tests currently running at CIEMAT (initiated during EU projects FEBEX, NF-PRO and PEBS) were designed to complement the information acquired from the *in situ* test. The dismantling and analysis of one of those tests [5][6] after running during 10 years will be part of CEBAMA. Its modelling will help the upscaling activities.

In addition, transport properties of the cementitious materials used in the LILW (OPC-based) facility at El Cabril and at interim storage facilities will be tested in the context of CEBAMA. In these concepts, high resistivity and salt resistant cementitious materials are used as elements of the engineering structure of the repositories, as well as for the encapsulation and immobilization of the LILW.

**Reference**s

[1]    ENRESA. 1995. Almacenamiento geológico profundo de residuos radiactivos de alta actividad (AGP). Diseños conceptuales genéricos. Publicación Técnica ENRESA 11/95, Madrid, 105 p.

[2]    Astudillo J. 2001. El almacenamiento geológico profundo de los residuos radiactivos de alta actividad: Principios básicos y tecnología. ENRESA 2001. 205 pp.

[3]    Huertas F., Fariña P., Farias J. [et al.]. 2006. Febex Full-scale Engineered Barriers Experiment. Updated Final Report 1994-2004. ENRESA Publicación Técnica PT 05-0/2006. Madrid. 590 pp.

[4]    http://www.grimsel.com/gts-phase-vi/febex-dp

[5]    Torres E., Turrero M.J., Escribano A., Martín P.L. 2013. Geochemical interactions at the concrete-bentonite interface of column experiments. PEBS EU Project. Deliverable D2.3-6-1. 75 pp.

[6]    Turrero M.J., Villar M.V., Torres E., Escribano A., Cuevas J., Fernández R., Ruiz A.I., Vigil de la Villa R., de Soto I. 2011. Laboratory tests at the interfaces: First results on the dismantling of tests FB3 and HB4. PEBS EU Project. Deliverable D2.3-3-1. 64 pp.

## 2.7 Sweden

### 2.7.1 SKB´s repository concepts for low- and intermediate level waste

*Per Mårtensson*

*Swedish Nuclear Fuel and Waste Management Co (SKB), Stockholm, Sweden*

The Final repository for short-lived radioactive waste, SFR, was taken into operation by SKB in 1988 and was at that time the first facility of its kind. At current, SFR comprises 4 different rock vaults and one silo, each with different types of barrier systems optimized for the different waste types disposed therein. An extension of SFR is now being planned and once taken into full operation SFR will comprise a total of 10 rock vaults and one silo, Figure 2.7.1.1.
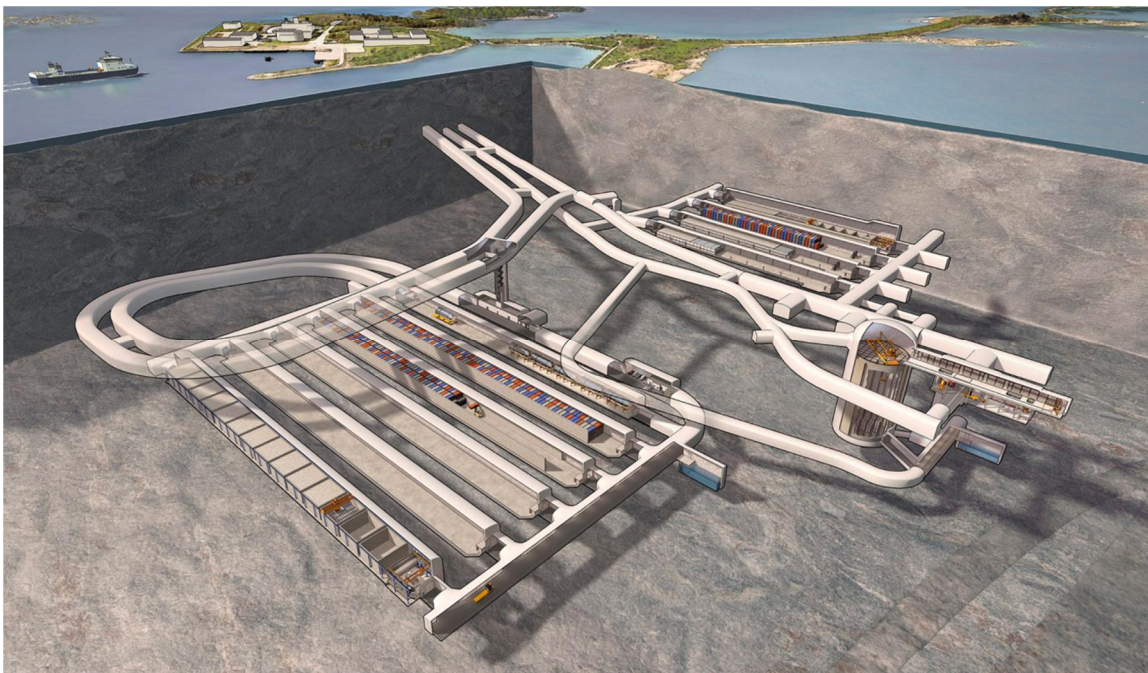


*Figure 2.7.1.1. A schematic illustration of SFR. The current facility comprises the rock vaults and silo in the upper right of the image whereas the extension comprises the rock vaults in the lower left.*

In SFR vast amounts of cementitious materials are used and are planned to be used in the engineered barrier systems of the different rock vaults and silo but such materials will also be used in the plugs used to seal the rock vaults and the tunnel system.

The silo is a cylindrical vault in which a free-standing concrete cylinder has been built. The concrete cylinder is made of *in-situ* cast concrete and founded on a bed of 90% sand and 10% bentonite. The concrete cylinder is divided into a number of vertical shafts, and the gap between the concrete cylinder and the surrounding bedrock is filled with bentonite. The bentonite is a bentonite from Milos (Greece) converted from its original Ca-form to the Na-state by soda treatment. The rock walls are lined with shotcrete, and a rock drainage system is installed between the bentonite and the bedrock [1].

*Figure 2.7.1.2. An illustration of the topmost part of the silo showing the concrete structure and the bentonite layer in the slit between the concrete structure and the surrounding bedrock.*

Bentonite will also be used in the plugs in the tunnel system (Figure 2.7.1.3) but also in plugs sealing the rock vaults. The purpose of these plugs is to minimize the flow of water in the tunnel system as well as between the tunnels and the rock vaults.
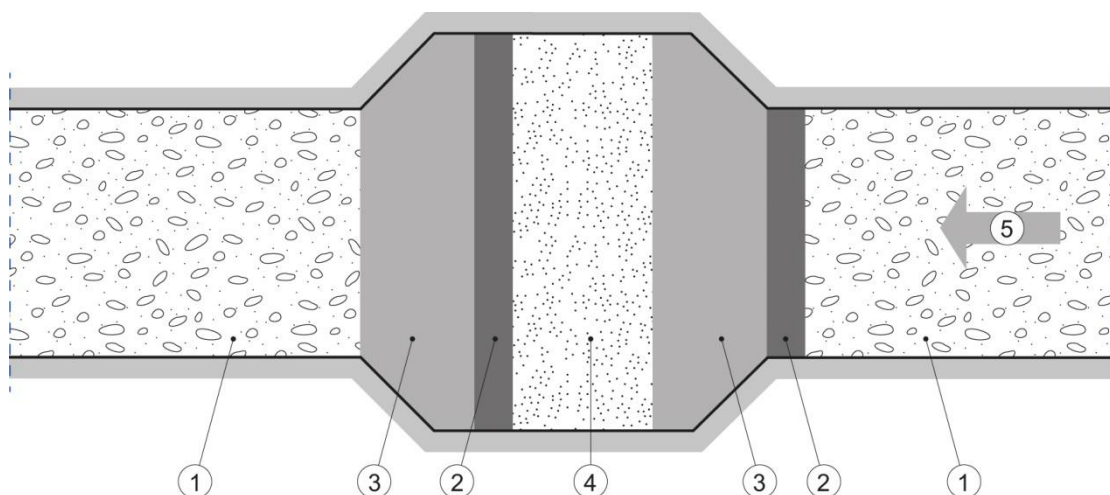


*Figure 2.7.1.3. Schematic reference design of plug in access tunnels. Legend: 1) Backfill of macadam 2) Constraining wall 3) Concrete 4) Bentonite 5) Working direction.*

SKB is currently also planning for the Final repository for long-lived radioactive waste, SFL which will be located at a depth of 300–500 meters in granitic bedrock [2]. This repository is planned to be taken into operation around the year 2045 and comprises two rock vaults, one for metallic waste such as reactor pressure vessels and core components from the dismantling of the Swedish nuclear power plants, BHK, and one for the legacy waste from the development of the Swedish nuclear programme, BHA.

In BHK, the barrier system comprises a concrete structure surrounded by a layer of concrete with a thickness of about 2 meters on all sides, Figure 2.7.1.4 left image, whereas in BHA the concrete structure is instead surrounded by a thick layer of bentonite clay, Figure 2.7.1.4 right image.
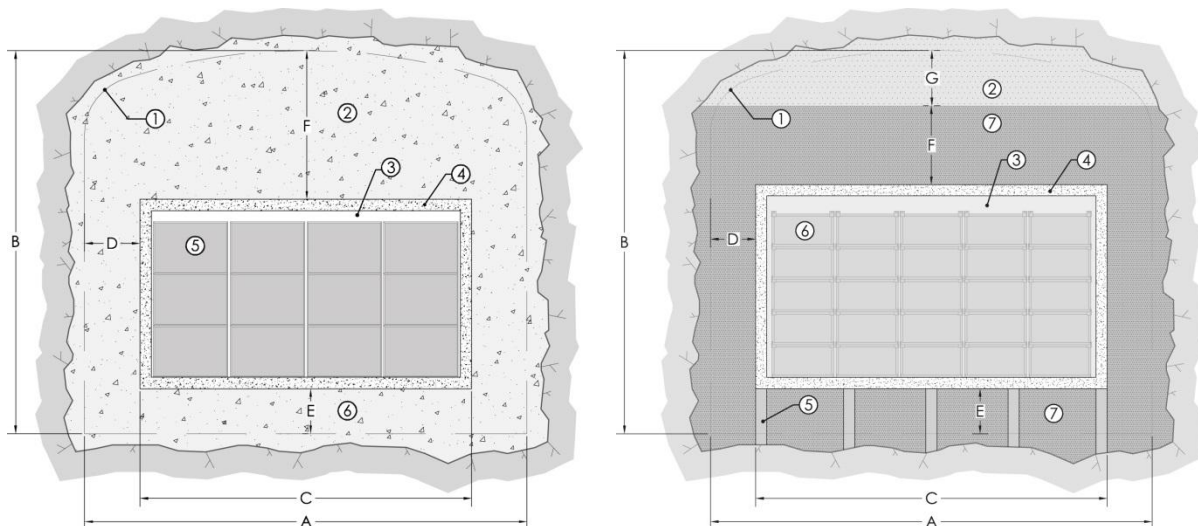
*Figure 2.7.1.4. Left image: Schematic illustration of the preliminary cross-sectional layout of the repository section for the metallic waste, Legend: 1) Theoretical tunnel contour. 2) Concrete. 3) Grout. 4) Reinforced concrete (0.5 m). 5) Steel tank. 6) Concrete. Right image: Schematic illustration of the preliminary cross-sectional layout of the repository section for the legacy waste. Legend: 1) Theoretical tunnel contour. 2) Bentonite pellets. 3) Grout. 4) Concrete structure for the operating phase (0.5 m). 5) Granite pillars. 6) Waste container. 7) Bentonite blocks.*

In the repository components described here interactions will occur between the cementitious materials and the bentonite clay (silo, BHA and plugs) or between the cementitious materials and the adjacent bedrock (BHK) affecting the properties of these materials. Previous studies (see e.g. [3] and [4]) have indicated significant alterations (though not detrimental from the perspective of long term safety) of the mineral composition in both the silo concrete structure and the surrounding bentonite during the period after closure. However, further studies are required in order to ensure that similar alterations do not compromise the safety functions of the engineered barrier system as a whole in other repository components.

## References

[1] SKB 2014. Safety analysis for SFR, long term safety. Main report for the safety assessment SR-PSU, SKB TR-14-01, Swedish Nuclear Fuel and Waste Management Co.

[2] Elfwing M, Evins L Z, Gontier M, Grahm P, Mårtensson P, Tunbrant S, 2013. SFL Concept study, Main report, SKB-TR-13-14, Swedish Nuclear Fuel and Waste Management Co.

[3] Gaucher E, Tournassat C, Nowak C, 2005. Modelling the geochemical evolution of the multi-barrier system of the Silo of the SFR repository. SKB R-05-80, Swedish Nuclear Fuel and Waste Management Co.

[4] Cronstrand P, 2016. Long-term performance of the bentonite barrier in the SFR silo. SKB TR-15-08, Svensk Kärnbränslehantering AB.

## 2.8 Switzerland

### 2.8.1 Swiss repository concept and cementitious materials

*Veerle Cloet [1] and Urs Mäder [2]*
*[1] Nagra - National Cooperative for the Disposal of Radioactive Waste, Switzerland*
*[2] University of Bern, Switzerland*

The overall approach to implementing deep geological disposal in Switzerland foresees two types of geological repositories: a high-level waste repository (HLW repository) for spent fuel (SF), vitrified high-level waste (HLW) and long-lived intermediate-level waste (ILW); and a repository for low- and intermediate-level waste (L/ILW repository). The procedure and the criteria for the selection of sites for deep geological repositories are specified in the concept part of the "Sectoral Plan for Deep Geological Repositories" (BFE 2008). The procedure consists of three stages and will ultimately lead to the identification of the sites for repository implementation, the definition of the main features of the repositories and the granting of the general licences. In Stage 1 of the Sectoral Plan, potential host rocks and associated geological siting regions were identified and entered in the Sectoral Plan with a decision by the Federal Council (BFE 2011). In the course of Stage 2, Nagra proposed for both repository types the two geological siting regions "Jura Ost" and "Zürich Nordost" (Nagra 2014) for further investigations in Stage 3. In these siting regions, Opalinus Clay has been identified as the preferred host rock for both repository types.

The HLW repository concept in Opalinus Clay envisions an array of long (ca. 800 m) parallel emplacement rooms (tunnels) at a depth of 600 to 900 m containing SF or HLW canisters, with the region around the canisters filled with bentonite, as shown in Fig. 3-1a. ILW, with much lower activity than SF or HLW, is emplaced in separate rooms (caverns), each about 8 m in width and up to 200 m in length, which are supported by concrete liners and backfilled with cementitious mortar. Access to the repository will be provided, during construction and operation, by a ramp and/or by shafts. For tunnel support, a low-pH shotcrete liner would be used, with an intermediate hydraulic seal placed between every tenth canister (Nagra 2010). The hydraulic seal would comprise bentonite of higher density than that used around the disposal canisters, constructed using a combination of blocks and pellets. The purpose of this structure is to maintain a certain hydraulic and gas permeability in case skin formation between concrete and either claystone or bentonite might lead to unwanted complete sealing.
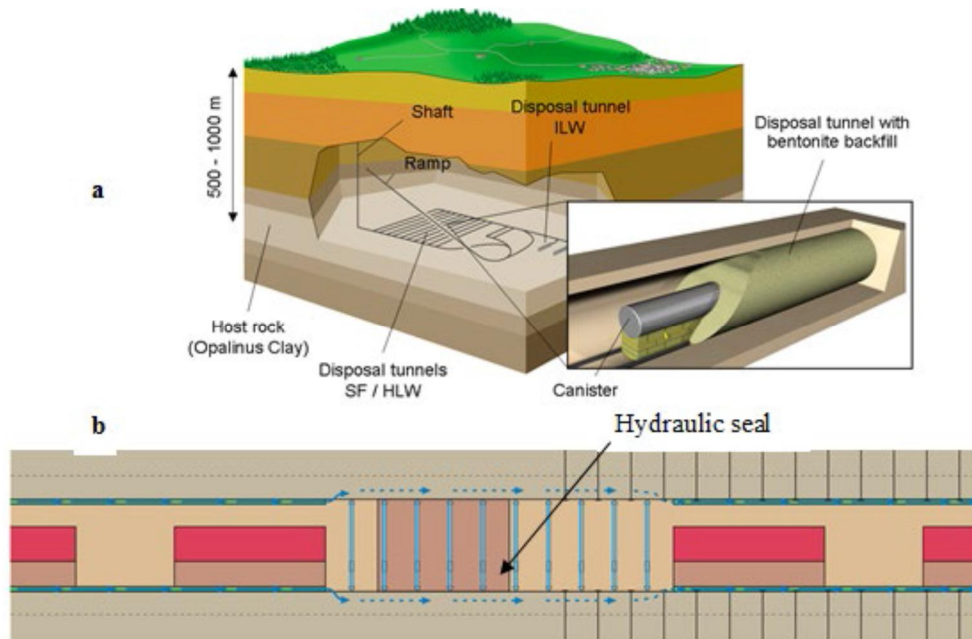
*Figure 2.8.1.1. Nagra HLW repository concept: (a) repository layout and detail of Engineered Barrier System; (b) longitudinal section of emplacement tunnel showing liner and hydraulic seal.*

Figure 2.8.1.2 presents a schematic view of a generic layout of the L/ILW repository, displaying the main elements of the underground structures, namely the access tunnel and shafts, the operations and access tunnels, the pilot repository, the rock laboratory, and the emplacement tunnels (also termed caverns).
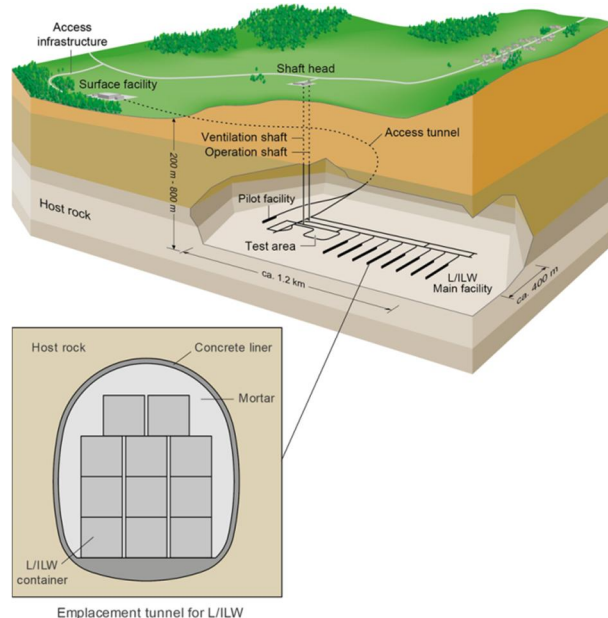


*Figure 2.8.1.2. Schematic layout of a generic concept for a L/ILW repository.*

The disposal containers for L/ILW are emplaced in caverns with a cross section of approximately 11.0 × 13.2 m (design variant K09)[1]. The length of the caverns is approximately 200 m, but can be

---

[1]  Several cavern size options have been considered by Nagra for L/ILW caverns (Nagra 2010). Because of stability considerations and concerns about excavation disturbance having a negative impact on characteristics of Opalinus Clay, the large diameter cavern concepts, K12, K16 and K20 are considered much less suitable than K04, K06 and K09.

longer or shorter. The caverns need to be supported with rock bolts and sprayed concrete lining including reinforcement (steel wire mesh).

As soon as the emplacement of waste containers in one disposal section of a cavern is completed, the voids between the containers and the cavern lining are backfilled with cementitious mortar (Jacobs et al., 1994). Once all sections of the cavern and the top heading are backfilled the enlarged section of the branch tunnel at the caverns entrance is also backfilled with the same mono-grain mortar. Each cavern is closed with a concrete plug.

The cementitious materials have not yet been specified for some components (Tab. 2.8.1.1). Different types of plugs and seals are not considered in this summary, and are not yet finalized. Currently, Nagra has developed one reference mortar recipe (Mortar 1) that will be used for the backfilling of the ILW and L/ILW caverns. A previously developed recipe (Mortar 2) which is a highly porous, low viscosity mortar will not be developed any further as it contained Aluminium powder, which is disadvantageous for long-term safety (gas production). Preliminary requirements on the porosity and permeability of the concrete components in the L/ILW repository (plugs, seals, construction concrete, backfill) were described in Nagra (2008). However, the concrete recipes to achieve these requirements were not yet defined. The concrete/mortar recipes used for the waste emplacement and repository containers are confidential in nature as they are being defined by the waste producers (NPP).

*Table 2.8.1.1. Cementitious components in repositories.*

| Repository | Component | Specification/options |
|---|---|---|
| HLW/ILW | Liner for SF drifts | No reference recipe defined yet, currently ESDRED* as most likely cement |
| | Liner for ILW caverns | No reference recipe defined yet: ESDRED or OPC |
| | ILW waste matrix | No publicly accessible reference reports available |
| | ILW back-fill | NTB 12-11: Jacobs et al (1994): Hochpermeable, zement-gebundene Verfüllmörtle für SMA Endlager |
| L/ILW | Liner for caverns | No reference recipe defined: ESDRED or OPC |
| | LLW waste matrix | No publicly accessible reference reports available |
| | LLW back-fill | NTB 12-11: Jacobs et al: Hochpermeable, zement-gebundene Verfüllmörtle für SMA Endlager |

The long-term geochemical evolution of the near-field for a HLW repository, including cement/clay interaction is described in Bradbury et al. (2012), including reactive transport modelling. The authors use a low-alkali cementitious product (ESDRED shotcrete, Alonso et al. 2009) – one option in Nagra's concept – in their calculations, in contact with MX-80 compacted bentonite and Opalinus Clay. The thermodynamic approach chosen is based on global free energy minimization and assuming chemical equilibrium. The geochemical evolution of the near-field surrounding an LLW is described in Kosakowski et al. (2014).

**References**

Alonso, J., García-Siñeriz, J.L., Bárcena, I., Alonso, M.C., Fernández Luco, L., García, J.L., Fries, Th., Petterson, S., Bodén, A., Salo, J-P. (2009). ESDRED, Module 4 (Temporary Sealing Technology) Final Technical Report. European Commission, Contract FI6W-CT-2004-508851.

BFE (2008): Sachplan geologische Tiefenlager. Konzeptteil. Bundesamt für Energie BFE, Bern, Schweiz.

BFE (2011): Sachplan geologische Tiefenlager. Ergebnisbericht zu Etappe 1: Festlegungen und Objektblätter. 30th November 2011. Swiss Federal Office of Energy SFOE, Bern, Switzerland.

Bradbury, H.M., Berner, U., Curti, E., Hummel, W., Kosakowski, G. and Thoenen, T. (2012). The long term geochemical evolution of the nearfield of the HLW repository. Nagra Technical Report NTB 12-01. Nagra, Wettingen, Switzerland.

Jacobs, F., Mayer, G. and Wittmann, F.H. (1994). Hochpermeable, zementgebundene Verfüllmörtel für SMA Endlager. Nagra Technical Report NTB 92-11.

Kosakowski, G., Berner, U., Wieland, E., Glaus, M. and Degueldre, C. (2014). Geochemical evolution of the L/ILW near-field. Nagra Technical Report NTB 14-11. Nagra, Wettingen, Switzerland.

Nagra (2008). Effects of post-disposal gas generation in a repository for low-and intermediate-level waste sited in the Opalinus Clay of Northern Switzerland. NTB 08-07

Nagra (2010). Beurteilung der geologischen Unterlagen für die provisorische Sicherheitsanalyse in SGT Etappe 2: Klärung der Notwendigkeit ergänzender geologsicher Untersuchungen. Nagra Technical Report NTB 10-01. Nagra, Wettingen, Switzerland.

Nagra (2014). Sicherheitstechnischer Vergleich und Vorschlag der in Etappe 3 weiter zu untersuchenden geologischen Standortgebiete (Textband). Nagra Technical Report NTB 14-01. Nagra, Wettingen, Switzerland.

## 2.9 United Kingdom

### 2.9.1 State of the art review of the NRVB: A UK high pH backfill cement

*R. G. W. Vasconcelos, J. L. Provis, C. L. Corkhill*

*Immobilisation Science Laboratory, Department of Materials Science and Engineering, University of Sheffield, Sheffield, S1 3JD, United Kingdom*

**Introduction**

The current concept for the disposal of intermediate level radioactive waste (ILW) and high level waste (HLW) in the UK is based on a multi-barrier Geological Disposal Facility (GDF) [1]. In one of the concepts under consideration for geological disposal of ILW, waste will be conditioned (e.g. by encapsulation with a cementitious grout), packaged in steel or concrete containers and placed in vaults excavated deep underground in a higher strength fractured rock. The vaults will be backfilled with a cement-based material, the NRVB (Nirex Reference Vault Backfill), which was specifically designed for this purpose [2].

The main function of the backfill is to provide a chemical barrier to radionuclide release to the far field [2]. For this purpose, the NRVB has an important role as an engineered barrier to achieve the necessary degree of long-term waste isolation and containment for the GDF. This cementitious backfill material has been specified to fulfill a number of benefits [2]:

- Long-term maintenance of alkaline porewater chemistry to suppress dissolved concentrations of many important radionuclides. The NRVB can chemically condition the groundwater to high pH for long-time scales;
- Long-term maintenance of a high active-surface-area for sorption of key radionuclides, mainly due to the calcium silicate hydrate (C-S-H) formed during the hydration of cement. This amorphous cement hydrate mineral is highly porous and can provide a very large surface area onto which many key radionuclides would sorb;
- Relatively high permeability and porosity to ensure homogeneous chemical conditions and to allow the escape of gas generated by chemical reactions within the repository;
- Long-term reactivity with carbon dioxide. NRVB will remove carbonates from inflowing groundwater and also non-active and $^{14}$C-containing $CO_2$ produced from the degradation of particular radioactive wastes, such as graphite, cellulose and irradiated metals, by forming low solubility carbonates;
- Possibility for reversibility / retrievability due to the low strength of NRVB, which facilitate the possibility of re-excavation of the vault to gain access to or remove waste packages [3, 4].

We here present a review of the literature pertaining to the NRVB, detailing the current understanding of the characteristics and properties relevant to its use as a backfill material in a UK GDF constructed in high strength rock.

**Composition and Chemical Analysis**

The NRVB is a high porosity cement composed of Portland cement (CEM I 52 5N), hydrated lime (calcium hydroxide, $Ca(OH)_2$) and limestone flour (calcium carbonate, $CaCO_3$). The target formulation for this material is: 450 kg m$^{-3}$ Portland Cement (PC), 170 kg m$^{-3}$ hydrated lime, 495 kg

m$^{-3}$ limestone flour and 615 kg m$^{-3}$ water; water / cement ratio of 1.37 and a water / solids ratio of 0.55, by mass [2].

When in contact with water, the hydration of PC occurs forming a mixture of mineral phases that provides the main properties of this cementitious backfill. The products from this reaction are calcium silicate hydrate ($3CaO \cdot 2SiO_2 \cdot 4H_2O$ or C-S-H), calcium hydroxide (also known as portlandite, $Ca(OH)_2$ or CH), ettringite ($Ca_6Al_2(SO_4)_3(OH)_{12} \cdot 26H_2O$ or $C_6A\bar{S}_3H_{32}$) and monosulphate aluminate hydrate ($Ca_4Al_2SO_4 \cdot 6H_2O$ or $C_4A\bar{S}H_{12}$) [1, 2, 5, 6]. C-S-H and CH are considered to be the most significant cement hydrate phases, because they are expected to provide the majority of the buffering capacity [2]. According to a model based on the mineral assemblages (at short-term (early ageing) and high temperature (80 °C)) studied by [7], the initial mineralogy (28 days of curing) of NRVB can be presented as:

*Table 2.9.1.1. Short-term high temperature model (80 ºC) (adapted from [7]).*

| Component | Abbreviation | Content in dry NRVB (mol m$^{-3}$) |
|---|---|---|
| Portlandite | CH | 3704 |
| Calcium silicate hydrate | C-S-H | 758 |
| Hydrogarnet | $C_3AH_6$ | 311 |
| Calcite | $CaCO_3$ | 4950 |

Figure 2.9.1.1 shows X-ray diffraction (XRD) patterns from fresh NRVB and NRVB cured for 4 months and 3 years [8]. The fresh NRVB is dominated by calcite, whereas in cured NRVB (both 4 months and 3 years) the phase assemblage is dominated by portlandite, with also a significant calcite contribution. These analyses do not identify C-S-H, because C-S-H, and possibly other hydrated products, may exist in the form of amorphous rather crystalline structures [9], hence no crystalline diffraction peak is observed.
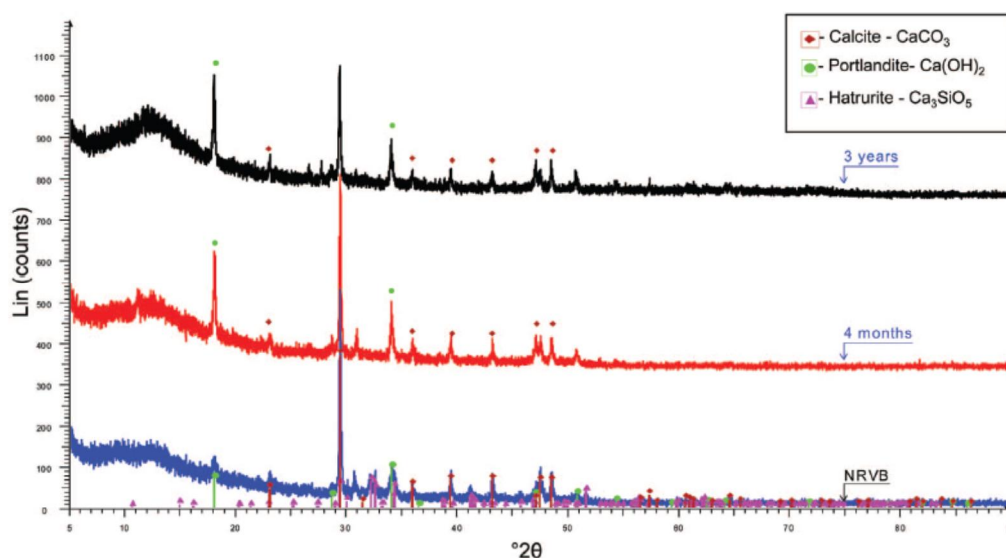


*Figure 2.9.1.1. XRD spectra of fresh NRVB powder, NRVB after 4-months curing and NRVB after 3-years curing (from [8]).*

Figure 2.9.1.2 shows the relationship between the temperature and weight loss of the NRVB when heated to 1000 °C, using differential thermal analysis (TGA) and derivative thermogravimetric

analysis [9]. The peak identified at 130 ℃ is attributed to the loss of chemically bound water in C-S-H. Between 400 to 460 °C, a peak related to the dehydration of calcium hydroxide is observed [9]. A third peak, at 650 to 770 °C, is attributed to the weight loss due to the decomposition of $CaCO_3$ and the consequent release of $CO_2$ [9].
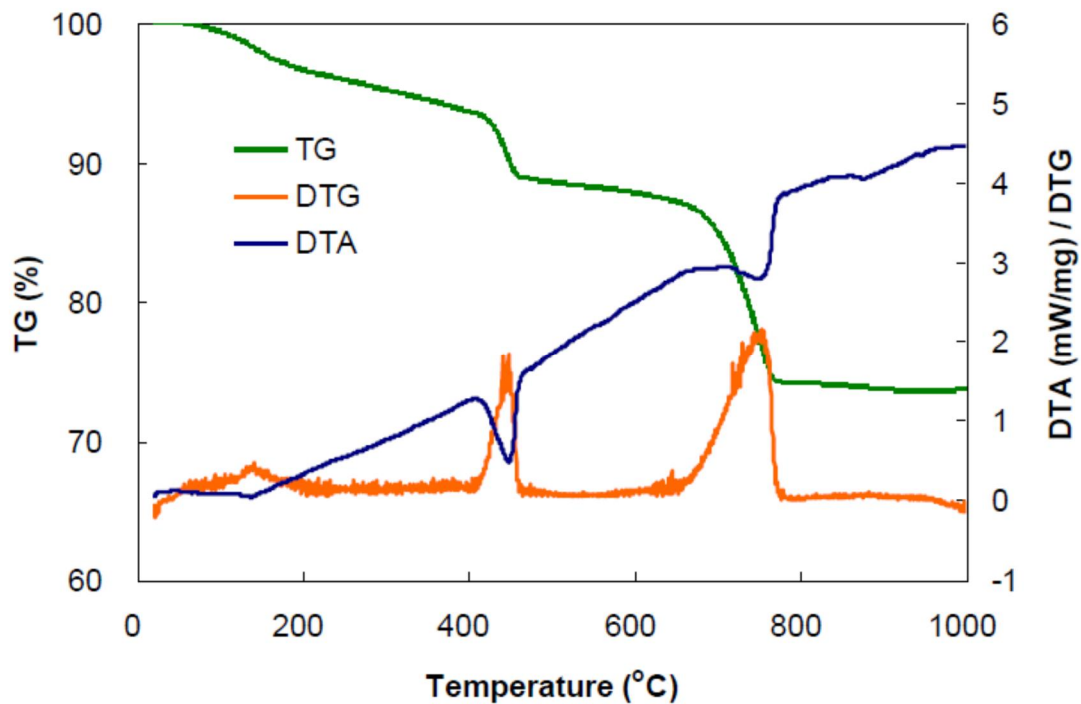


*Figure 2.9.1.2. TG/DTA/DTG curves of fresh NRVB (from [9]).*

**Properties**

The general properties of NRVB, summarized by [2, 10] are detailed in Table 2.9.1.2.

*Table 2.9.1.2. NRVB properties (adapted from [2, 10]).*

| Property | Measured value |
|---|---|
| Bleed (standard 100mm high column and 900 mm column) | 1.7% |
| Adiabatic temperature rise | ± 40 ℃ |
| Setting time | Initial - 4 hours<br>Final - 4 hours 50 minutes |
| Density (100 mm cubes) | Saturated - 1731 kg m$^{-3}$<br>Oven dried - 1095 kg m$^{-3}$ |
| Compressive strength | 7 days - 4.95 MPa<br>28 days - 5.95 MPa<br>90 days - 6.26 MPa |
| Flow time | Initial - 12.0 seconds<br>At 1 hour - 14.0 seconds |
| Gas permeability | Dry - 2 x 10$^{-15}$ m$^2$<br>Saturated - 5 x 10$^{-17}$ m$^2$ |
| Water permeability | 1 x 10$^{-16}$ m$^2$ |

It is clear that NRVB is a very porous cement that allows: gas migration; high alkalinity for chemical conditioning; low bleed and high fluidity for good void filling; and relatively low strength to facilitate the possibility of re-excavation of the vault to gain access to or remove waste packages, if required [2]. The literature pertaining to the key mechanical properties of NRVB are detailed in the following section.

*Strength (compressive strength)*

The compressive strength of NRVB is gained mostly in the first 7 days of curing, with a final value of about 4.95 MPa [2]. After this time, the compressive strength increases a small amount from ~ 5.95 MPa to 6.26 MPa from 28 to 90 days.

Since the repository operating temperatures will be higher than the 20 °C used for standard cement curing, studies have been performed to assess the effect of elevated temperature curing on strength [2]. Results showed that by increasing the temperature of curing there is a reduction in the strength, for example after 28 days of curing at 90 °C the strength was about half the strength achieved at 30 °C [2]. Similar results have been obtained with Portland-limestone cement (PLC), where the increase of the temperature influences negatively compressive strength [10, 11].

This relatively low strength of NRVB, for example compared to a BFS/PC grout, which has a compressive strength (depending on the proportion of BFS (between 10% and 35%) and PC used) between 26 and 32 MPa (at 7 days of curing), approximately 40 MPa (at 28 days of curing) and between 44 and 51 MPa (at 90 days of curing) [12], is to facilitate the possibility of re-excavation of the vault to gain access to or remove waste packages, if necessary [13]. This was identified as a stakeholder requirement for the siting of a geological disposal facility [3].

*Porosity*

NRVB was developed to be highly porous. High porosity is advantageous for the following purposes [2]:

- Allows the diffusion of any gaseous discharge from the waste packages (e.g. $H_2$, $CO_2$ or $CH_4$ gas), that would otherwise build up and pressurize the geological disposal facility vault;
- Allows the ingress of groundwater, leading to rapid saturation. Under these conditions, the chemical buffering capacity of the backfill will be initiated due to dissolution of the cement phases by groundwater. Additionally, water will begin to corrode the steel waste containers, leading to hydrogen production and the onset of reducing conditions.
- The high surface area afforded by such high porosity gives rise to a large surface area capable of sorbing radionuclide species, as discussed in Section 4.

Mercury intrusion porosimetry for large pores and nitrogen desorption for small pores was used to determine a fractional porosity of approximately 0.55 [2,14]. However, as stated by Bamforth et al. [15], these measurements involve drying samples, which tends to increase the porosity by generating capillary stress, cement hydrates (ettringite, AFm, C-S-H) desiccation and potential microcrack generation in relationship with internal thermohydric stress [16], and therefore some uncertainty in the porosity measurement may be expected; this is unlikely to significantly influence the post closure safety case [14]. It is not currently well understood how interaction of NRVB with groundwater, which may induce precipitation of phases throughout the grout matrix, may influence the porosity.

*Permeability*

The NRVB permeability coefficient is approximately $1 \times 10^{-16}$ m$^2$ [2]. This value was obtained in uncracked backfill by monitoring inflow and outflow rates until they reached a steady state (reported on the basis of an unspecified testing method). Because cracks may develop as a result of plastic settlement, early-age thermal contraction and expansion of the waste packages (corrosion), and they contribute to the effective permeability, a value for cracked NRVB of about $4 \times 10^{-13}$ m$^2$ has been estimated [15]. Consequently, groundwater may flow through the cracks.

*Gas Permeability*

After closure, the formation of gases is expected to occur. These gases can be generated by different mechanisms: i) Magnox spent fuel cladding (a Mg metal alloy) will generate hydrogen gas upon contact with water; ii) under anaerobic conditions, uranium metal and steels will corrode to produce hydrogen; iii) microbial degradation of organic compounds may generate methane and carbon dioxide and; iv) radiolysis of water will lead to the generation of hydrogen and oxygen [17].

One of the requirements for NRVB is that the permeability should be sufficient to allow gas movement without significant over-pressurisation and cracking [2]. Harris and colleagues [17] studied the gas permeability coefficients for argon and helium in a membrane of NRVB 20 mm thick (average pressure of 100 kPa), and obtained a permeability coefficient of approximately $2 \times 10^{-15}$ m$^2$ in dry conditions and $5 \times 10^{-17}$ m$^2$ in saturated grout. It was also possible to conclude that the NRVB is able to release gas in a sufficient rate without generating cracks [17].

*Cracking*

The formation of cracks in the backfill material could influence the post-closure performance, since they can influence the flow of groundwater through the repository (as stated above), effect the chemistry of the pore water in the cracks, and impact upon the transport of radionuclides in solution and the migration of gases [18].

When the tensile strain exceeds the tensile strain capacity of the material, cracking occurs [2]. The cracking of NRVB may occur soon after backfill placement and as the backfill ages. The processes by which the cracks are formed include:

- Differential movement between backfill and waste packages or vault walls, where backfill strains would arise from changes in temperature, moisture content, etc;
- Internal pressures from the expansive corrosion of waste and containers or from gas generated by metal corrosion or organic waste decomposition;
- The precipitation of minerals such as magnesium hydroxide (or brucite) (formed by interactions between groundwater or other components of the repository and the NRVB), within the backfill porosity and the dissolution of calcium hydroxide and C-S-H minerals (although this may also block cracks).

The mechanisms of crack formation include plastic shrinkage cracking, plastic (differential) settlement cracking, and thermal cracking [19]. The former occurs when the water is evaporated from the surface more quickly than the rate of bleed water arrival. When there are different depths of backfill adjacent to each other at the top of a waste package, this produces a plastic settlement cracking. Also, when there are changes in temperature this can create thermal expansion and contraction and, potentially, strain that could cause thermal cracking. These changes in temperature may be caused by the heat generated by the cement hydration reaction in the NRVB and by the radiogenic heat produced by radioactive decay of the radionuclides in the waste packages [19].

Backfill separation from the vault walls may be a consequence of the chemical and thermal shrinkage. This gap may provide a flow-path for the groundwater to bypass the waste, and reduce the likely transport of radionuclides out of the waste [19].

*Sorption Capacity*

The primary function of NRVB is to chemically condition the environment of the near field. This is achieved by maintaining a high pH and establishing reducing conditions, produced by the corrosion of metals in the wastes and containers, which minimizes the solubility of many radionuclides present in the waste. The backfill also provides a high sorption capacity that, together with the limitation of solubility, reduces the mobility of radionuclides [8, 20–22].

To produce a near field pH of 10.5 or greater, and a reducing redox potential determined by the iron-uranium redox couple, it is necessary that the chemical condition is dominated by the dissolution of the NRVB, the corrosion of iron and the presence of uranium oxides in the waste. With these conditions, the thermodynamically-stable solid phases will be predominantly oxides or hydroxides, which for many radionuclides are relatively insoluble [2, 13].

There are two processes for the removal of dissolved chemical species from a solution, namely precipitation (including substitution in existing solids) and sorption [22]. Precipitation requires the formation of new solids, where the chemical species removed from solution are transferred. This occurs when the concentration of solute species reaches saturation or supersaturation with respect to the relevant solid phase, so radionuclides that are present in the waste as soluble chemical compounds will react with the high pH water to form oxides and hydroxides (relatively insoluble). This will cause the precipitation of radionuclides from solution, resulting in a reduction of the transport of radionuclides in groundwater [13]. Sorption, the binding of soluble chemical species to solid surface, includes all the processes that can retard the migration of aqueous species by reducing the apparent concentration in solution. These include two processes that can operate simultaneously: absorption and adsorption, the latter of which can be either chemical or physical [2]. NRVB has a high internal surface area of about $2.8 \times 10^4$ $m^2$ $kg^{-1}$ for sorption [2].

The main elements that are affected by the chemical containment of NRVB are the actinide elements, such as thorium, uranium, plutonium, and others, and other metallic elements such as nickel, zirconium and tin [13]. Other long-lived, non-sorbing radionuclides such as iodine-129 and chlorine-36 may be partially retained by NRVB, however technetium-99 sorption occurs only when anaerobic conditions prevail [8, 14, 23].

Of the cement hydration products, the phase that contributes significantly to the cation sorption capacity of NRVB is C-S-H gel, because it has a large specific surface area comprised of acidic silanol sites (Si-OH) where most of the radionuclides bind [24, 25]. However, because the silanol surface is modified by sorption of calcium ions present in the pore water (concentration controlled by the Ca/Si ratio of NRVB), dissolved cationic radionuclides compete with the calcium ions in solution for silanol sites [2].

Several studies have been made to access the sorption capacity of NRVB, and three techniques were used: batch-sorption, through-diffusion and pore-expression [2]. In the batch-sorption technique samples of NRVB are crushed and equilibrated with solutions of sorbing radionuclide, and the distribution coefficient, $R_d$, is obtained (Equation 1):

$$R_d = V (C_0 - C_t) / M C_t \text{ \textit{(Equation 1.)}}$$

Where V is the volume of solution, M is the mass of solid, $C_0$ is the initial concentration of the radioelement in the solution and $C_t$ is the final concentration of the element in solution at the end of the experiment. The main advantage of the batch-sorption method is the measurement of strongly-sorbing species and this has been extensively used to obtain data for a range of radionuclides and materials [2]. The disadvantages are related to the fact that the samples are crushed, giving a modified surface area, and also the low solid to liquid ratios. However, some authors argue that because NRVB is a highly porous material, variations in particle size are found to have little effect [2].

In the through-diffusion test, a disc of NRVB separates two reservoirs; one containing a solution of the radionuclide of interest, and the other containing a radionuclide-free solution. The diffusion and sorption properties of the radionuclide can be obtained from analysis of the breakthrough curve, i.e. the time and rate at which radionuclide builds up in the second reservoir. For some strongly-sorbing radionuclides it can take many years to achieve breakthrough. In this case, sorption parameters can be obtained from the concentration profile in the disc [2]. This method has the beneficial of being simple, robust, cost-effective and provided reproducible results [21].

In the pore-expression method, small cylinders of cured NRVB are used for the extraction and analysis of pore fluid using a high force hydraulic press. This technique has the advantage of allowing data to be obtained at realistic water-to-solid ratios and is suitable for both weak and strongly sorbing species.

Felipe-Sotelo et al. [8] studied the sorption behavior of $I^-$, $Cs^+$, $Ni^{2+}$, $Eu^{3+}$, $Th^{4+}$ and $UO_2^{2+}$ on NRVB, at a pH of 12.8, by using batch sorption experiments. It was possible to observe that $I^-$ and $Cs^+$ had low sorption onto NRVB, and in the case of $Th^{4+}$ and $UO_2^{2+}$ significant concentrations were retained in this cementitious backfill. For the uptake of $Ni^{2+}$, it was postulated that this was primarily due to solubility related factors, and not by sorption alone. It was observed that for Ni and Eu, the limestone flour proportion of NRVB showed the highest partition coefficient, while in the case of Cs, Th and U it was the Portland cement [8].

One important aspect to be considered when studying the sorption capacity of NRVB is the ageing of this material, because it is known that cementitious materials alter with time [2, 20, 26]. Several factors can contribute to these alterations: the evolution of the amorphous phases to more stable crystalline forms, as the case of C-S-H; the elevated temperatures observed post closure, also known as hydrothermal ageing; and interactions with groundwater, resulting, for example, in the dissolution of portlandite and C-S-H [20]. An experiment was carried out by Baston et al. [20] to assess the main changes in the composition and characteristics of aged NRVB. X-ray diffraction analysis of aged NRVB (Figure 2.9.1.3) revealed the absence of portlandite. Despite this deviation from un-aged NRVB, little alteration in the sorption of uranium, neptunium, zirconium and tin onto NRVB was observed. The authors contributed this to a high sorption capacity of C-S-H, even after conversion from a gel to more crystalline forms [20].
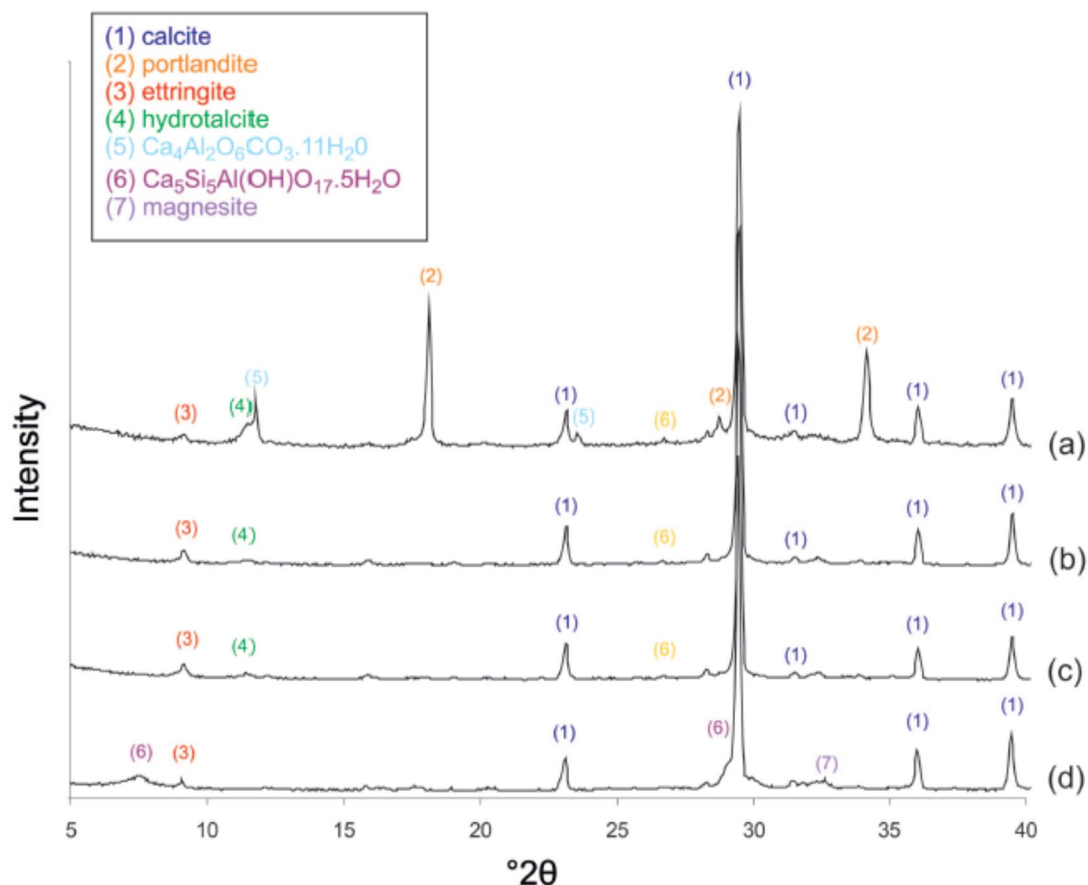
*Figure 2.9.1.3. X-ray diffractograms for (a) untreated NRVB; (b) leached for 541 days; (c) NRVB leached for 1272 days; and (d) NRVB subjected to leaching followed by hydrothermal treatment, with principal peaks indicated (from Baston et al. [20]).*

Some authors consider that radionuclides sorbed onto backfill may be slowly mineralized, and with this incorporated in solids with lower solubility phases, as the backfill ages. This process may provide an irreversible mechanism of retention of radionuclides but has not been fully investigated in NRVB over long time scales or in the presence of groundwater species [2].

*Buffering Capacity*

To achieve chemical containment of long-lived radionuclides in the waste, NRVB has the capacity to buffer repository porewater at high alkalinity for a long period of time [2]. In the beginning, the main components of NRVB are expected to be alkali (i.e. Na, K) hydroxides/sulfates; portlandite $Ca(OH)_2$; calcium-silicate-hydrate (C-S-H) gels; calcium carbonate $CaCO_3$; and hydrated calcium aluminates [1, 2, 5–7]. The total calcium hydroxide content of the NRVB (from lime additive and PC) is approximately 4700 moles $m^{-1}$. The initial porewater pH will be of about 13.5 caused by the dissolution of the more soluble sodium and potassium hydroxides. After the removal of the alkali metal salts, buffering will continue by the dissolution of portlandite. A solution saturated with respect to portlandite is formed with a pH of about 12.5 at 25 °C, equivalent to a hydroxyl molality of 0.03 mol $kg^{-1}$ water and a total calcium concentration of about 0.02 mol $kg^{-1}$ [2]. After the calcium hydroxide has been exhausted, pH buffering will occur by the incongruent dissolution of C-S-H phases with relatively high calcium/silicon molar ratios (Ca/Si) of ~1.5. From this, dissolution will result in the release of calcium and hydroxide ions, thus lowering the Ca/Si ratio and reducing the pH value at which the water is buffered [6, 29].

The timescale and capacity for buffering by portlandite is dependent on the initial quantity of NRVB in a vault, the amount of the calcium hydroxide-content of the NRVB consumed by reaction with wasteforms and the rate of groundwater leaching [2]. Also, the quantity of C-S-H gel that will be available to buffer porewater pH will depend on the quantity of backfill material used to achieve buffering by calcium hydroxide under a given set of conditions.

*Influence of groundwater on buffering capacity*

High pH cementitious backfill materials are expected to strongly influence the chemistry of the near field. The evolution of the chemistry of these materials in a GDF is mainly dependent on the geochemistry and flow rate of the groundwater [10, 28].

Groundwater is expected to react with NRVB and the intermediate level wastes it encapsulates, which contain magnesium, sulfur and aluminum. These interactions may result in the formation of some secondary minerals, such as calcite, brucite, ettringite, hydrogarnet, $CO_3$-hydrotalcite and Al-monocarbonate [1, 6]. Such secondary minerals could continue to buffer the porewater at pH values of 10 to 12 [6] and are expected to precipitate in the NRVB porosity and subsequently become mineralized or re-dissolved [2]. The main consequence of the precipitation of secondary phases is the reduction in the NRVB porosity in the region where groundwater flows into a vault. This is particularly the case for high carbonate-containing ground waters, due to the precipitation of calcite and other Mg/Ca bearing phases. The result is that subsequent inflow, and gas migration pathways, will be reduced [2]. It is important to emphasize that these precipitation reactions will depend on the composition and concentration of the groundwater solutes [28], which will depend on the specific location of the GDF (e.g. in a clay, granite or evaporite host rock).

Numerous modeling studies have been performed to understand the pH evolution on leaching NRVB [1]. Figure 2.9.1.4 describes one such study [1], which gives the four sequential stages of cement dissolution.
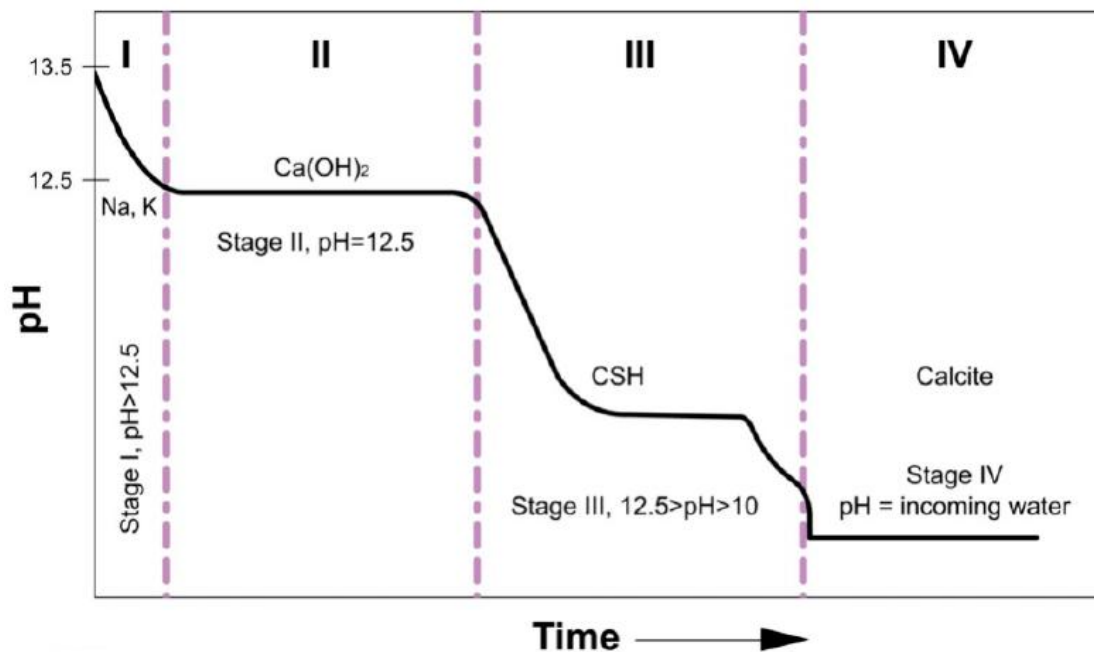


*Figure 2.9.1.4. Schematic representation of the evolution of pH at 25 °C in cement pore fluid as a result of groundwater leaching (from [1]).*

A series of accelerated leach testing experiments have been performed to demonstrate the ability of NRVB to buffer simulated groundwater [30]. In these experiments, it was possible to observe the removal of all calcium hydroxide, and consequent buffering controlled by the dissolution of the C-S-H gel, at a pH of about 11. During the test, the porosity was measured and an increase of about 20% was observed, but the sample remained intact. A surface coating of brucite (magnesium hydroxide) was formed at the region of inflow, which reduced the permeability coefficient by about an order of magnitude [2].

A long-term leaching study (run for up to two years) was carried out to provide data on the evolution of pH during extensive leaching of the NRVB [5]. Three different leachant compositions were used (deionized water, 0.1 M and 1 M NaCl solutions). In this study it was found that there is sufficient alkaline buffering capacity present to maintain the leachate above pH 10 for 1000 cumulative specimen volumes for all three leachants. It was also observed that the trend of reduction in pH from the pH 12.5–12.6 plateau was in the order of 1 M NaCl > 0.1 M NaCl > deionized water. This indicates that chloride will increase the rate of leaching of the calcium within cementitious materials.

*NRVB Carbonation*

In GDF conditions, carbonation of the NRVB may occur at several stages: during backfilling at the end of the operational phase of a repository (NRVB could react with carbon dioxide in the air of the vaults); during the post-closure phase when the repository has re-saturated and alkaline degradation of organic material in the waste could produce carbon dioxide; and also during this last phase when carbon dioxide or carbonate species could be introduced in inflowing groundwater [2, 19].

For cement carbonation to occur, carbon dioxide must be dissolved in water and react with high alkalinity components present in NRVB, i.e. products of cement hydration (for example, calcium hydroxide, calcium silicate hydrate and various calcium aluminate hydrate or ferro-aluminate hydrates). From this reaction, the products formed will be calcium carbonate, silica gel and hydrated aluminium and iron oxides, while sulfate will convert to gypsum after complete carbonation [9, 31]. The main effects of the carbonation are: the reduction in the buffering capacity (i.e. in the pH) due to the consumption of calcium hydroxide and alterations to the physical properties by decreasing the pore volume and permeability [9, 32]. Because there is a precipitation of the $CaCO_3$ in the pore structure, this will increase in volume and lead to structural changes, including changes to the density and porosity (Figure 2.9.1.4) [9, 31]. In Figure 2.9.1.5, VOI (Volume-of-Interest) images from samples of NRVB that are carbonated and non-carbonated are shown, with the respective differences in the fraction of pores. It can be observed that the carbonated samples presented a reduced porosity compared to the non-carbonated samples, associated with the precipitation of calcium carbonates [31].
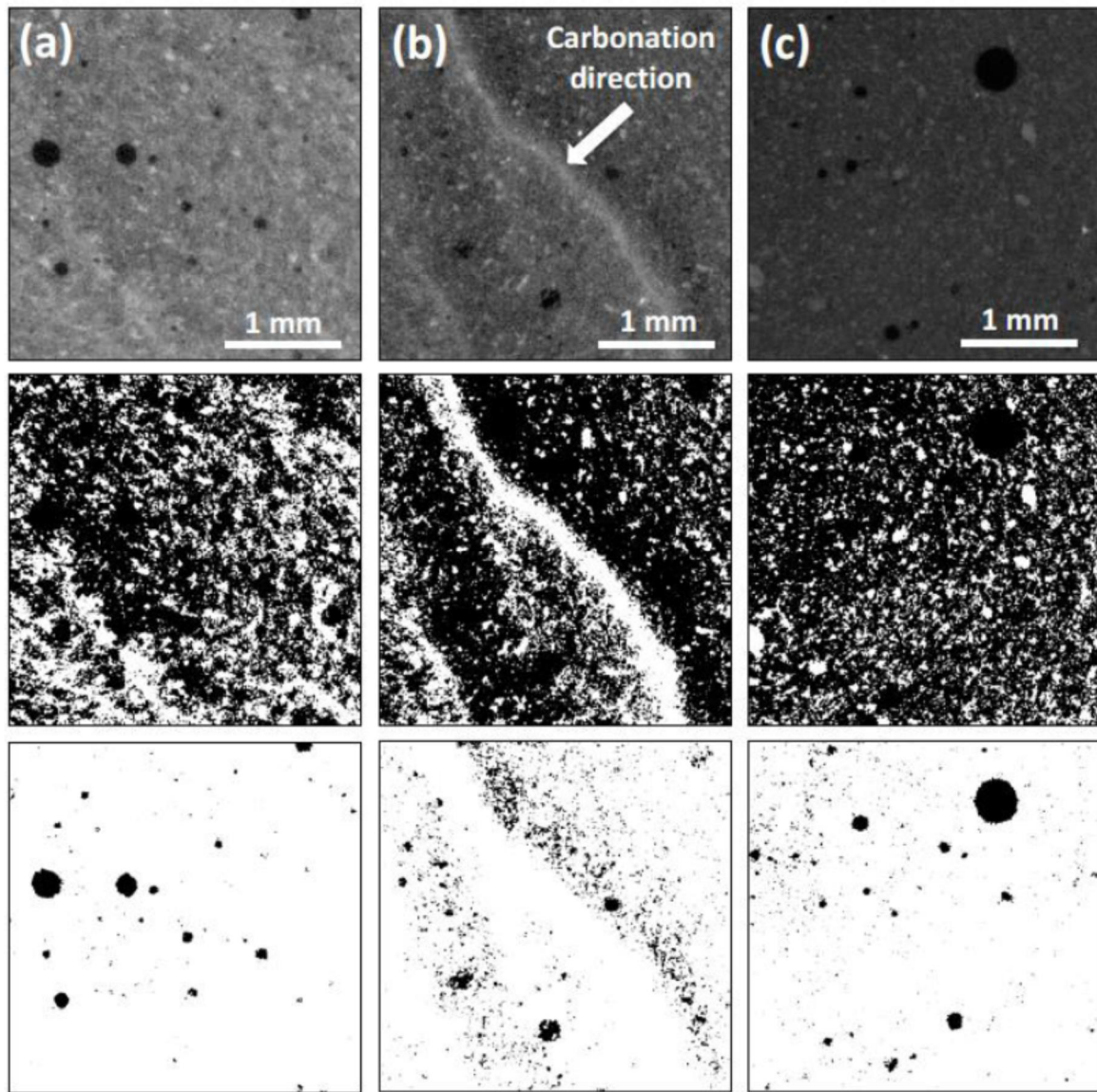
*Figure 2.9.1.5. Selected VOI (a) carbonated sample, (b) partially carbonated sample, and (c) non-carbonated sample. Top image: grey scale image, centre image: segmented into solid (white) and pore (black) regions, and bottom image: segmented into large pores (black) (from Heyes et al. [31]).*

Some authors have observed that carbonation can also be associated with crack sealing, due to the precipitation of $CaCO_3$ [2]. It was also found that the gas permeability is reduced by half on carbonation, but it was concluded that this will not adversely affect the transport of gases and fluids through NRVB [32]. One advantage of carbonation is that the $^{14}CO_2$ (g) generated will be absorbed by the calcium component of the cement, thereby preventing the release of $^{14}CO_2$ as a gas phase to the far field or the biosphere [9].

Because of the changes in the physical and chemical properties of the cementitious backfill, some studies have been carried out to understand the extent of carbonation in NRVB. The main conclusions were: NRVB retards the migration of any released $CO_2$; carbonation resulted in consumption of portlandite; and XRD results showed that the hydrated cement phases were completely replaced by calcium carbonate within the main region of carbonation [9, 31], as can be

seen in Figure 2.9.1.6. When carbonation occurs, the peaks corresponding to calcium hydroxide are no longer visible and the intensity of the peaks corresponding to calcium carbonate increase [9].
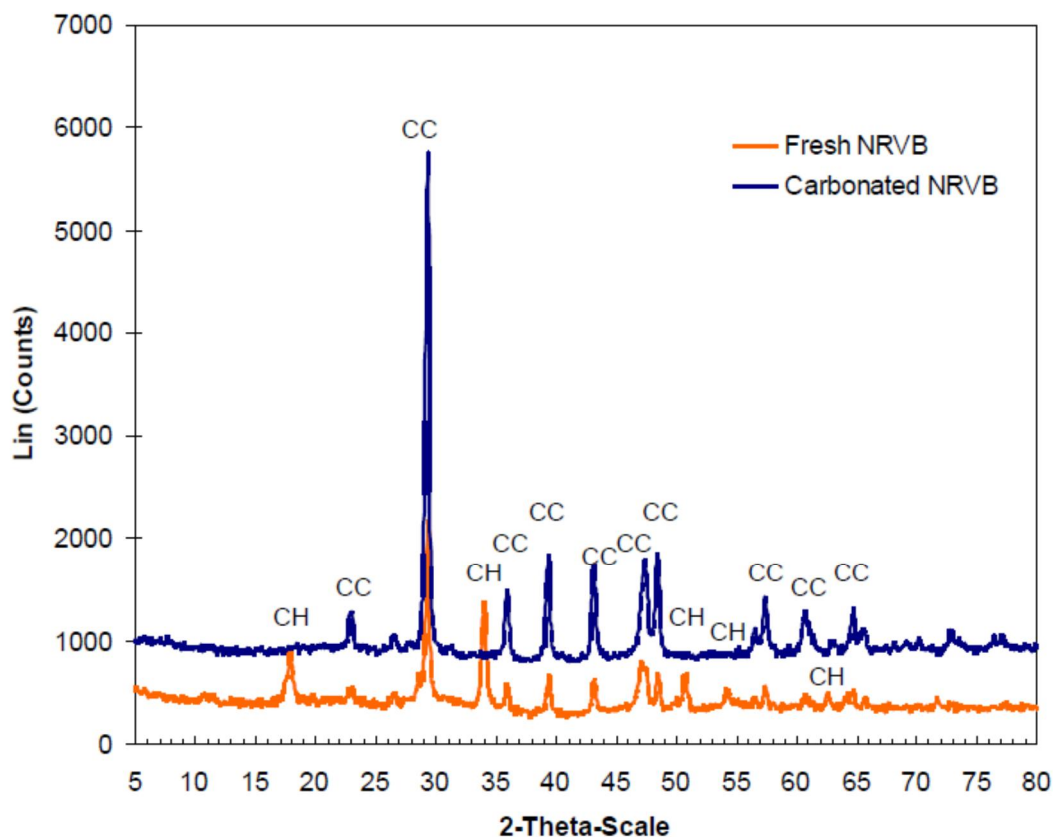


*Figure 2.9.1.6. XRD diffractograms of fresh NRVB and carbonated NRVB; CC represents calcium carbonated, and CH represents calcium hydroxide (from [9]).*

C-S-H can also be affected during carbonation. Morandeau et al. [33] show that a decalcification of C-S-H occurs in the presence of $CO_2$. This will consequently lead to a smaller molar volume and smaller Ca/Si ratio of C-S-H when compared to non-carbonated C-S-H. Moreover, C-S-H does not release physical water during carbonation, unlike portlandite. This will result in a highly hydrated silica gel [33].

**Summary and Conclusions**

For one of the UK GDF conceptual scenarios, intermediate level radioactive waste would be backfilled by a cementitious material, called NRVB. NRVB is composed of Portland cement, hydrated lime and limestone flour. This composition contributes to its specific properties, including high porosity that allows the inflow of porewater and gas migration, low bleed and high fluidity for good void filling, and relatively low strength to facilitate the possibility of re-excavation of the vault to gain access to or remove waste packages, if necessary.

The primary function of NRVB is to maintain a high pH and reducing conditions that minimises the solubility and transport of many radionuclides, and also to provide a high sorption capacity. C-S-H is the by-product of cement hydration that contributes significantly to the sorption capacity of NRVB, since it has a large specific surface area where most of the radionuclides bind (Si-OH). Some factors can affect the capacity of sorption of NRVB, for example, ageing, the presence of cellulose degradation products and colloids, the inflow of groundwater, and carbonation.

A number of studies have been performed to understand how these factors can influence the long-term capacity of NRVB to physically and chemically condition the radioactive waste, however many of these are geochemical models with little experimental verification. It is recognised that modeling is important to comprehend what happens in a long time scale (most of the times difficult to replicate in a laboratory scale), however further experiments are required to obtain more precise and confident data that can support the modeling findings, particularly with respect to the influence of groundwater chemistry on the microstructure and buffering capacity.

In the Cebama project, we aim to further our understanding of the NRVB material through the following tasks:

1. Develop a mechanistic understanding of the processes governing interfacial groundwater/NRVB reactions under a variety of relevant conditions. Influence of such reactions on the physical properties of cement will be the main focus.
2. Develop a quantitative understanding of how interfacial cement alteration affects microstructure under a variety of relevant groundwater conditions, including an interpretation of changes to diffusive transport.

## Acknowledgements

## References

[1] Nuclear Decommissioning Authority, Geological Disposal: Near-Field Evolution Status Report, 2010. Report no. NDA/RWMD/033.

[2] A.J. Francis, R. Cather, I.G. Crossland, Nirex Safety Assessment Research Programme: Development of the Nirex Reference Vault Backfill; Report on Current Status in 1994, (1997). Report no: S/97/014.

[3] Nuclear Decommissioning Authority, Retrievability of Waste Emplaced in a Geological Disposal Facility Retrievability of Waste Emplaced in a Geological, 2010. Doc No RWMDPP03 December.

[4] Nirex, Context Note 4.1: Retrievability, United Kingdom Niex Ltd. (2005). Number: 484424 December.

[5] E.J. Butcher, J. Borwick, N. Collier, S.J. Williams, Long term leachate evolution during flow-through leaching of a vault backfill (NRVB), Mineral. Mag. 76 (2012) 3023–3031.

[6] A.R. Hoch, G.M.N. Baston, F.P. Glasser, F.M.I. Hunter, V. Smith, Modelling evolution in the near field of a cementitious repository, Mineral. Mag. 76 (2012) 3055–3069.

[7] T.R. Holland, W.M. Tearle, Serco Assurance A Review of NRVB Mineralogy, Serco Assur. SERCO/ERRA (2003). SERCO/ERRA-0455 January.

[8] M. Felipe-Sotelo, J. Hinchliff, N. Evans, P. Warwick, D. Read, Sorption of radionuclides to a cementitious backfill material under near-field conditions, Mineral. Mag. 76 (2012) 3401–3410.

[9] J. Sun, PhD Thesis, Carbonation kinetics of cementitious materials used in the geological disposal of radioactive waste, 2011. http://discovery.ucl.ac.uk/1306875/.

[10] B. Lothenbach, F. Winnefeld, C. Alder, E. Wieland, P. Lunk, Effect of temperature on the pore solution, microstructure and hydration products of Portland cement pastes, Cem. Concr. Res. 37 (2007) 483–491.

[11] B. Lothenbach, T. Matschei, G. Möschner, F.P. Glasser, Thermodynamic modelling of the effect of temperature on the hydration and porosity of Portland cement, Cem. Concr. Res. 38 (2008) 1–18.

[12] G. Menéndez, V. Bonavetti, E.F. Irassar, Strength development of ternary blended cement with limestone filler and blast-furnace slag, Cem. Concr. Compos. 25 (2003) 61–67.

[13] I.G. Crossland, S.P. Vines, Why a cementitious repository, Nirex Rep. N/034. (2001).

[14] A.W. Harris, A.K. Nickerson, A.E.A. Technology, The Physical Properties of the Nirex Reference Vault Backfill, NSS/R335. (1997).

[15] P.B. Bamforth, G.M.N. Baston, J.A. Berry, F.P. Glasser, T.G. Heath, C.P. Jackson, et al., Cement materials for use as backfill, sealing and structural materials in geological disposal concepts. A review of current status, (2012) 1–235. SERCO/005125/001 Issue 3.

[16]    C. Gallé, Effect of drying on cement-based materials pore structure as identified by mercury porosimetry—a comparative study between oven-, vacuum-, and freeze-drying, Cem. Concr. Res. 33 (2001) 169–170.

[17]    A.W. Harris, A. Atkinson, P.A. Claisse, Transport of Gases in Concrete Barriers, Waste Manag. 12 (1992) 155–178.

[18]    B.T. Swift, P.B. Bamforth, A.R. Hoch, C.P. Jackson, D.A. Roberts, G.M.N. Baston, Cracking, Flow and Chemistry in NRVB Report to the NDA RWMD, Serco. (2010) 155. SERCO/TAS/000505/001 Issue 3.

[19]    I.G. Crossland, Cracking of the Nirex Reference Vault Backfill: A review of its Likely Occurence and Significance, NDA. (2007) 1–49. Report CCL/2007/1.

[20]    G.M.N. Baston, M.M. Cowper, T. a. Marshall, Sorption properties of aged cements, Mineral. Mag. 76 (2012) 3411–3423.

[21]    M. Felipe-Sotelo, J. Hinchliff, D. Drury, N.D.M. Evans, S. Williams, D. Read, Radial diffusion of radiocaesium and radioiodide through cementitious backfill, Phys. Chem. Earth, Parts A/B/C. 70-71 (2014) 60–70.

[22]    Nuclear Decommissioning Authority, Geological Disposal: Radionuclide Behaviour Status Report, 2010. NDA Report no. NDA/RWMD/034.

[23]    C.L. Corkhill, J.W. Bridge, X.C. Chen, P. Hillel, S.F. Thornton, M.E. Romero-Gonzalez, et al., Real-time gamma imaging of technetium transport through natural and engineered porous materials for radioactive waste disposal, Environ. Sci. Technol. 47 (2013) 13857–13864.

[24]    G. Baston, M.M. Cowper, T.A. Marshall, Sorption of Np , Zr and Sn onto Leached and Hydrothermally-aged NRVB Report to NDA RWMD, (2010). SERCO/TAS/002097/001 Issue 02.

[25]    S.Y. Hong, F.P. Glasser, Alkali sorption by C-S-H and C-A-S-H gels: Part II. Role of alumina, Cem. Concr. Res. 32 (2002) 1101–1111.

[26]    F.P. Glasser, J. Marchand, E. Samson, Durability of concrete - Degradation phenomena involving detrimental chemical reactions, Cem. Concr. Res. 38 (2008) 226–246.

[27]    G.M.N. Baston, a. P. Clacher, T.G. Heath, F.M.I. Hunter, V. Smith, S.W. Swanton, Calcium silicate hydrate (C-S-H) gel dissolution and pH buffering in a cementitious near field, Mineral. Mag. 76 (2012) 3045–3053.

[28]    C.S. Walker, S. Sutou, C. Oda, M. Mihara, A. Honda, Calcium silicate hydrate (C-S-H) gel solubility data and a discrete solid phase model at 25 °C based on two binary non-ideal solid solutions, Cem. Concr. Res. 79 (2016) 1–30.

[29]    A.W. Harris, M.C. Manning, W.M. Tearle, C.J. Tweed, Testing of models of the dissolution of cements - Leaching of synthetic CSH gels, Cem. Concr. Res. 32 (2002) 731–746.

[30]    A.W. Harris, A. Atkinson, V. Balek, K. Brodersen, G.B. Cole, A. Haworth, et al., The Performance of Cementitious Barriers in Repositories, Nucl. Sci. Technol. (1994). EUR 17643.

[31]    D.W. Heyes, E.J. Butcher, J. Borwick, A.E. Milodowski, L.P. Field, S.J. Kemp, et al., Demonstration of Carbonation of the NRVB, Natl. Nucl. Lab. 16 (2015). NNL (14) 13296 Issue 4.

[32]    G. Purser, A.E. Milodowski, J.F. Harrington, C.A. Rochelle, A. Butcher, D. Wagner, Modification to the Flow Properties of Repository Cement as a Result of Carbonation, Procedia Earth Planet. Sci. 7 (2013) 701–704.

[33]    A. Morandeau, M. Thiery, P. Dangla, Investigation of the carbonation mechanism of CH and C-S-H in terms of kinetics, microstructure changes and moisture properties, Cem. Concr. Res. 56 (2014) 153–170.

# 3  Research methods

## 3.1  Testing methods for water-concrete interaction characterization

*M.C. Alonso, J.L. Garcia-Calvo*

*CSIC High Research Council of Spain, Madrid, Spain*

**Leaching tests classification and selection criteria**

Numerous types of leaching tests have been developed in order to verify the stability and confinement of nuclear and hazardous wastes in construction materials [1–7]. Some tests methods are focused to the confinement ability of the cement paste to retain the waste [7-9], while others consider the leachability of cementitious materials in aqueous media [1, 10–14], focusing in studying the stability of hydrated solid phases to know their integrity under water contact [10, 15–23]. The characterisation of water concrete interaction using leaching tests have also devoted to study the kinetics of the leaching process and the mechanisms of concrete degradation that are involved in landfill [1, 7, 8, 10–13].

The appropriate selection of a testing method for characterisation of concrete performance under different waters implies to know two main aspects:

1) The type of scenario to simulate.
2) The reproducibility of the leaching mechanisms involved.

Several testing protocols exist and have demonstrated their capacity; however, the classification of leaching tests is a complex matter due to the wide number of parameters that influence the leaching process:

- With respect to the <u>leachant</u>: some factors include the type of water/concrete contact regime, frequency of renewal, pressure, temperature, pH and ionic composition of the leaching solution or the liquid/solid ratio.
- With respect to the <u>solid leaching sample:</u> the size and geometry of leaching material, the surface condition and porosity are important factors.
- Also the <u>field of application and the type of scenario</u> to reproduce real conditions affect the appropriate selection of the leaching test.

CEN/TC 292 [24] adopted a distinction of leaching methods in relation to the level of understanding needed in practice, of the type: a) basic characterisation tests, b) compliance tests, and 3) on-site verification tests. Another classification for laboratory leaching tests follow a division into three groups based on the type of the specimen [14]: 1) Extraction or Batch Extraction Tests/Acid Neutralisation Tests (ANT), 2) Leach Tests/Tank Water Test (TWT), and 3) Column Leach Tests/Running Water Test (RWT). The main characteristics of this classification are summarised in table 3.1.1. Besides other leaching tests based on the type of water interaction mechanism used have been more recently developed, also included in table 3.1.1, identified as: 4) Permeability/Percolation Tests and 5) Migration Tests.

The leachability of concretes (leaching kinetics) with respect to water aggression depends significantly on the convection and contact regime, (water/concrete), the water running velocity or the frequency of water renewal at the concrete surface. The Leach Test using [9] (Tank Water Test) is more aggressive in the first stages of contact but the Column Leach Tests with running water

leacheate more calcium at long-term [37, 41]. Besides, teaching mechanism may be altered due to the convection regime of the water in contact with the concrete surface [30–33].

*Table 3.1.1. Summary of the main characteristics of leaching tests types from the literature according with classification described.*

| Type of Leaching Tests | Waste form | Agita-tion | Leachant | Num. of extrac-tions | Leaching conditions | Expression of the results | Length | Objective |
|---|---|---|---|---|---|---|---|---|
| **Extraction or Batch extraction Tests/Acid Neutralisation Tests (ANT) [8, 25–34]** | Grounded/ Pulverised | YES | Acid orwater (control of pH) | One or more | Leaching is assumed to reach equilibrium by the end of one extraction period. The maximum, or saturated, leachate concentration | Leachate concentration or cumulative fraction of total mass leached. | Hours/ days | Accelerated, to simulate worst case of leaching conditions. |
| **Leach Tests/Tank Water Test (TWT) [1, 9, 10, 19–23, 35–37]** | Monolithic | NO | Deionised/ ionic water | One (static) | Leaching takes place under static hydraulic conditions. Low leaching rates and maximum leachate concentration | Flux or mass transfer parameter like the leaching rate Diffusivity | Weeks/ years | To simulate leaching under controlled conditions, short-term scenarios, in which the waste form is intact |
| | | | Deionised/ ionic water | Several (dyna-mic) | Non equilibrium conditions in which maximum saturation limits are not obtained and leaching rates are high | | | |
| **Column Leach Tests/Running Water Test (RWT) [21–24, 37–42]** | Grounded/ Monolithic | NO (Flow in co-lumn) | Deionised/ ionic water | Several | Local steady state (for up-flow test) | Leaching rate | Weeks/ years | Representative of field leaching conditions |
| **Permeability/ Percolation-Infiltration Tests [20, 40, 43–47]** | Monolithic | NO | Deionised/ ionic water | Several | Non equilibrium conditions | Water permeability coefficient Ion leached | Weeks/ years | Representative of field leaching conditions |
| **Migration Tests [48–57]** | Monolithic | NO | Deionised | one | Non equilibrium conditions | Ion leached | weeks | Accelerated to simulate worst-case leaching conditions |

As indicated above there is no agreement between the leaching method used concerning the regime of leachant/concrete contact but also no agreement exists in testing methodologies with the selection of leachant composition. For instance, tests using acid media as leachant agent are been employed [1, 7, 10, 30], also deionised water [10], or water with chlorides [47], or even bubbling of $CO_2$ through the demineralised water [4], that affects the leaching of Ca. Deionised water [10, 13] informs on the degradation stages, but in comparison with natural waters it may be considered too aggressive. Bubbling of $CO_2$ makes more representative the testing method, as this component usually is present in real conditions [1]. The lower pH of the $CO_2$-bubbling test provides a marked degree of acceleration. Besides, the leaching mechanism is affected due to the precipitation of calcite into the degraded zone [1, 37, 41]. Natural waters contain ionic species that may also affect

the leaching process, such as, $Ca^{+2}$, $Si^{+4}$, $Cl^-$, $SO_4^=$, even $Mg^{+2}$ and alkalis ($Na^+$, $K^+$) and also $HCO_3^-$. Obviously the hardness of the waters affects the leaching resistance of concretes [30–33, 47].

## Description and protocols of leaching tests

A more detailed information of the leaching tests protocols included in table I are described below.

*Extraction or batch extraction tests /Acid Neutralisation Tests (ANT) [8, 25–34]*

Batch extraction tests have been used to identify the processes involved in the leaching of the cement hydration phases [25–27, 31]. The leaching of cements pastes using this type of leaching test proceeds towards the characterisation of the different stages and plateaus of the pH involved in the process [31]. Therefore, the objective of extraction tests is to determine the maximum leachate concentrations under a given set of testing conditions.

This test type involves agitation of ground or pulverized waste forms in a leaching solution in a close system, as that shown in figure 1-left [30]. The leaching solution may be acidic, neutral or variable throughout the extraction test. The tests may involve one-time or multiple extractions. In either case, leaching is assumed to reach equilibrium by the end of one extraction period. A derivation from these tests is that the pH may be adjusted to a specific value in order to determine its influence on the release of the waste [10, 30]. The total acid or base neutralisation capacity of the waste is so determined.

The progressive neutralisation of the alkaline cement paste may be followed by an acid attack and the continuous measurement of the evolution of pH. It can be characterised by the milliequivalents of acid ($H_3O^+$) needed to get the particular pH value, per gram of cement paste sample. The experimental procedure consisted of a batch test, figure 3.1.1-left [30]. Mixes are ground and sieved until a small particle size, less than 75 $\mu$m are recommended. The powder (S) is then mixed with the water (L) in a specific ratio, S/L = 1 is highly recommended [30], producing a homogeneous slurry. Accelerated neutralisation test is performed in this slurry by adding acid or even granitic water at a specified rate and stirring the sample vigorously to favour continuous mixture of the leachant and the sample to reach the equilibrium. A nitrogen flow can be also bubbled in the system to avoid carbonation [33, 34]. The leaching process can be interrupted at different stages and liquid and solid phase sampling can be taken at different pHs, corresponding to progressive degradation stages of cement paste. The solid part of the degraded cement paste is then freeze with acetone and ethanol and samples vacuum filtered to avoid further continuation of interaction with water processes [33]. Further analysis of the leachates and solid phases can then be carried out with Batch extraction tests.

The acid neutralisation capacity of various cements pastes have being determined in contact with different acidic media (sulphuric, chloric and nitric acids) [10, 30, 34] in powdered samples, differences in performance under a neutralisation test are shown in figure 3.1.1-right [30, 31, 33].
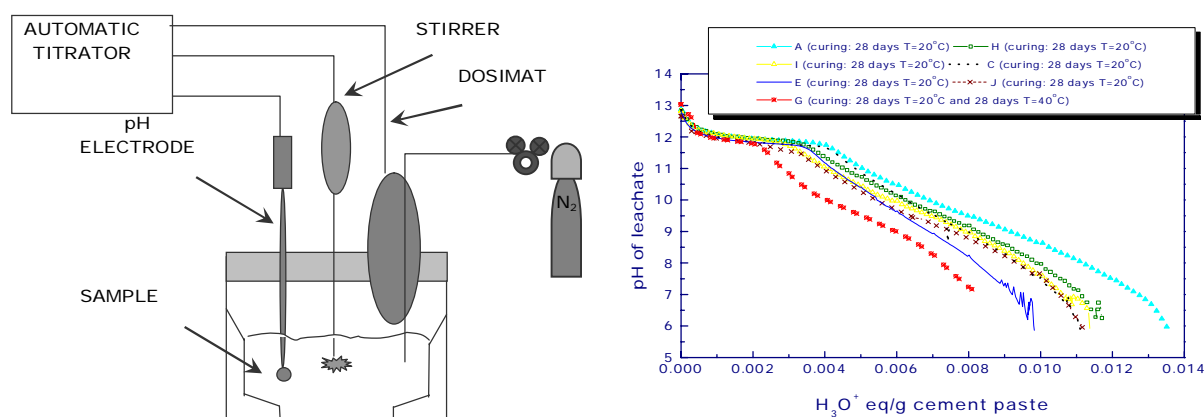
*Figure 3.1.1. Experimental set-up of a neutralisation test method and stages of acid neutralisation of different cement pastes, from [31].*

Respect to the type of acid to study the effect of decreasing pH (protonation) simulated of cement paste, in case of using $HNO_3$ as acid neutralisation media reactions between nitric acid and hydrated cement are based in the neutralisation of the cement alkalinity with formation of soluble calcium nitrate [30, 31, 33, 34]. For this reason, nitric acid is used to simulate the pH decrease due to the dilution processes that occur when groundwater diffuse into the concrete. $HNO_3$ has the advantage of forming soluble salts which simplifies the study of acid attack. Chemical effects on cement pastes due to the protonation by an acid will be:

1) Dissolution of minerals.
2) Precipitation of secondary alteration solid phases such of amorphous hydroxides or other.
3) Released by dissolution of crystalline hydrates.
4) Precipitation of insoluble solid phases.

The use of granitic water is interesting due to its realistic nature. In this case the degradation process is due to a combination of:

1) Dissolution of minerals.
2) Continued hydration (anhydrous clinker grains react with water forming more portlandite and CSH gel).
3) Carbonation and precipitation of calcite as the principal secondary alteration phase.

*The Leach Tests/Tank Water Tests (TWT) [1, 9, 10, 19–23, 35–37]*

The typical Leach Test or Tank Water Tests (TWT) involves no agitation of the waste form, which is monolithic, having a well-defined geometry. The leaching may occur under static or dynamic conditions, depending on the frequency of the leaching solution renewal. In static leach tests, the leaching solution is not replaced by fresh solution. In dynamic leach tests, the leaching solution is periodically replaced; therefore, this test simulates the leaching of a monolithic waste form under non-equilibrium conditions in which maximum saturation limits are not obtained and leaching rates are high.

Some authors have used Leach Tests to study the leaching of hydrated cement phases, either in static or dynamic conditions [1, 10, 19, 23, 28, 29, 35, 37]. The tests employed vary from one to other on:

a) The size of the specimen used, monolithic, although most usual shape is cylindrical,
b) The periodicity of renewing of the leachant, and

45

c) The composition of aggressive water, (acid, deionised water or granitic waters).

The kinetics of the leaching processes involved is better identified with this type of tests. In [28, 29, 35] cement pastes and mortars made of OPC were immersed in solutions containing acetic, nitric, chloric or sulphuric acids and ammonium nitrate. A static regime of the leachant was considered.

The Leach Tests method used for studying the leaching resistance of cement pastes has been modified based on the idea that acidic media are too aggressive and demineralised water has been used [36]. In this last case two contact regimes are considered:

1) Using a dynamic system with a periodic renewal of the leachate, and
2) Modifying the leaching method fixing the pH of the water in contact with cement paste at pH = 7, by continuous addition of nitric acid.

The second method allowed the determination of the amount of ions released and the kinetics of the leaching process [23].

In the Leach Tests methods the steady-state concentration of an element in the liquid would depend on the temperature and water velocity renewal frequency [36]. However, deionised water may be considered a no realistic system and certain content of $HCO_3^-$ in the leachate are more representative [23]. The predictive accuracy of short-term accelerated tests is also questioned [23].

Most of the experience using Leach Tests follows the standard ANSI/ANS-16.1-1986 [9]: "Measurement of the leachability of solidified low-level radioactive wastes by short-term test", procedure commonly used in testing cementitious materials for the nuclear industry. Testing protocol and leaching estimation parameters are described below.

The test consists of a procedure in which the leachant is sampled and replaced at designated intervals, as shown in figure 3.1.2. The procedure permits the accumulation of sufficient data in a reasonably short time for quality assessment purposes. The data obtained from this standard are expressed as a material parameter of the leachability of specific leached specie considered. This parameter is called "Leachability Index", also the effective diffusivity of leached species can be obtained.

Figure 3.1.2-left shows a schematic drawn of the leaching arrangement employed [37]. The sample must have a well-defined shape, mass and volume. The preferred test specimen geometry is cylindrical and it shall have a length to diameter (L/D) ratio in the range of 0.2 to 5. The test does not prescribe to maintain a fixed value of the pH of the leachant in contact with the concrete.

In this test the leachate is sampled and entirely replaced at designated time intervals, as suggested in the ANSI test protocol [9], the water solution shall be sampled and replaced after cumulative leach times. Under these conditions the mass-transferred equations permit the calculation of an effective diffusivity of the concretes by the expressions given in the standard [9]. If they are applied to the amount of calcium leached from the concretes, the effective diffusivity of Calcium, $D_{nsCa}$, is estimated from (Eq. 1and 2). The leachability index of Calcium, $L_{iCa}$, is also obtained using the (Equation 3).

$$D_{nsCa} = \pi \left[ \frac{a_n/A_0}{(\Delta t)_n} \right]^2 \left[ \frac{V}{S} \right]^2 \bullet T \quad \textit{(Equation 1.)}$$

DnsCa = effective diffusivity of Calcium, $cm^2/s$.

V = volume of specimen, $cm^3$.

S = geometric surface area of the specimen from measured dimensions, $cm^2$.

T = leaching time representing the «mean time» of the leaching interval, s.

$a_n$ = activity of calcium released from the sample during leaching interval n.

$A_o$ = total activity of calcium at the beginning of the first leaching interval, 30 s.

$$T = \left[ \frac{1}{2} \left( t_n^{1/2} + t_{n-1}^{1/2} \right) \right]^2 \text{ (Equation 2.)}$$

$(\Delta t)_n = t_n - t_{n-1}$, duration of the $n^{th}$ leaching interval, s.

The Leachability Index of Calcium from the tested concretes is obtained through next (Equation 3):

$$L_{iCa} = \frac{1}{10} \sum_{1}^{10} \left[ \log(\beta / D_{nsCa}) \right]_n \text{ (Equation .3)}$$

Constant $\beta = 1.0 \ cm^2 \ s$

$D_{nsCa}$ is the effective diffusivity of calcium calculated from the test data using (Equation 1).

$L_{iCa}$ = Leachability index of calcium.

Calcium leach follow a potential response from these method, as shown in figure 3.1.2-right, that also depends on the frequency of water renewal, as studied in [37].
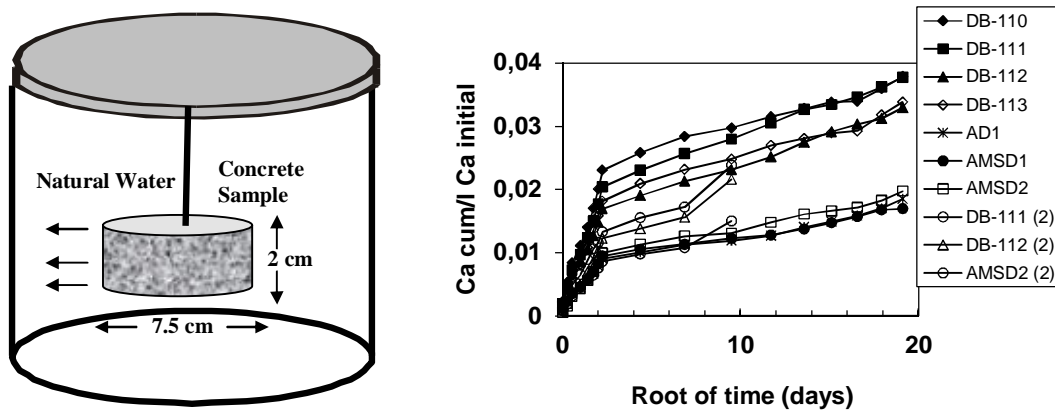


*Figure 3.1.2. Tank water test, left and cumulative calcium leached from different type of concretes, right, from [37].*

*The Column Leach Tests/Running Water Test (RWT) [21–24, 37–42]*

Column Leach Tests with flowing water have not commonly applied in testing degradation of cement matrixes, in spite of running water simulates a real situation occurring when an aquifer enters in contact with a repository. Few papers have been published employing a column leach test type [21–24, 37–42].

The materials used were cementitious materials with variable geometries, granular [23] or monolithic [22, 23], that are placed in a column, with a continuously contact with a new leaching solution at a specified flow rate. The leaching solution is generally pumped through the waste in an up-flow column set-up. A local steady state is assumed to be reached.

While some experiences employed de-ionized water [21] also has been considered the addition of sodium and magnesium sulfates [23] and also granitic waters with low ionic content [37, 41]. The flow rates of water have been varied from 24–202 ml/h [21] to 140–210 ml/h [23]. However, slower flows are expected in underground repositories as those tested in 7–14 ml/h [37, 41]. Also it is expected that natural waters that contain dissolved ions are more representative than de-ionized water.

Different leaching devices are used for running water test, as those used in [37, 41]. The method works in an open system, similar to a leaching column with a continuous flow-up, as indicated in Figure 3.1.3. In this particular arrangement, the water flow follows the up direction at a specified rate [41]. Once the chamber is in contact with the concrete face (a) is filled, the leachant passes to the next chamber, in contact with face (b) filling also in the up direction of the water flow. Periodic sampling of the leachate can be made, so that the evolution of the ionic leaching water is followed to characterise the leaching process and concrete degradation. Also the pH of the leaches evolution is possible to follow, as shown in figure 3.1.3-right experience [37].
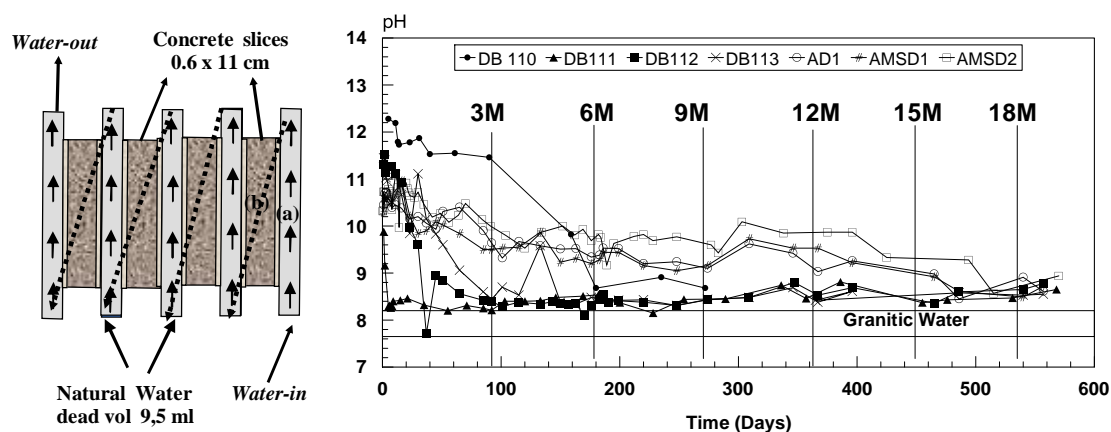


Figure 3.1.3. Running Water Test, left and pH of the leachates from different concretes, right, as from [37].

Permeability/Percolation-Infiltration test [24, 40, 43–47]

This leaching method looks for the extraction of the concrete pore solution, in this case by miscible displacement of the liquid inside the concrete pores using high pressure permeameter [24, 40] and the eluted water allows the measurement of the ionic concentration and the pH [44, 45, 47]. The method is also employed for the hydraulic permeability factor to be determined in cementitious materials. Also hybrid systems made of monolitic concrete plus monolithic bentonite can be placed in contact and interaction with ground waters flowing first through the concrete towards the bentonite what made possible the study with this percolation test of both systems.

The Percolation leaching method is mainly developed to be used for characterizing the leaching behaviour of the engineer barriers in radioactive waste repositories and for measuring the liquid conductivity of porous construction materials but also pH alkaline plume from concrete can be followed and water permeability coefficient can be also determined. There are two main testing protocols used [43–46] that will be described.

*Percolation leaching test from [44, 45]*

The objective of this testing method is to study the evolution of chemical and microstructural changes occurring when materials are subjected to a continuous flow of groundwater. The arrangement of the equipment used is showed in figure 3.1.4.

The sample preparation needs to employ monolithic samples, usually cylinders. The leaching tests procedure is based in the next assumptions: Concrete or mortar sample is placed between two cylinders of methacrylate containing holes for water inlet and outlet. The block is sealed with an epoxy-resin in order to be sure that water pass only through the sample and measured fluxes are correct. Once the samples are placed in contact, a water head between 0.5 and 5 bars (depending on the sample tested) pressure is maintained to pass water from the concrete side and it is collected for analysis. The permeability of the samples and the pressure applied to the water regulate the water flow rate.
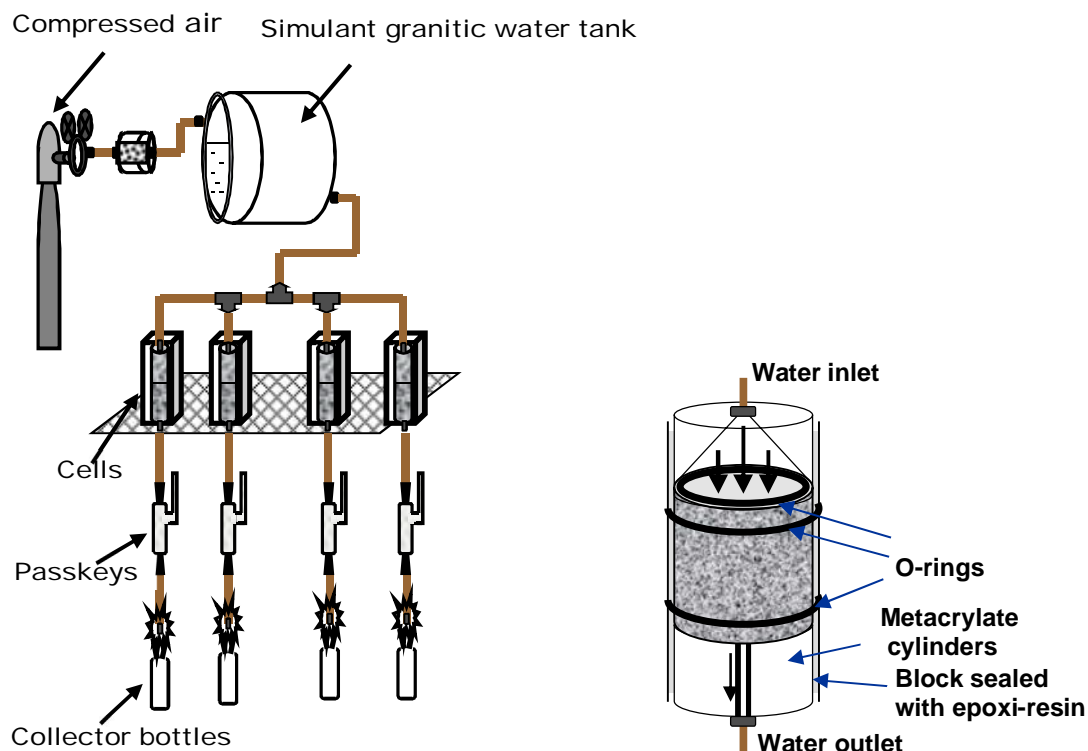


*Figure 3.1.4. Arrangement of concrete sample under percolation test [44].*

The main characteristics of this percolation test arrangement are:

3) Column leaching test (open system).
4) Unidirectional flow.
5) Control of the inflow and outflow solutions.
6) Material shape: monolithic (cylinders 50 mm diameter and 50 mm length).
7) Samples are saturated for 24 hours, before the starting of the test.
8) Water head of 0.5–5 bars

*Percolation leaching test from [43, 46]*

The authors develop a water percolation method in which pore solution is removed by miscible displacement with water in a high pressure, Hassler cell permeameter described by Green [43],

shown in figure 3.1.5. They studied different mortar samples and in this case the resultant solution was analysed for chloride ion leaching (in this study the chloride have been deliberately introduced into the mortar due to it focuses on the corrosion protection in embedded steel reinforcement).

The Hasller cell permeameter is a high pressure axial-flow permeameter designed to accommodate the cylindrical core 25 mm in diameter and between 25 and 75 mm in length. Before being loaded into the Hasller cell the sample must be saturated with water. The core is encased in a nitrile rubber sleeve to which a containing pressure is applied such that the containing pressure exceeds the pressure of the liquid flowing through the sample. The containing pressure seals the circumferential face of the sample and ensures axial-flow. A chromatography pump provides a pulse-free constant flow rate of liquid through the sample and the pressure necessary to maintain this flow is recovered. A flow rate of 1 ml/min is used in each case, resulting in fluid pressures ranging between 0.1 and 1 MPa depending on the mortar composition. The containing pressure is held constant at 4 MPa. The eluent is collected over the first 400 s and subsequently over 200 s intervals for a total of 30 min. Both containing and fluid pressures are measured. For the pumped and saturated liquids being completely miscible the latter is completely displaced. The pore solution is that eluted by the pumped liquid, collected and then analysed for ions.



KEY:

A: Retaining ring,
B: Nitrile rubber O ring,
C: Sleeve carrier,
D: Fixed platen,
E: Nitrile rubber sleeve,
F: Stainless steel case,
G: Sample,
H: Movable platen,
I : Platen carrier,
J: End cap.
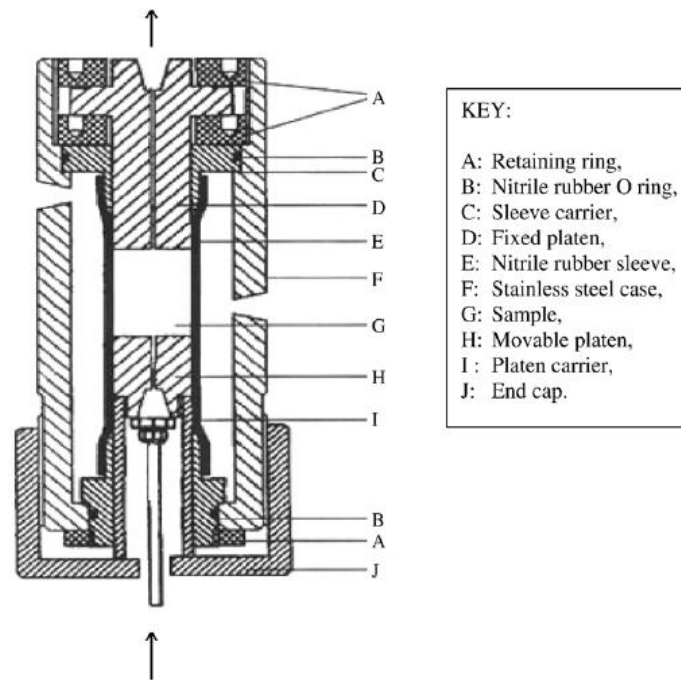
*Figure 3.1.5. Hassler cell permeameter [43].*

Changes in solid phases microstructure of concrete leached samples can be well characterised with Percolation Leach Tests methods, as the experienced shown in figure 3.1.6-left at different thickness from the water source, and also the evolution of leached ions or pH as the example of figure 3.1.6-right for low pH concrete experience with Aspöo granitic waters [47].

There is a decrease in ion concentration as the eluted water progresses: this means that in the particular case of initial concrete pH determination only the first ml of water eluted could be used, but the evolution of pH changes with leaching of concrete can be followed to determine the duration of the alkaline plume of concrete. The water flow evolution induces changes in the equilibriums of solid phases and dissolution of some soluble solids as portlandite. Samples with low porosity, low water /cement ratio, etc., are too impermeable to allow measurable water flow in a short time.
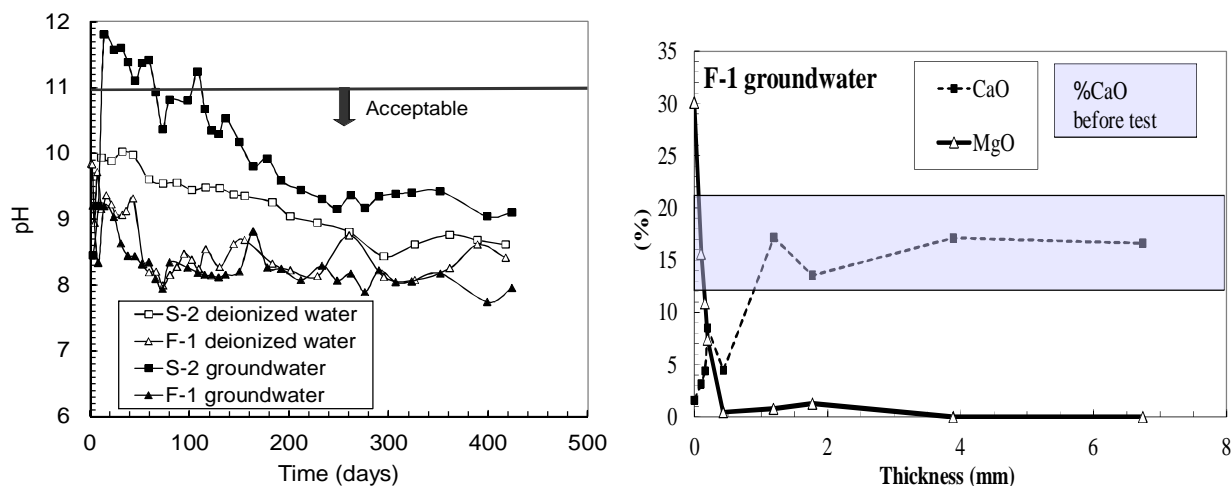
*Figure 3.1.6. Solid changes in low-pH concrete depth in contact with granitic waters (left). pH change evolution of eluates with leach time (Right), from [47].*

*Migration tests [48–57]*

The more recent development of accelerated leaching tests is based on the application of electrical fields (migration tests) to simulate the natural degradation of cementitious materials. The challenge of this method is based on the assumption that cementitious materials have an internal pore network full of an aqueous phase with different ions, therefore when they are submitted to an external electrical field, they behave as an electrolyte and ions inside are able to move driven by the electrical field, causing the simultaneous dissolution of the solid phases which are no longer in equilibrium with the pore solution, as the portlandite and calcium silicates hydrates [48, 49, 51, 53, 54].

Several researchers have applied this kind of methods to the study of the deterioration of cementitious materials in contact with water [48–54]. In [50], after a very complete research program it was stated that the application of an electrical field allowed the degradation of the cement paste following simila mechanisms than in natural scenarios, although more aggressive for work conditions water/concrete interaction. Therefore, this kind of test might be considered as representative of the long-term leaching degradation.

Most of the work that can be found in the literature on this subject has been carried out on cement paste or mortars [48–54]. However, as it is also some experience in concrete [55–57], but the study of the leaching in concretes by this method is more difficult because the high resistivity of cementitious materials implies a quite low current passing through the concrete even at high voltage applied. In addition, characterisation of the degraded zones is difficult due to the presence of aggregates, and also the determination, in a quantitative manner of the microstructure changes that take place during these tests, becomes very doubtful.

In paper [55] the arrangement used was that shown in figure 3.1.7-left. In this migration test concrete leaching acceleration was the main objective. A 10 mm thick concrete disc, previously saturated under vacuum is used for separating the two chambers where cathode and anode were placed. The electrodes used were of activated titanium, and the volume of each compartment filled with granitic water. Galvanostatic tests were performed applying a constant current density passing. A current density of 36 mA/m$^2$ was imposed during 18 days. Periodically, samples in both compartments were analysed, and the evolution of Ca ion which mainly indicates the state of degradation of the concrete in the catholyte can be monitored. Also potentiostatic tests applying

voltages of at least 30V were performed. Different levels of concrete degradation were obtained following several periods of treatment. The coulombs, Q, passed were confirmed as the variable that may define degradation. As a result, acceleration of the degradation process of concrete is characterised and results are obtained within few weeks [55, 56].
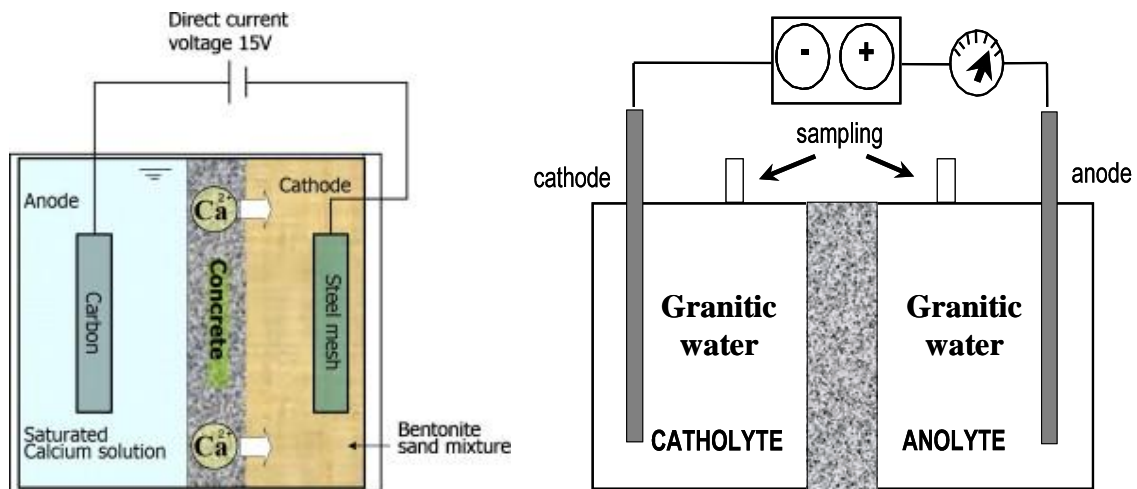


*Figure 3.1.7. Sketch of the fundamentals of the migration methods. Left from [55], right from [57].*

Besides, the migration leaching test method has been employed to composite specimens of compacted bentonite and hardened concrete that are connected each other. The arrangement used was that shown in figure 3.1.7-right [57]. The steel cathode was immersed inside the compacted bentonite and the anode immersed in the saturated calcium solution which is them in contact with one cross section of concrete. A direct current of 15V was applied to the migration cell for acceleration of the Ca migrations ions from the concrete towards the bentonite. This arrangement allows studying the effect of different mix proportions of concrete on the alteration of the characteristics of compacted bentonite. Also quantitative evaluation of the compacted bentonite was provided.

## References

[1]     M. Andac and F. P. Glasser. Long-term leaching mechanism of Portland cement- stabilized municipal solid waste fly ash in carbonated water. *Cem. and Conc. Res., vol 29 (1999) 179–186.*

[2]     M. Furhrmann, R. Pietrzark, J. Heiser III, E. Franz and P. Colomo. The effects of temperature on the leaching sulphate-system. *Mat. Res. Soc. Symp. Proc., vol 176 (1990) 75–80.*

[3]     I. B. Plecas, A. D. Peric, J. D. Drejaca, A.M. Kostadinovic and S .D. Glodic. Immobilisation of radioactive waste residues in cement matrix. *Cem. and Conc. Res., vol 22 (1992) 571–576.*

[4]     S. Goñi, M.S. Hernández, A. Guerrero and M.P. Lorenzo. Effect of temperature on the leaching performance of a simulated cement based immobilisation system. Calcium and hydroxyl behaviour. *Const. of Build. Mat., vol 10, N. 3 (1996) 171–177.*

[5]     E. Zamorani. Deeds and misdeeds of cement composites in waste management. *Cem. and Conc. Res., vol 22 (1992) 359–367.*

[6]     I. Hohberg, G. J. de Groot, A. M. H. Van der Veen and W. Wassing. Development of a leaching protocol for concrete. *Waste Management, vol 20 (2000) 177–184.*

[7]     H. A. Van der Sloot. Comparison of the characteristic leaching behaviour of cements using standard (EN 196-1) cement mortar and an assessment of their long-term environmental behaviour in construction during service life and recycling. *Cem. and Conc. Res., vol 30 (2000) 1079–1096.*

[8]     NEN 7341. Determination of the availability from leaching granular and monolithic construction materials. *Netherlands Standardization Institute (NNI), (1995).*

[9]     ANSI/ANS 16.1. Measurement of the Leachability of Solidified Low-Level Radioactive Wastes by a Short-Term Test Procedure. *American Nuclear Society, (1986).*

[10]    F. Adenot. Durabilité du béton: Caractérisation et modélisation des processus physiques et chimiques de

dégradation du cément. *Doctoral Theses, Univ. D´Orleans (1992).*

[11] B. Gerard. Contribution of the mechanical, chemical and transport coupling in the long-term behaviour of radioactive waste repository structures. *Doctoral Thesis, Univ. Laval (1996).*

[12] P. Faucon, B. Gerar, J. F. Jacquinot and J. Marchand, Water attack of a cement paste. Towards an improved accelerated test?, *Adv. in Cem. Res., vol 10, N 2 (1998) 67–73.*

[13] V. Matte, Durabilité des bétons ultrahautes performance: rôle de la matrice cimentaire. *Doctoral thesis, Ecole Sup. of Cachan (1999).*

[14] E. F. Barth, P. de Percin, M.M. Arozarena, J. L. Zieleniewski, M. Dosani, H. R. Maxey, S. A. Hokanson, C. A. Pryately, T. Whipple, R. Kravith, M. J. Cullinane, Jr. L.W. Jones and P. G. Malone. Stabilization and solidification of hazardous wastes. *U.S. Environmental Protection Agency. Chap 5 (1990) 35–46.*

[15] G. Sergi. Corrosion of steel in concrete: cement matrix variables. *Doctoral Thesis, Aston University (1986).*

[16] A. Hidalgo, S. Petit, C. Domingo, C. Alonso, C. Andrade. Microstructural characterisation of leaching effects in cement paste due to neutralisation of their alkaline nature. Part I. Portland cement pastes, *Cem. and Conc. Res., 37 (2009) 63–70.*

[17] A. Hidalgo, C. Andrade and C. Alonso. Evaluation of the long term behavior of concrete used in high level nuclear waste disposal (HLW). *An accelerated leaching test, in G. Ortiz de Urbina, H. Goumans (EDS.), Environmental and technical Implications of construction with alternative materials, Iscowa-Inasmet, San Sebastian (2003) 857–860.*

[18] E. Revertegat, C. Richet and P. Gegout. Effect of pH on the durability of cement pastes. *Cem. and Conc. Res., vol 22 (1992) 255–272.*

[19] V. Pavlik. Corrosion of hardened cement paste by acetic and nitric acids. Part I: Calculation of the corrosion depth, *Cem. and Conc. Res., vol 24, N. 3 (1994) 551–562.*

[20] C. Carde and R. François. Effect of ITZ leaching on durability of cement based materials, *Cem and Conc. Res., vol 27, N 7 (1997) 971–978.*

[21] V. Matte. Durabilité des bétons ultrahauts performance: rôle de la matrice cimentaire. *Doctoral thesis, Ecole Sup. Of Cachan (1999).*

[22] E. Zamorani, F. Lanza, G. Serrini and H. Blanchard. Water leachability of cement forms for médium- level waste immobilization. *Nuclear and chemical waste management, vol 6, (1986) 197–202.*

[23] F. Bermejo. Resistencia química del hormigón. Acción del agua desionizada, y de disoluciones de sulfatos de sodio y de magnesio sobre dos cementos Pórtland hidratados. *Tesis Doctoral Univ. Compl. Madrid (1988).*

[24] CEN/TC292/WG6. Leaching Behaviour Test: Percolation Simulation Test.

[25] SW846-1311. Toxicity Characteristic Leaching Procedure (TCLP), *U.S. Environmental Protection Agency (EPA), (1992).*

[26] SW846-1312. Synthetic Precipitation Leaching Procedure (TCLP), *U.S. Environmental Protection Agency (EPA), (1994).*

[27] AFNOR X31-210. Déchets. Essais de Lixiviation, *Association Française de Normalisation, (1998).*

[28] J. Insemburg and M. Moore. Generalised Acid Neutralisation Capacity Test (GANC), in Stabilization and Solidification of Hazardous, Radioactive and Mixed Wastes, *vol. 2, ASTM STP 1123, Gilliam T.M. and Wiles, C.C. Eds., American Society for Testing and Materials, (1992) 361–377.*

[29] L. Helard, J. P.Letourneux and H. Fryda. Examples of Chemical Interactions Between Pollutants and Hydraulic Binders., *in Actes du Congrès International sur les Procédés de Solidification et de Stabilisation des Déchets, J. M. Cases and F. Thomas Eds., (1995) 239–245.*

[30] A. Hidalgo, C. Andrade and C. Alonso. An accelerated leaching test to evaluate the long term behaviour of concrete in waste disposal. *5th CANMET/ACI Inter. Conf. on Durability of Concrete. Barcelona June (2000) 373–381.*

[31] A. Hidalgo, C. Andrade and C. Alonso. Role of alkaline reserve in the acidic resistance of cement pastes. Calcium hydroxide in concrete. *Edt. Am. Cerm. Sc., J.Skalny, J.Gebauer and I. Odler. (2001) 93–110.*

[32] E. Revertegat, C. Richet and P. Gegout. Effect of pH on the durability of cement pastes. Cem. and Conc. Res., vol 22 (1992) 255–272.

[33] A. Hidalgo, C. Andrade and C. Alonso. An accelerated leaching test to evaluate the long term behaviour of concrete in waste disposal. *Ind. Ital. Cem, 766 (2001) 498–507.*

[34] E. Roziene, A. Loukili. Performance based assessment of concrete resistance to leaching, *Cem. and Conc. Comp., 33 (2011) 451–456.*

[35] MCC-1P. Static Leach Test Method, *Materials Characterization Centre, Pacific Northwest Laboratory, (1983).*

[36] NEN 7345. Determination of leaching from monolithic construction materials and waste materials by means of diffusion test. *Oct (1994).*

[37] C. Alonso M. Castellote, I. Llorente and C. Andrade. Ground water leaching resistance of high and ultrahigh performance concretes in relation to the testing convection regime, *Cem. and Conc. Res., Vol. 36 (2006) 1583–*

1594.

[38]    ASTM D4874-95. Standard Test Method for Leaching Solid Material in a Column Apparatus, *American Society for Testing and Materials, (1995).*

[39]    NEN 7343. Leaching characteristics of solid earthy and stony building and waste materials - Leaching tests: Determination of the leaching of inorganic components from granular materials with the column test, *Netherlands Standardization Institute (NNI), (1995).*

[40]    Meteoric Water Mobility Procedure (MWMP), Standardized Column Percolation Test Procedure, *Nevada Mining Association, Reno NV, EE.UU., (1996).*

[41]    C. Vernet, C. Alonso, C. Andrade, M. Castellote, I. Llorente and A. Hidalgo. A new leaching test based in running water system to evaluate long-term resistance of concretes. *Adv. in Cem. Res. , vol 14, N 4, October (2002) 157–168.*

[42]    N. Marinoni, A. Pavese, M. Voltolini, M. Merlini. Long -term leaching test in concrete: An X-ray powder diffraction study. *Cem. and Conc. Comp., 30 (2008) 700–705.*

[43]    K.M. Green, W.D. Hoff, M.A. Carter, M.A. Wilson and J.P. Hyatt. A high pressure permeameter for the measurement of liquid conductivity of porous construction materials. *Review of Scientific Instruments, 70 (1999) 3397–3491.*

[44]    A. Hidalgo, I. Llorente, C. Alonso and C. Andrade. Study of concrete bentonite interaction using accelerated and natural leaching test. *CSNI/RIL.*

[45]    *EM WS on use and performance of concrete in NPP fuel cycle facilities, NEA/CSNI/R (2004) 125–135.*

[46]    A. Hidalgo, M. Castellote, I. Llorente, C. Alonso and C. Andrade. Ecoclay II. Effects of cement and clay barrier performance. Phase III. Final report, EC contract *NFIKW-CT 2000-00028 European Commission (2004).*

[47]    L.J. Bucley, M.A. Carter, M.A. Wilson and D.J. Scantlebury. Methods of obtaining the pore solution from cement pastes and mortar for chloride analysis. *Cem. and Conc. Res., 37 (2007) 1544–1550.*

[48]    J.L. Garcia-Calvo, A. Hidalgo, C. Alonso, L. Fernandez-Luco, Development of low-pH cementitious materials for HLRW repositories. Resistance against ground water aggression. *Cem. and Conc. Res. (2010) 1290–1297.*

[49]    H. Saito, S. Nakane, S. Ikari, S. and A. Fujiwara. Preliminary experimental study on the deterioration of cementitious materials by an acceleration method. *Nuclear Engineering and Design, 138 (1992), 151–155.*

[50]    P. Faucon, B. Gerard, J.F. Jacquinot and J. Marchand. Water attack of a cement paste: towards an improved accelerated test?, *Advances in Cement Research, 10, N° 2, 1998, 67–73.*

[51]    B. Gerard. Contribution des couplages mécanique-chimique-transfert dans la tenue à long terme des ouvrages de stockage de déchets radioactifs. *Doctoral thèses. Laboratoire de Mécanique et Technologie (E.N.S. de Cachan, C.N.R.S. Université Paris 6). Université Laval. Dpt. De Génie Civil C.R.I.B. Québec, Canada. (1996).*

[52]    T. Kuroi, T. and T. Sueyoshi. Basic study on softening phenomenon of cement paste due to action of electric current, *CAJ review, march 1987, 164–167.*

[53]    J. Le Maréchal, B. Gerard, J. Marchand, J. Gagnon and O. Didry, O. New accelerated leaching experiment: The LIFT procedure. *Proceedings Fourth CANMET/ACI/JCI International Conference. SP 179-55, Tokushima, Japan, 1998.*

[54]    M. Castellote, A. Andrade and C. Alonso. Changes in the concrete pore size distribution due to electrochemical chloride migration trials. *ACI Materials Journal, Vol 96, n° 3, May-June 1999, pp 314–319.*

[55]    H. Saito and A. Deguchi. Leaching tests on different mortars using accelerated electrochemical method. *Cem. and Conc. Res., 30 (2000), 1815–1825.*

[56]    M. Castellote M. Castellote, I. Llorente, C. Andrade and C. Alonso, In situ accelerated leaching of cement paste by application of electrical fields monitored by syncrotron X-ray diffraction, *Applied Physics A, 79 (2004) 661–669.*

[57]    M. Castellote, I. Llorente, C. Andrade and C. Alonso. Accelerated leaching of ultrahigh performance concretes by application of electrical fields to simulate their natural degradation, *Mat. and Structures, 36 (2003) 381–391.*

[58]    T. Sugiyama and Y. Tsuji, Use of a migration technique to study alteration of compacted sand-bentonite mixture in contact with concrete, *Physics and chemistry of the earth, 33 (2008) S276–S284.*

## 3.2 Methodologies to determine permeability and diffusivity in cementitious materials

*Q. T. Phung, N. Maes*

*Belgian Nuclear Research Centre (SCK•CEN), Belgium*

### General introduction

Durability and performance of concrete are affected by a number of chemical degradation phenomena such as carbonation, calcium leaching, sulphate attack, chloride attack, and corrosion of the reinforcement bars [1, 2]. Diffusivity and permeability as macroscopic properties of concrete determine how fast aggressive substances penetrate into concrete, thereby influencing almost all mentioned degradation mechanisms. Therefore, these are fundamental parameters for characterizing long-term performance of concrete rather than the standard compressive/tensile strengths. In this section, a critical review on permeability and diffusion of cement-based materials is presented. The existing methods, influencing factors and prediction of transport properties are introduced. The advantages and disadvantages of different techniques are discussed.

### Permeability

*Introduction*

The intrinsic permeability is the capacity of a porous material to transfer liquids through a fully saturated pore network under a pressure gradient, $\nabla p$ [Pa/m], and is determined by Darcy's law [3]:

$$J = -\frac{k}{\eta}\nabla p \quad \textit{(Equation 1.)}$$

Within the field of engineering, water permeability is normally expressed by the hydraulic conductivity, $k_w$, which is related to the intrinsic permeability, $k$, as:

$$k_w = \frac{\rho g}{\eta} k \textit{ (Equation 2.)}$$

where $\rho$ is the density of water [kg/m$^3$]; $\eta$ is the dynamic viscosity for water [kg/m.s]; and $g$ is the gravitation constant [m/s$^2$]. The unit of the hydraulic conductivity (also called as permeability coefficient) is [m/s], while the SI unit of intrinsic permeability is [m$^2$].

Permeability generally depends on the features of the pore network of cementitious materials which are quantified by variables as porosity, size distribution, tortuosity, connectivity, specific surface and also micro cracks. These parameters are, amongst others, controlled by the water/cement (w/c) ratio, the particle size distribution, the age of hardened cementitious materials and the ingress of aggressive substances. Due to the importance of permeability, many methods to determine permeability have been proposed [4–11] but none of them seems fully accepted worldwide.

*Review of existing water permeability measurement techniques*

A variety of methods has been proposed to measure permeability of cementitious materials but a lot of arguments/problems/issues still remain. One of the main challenges is to cope with the continuous change in microstructure as a result of hydration of early age cementitious materials.

Therefore, an appropriate method for measuring permeability requires a short measurement time. In general, permeability measurements can be classified in two categories: direct and indirect methods.

*Direct methods*

Most direct methods for determining the permeability of porous materials rely on Darcy's law. In its basic form, the water flux through a disk-shaped sample is measured under a pressure gradient by having a water head at one side of the sample, while maintaining the other side at atmospheric pressure [12]. Based on the geometry of the sample, the permeability is calculated directly from Darcy's law. Although these methods are relatively simple, it can take a long time to reach steady state flow conditions (in the order of several weeks for $k_w$ of $10^{-11}$ m/s). Unfortunately, hydration during such long testing time can change the pore structure which could lead to changes in permeability (usually decreasing the permeability). To reduce the required measurement time, researchers propose to apply an additional pressure (e.g. 15 bar in [5]) rather than self-gravity of a water head [5, 7, 13]. Nevertheless, due to the higher applied pressure, the probability of leakage at the interface of the sample and the testing cell might be larger.

El-Dieb and Hooton [14, 15] introduced a triaxial cell that can measure permeability as low as $10^{-15}$ m/s which is a typical value for extremely low-permeable materials such as high performance concrete or high strength concrete. A confining pressure is applied to a cylindrical sample through a rubber sleeve to prevent leakage around the sides. The ratio of confining pressure to driving pressure is recommended to be approximately 4 in order to increase the stability of the measurement. The high-confining pressure condition raises the question whether it may modify the pore structure due to the compression of pores or due to creation of artificial micro cracks, thereby, leading to unrepresentative permeability values.
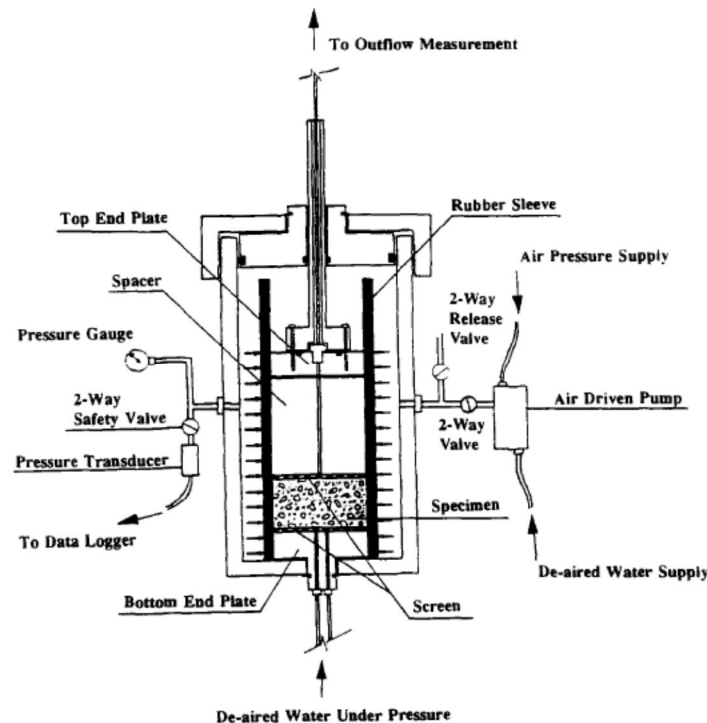


*Figure 3.2.1. Triaxial cell to measure permeability [14].*

Instead of imposing longitudinal flow, a radial flow through the sample is created by applying a hydrostatic pressure to the outer surface of a hollow cylindrical sample resulting water to move from the outer to the inner surface of a sample [7, 13]. By measuring the out-flow rate with a linear

variable differential transformer [13] or with an out-flow measurement device [7], the permeability is calculated by a modified form of Darcy's law. There are several advantages by using the radial flow method. Firstly, because of a larger contact area of the fluid compared to a longitudinal flow setup, flow rates are higher and, thus, the accuracy of the measurements increases. Secondly, the area which needs to be sealed is minimized; as a result the potential of leakage is decreased. Finally, a hollow cylindrical sample may be easier to saturate than an equivalent solid sample. However, it is quite difficult to prepare a hollow sample, especially, in the case of in-situ concrete.
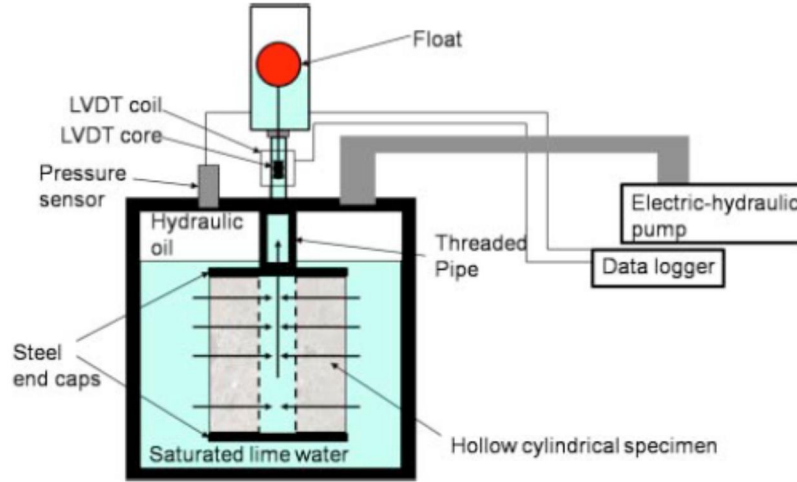


*Figure 3.2.2. Hollow cylinder dynamic pressurization test for measuring permeability [13].*

Another promising method is the centrifuge technique which was first applied on soil materials by Nimmo *et al.* [16, 17]. This method was recently standardized in the ASTM standard D6527 which covers permeability measurements of any porous material [18]. A cylinder-shaped sample is put in a centrifuge with a centrifuge radius of $r$ [m], and a rotation speed of $\omega$ [rad/s]. The centripetal force per unit volume, $-\rho r \omega^2$, is the main fluid driving force. The permeability can be calculated as follows (the Eq. (1a) is probably wrongly written in reference [19] due to missing term $\rho g$ which leads to unit for permeability [m$^3$.s/kg]):

$$k = -\frac{q\rho g}{d\psi/dr - \rho r \omega^2} \ (Equation\ 3.)$$

where $q$ is the flux [m/s] and $d\psi/dr$ [kg/m$^2$.s$^2$] is the matric potential gradient which is negligible if rotation speed is above 400 rotations per minute [19]. An important advantage of the centrifuge technique is that the centrifugal force is a body force which acts, similar to gravity, independently of other driving forces over the entire porous material [19]. The magnitude of centrifugal force per unit volume can be increased by increasing the rotation speed such that it dominates any matric potential gradients. However, if the rotation speed is too large, the sample can be compacted under equivalent pressure exerted by centrifugal acceleration. Additionally, this method can be used to determine out-flow of unsaturated porous materials because it can fix the water content to achieve hydraulic steady state which cannot be done by pressure driven techniques [19]. The centrifuge technique is normally applied for materials of which permeability is not too low as stated in ASTM standard D6527 ($10^{-6}$–$10^{-13}$ m/s) [18].
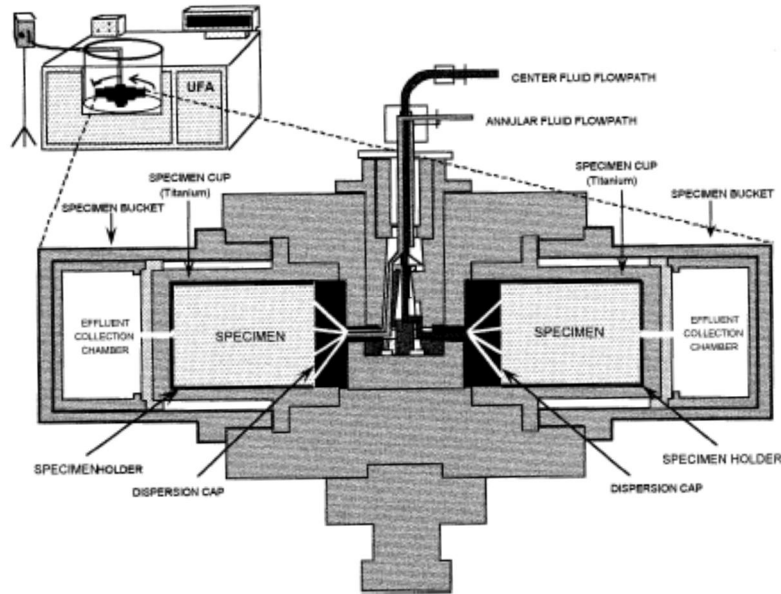
*Figure 3.2.3. Steady-state centrifugation-unsaturated flow apparatus for measuring permeability [18].*

Recently, Phung et al. [20] proposed a novel method to measure water permeability of cement-based materials based on the application of a constant flow instead of a constant pressure in traditional methods, which overcomes the problem of measuring extremely low flow rate. This method seems promising in terms of the required experimental time and the parameter control. It is also very flexible for further testing in which carbonation, leaching and diffusion tests can be performed on the same sample to study the effects of chemical degradation on transport properties. It can determine the permeability coefficient of cement paste in a relative short time compared to other methods (within 1 week for permeability of $10^{-13}$ m/s).
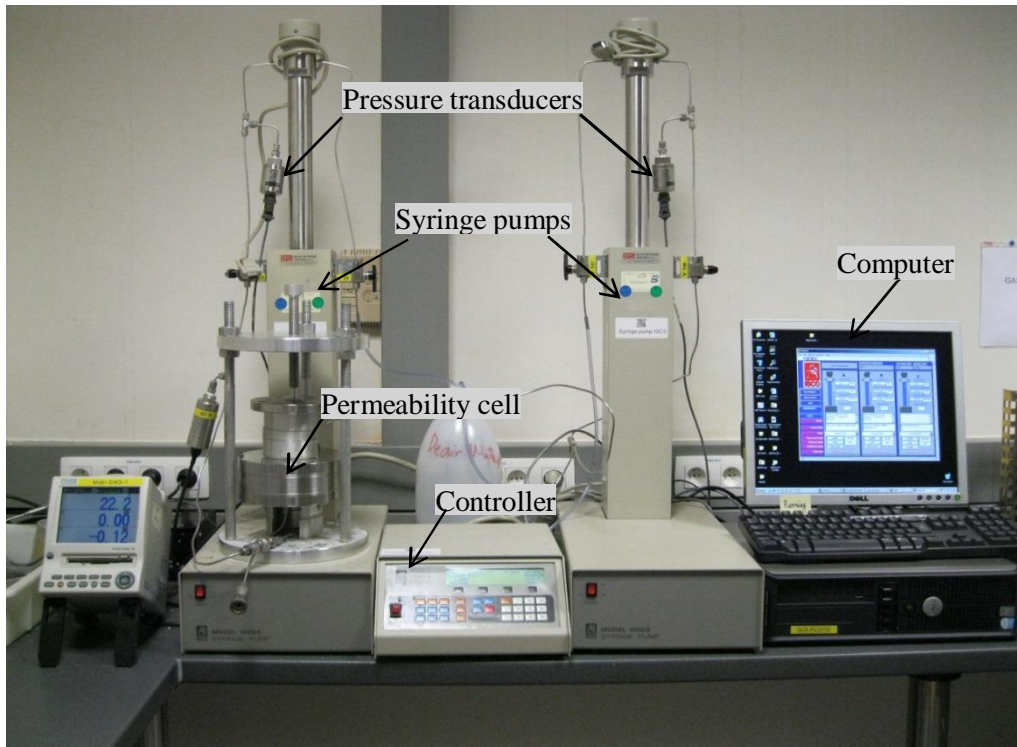


*Figure 3.2.4. Schematic permeability setup using a controlled constant flow method [20].*

In general, direct methods are quite simple and easy to setup. No additional parameters are needed to interpret the results when using Darcy's law directly. On the other hand, it takes a long time to reach the steady state flow conditions needed to apply Darcy's formula. Therefore, concrete samples are more susceptible to microstructural changes as a consequence of hydration, especially at early hydration stage. Potential for leaks around the sample is high if seal and/or confining pressure are not sufficient. Because of these limitations, the direct methods can only be applied to materials of which the permeability is not too low.

*Indirect methods*

Indirect methods involve either the application of a transient pressure pulse technique or the application of poromechanical techniques.

In 1968, Brace *et al.* [21] introduced a transient pressure method for determining the permeability of granite. The principle of this method is to measure the decay characteristics of pressure, which depend on permeability, after a sudden change of applied pressure. This method can measure permeability coefficient as low as $4 \times 10^{-14}$ m/s. This method, already applied to cement-based materials [4, 22], needs only measured time series of pressure instead of the extremely low flow rate measurement in the direct methods.



*Figure 3.2.5. Confining cell to measure gas permeability using a low-transient pressure method [22].*

Alternatively, poromechanical techniques measure the strain-time history, which depends on the fluid movement in a pore network, of a sample under an applied pressure or heating. Especially the beam bending method, proposed by Scherer *et al.* [23], is of great interest since it is extremely fast

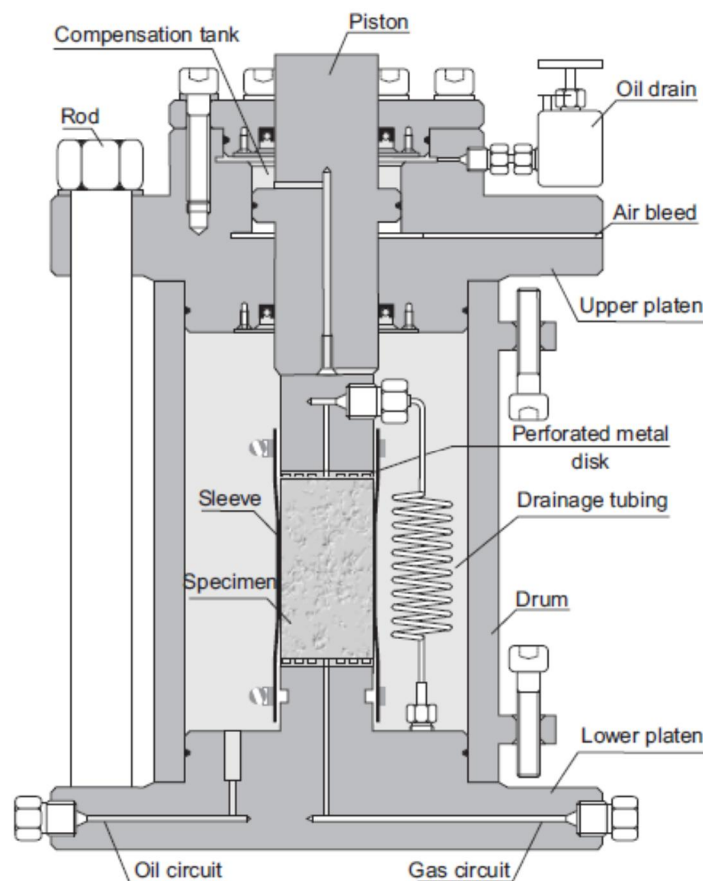(several minutes to hours compared to days of conventional methods for permeability of the same order of magnitude), and thus suitable for low-permeable materials, and provides also viscoelastic properties (i.e. shear modulus, Young's modulus). This method was originally developed for silica gels [24] and then extended for glass [25] and cementitious materials [6, 26]. However, it is difficult to apply the beam bending method for concrete because the sample must be long and slender enough to avoid micro cracking. For example, the concrete sample should be more than one meter long if it is 10 cm thick [10].
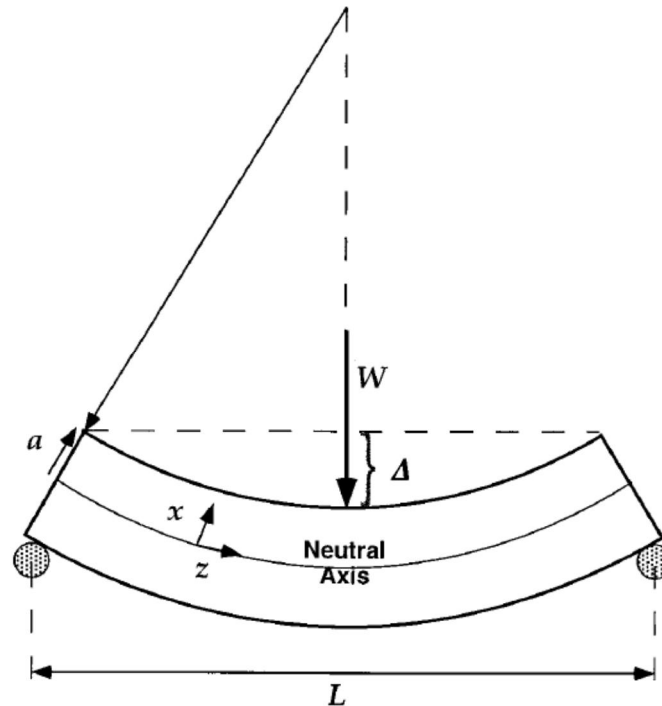


*Figure 3.2.6. Schematic of cylindrical beam: beam on end supports with span L; z-axis along axis of beam, x-axis vertical; deflection Δ is displacement of upper surface caused by applied force W [23].*

Thermopermeametry and dynamic pressurization are other examples of applying poromechanics to measure permeability. Thermopermeametry was also first introduced for gels [27, 28] and afterwards applied for cementitious materials [29, 30]. The main principle of this method is based on the difference in expansion of liquid and solid phase when heated. This method requires a complete saturation of the sample because water will first fill the pores before flowing out when air is still entrapped. This leads to an underestimation of the permeability. Therefore, this method may not work well for mortar or concrete for which full saturation state is not easy to obtain within a short time. Dynamic pressurization involves applying a sudden hydrostatic pressure on a cylindrical sample in a closed system. By measuring the history of the re-expansion, the permeability of the sample can be obtained in a relative short time. The sample can be a solid cylinder [8, 9] or a hollow cylinder [13]. The permeability measured by the hollow dynamic pressurization method seems to agree well with the one measured by the solid dynamic pressurization method [31]. However, the hollow dynamic pressurization method probably measures a wider range of concrete permeability because it can also be tested as a radial flow through method.

*Figure 3.2.7. Schematic diagram of the thermopermeametry [30].*

In general, the indirect methods for measuring permeability are much faster than direct methods because they are based on measurements obtained during non-steady state flow conditions. Potential of leakage is actually eliminated. These techniques can determine very low permeability. However, a full saturation of the sample, which is extremely difficult to obtain for low-permeable materials such as high performance concrete, is absolutely required because the degr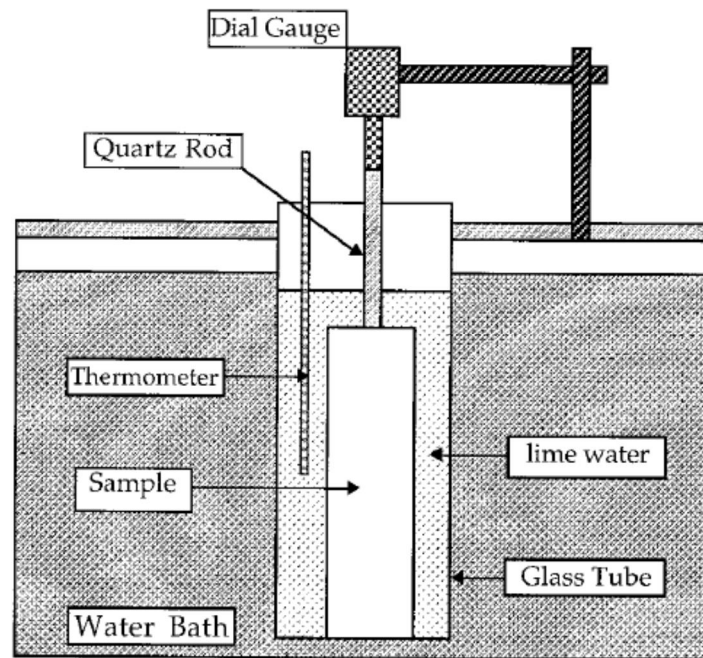ee of saturation hugely affects test result. With direct methods, the sample saturates during the test until steady state is reached, which also can take a long experimental time. Application of heating or high pressure may also change the microstructure of the cementitious materials. Another disadvantage of these methods is that the experimental setup and the interpretation or analysis are quite complex.

*Gas permeability*

It is well-known that the intrinsic gas permeability is higher than the intrinsic water permeability of cement based-materials (around 2 orders of magnitude) despite the fact that permeability is an intrinsic property of the material [5]. In addition, lower viscosity of gas results in higher fluxes in gas permeability measurement than water permeability measurement. As such, measuring the gas permeability and converting it to the water permeability would be easier because gas permeability determination is less time consuming. Unfortunately, the intrinsic permeability cannot be derived directly from the measured gas permeability because of gas slippage or the so-called Klinkenberg effect [32] which increases the amount of gas passing through the capillaries of porous media compared to prediction from a physical law. Some studies established a statistical, thus empirical, log-log linear correlation between air and water permeability using a huge amount of experimental data [33, 34].

*Factors influencing water permeability*

There are many factors influencing the permeability of cement-based materials. Several factors are classified as extrinsic related to experimental conditions such as applied pressure, size of sample [35] and confining pressure [7]. Variation of these factors can cause a change of several orders of magnitude in permeability. Another factor which can significantly affect the permeability is the fluid-cement matrix interactions during measurement. In the case of using water as a testing fluid,

61

the time dependent reduction of permeability is mainly due to continuing hydration, autogenous healing and the self-sealing effects [5, 36, 37]. However, these phenomena likely occur in cracked [38, 39] and/or early aged cement-based materials rather than virgin and/or mature materials. Unreactive fluids such as ethanol [5], glycol [40] or 2-propanol [6] may be used instead of water to eliminate the fluid-cement matrix interactions. However, the replacement of water by unreactive fluid may require longer experimental time and especially the fluid exchange would create micro cracks which hugely increase the permeability. In some cases, the permeability can increase 2 orders of magnitude [6].

Intrinsic factors are related to material properties such as pore network characteristics of the cementitious material which include porosity, pore size distribution, tortuosity, specific surface and micro cracks. These parameters are basically controlled by the water to cement ratio, particle size distribution (cement + aggregate), age of sample and type of constituent materials. Concrete with larger pore size has higher permeability than concrete with smaller pore size despite the same total porosity. This effect is normally reflected through the critical pore size (which is the most frequently occurring pore size in interconnected pores). It is obvious that pore connectivity is one of the most critical factors influencing the permeability. Pores which are blocked cannot transport any fluid. The type of constituent materials mainly affects permeability through hydration degree, especially at early ages. As shown in many studies [6, 41–44], the permeability increases with increasing w/c ratio because of a higher porosity at higher w/c ratio. However, to the knowledge of the author, no direct connection between water to cement ratio and permeability has been proposed. A direct relation between porosity and permeability has been introduced by some researchers [45–49]. Nevertheless, porosity alone should not be a unique factor influencing the permeability, i.e. samples with same porosity may have different permeability.

## Diffusion

### Introduction

Diffusion of chemical substances plays an important role in many degradation processes (e.g. corrosion of steel bars; chloride, sulphate attacks). Knowledge of diffusion coefficients helps to better design and evaluate concrete structures. Diffusion is a mass transport induced by the random Brownian motion of substance. The diffusion coefficient (diffusivity) is the capacity of a medium to transfer substances (gases, dissolved gases, ions) under a concentration gradient expressed by Fick's first law (1D):

$$J = -D\frac{\partial C}{\partial x} \text{ (Equation 4.)}$$

where $J$ is the substance flux [kg/m$^2$.s]; $\frac{\partial C}{\partial x}$ is the concentration gradient [kg/m$^4$]; and $D$ is the diffusion coefficient [m$^2$/s]. In porous materials, diffusion is affected by the characteristics of pore network (porosity $\phi$ [-], tortuosity $\tau$ [-], constrictivity $\delta$ [-]) which leads to the need to define different diffusion coefficients for practical application [50]. The pore diffusivity, $D_p$, is smaller than the diffusivity in free water or ideal solutions $D_0$, which takes into account the effects of tortuosity and constrictivity (a dimensionless parameter depending on the ratio of the size of diffusion species and pore size) and is expressed as:

$$D_p = D_0 \frac{\delta}{\tau^2} \text{ (Equation 5.)}$$

The effective diffusivity, $D_e$, takes into account the volume of porous media available for diffusion and is defined as:

$$D_e = \phi D_p = D_0 \frac{\phi \delta}{\tau^2} \ \textit{(Equation 6.)}$$

The apparent diffusivity, $D_a$, takes into account the sorption/binding which retards the diffusion and is linked to the pore diffusivity through a retardation factor ($\geq 1$), $R_e$, as follows:

$$D_a = \frac{D_p}{R_e} = D_0 \frac{\delta}{R_e \tau^2} \ \textit{(Equation 7.)}$$

*Review of existing diffusivity measurement techniques*

Due to the importance of diffusion, many methods to determine diffusivity have been proposed. The diffusion coefficients can be obtained under steady state or transient state conditions. We distinguish between four main types of experiments to determine diffusivity: (i) through-diffusion based on measuring fluxes, (ii) in-diffusion based on measuring concentration profiles in the sample, (iii) electro-migration experiments, either by through- or in-diffusion, in which ion diffusion is accelerated by an electric field, and (iv) techniques in which proxy variables are used to determine diffusivity, for example, electrical resistivity techniques. A summary of the measurement techniques is given in Table 3.2.1.

*Table 3.2.1. Summary of methods to measure diffusion coefficients of cement-based materials.*

| Technique | | Through-diffusion | In-diffusion | Electro-migration | Electrical resistivity |
|---|---|---|---|---|---|
| **Description/principle** | | • Thin sample located between two compartments; <br>• The diffusing species is injected to the upstream compartment; <br>• The concentration of diffusing species in the downstream compartment is measured regularly until a steady state flux is reached. | • Based on the measurement of the concentration profile of the diffusing species inside the sample. | • Thin sample located between two electrodes; <br>• Transport of ionic species is accelerated by an electrical potential difference; <br>• Non-steady-state: concentration profile of ion is measured inside the sample; <br>• Steady-state: concentration of ion in the downstream compartment is monitored until steady-state is reached. | • The electrical resistivity of the sample is measured by applying a known alternating current/voltage; <br>• Diffusivity can be obtained from the link between resistivity and diffusion. |
| **Interpretation** | | Fick's first law | Fick's second law | Nernst–Planck equation | Nernst–Einstein equation |
| **Pros** | | • Simple <br>• Accurate | • Possible to measure diffusivity of *in situ* concrete | • Relatively fast | • Very fast |
| **Cons** | | • Time-consuming, <br>• Requires constant concentration gradient <br>• Very thin sample <br>• Microstructural changes due to long testing duration | • Laborious | • Complicate interpretation, many assumptions needed; <br>• Electro-osmotic flow and heat generation due to current; <br>• All ions in pore solution involved; <br>• Scattered results. | • Need to determine the resistivity of pore solution to calculate the effective diffusivity; <br>• Gives only approximate diffusivity of the sample, not for specific species. |
| **Application on:** | Cement | Usually for cement paste | x | x | x |
| | Mortar | | x | x | x |

| Technique | | Through-diffusion | In-diffusion | Electro-migration | Electrical resistivity |
|---|---|---|---|---|---|
| | Concrete | | Limited due to difficulty in slicing the sample | x | x |
| **Obtained parameters:** | $D_e$ | x | | x | x |
| | $D_a$ | x | x | x | |
| | $\phi$ | x | | x | |
| **Test duration** | | Few months | Few weeks | Few days | Instantaneous |
| **Diffusing species** | | Dissolved gases; Ions | Ions; Radioactive elements | Ions | Not specific |

*Through-diffusion technique*

The diffusion coefficients of a variety of diffusing species (e.g. HTO, ions and dissolved gases) are classically determined by the through-diffusion technique because of its simplicity and convenience. The setup (Figure 3.2.8a) consists of a thin sample located between two compartments. The diffusing species is injected/filled to the upstream compartment. For measuring diffusivity of dissolved gases, two gases with the same pressure are injected to the downstream and upstream compartments to balance the pressure in the two compartments which prevents advective transport. This setup usually allows measuring the diffusivity of two dissolved gases in a single experiment [51–53]. Under the concentration gradient, the diffusing species diffuses toward the downstream compartment. The concentration of diffusing species in the downstream compartment is measured regularly until steady state flux is reached.
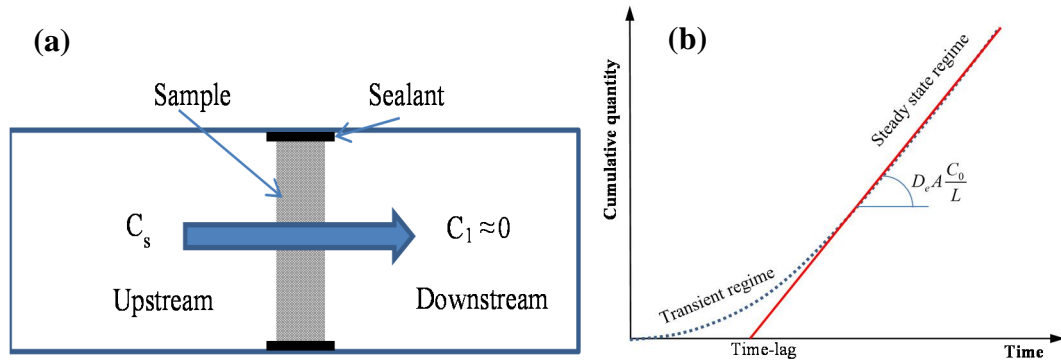


*Figure 3.2.8. (a) Through-diffusion setup (b) cumulative quantity in the upstream compartment.*

Figure 3.2.8b shows a typical cumulative quantity of a diffusing species over time. When steady-state is reached, the slope becomes constant which means the diffusive flux across the sample is constant. Fick's first law can then be applied to calculate the cumulative quantity $Q(t)$ [mol] of diffusing species passed through a sample with a cross-sectional area $A$ [m$^2$]:

$$Q(t) = \int_0^t -D_e A \frac{\partial C}{\partial x} dt' = D_e A \frac{C_s}{L} t \quad \text{(Equation 8.)}$$

*where L is the length of sample [m], C is the concentration [mol/m$^3$] and $C_s$ is the concentration of diffusing species in the upstream compartment [mol/m$^3$]. Note that the concentration of diffusing species in the downstream compartment should be negligible compared to $C_s$ in order to apply Eq. (8). The effective diffusivity in this case can be easily computed from the slope of Q(t) curve. In case of no sorption/binding, the accessible porosity of the sample can be determined from the time-lag*

$t_{lag}$ [s] (Eq. 9), which is the intercept of the straight line with the x axis in Figure 3.2.8b and expressed as follows:

$$\phi = \frac{6D_e t_{lag}}{L^2} \quad (Equation\ 9.)$$

However, it has been reported that the porosity determined from time-lag is less precise than traditional porosity measurements [50].

To maintain a constant concentration gradient, the gas/solution in upstream and downstream compartments is regularly refreshed. In spite of this, the constant gradient condition is difficult to achieve and small variations in concentration gradient at steady state can be permitted [50]. If the variations are too large, the effective diffusion coefficient can be obtained through fitting using a numerical solution of diffusion equation [51, 52].

The through-diffusion technique has been used to determine the steady-state diffusion coefficients of ions (chloride, sulphate) [54, 55]. However, through-diffusion is not an optimal method to measure the steady-state diffusion coefficient for interacting (sorbing) species as it takes long time to reach steady-state. Alternatively, electro-migration technique (see section 2.3) enables to obtain the steady-state diffusion coefficient in a short period. The data on diffusion of dissolved gases in saturated cement-based materials measured using through-diffusion technique are very scarce in literature. However, the knowledge of the diffusion of specific dissolved gases is very important, especially the diffusion of dissolved oxygen which is involved in the corrosion process of steel bars in reinforced concrete. Recently, Phung [51, 52] applied the through-diffusion technique to measure the effective diffusion coefficients of two dissolved gases in a single experiment.
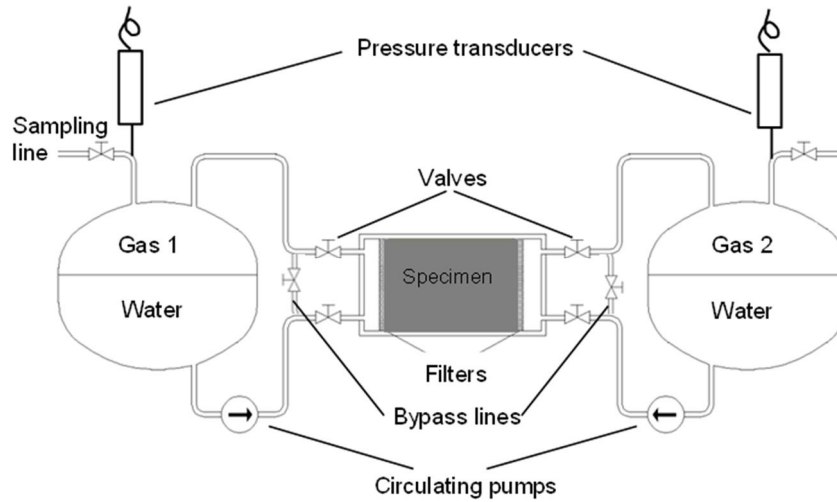


Figure 3.2.9. Schematic experimental setup to measure diffusivities of dissolved gases [51, 52].

The effective diffusion coefficients of dissolved oxygen are usually determined by an electrochemical method involving cathodic consumption of the diffused oxygen [56]. The method is actually a through-diffusion based technique. However, instead of measuring the concentration of diffusing species at the downstream compartment, the cumulative quantity is calculated from the charge passed based on Faraday's law:

$$Q(t) = \frac{E_C}{F} \frac{M}{z} \quad (Equation\ 10.)$$

where $E_C$ [coulomb] is the total electric charge passed, $F$ is the Faraday number (96485 coulomb/mol), $M$ [kg/mol] is the molar mass of species, and $z$ is the number of electrons transferred per molecule of species ($z = 4$ for oxygen).

*In-diffusion technique*

Instead of waiting for a steady state flux as in the case of through-diffusion set-up, in-diffusion is a transient method, which is less time consuming. However, the technique is only applicable on easily traceable species (chloride, radioactive elements). The technique is based on the measurement of the concentration profile of the diffusing species inside the sample by cutting the sample into small slices at a given time. Experiments are usually designed in such a way that the source concentration of the diffusing species is kept constant and the sample is long enough to consider a semi-infinite medium. The apparent diffusion coefficient is then obtained by fitting the concentration profile with the solution of the Fick's second law [57]:

$$C(x,t) - C_0 = (C_s - C_0) erfc\left(\frac{x}{2\sqrt{D_a t}}\right) \ (Equation\ 11.)$$

where $C(x,t)$ is concentration at depth $x$ [m] and time $t$ [s], $C_0$ and $C_s$ are the initial and source concentrations, respectively [mol/m$^3$] and *erfc* is the complementary error function.
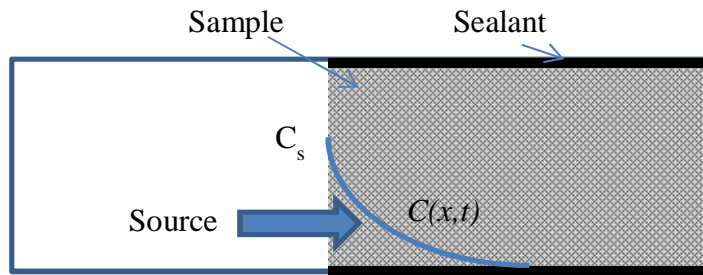


*Figure 3.2.10. In-diffusion setup.*

Chloride diffusion coefficients are commonly determined using long-term immersion tests based on the in-diffusion method which have been standardized in ASTM C1556-04 [58] and Nordtest NT Build 443 [59]. The diffusivity obtained from long-term immersion tests is frequently based on Fick's law which does not take into account ion-ion interactions. This leads to controversial results, for example, the diffusivity of chloride in sodium chloride solution is smaller than in potassium chloride because the diffusivity of potassium is higher than that of sodium [60] resulting in a larger charge influence of chloride diffusion. Furthermore, chloride diffusivities obtained from long-term immersion tests are higher than electro-migration tests despite the good correlation between two obtained diffusivities [61, 62]. In theory, the Nernst-Planck relationship instead of Fick's law (see next section) should be applied to interpret data from long-term immersion tests even when there is no electrical gradient applied.

Besides chloride ions, diffusion of sulphate ions is also a relevant research area because sulphate attack is an important durability problem in coastal concrete structures. The diffusion coefficient of sulphate ions is normally measured by an in-diffusion method in which the sample is placed in a sodium sulphate solution (5%) [63]. A similar migration test protocol for chloride can also be applied for the determination of sulphate diffusion coefficient [64, 65].

*Electro-migration technique*

Electro-migration tests have been developed to accelerate the ionic transport by applying an electrical field. The setup consists of a thin sample located between two electrodes immersed in electrolyte solutions (see Figure 3.2.11). The ionic species for which diffusivity has to be measured is added to the upstream compartment. A constant electrical potential difference is applied across the sample. In steady state migration tests, the evolution of the concentration of a given ionic species in the downstream compartment is monitored until steady-state is reached. For non-steady-state migration tests, the concentration profile of the ionic species within the sample is measured after a given period. The calculation of the diffusion coefficient is based on the Nernst–Planck equation without advection term [66]:

$$J = -D_a \nabla C - D_a C \frac{zF}{RT} \nabla \Psi \ \textit{(Equation 12.)}$$

$$\frac{\partial C}{\partial t} = -\nabla J$$

where $z$ is the valence number; $F$ is the Faraday constant (96485.33289 C mol$^{-1}$), $R$ is the ideal gas constant (8.3145 J/mol $^{\circ}$K), $T$ is the temperature of the liquid [$^{\circ}$K] and $\Psi$ is the electrical potential [kg.m$^2$/s$^2$.coulomb]. On the right-hand side of Eq. (12), the first term stands for diffusion and the second term stands for electro-migration. The dominant movement of ionic species in this setup is the electro-migration, which is dependent on both the diffusion coefficient and the potential gradient. Note that chemical activity effects are neglected in Eq. (12). At steady-state and with the assumption that electro-migration is the dominant transport process, it is possible to calculate the effective diffusion coefficient as follows:

$$D_e = \frac{J_{SS} R T L}{z F C_s \Delta \Psi} \ \textit{(Equation 13.)}$$

where $C_s$ is the source (boundary) concentration [mol/m$^3$], $L$ is the length of sample [m] and $\Delta\Psi$ is the potential difference [kg.m$^2$/s$^2$.coulomb]. The steady state flux $J_{SS}$ [mol/m$^2$.s] can be calculated from the concentration evolution in the downstream compartment.
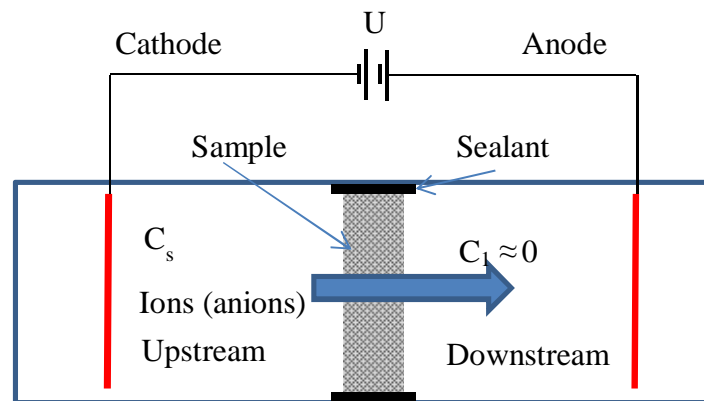


*Figure 3.2.11. Electro-migration diffusion setup.*

In non-steady-state tests, concentration profiles (as in the case of in-diffusion technique) are used and, if the advection term is negligible, the following analytical solution of Equation (12) is valid [67]:

$$C = \frac{C_s}{2}\left[ e^{ax} erfc\left(\frac{x+aD_a t}{2\sqrt{D_a t}}\right) + erfc\left(\frac{x-aD_a t}{2\sqrt{D_a t}}\right)\right] \text{(Equation 14.)}$$

where $a = \frac{zF\Delta\Psi}{RTL}$. Electro-migration tests offer a possibility to significantly shorten the measurement time for ionic species [67-70]. The method was also standardized in ASTM C1202-97 [71] and Nordtest NT Build 492 [72]. For cement-based materials, the most commonly investigated ion is chloride, because of the extent of reinforcement corrosion damage due to de-icing and exposure to marine environment. The non-steady-state diffusion coefficient is about one order of magnitude higher than the steady-state diffusion coefficient due to binding effects and up to several times higher than that from the electrical resistivity technique [73].

*Electrical resistivity technique*

The diffusion coefficient can be alternatively obtained by exploiting the analogy between electrical conductivity and diffusion of ions in a porous material. Based on the Nernst–Einstein equation, diffusion, electrical conductivity and resistivity are linked as:

$$\frac{D_e}{D_0} = \frac{\sigma_e}{\sigma_0} = \frac{\rho_0}{\rho_e} \text{ (Equation 15.)}$$

where $\sigma_e$ and $\sigma_0$ [S/m] are the electrical conductivity of the sample and of pore solution, respectively and $\rho_e$ and $\rho_0$ [m/S] are the electrical resistivity of the sample and the pore solution, respectively. The electrical resistivity of the sample is measured by applying a known current/voltage. The resistivity of the sample can be then determined as:

$$\rho_e = \frac{\Delta\Psi}{I}\frac{A}{L} \text{ (Equation 16.)}$$

where $\Psi$ and $I$ [A] are the electrical potential and current passed through the sample, respectively and $A$ [m$^2$] and $L$ [m] are the cross sectional area and length of the sample, respectively. However, determination of the pore solution resistivity is difficult. The pore solution has to be extracted under extremely high pressure (up to 400 MPa) in order to determine its resistivity. The electrical resistivity can also be estimated if the pore water composition of cement paste is known [74]. An alternative way is to replace the pore solution by a known resistivity solution, which is time consuming and the electrical properties of the known solution may change due to the interaction with the cement matrix.

*Factors influencing diffusion*

One may expect that the intrinsic factors (e.g. porosity, size distribution, tortuosity, specific surface area) would affect diffusion in the same way as for permeability. However, as permeability transport mainly occurs in meso and macro pore sizes, while diffusive transport could also occur in micro (gel) pore sizes (and dead-end pores), the impacts would be different at different ranges of

pore sizes. In micropore level, Knudsen diffusion is the main mechanism, while molecular diffusion is the dominant process in larger pore size ranges.

Different methods might result in inconsistent effective diffusion coefficients. The difference is sometimes not only because of the setup itself but also because of the way to interpret experimental data. In order to obtain the diffusion coefficients, a number of assumptions (e.g. constant source concentration, dominant transport mechanisms, multi/single species transport) have to be made. If the experiments do not fulfil these assumptions, results will significantly differ. In case of ionic diffusion determined by the migration methods, a higher applied potential results in higher diffusion coefficients [75]. The source concentration significantly affects the interpretation of diffusion coefficients in non-steady state; but not in steady state [76]. The non-steady state migration method results in a higher chloride diffusivity compared to the diffusivity obtained from the steady state migration test [54, 73].

**Concluding remarks**

Since its importance and hard measurement, a variety of test methods have been developed to measure transport properties of cement-based materials and in this chapter available test methods for the determination of permeability and diffusion in the laboratory have been reviewed. It becomes clear that different methods do not always lead to consistent results. For permeability measurements, the variation of measured values is sometimes up to 2 orders of magnitude. For diffusion measurements, the values obtained by different methods are less scattered. Most of the test procedures are applicable for a specific purpose or to certain testing species. The straightforward comparison of observed experimental data may not give a true indication of the relative properties of different materials unless they are determined using the same or at least similar test methods.

Traditional experimental methods require steady state conditions to be reached, which is very time consuming but normally results in reliable results due to its simple interpretation and fewer (or no) assumptions to be made. However, to reduce the measurement time, many methods have been proposed to accelerate the transport by applying a high pressure/concentration gradient or applying an electrical field. These accelerated methods are usually accompanied by many practical problems (e.g. cracking, heating). Furthermore, many assumptions are made to simplify the problem allowing the application of conventional physical/chemical laws to interpret the experimental data.

To conclude, the measurement methods for the determination of transport properties are, to some extent, not accepted worldwide, which leads to a difficulty in comparison of the values obtained from different methods. There is still a need to develop methods which meet some key requirements such as high repeatability, short measurement time, high accuracy, easy application and fewer assumptions made.

**References**

[1] Glasser FP, Marchand J, Samson E. Durability of concrete - Degradation phenomena involving detrimental chemical reactions. Cement and Concrete Research. 2008;38(2):226–246.
[2] Pabalan RT, Glasser FP, Pickett DA, Walter GR, Biswas S, Juckett MR, et al. Review of Literature and Assessment of Factors Relevant to Performance of Grouted Systems for Radioactive Waste Disposal. CNWRA 2009-001: Center for Nuclear Waste Regulatory Analyses, San Antonio, Texas; 2009. p. 359.
[3] Dullien FAL. Porous media : fluid transport and pore structure. San Diego: Academic Press; 1992.
[4] Selvadurai APS, Carnaffan P. A transient pressure pulse method for the measurement of permeability of a cement grout. Can J Civil Eng. 1997;24(3):489–502.
[5] Loosveldt H, Lafhaj Z, Skoczylas F. Experimental study of gas and liquid permeability of a mortar. Cement and Concrete Research. 2002;32(9):1357–1363.

[6] Vichit-Vadakan W, Scherer GW. Measuring permeability of rigid materials by a beam-bending method: III, cement paste. J Am Ceram Soc. 2002;85(6):1537–1544.

[7] Bhargava A, Banthia N. Measurement of concrete permeability under stress. Exp Techniques. 2006;30(5):28–31.

[8] Scherer GW. Dynamic pressurization method for measuring permeability and modulus: I. theory. Mater Struct. 2006;39(10):1041–1057.

[9] Grasley ZC, Scherer GW, Lange DA, Valenza JJ. Dynamic pressurization method for measuring permeability and modulus: II. cementitious materials. Mater Struct. 2007;40(7):711–721.

[10] Scherer GW, Valenza JJ, Simmons G. New methods to measure liquid permeability in porous materials. Cement and Concrete Research. 2007;37(3):386–397.

[11] Picandet V, Rangeard D, Perrot A, Lecompte T. Permeability measurement of fresh cement paste. Cement and Concrete Research. 2011;41(3):330–338.

[12] Ludirdja D, Berger RL, Young JF. Simple Method for Measuring Water Permeability of Concrete. Aci Mater J. 1989;86(5):433–439.

[13] Jones CA, Grasley ZC. Correlation of Radial Flow-Through and Hollow Cylinder Dynamic Pressurization Test for Measuring Permeability. J Mater Civil Eng. 2009;21(10):594–600.

[14] Eldieb AS, Hooton RD. A High-Pressure Triaxial Cell with Improved Measurement Sensitivity for Saturated Water Permeability of High-Performance Concrete. Cement and Concrete Research. 1994;24(5):854–862.

[15] Eldieb AS, Hooton RD. Water-Permeability Measurement of High-Performance Concrete Using a High-Pressure Triaxial Cell. Cement and Concrete Research. 1995;25(6):1199–1208.

[16] Nimmo JR. Experimental Testing of Transient Unsaturated Flow Theory at Low Water-Content in a Centrifugal Field. Water Resour Res. 1990;26(9):1951–1960.

[17] Nimmo JR, Rubin J, Hammermeister DP. Unsaturated Flow in a Centrifugal Field - Measurement of Hydraulic Conductivity and Testing of Darcy Law. Water Resour Res. 1987;23(1):124–134.

[18] ASTM. ASTM Standard D6527 - 00(2008), "Standard Test Method for Determining Unsaturated and Saturated Hydraulic Conductivity in Porous Media by Steady-State Centrifugation". ASTM International, West Conshohocken, PA; 2008. p. 10.

[19] Conca JL, Wright J. Diffusion And Flow In Gravel, Soil, And Whole Rock. Applied Hydrogeology. 1992;1(1):5–24.

[20] Phung QT, Maes N, De Schutter G, Jacques D, Ye G. Determination of water permeability of cementitious materials using a controlled constant flow method. Constr Build Mater. 2013;47(0):1488–1496.

[21] Brace WF, Walsh JB, Frangos WT. Permeability of Granite under High Pressure. J Geophys Res. 1968;73(6):2225–2236.

[22] Meziani H. Gas permeability measurements of cement-based materials under hydrostatic test conditions using a low-transient method. Magazine of Concrete Research. 2006;58(8):489–503.

[23] Scherer GW. Measuring permeability of rigid materials by a beam-bending method: I, theory. J Am Ceram Soc. 2000;83(9):2231–2239.

[24] Scherer GW. Bending of Gel Beams - Method for Characterizing Elastic Properties and Permeability. J Non-Cryst Solids. 1992;142(1-2):18–35.

[25] Vichit-Vadakan W, Scherer GW. Measuring permeability of rigid materials by a beam-bending method: II, porous glass. J Am Ceram Soc. 2000;83(9):2240–2245.

[26] Vichit-Vadakan W, Scherer GW. Measuring permeability and stress relaxation of young cement paste by beam bending. Cement and Concrete Research. 2003;33(12):1925–1932.

[27] Scherer GW, Hdach H, Phalippou J. Thermal Expansion of Gels: A Novel Method for Measuring Permeability. J Non-Cryst Solids. 1991;130(2):157–170.

[28] Scherer GW. Measuring permeability by the thermal expansion method for rigid or highly permeable gels. Journal of Sol-Gel Science and Technology. 1994;3(1):31–40.

[29] Scherer GW. Thermal expansion kinetics: Method to measure permeability of cementitious materials: I, theory. J Am Ceram Soc. 2000;83(11):2753–2761.

[30] Ai H, Young JF, Scherer GW. Thermal expansion kinetics: Method to measure permeability of cementitious materials: II, application to hardened cement pastes. J Am Ceram Soc. 2001;84(2):385–391.

[31] Jones CA, Grasley ZC. Correlation of hollow and solid cylinder dynamic pressurization tests for measuring permeability. Cement and Concrete Research. 2009;39(4):345–352.

[32] Klinkenberg LJ. The Permeability of Porous Media to Liquids and Gases. Drilling and Production Practice: American Petroleum Institute; 1941. p. 14.

[33] Iversen BV, Moldrup P, Schjonning P, Jacobsen OH. Field Application of a Portable Air Permeameter to Characterize Spatial Variability in Air and Water Permeability. Vadose Zone J. 2003;2(4):618–626.

[34] Loll P, Moldrup P, Schjonning P, Riley H. Predicting saturated hydraulic conductivity from air permeability: Application in stochastic water infiltration modeling. Water Resour Res. 1999;35(8):2387–2400.

[35] Alarcon-Ruiz L, Brocato M, Dal Pont S, Feraille A. Size Effect in Concrete Intrinsic Permeability Measurements. Transport Porous Med. 2010;85(2):541–564.

[36] Hearn N. Self-sealing, autogenous healing and continued hydration: What is the difference? Mater Struct. 1998;31(212):563–567.

[37] Hearn N, Morley CT. Self-sealing property of concrete - Experimental evidence. Mater Struct. 1997;30(201):404–411.

[38] Edvardsen C. Water permeability and autogenous healing of cracks in concrete. Aci Mater J. 1999;96(4):448–454.

[39] Picandet V, Khelidj A, Bellegou H. Crack effects on gas and water permeability of concretes. Cement and Concrete Research. 2009;39(6):537–547.

[40] Charron J-P, Denarié E, Brühwiler E. Transport properties of water and glycol in an ultra high performance fiber reinforced concrete (UHPFRC) under high tensile deformation. Cement and Concrete Research. 2008;38(5):689–698.

[41] Christensen BJ, Mason TO, Jennings HM. Comparison of measured and calculated permeabilities for hardened cement pastes. Cement and Concrete Research. 1996;26(9):1325–1334.

[42] Goto S, Roy DM. The Effect of W-C Ratio and Curing Temperature on the Permeability of Hardened Cement Paste. Cement and Concrete Research. 1981;11(4):575–579.

[43] Soongswang P, Tia M, Bloomquist D. Factors Affecting the Strength and Permeability of Concrete Made with Porous Limestone. Aci Mater J. 1991;88(4):400–406.

[44] Wong HS, Zimmerman RW, Buenfeld NR. Estimating the permeability of cement pastes and mortars using image analysis and effective medium theory. Cement and Concrete Research. 2012;42(2):476–483.

[45] Lafhaj Z, Goueygou M, Djerbi A, Kaczmarek M. Correlation between porosity, permeability and ultrasonic parameters of mortar with variable water/cement ratio and water content. Cement and Concrete Research. 2006;36(4):625–633.

[46] Katz AJ, Thompson AH. Quantitative Prediction of Permeability in Porous Rock. Phys Rev B. 1986;34(11):8179–8181.

[47] Das BB, Kondraivendhan B. Implication of pore size distribution parameters on compressive strength, permeability and hydraulic diffusivity of concrete. Constr Build Mater. 2012;28(1):382–386.

[48] Carman PC. Fluid flow through granular beds. T I Chem Eng-Lond. 1937;15:150–166.

[49] Kozeny J. Über kapillare Leitung des Wassers im Boden. Akad Wiss Wien. 1927;136:271–306.

[50] García-Gutiérrez M, Cormenzana JL, Missana T, Mingarro M, Molinero J. Overview of laboratory methods employed for obtaining diffusion coefficients in FEBEX compacted bentonite. Journal of Iberian Geology. 2006;32(1):37–53.

[51] Phung QT, Maes N, Jacques D, Jacop E, Grade A, Schutter GD, et al. Determination of diffusivities of dissolved gases in saturated cement-based materials  In: Dehn F, Beushausen H-D, Alexander MG, Moyo P, editors. International Conference on Concrete Repair, Rehabilitation and Retrofitting IV. Leipzig, Germany: CRC Press; 2015. p. 1019–1027.

[52] Phung QT. Effects of Carbonation and Calcium Leaching on Microstructure and Transport Properties of Cement Pastes [PhD thesis]. Belgium: Ghent University; 2015.

[53] Jacops E, Volckaert G, Maes N, Weetjens E, Govaerts J. Determination of gas diffusion coefficients in saturated porous media: He and $CH_4$ diffusion in Boom Clay. Applied Clay Science. 2013;83–84(0):217–223.

[54] Castellote M, Andrade C, Alonso C. Measurement of the steady and non-steady-state chloride diffusion coefficients in a migration test by means of monitoring the conductivity in the anolyte chamber - Comparison with natural diffusion tests. Cement and Concrete Research. 2001;31(10):1411–1420.

[55] Park B, Jang SY, Cho J-Y, Kim JY. A novel short-term immersion test to determine the chloride ion diffusion coefficient of cementitious materials. Constr Build Mater. 2014;57(0):169–178.

[56] Yu SW, Page CL. Diffusion in cementitious materials: 1. Comparative study of chloride and oxygen diffusion in hydrated cement pastes. Cement and Concrete Research. 1991;21(4):581–588.

[57] Crank J. The mathematics of diffusion: Clarendon Press; 1975.

[58] ASTM. ASTM Standard Test Method for Determining the Apparent Chloride Diffusion Coefficient of Cementitious Mixtures by Bulk Diffusion (C 1556-04). 2004.

[59] Nordtest. Concrete, hardened: Accelerated chloride penetration (NT BUILD 443). 1995.

[60] Ollivier J-PTJ-MCM. Physical properties of concrete and concrete constituents. London; Hoboken, N.J.: ISTE/Wiley; 2012.

[61] Claisse PA. Transport properties of concrete: measurement and applications. Waltham, MA: Woodhead Pub.; 2014.

[62] Lizarazo-Marriaga J, Claisse P. Determination of the concrete chloride diffusion coefficient based on an electrochemical test and an optimization model. Mater Chem Phys. 2009;117(2-3):536–543.

[63] Sun C, Chen J, Zhu J, Zhang M, Ye J. A new diffusion model of sulfate ions in concrete. Constr Build Mater. 2013;39(0):39–45.

[64] Moon H-Y, Lee S-T, Kim H-S, Kims S-S. Experimental Study on the Sulfate Resistance of Concrete Blended Ground Granulated Blast-furnace Slag for Recycling. Geosystem Engineering. 2002;5(3):67–73.

[65] Tumidajski PJ, Turc I. A rapid test for sulfate ingress into concrete. Cement and Concrete Research. 1995;25(5):924–928.

[66] Bockris JOM, Reddy AKN. Modern Electrochemistry: An Introduction to an Interdisciplinary Area: Plenum Press; 1974.

[67] Luping T, Nilsson L-O. Rapid Determination of the Chloride Diffusivity in Concrete by Applying an Electric Field. Aci Mater J. 1993;89(1): 49–53.

[68] Aguayo M, Yang P, Vance K, Sant G, Neithalath N. Electrically driven chloride ion transport in blended binder concretes: Insights from experiments and numerical simulations. Cement and Concrete Research. 2014;66(0):1–10.

[69] Yang CC, Chiang SC, Wang LC. Estimation of the chloride diffusion from migration test using electrical current. Constr Build Mater. 2007;21(7):1560–1567.

[70] Truc O, Ollivier JP, Carcasses M. A new way for determining the chloride diffusion coefficient in concrete from steady state migration test. Cement and Concrete Research. 2000;30(2):217–226.

[71] ASTM. Standard Test Method for Electrical Indication of Concrete's Ability to Resist Chloride Ion Penetration (C1202-97). 1997.

[72] NT BUILD 492: Concrete, mortar and cement-based repair materials: Chloride migration coefficient from non-steady-state migration experiments Finland: Nordtest; 1999.

[73] Tong L, Gjørv OE. Chloride diffusivity based on migration testing. Cement and Concrete Research. 2001;31(7):973–982.

[74] Snyder KA, Feng X, Keen BD, Mason TO. Estimating the electrical conductivity of cement paste pore solutions from OH-, K+ and Na+ concentrations. Cement and Concrete Research. 2003;33(6):793–798.

[75] McGrath PF, Hooton RD. Influence of voltage on chloride diffusion coefficients from chloride migration tests. Cement and Concrete Research. 1996;26(8):1239–1244.

[76] Narsillo GA, Li R, Pivonka P, Smith DW. Comparative study of methods used to estimate ionic diffusion coefficients using migration tests. Cement and Concrete Research. 2007;37(8):1152–1163.

## 3.3  Laboratory observation of processes in heterogeneous material

*J. Kulenkampff*

*Helmholtz-Zentrum Dresden-Rossendorf, Forschungsstelle Leipzig - Interdisziplinäre Isotopenforschung, Germany*

The interface between cement-based barrier constructions and the host rock should be considered as highly heterogeneous zone: The contact area between cement and rock is heterogeneous on principle. The host rock in this zone has to be attributed to the excavation damage zone which is inevitable caused by stress release during excavation and characterized by a network of fractures with elevated porosity and transport parameters. Also the cement in the interfacial zone should be considered as heterogeneous material, because the technical constraints at the breast limit efficient homogenisation and compaction. The typical largest scale of these heterogeneities is in the order of centimetres.

Therefore, reactive transport processes are progressing in a highly heterogeneous material with disorder on the centimetre scale. This issue is relevant for the function of the barrier, because one consequence is the evolution of preferential transport zones of reactive flow and diffusion. Preferential zones with higher transport rates generally are less tortuous, which also means a smaller effective internal surface area. Therefore, these zones delimit the barrier function both by increased transport rate and decreased retention by sorption. One possible hypothetical scenario therefore is transport along preferential pathways with inconsiderable sorption. This worst case could be mitigated by precipitation reactions that are due to the transport of water that is not in equilibrium with the material. Precipitation could clog preferential pathways, but also amplify the heterogeneous effects.

Experimental determination of such heterogeneous effects with common flow or diffusion experiments is laborious and requires a large number of studies in order to match these delimiting zones. Another approach is the comprehensive description of the pore structure, material properties, and reactions as parameters for model simulation on the pore scale. The detailed characterization on the pore space with multiscale imaging methods is particularly intricate, because a hierarchy of structures over many orders should be considered, from surface characteristics on the molecular scale to fine-layering on the centimetre scale. This range can only be covered by a hierarchical suite of different methods with different spatial resolution (1). However, the huge size of these hierarchical tomographic data currently precludes composition and processing of pore-scale simulation models in such detailed structures. Typical model simulations are conducted on structural models that are based on the limited resolution range of a particular tomographic method.

These issues can be overcome by direct tomographic observation of the transport processes itself (2, 3). Frequently, the most meaningful observable is the concentration of dissolved or dispersed species, which is an intensive thermodynamic parameter that is most relevant for aligning observations with simulation results from models of the processes. Concentration is a continuous value, referred to a finite test volume which is defined by the spatial resolution of the measuring method. Here, spatial resolution is merely the response function which controls the smoothing of the image.

Ionic concentrations can be monitored with different types of Electrical Impedance Tomography (EIT). These are frequently applied to investigate transport processes of conductive solutions in soils and rocks. However, electrical resistivity, as one of these parameters, depends on a variety of

material parameters and rock-fluid interactions; therefore the result is not univocal. Other imaging methods apply tracers for labelling, which facilitates detection and quantification of the species. Spatiotemporal visualization of labelled substances requires tomographic methods with selective response to the tracer. In the field of biomedical research these techniques are called "molecular imaging methods" (4). From these methods, magnetic resonance imaging (MRI), single photon emission computed tomography (SPECT), and positron emission tomography (PET) are suited for opaque media. In contrast to ERT, these methods selectively respond to the concentration of protons or specific tracer isotopes, respectively, but they are mere laboratory applications and barely suitable for field applications. The methods differ with regard to the matrix effect. In the case of MRI, distortions of the magnetic field by paramagnetic compounds of the matrix, and in the case of SPECT, radiation attenuation and scattering, are constricting their applicability. PET is least affected by material inferences.

PET is perfectly selective and by far the most sensitive method, because the response is directly and only related to the number of decaying positrons, and thus the number of tracer atoms. The sensitivity is better than pico-moles per µL, depending on the decay characteristics of the PET-nuclide and the noise level. With this ultimate sensitivity, PET can serve as gold-standard for tomographic imaging of tracer concentrations.

It is highly recommendable to apply high-resolution PET-scanners ("small animal PET scanner") with a resolution around 1 mm, otherwise major heterogeneous effects are not distinguishable. Also, this is a reasonable scale for process observations on the core scale, in the range of 10 cm, which also is the order of the representative elementary volume for a large group of inhomogeneous materials. The spatial resolution of clinical PET-scanners (3 to 5 mm) is rather poor, compared to the maximum sample diameter of 10 cm, and tends to equilibrate the major features of inhomogeneous transport patterns (5). We could prove the benefits of PET observation for different types of processes (6), especially for diffusion processes in Opalinus clay (7). The method is ready for spatio-temporal visualization of transport processes on the laboratory scale for enhanced process understanding of reaction and transport processes at the interface between cement and clay formations.

## References

[1]     Hemes S, Desbois G, Urai JL, Schröppel B, Schwarz J-O. Multi-scale characterization of porosity in Boom Clay (HADES-level, Mol, Belgium) using a combination of X-ray µ-CT, 2D BIB-SEM and FIB-SEM tomography. Microporous and Mesoporous Materials. 2015;208:1–20.
[2]     Wang M. Industrial Tomography. Cambridge (UK): Woodhead Publishing; 2015.
[3]     Williams RAB, M. S. Process tomography:principles, techniques, and applications. Oxford (UK): Butterworth-Heinemann Ltd; 1995.
[4]     Weissleder R, Ross, B.D., Rehemtulla, A., Gambhir, S.S. Molecular Imaging. Shelton, USA: People's Medical Publishing House; 2010.
[5]     Kulenkampff J, Gründig M, Richter M, Enzmann F. Evaluation of positron-emission-tomography for visualisation of migration processes in geomaterials. Physics and Chemistry of the Earth, Parts A/B/C. 2008;33(14–16):937–42.
[6]     Kulenkampff J, Gründig M, Korn N, Zakhnini A, Barth T, Lippmann-Pipke J. Application of high-resolution positron-emission-tomography for quantitative spatiotemporal process monitoring in dense material. 7 World Congress on Industrial Process Tomography, 02092013, Krakow, Polen2013.
[7]     Kulenkampff J, Gründig M, Zakhnini A, Gerasch R, Lippmann-Pipke J. Process tomography of diffusion, using PET, to evaluate anisotropy and heterogeneity. Clay Minerals. 2015;50(3):369–75.

# 4 Materials

## 4.1 Low hydration heat/Low pH formulations

*X. Bourbon*

*Andra - French National Agency for nuclear Waste Management, R&D Division, France*

**Principles of formulation**

**To lower the hydration heat**: to decrease the cement content and to use or to target a blended hydraulic binder (chemical reactive and non-reactive mineral additions).

**To lower the pH**: to neutralize the main alkaline hydrates in the hydrated cement and to immobilize the alkaline ions ($Na^+$ and $K^+$): substitution of the cement with chemical reactive mineral additives (pozzolanic or hydraulic compounds); to minimize the total initial amount in the raw materials: selection of a cement with a low alkali content (as low as achievable).

Thus, to reach both properties 'low hydration heat' and 'low pH' means decreasing the clinker content in the binder and to use a blend with an significant substitution level. From a chemical point of view (for Si-Ca cements), decreasing the pH of the hydrated cement means decreasing the Ca/Si ratio in the dry mix to have a mean composition in the hydrated cement with a C/S ratio less than 1.0 (Figure 4.1.1 from Greenberg & Chang, 1964, confirmed by Fuji & Kondo (1981), Harris et al. (2002) or Chen et al. (2004)). The C-S-H chemical stability domain ends at a C/S ratio close to 0.6. The chemical composition of the C-S-H phases to be considered in low pH concrete is then a C/S ratio from 0.6 to 1.0.
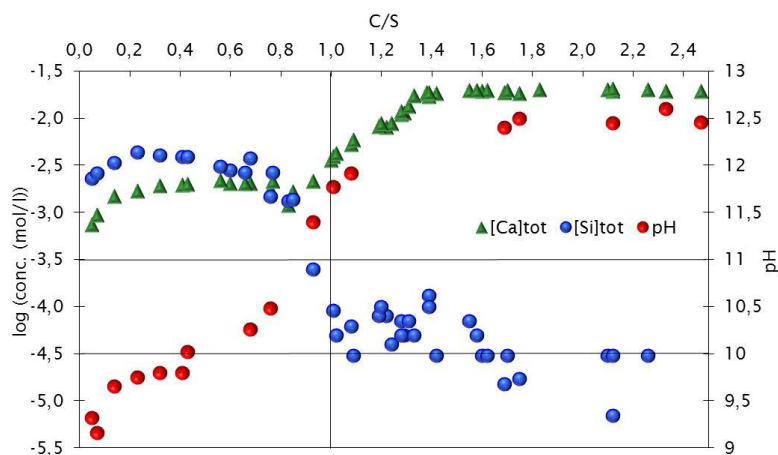


*Figure 4.1.1. pH, Ca and Si concentration evolutions with C/S ratio.*

Cau-dit-Coumes *et al.* (2006) tested binary and ternary blends using a CEM I (according to European standards) as reference material. The blends were made with the following Supplementary Cementitious Materials (SCM): metakaolin (MK), silica fume (SF), fly ashes (FA) and blast furnace slag (BFS) (Figure 4.1.2). To reach the limit of pH ~11, the total silica content in the "dry blend" has to be more than 50%, whatever the mix. Comparing these different SCM, neither ternary nor binary blends using metakaolin fulfill the chemical specification of pH 11 after hydration. In the case of binary blends with CEM I and SF, the SF content has to be equal or more than 40%. Ternary blends are more various and offer more possibilities. The most accurate binders

seem to be based on a CEM I/SF mix with fly ashes or blast furnace slag (ternary blends). Those using BFS fulfill more easily the chemical criterion (due to the lower chemical reactivity of FA compared to BFS).



*Figure 4.1.2. pH evolution according to total silica content in the dry mix.*

**Raw materials**

Raw materials have to be chosen with regards to the chemical expectations (low pH) and boundary conditions (chemical reactivity controlled by the geological medium and/or in situ clay materials – clay plug and backfill), as well as the physical requirements (low hydration heat, high performance cement).

1. **Clinker** (based on a CEM I use): A cement CEM I offers the possibility to adapt/control the clinker content in the blend and the total alkali content as well as the chemical resistanc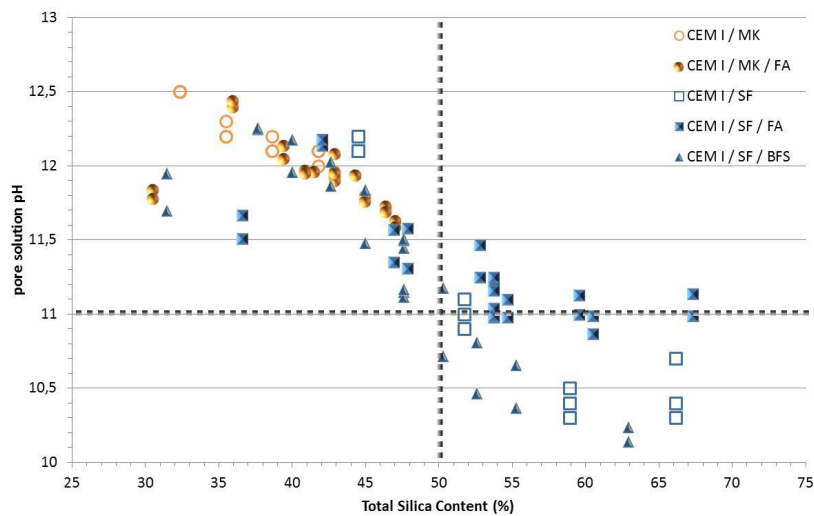e to chemical degradations such as delayed ettringite formation. The chemical boundary conditions, imposed by the geological medium and the clay materials, can be taken into account by various CEM I, such as sulfate resisting cement if required.

We should notice that low hydration heat cements (i.e. CEM III – slag cement) are available from an industrial point of view. These cements do not have any "low pH" properties but can constitute a raw material (the "clinker/BFS" mix is already done). In these conditions it is more difficult to change/to control precisely the clinker content in the dry mix. It is an alternative solution but offers less possibility to adapt the clinker content and then the final chemical properties.

2. **Pozzolanic compounds**: Silica fume (SF) and Fly Ashes (FA) are possible candidates for a low pH concrete composition. Proportions in the mix allow adjusting the total silica content as well as the kinetic of hydration and the final pH reached after full hydration. SF is a "pure" compound containing more than 95% of $SiO_2$. FA compositions are impossible to control. The compositions are strongly depending on the origin and may have chemical consequences on the chemical behaviour of the concrete.

3. **Hydraulic compounds**: Blast Furnace Slag (BFS) is a well know hydraulic compound, with a behaviour same as a cement in alkaline conditions. It could replace high amounts of clinker, keeping at a high level the performances of the concrete and promoting the pozzolanic reaction, then having a strong impact on the pH value. In ternary blends associated with silica fume, BFS are highly efficient to decrease quickly the pH value and to reach a value close to 10.5 within

few weeks. Moreover, slag cements are usually used/recommended in highly chemical reactive/aggressive media, enhancing the chemical stability of the concrete.

The compositions and recipe have to be adapted to the *in situ* conditions of use and the final requirements (regarding shrinkage, cracks evolution with time, water permeability and drying). At present it is impossible to define a HPC composition without admixtures. Their role is both at a short timescale and after setting. At first, the target is to facilitate the conditions of use. The main key issues are the workability and to delay the setting. Then expecting a HPC, as a result, the concrete have to be compact enough (especially lowering the water-to-binder (W/B) ratio). These different requirements, lead to the use of superplasticizers and water reducing admixtures. In the mix proportions, the admixture dosages have to be lowered as much as possible due to the impact of organic matter at a global scale (presence of organic complexing agents, bioactivity …).

### «Reference» low pH compositions

*Composition*

On the basis of ternary blends, potentially the most efficient to fulfill the chemical requirement within few weeks, two "reference" compositions have been developed and optimized (Cau-dit-coumes et al., 2006; Codina, 2007; Garcia & Verdier, 2009; Leung, 2015). From this point (a ternary blend) other surveys led to a shotcrete and a self-compacted concrete (see below '§ FSS').

*Table 4.1.1. Possible reference compositions.*

|  | Binder (kg/m$^3$) | CEM I (mass.%) | SF (mass.%) | FA (mass.%) | BFS (mass.%) | W/B | G/S | SP (mass.%) |
|---|---|---|---|---|---|---|---|---|
| $T_{FA}$ | 375 | 37.5 | 32.5 | 30.0 | 0 | 0.4 | 1.1 | 1.5 |
| $T_{BFS}$ | 380 | 20.0 | 32.5 | 0 | 47.5 | 0.4 | 1.1 | 1.5 |

*Note: $T_{FA}$ for ternary blend CEM I/SF/FA; $T_{BFS}$ for ternary blend CEM I/SF/BFS; G/S: Gravel to Sand ratio to keep possible pumping and workability; SP: superplasticizer*

*Hydration*

From a kinetic point of view, these concretes are significantly different from classical materials. Their hydration period occurs over several years, compared to few weeks or few months for blended cement such as CEM V.

Even if the target pH ~11 is reached after few weeks for most of the tested blends, their hydration (and the decrease of the pH) continues. Four to five years are required to reach, as close as possible, the full hydration of these materials. As a consequence, the maximum temperature reached during setting is very low (less than 10–12 °C) and delayed (between 36h and 48h) compared to classical concretes (El-Bitouri, 2015; Leung, 2015).

*Table 4.1.2. pH evolution with time for low pH cements (ternary blends).*

| pH | 7 days | 28 days | 90 days | 8 months | 4 years | 8 years |
|---|---|---|---|---|---|---|
| Ternary blend CEM I/SF/FA | 13,0 | 11,2 | 10,9 | 10,5 | 10,3 | 10,5 |
| Ternary blend CEM I/SF/BFS | 12,9 | 11,5 | 11,2 | 11,1 | 10,5 | 10,5 |

*Physical evolution*

Even if the thermal behaviour during setting is different, the mechanical evolutions of these formulations are similar to those of "classical HPC". The setting starts few hours after preparation and a period of 24 h is enough to have a concrete stable enough from a mechanical point of view, even if hydration continues and obviously change the physical properties of the material. After three months, more than 75% of the "final compressive strength" is reached, close to CEM V mechanical behaviour.

The estimated mechanical properties after full hydration are:

|            | Rc (MPa) | Rt (MPa) | E (GPa) |
|------------|----------|----------|---------|
| $T_{FA}$   | 86       | 4.1      | 43      |
| $T_{BFS}$  | 97       | 4.5      | 45      |
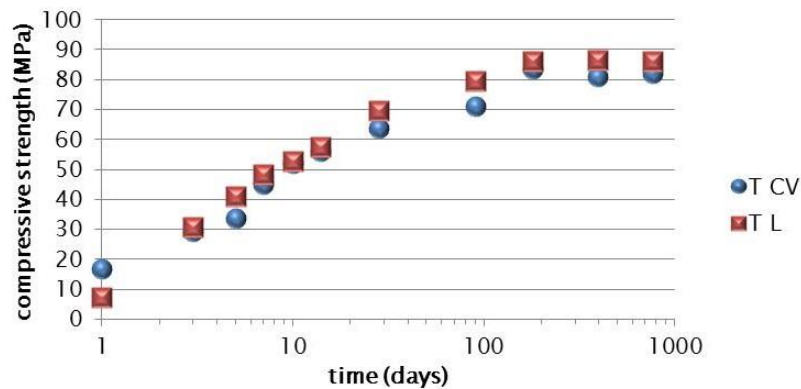


*Figure 4.1.3. Mechanical evolution with time of $T_{CV}$ and $T_L$ concretes.*

The mechanical properties are modeled on the basis of the hydration degree evolution using a De Schutter approach (De Schutter & Taerwe, 1996). This needs a characterization of each component of the blend independently and afterward a complete calculation as a mix (and not as the sum of single compounds) to validate the model. This validation has been done by Leung (2015) giving the opportunity to calculate the evolution of the mechanical properties with time (Figure 4.1.4 and Figure 4.1.5).
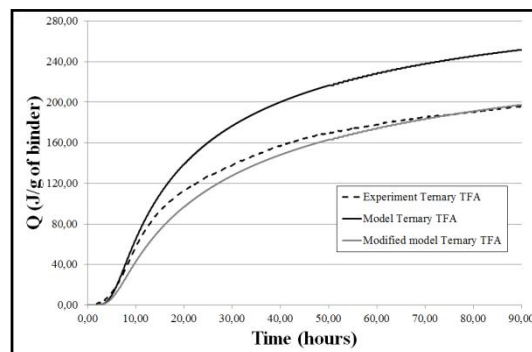


*Figure 4.1.4. Thermal release modelling during hydration ($T_{FA}$ formulation).*
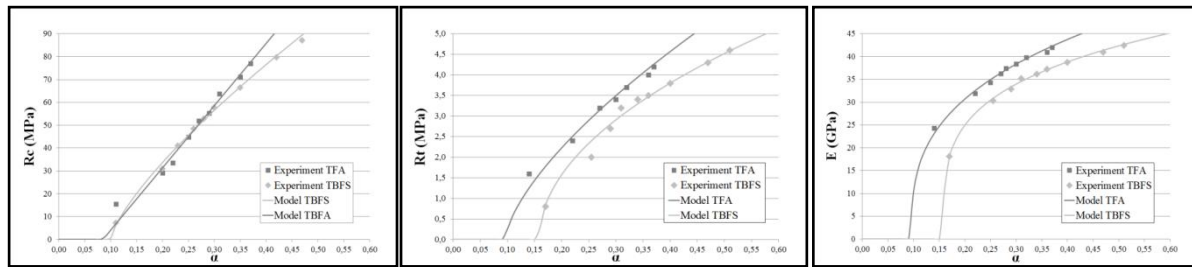
*Figure 4.1.5. Evolution of the mechanical properties of the $T_{FA}$ and $T_L$ concretes with the hydration degree.*

**«Candidate» low hydration heat/low pH mixtures**

Considering a Calcium/Silica chemical system, different mixes have been tested to fulfill the main chemical requirement (pH<11). Over the last decade, few countries have tested and developed low hydration heat/low pH mix compositions. Table summarizes the main types of blend and the resulting studies in eight countries through national or international programs (Canada, Finland, France, Japan, Spain, Sweden, Switzerland, USA). All these tested materials have as common characteristics, a high substitution level of the clinker (30% to 80%) and SCM are SF, FA and/or BFS.

*Table 4.1.3. Low hydration heat/low pH compositions.*

| Mix | Composition | pH (Eq. or interstitial Sol.) | |
|---|---|---|---|
| **Binary** CEM I/SF | CEM I 70%/SF 30% | 12.2 | Bach, 2010 |
| | CEM I 60%/SF 40% | 11.7 | Bach, 2010 |
| | | 12.2 11.1 | Garcia Calvo *et al.*, 2007 Alonso et al., 2008 |
| | | 11.0 11.4 | Vuorinen & Lehikoinen, 2005 Holt et al., 2014 |
| | | 11.3 | Fries *et al.,* 2007 |
| | CEM I 50%/SF 50% | 10.6 11.2 | Martino, 2007 Alonso et al., 2008 |
| **Ternary** CEM I/SF/FA | CEM I 37.5%/SF 32.5%/FA 30% | 11.1 | Bach, 2010 |
| | | 11.4 | Codina, 2007, 2008 |
| | CEM I 35% SF 35%/FA 30% | 10.9 10.5 | Garcia Calvo *et al.,* 2007 Alonso et al., 2008 |
| | CEM I 40%/SF 20%/FA 40% | 11.0 | Nishiuchi *et al.*, 2007; Kobayashi *et al.,* 2007 |
| | CEM I 37.5%/SF 32.5%/FA30% | 11.4 | Holt et al., 2014 |
| **Ternary** CEM I/SF/ BFS | CEM I 20%/SF 32.5%/BFS 47.5% | 11.0 | Codina, 2007, 2008; Bach, 2010 |
| | CEM I 37.5%/SF 31%/BFS 31.5% | 11.6 | Leung, 2015 |
| | CEM III 90%/nanosilica 10% | 12.3 | Lotenbach, 2008 |
| **Quaternary** CEM I/SF/ FA/BFS | CEM I 33%/BFS 13.5%/FA 13.5%/SF 40% | 12.1 | Codina, 2007, 2008 |
| | CEM I 40%/BFS 30%/FA 25%/SF 5% | 12.7 | Mattus & Dole, 2007 |

**International programs**

*TSX*

The Tunnel Sealing Experiment (TSX) was an international program performed at the Atomic Energy of Canada Limited (AECL) underground research laboratory close to 'lac du Bonnet' (MB, Canada) with international participation. The lead agencies were the Japan Nuclear Cycle Institute (JNC), French National Agency for Nuclear Waste Management (Andra), the United States Department of Energy (USDOE) (through the science advisor for Waste Isolation Pilot Plant (WIPP)) and Atomic Energy of Canada Limited (AECL). The TSX has been organized in two steps (1995/2002–2003/2008). The experiment began in 1995 with development of the concept and design. In 1997, the TSX tunnel and bulkhead keys were excavated. The installation of the bulkheads was completed in 1998 September, after which pressurization to 4 MPa was begun. The construction and pressurization took longer than initially anticipated extending the first unheated phase of the experiment to nearly seven years (Chandler et al. 2002). Japan, France and Canada then conducted the thermal/decommissioning phase of the experiment for an additional three years, where a temperature of 65 °C was reached at the upstream side of the bulkheads (Martino et al., 2008).

The TSX was designed to characterize and to assess the sealing potential of full-scale bulkheads made with swelling clay or concrete in a horizontal gallery at 420 m below the surface (Figure 4.1.6). One bulkhead was composed of approximately 9000 highly compacted sand-bentonite blocks, while the second was constructed using Low-Heat High-Performance Concrete (LHHPC) developed at AECL (Gray & Shenton 1998). These two plugs were separated by a "central chamber" filled with sand and then flooded with water. This test chamber was pressurized up to 4 MPa by means of a static water head in the first phase (1998/2002). A circulation pump and heaters were added for a second phase to reach the temperature of 65 °C in the bulkheads. Seepage data, together with solute transport data from tracer tests, were used to quantify the sealing characteristics of the two bulkheads. It should be noted here that the bulkheads in the TSX were not optimized tunnel seals. At the conclusion of heating, a three-month cooling period was followed by depressurization of the tunnel. Finally, samples were then taken to measure to physical properties of the materials.

The experiment was designed to characterize an achievable bulkhead performance using currently available technologies. In this context, the performance was defined as the ability of the bulkhead to restrict the flow of water in the axial direction of the tunnel. According to Chandler et al. (2002), the aims of the experiment were:

- to assess the applicability of technologies for construction of practicable concrete and bentonite bulkheads (to design and construct a concrete bulkhead as well as a bulkhead comprising highly compacted bentonite-based material);
- to evaluate the performance of each bulkhead, assessing seepage measurements through and around each bulkhead under an applied hydraulic gradient and to determine the factors which most influence the rate of seepage or transport;
- to identify and document the parameters that affect that performance.

The LHH-HP concrete has been formulated with:

> 97 kg/m$^3$ CEM I;
> 97 kg/m$^3$ silica fume;
> 2 129 kg/m$^3$ silica flour and siliceous aggregates.

The 76 m$^3$ were poured in eight hours (preparation in a surface facility, transferred with skips to the -420 level and pumped).
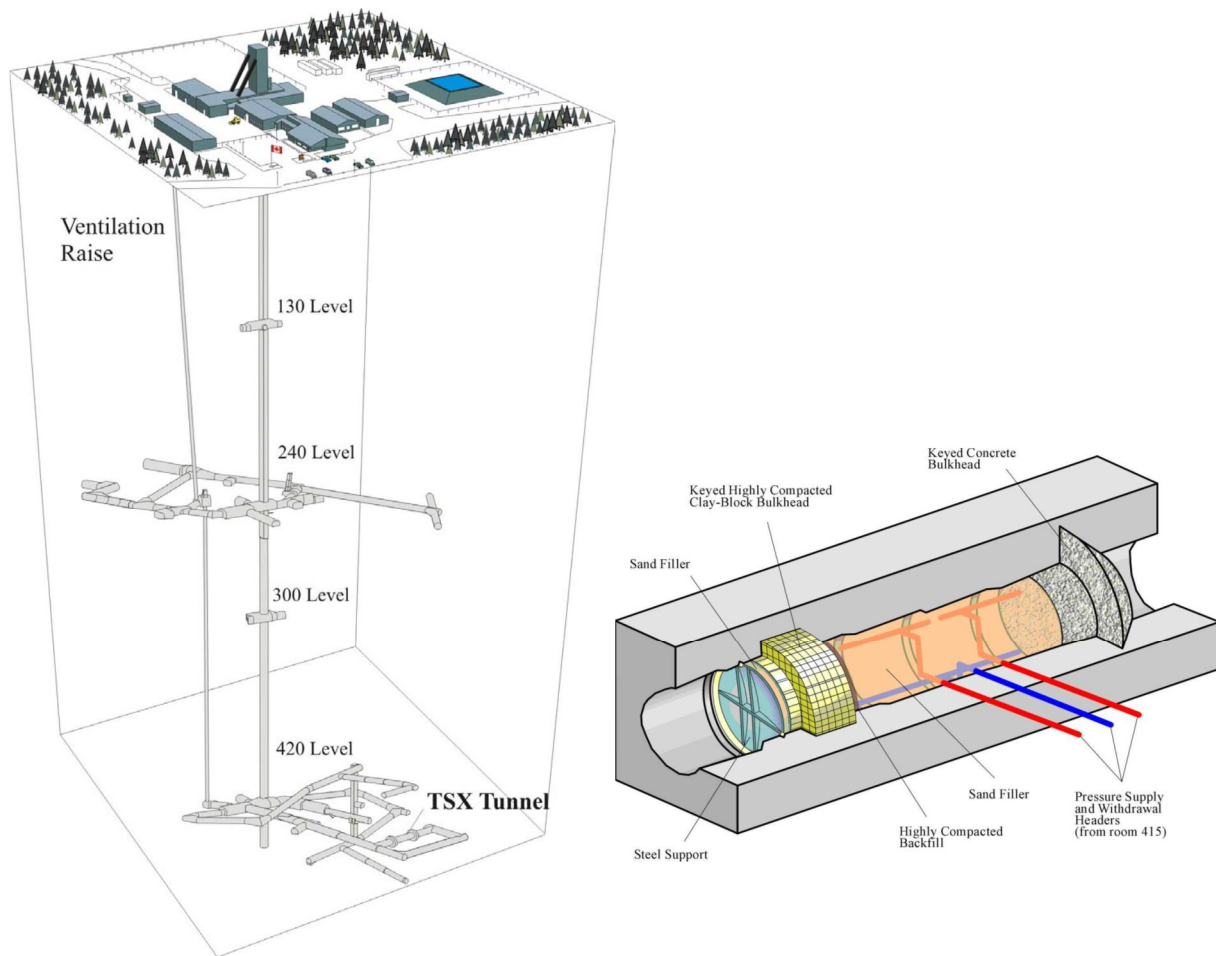


*Figure 4.1.6. AECL Underground Research Laboratory and TSX global layout.*

The physical behaviour assessment of the concrete seal revealed:

- Internal cracks detected by acoustic emission and observed afterward during sampling;
- Shrinkage/opening cracks at the interface with the geological medium;
- According to the hydraulic pressure increase, the seepage decreased after a transient period;
- Due to the thermal expansion, a significant decrease of the seepage has been observed during the heating phase.

The shrinkage has not been optimized. Then voids have been noticed especially at the interface with the geological medium. This has been anticipated and bentonite strips have been placed to close these voids after setting. Due to the geometry of the plug, an important crack due to endogenous shrinkage has been localized by acoustic emission and observed on samples in the central volume of the plug (Figure 4.1.7).
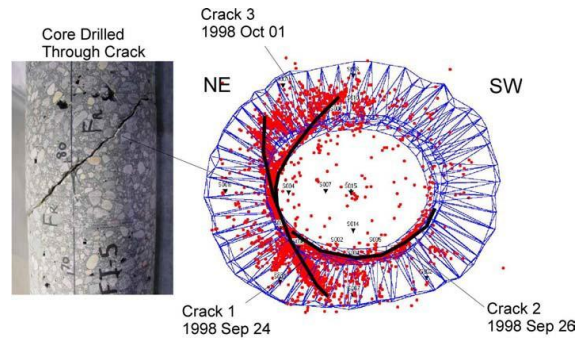
*Figure 4.1.7. Crack localization by acoustic emission measurements and sampling (Martino et al., 2008.)*

With the pressure increase and in a second step with the temperature increase, the concrete plug moved (axial displacement in the gallery and thermal expansion). As a consequence, seepage decrease has been measured (Figure 4.1.8).
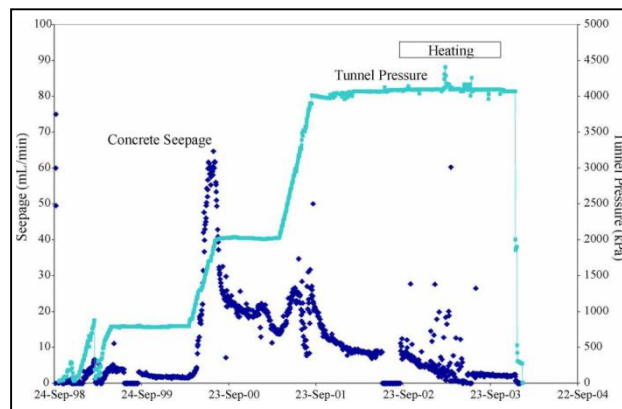


*Figure 4.1.8. Seepage evolution with time during pressure and temperature increases (Martino et al., 2008).*

The concrete properties, measured on samples taken in the global volume of the plug, indicate at the plug scale that the concrete fulfilled the specifications (Table 4.1.4).

*Table 4.1.4. TSX concrete physical properties.*

| Rc (MPa) | E (GPa) | Porosity (%) | Hydraulic conductivity (m/s) | Gas permeability (m²) | |
|---|---|---|---|---|---|
| | | | | dry | water saturated |
| $76 \pm 14$ | $36.6 \pm 4.8$ | 8.0 / 12.5 | $10^{-12}$ | $\sim 10^{-16}$ | $\sim 4.10^{-20}$ |

*ESDRED*

ESDRED (Engineering Studies and Demonstrations of Repository Designs; www.esdred.info) was a European project (2005–2009), involving seven waste management agencies and six R&D institutions, from Belgium (Ondraf/Niras, ESV Euridice EIG), Finland (POSIVA), France (Andra), Germany (DBE technology, GRS), the Netherlands (NRG), Spain (Enresa, Aitemin, CSIC), Sweden (SKB), the Switzerland (NAGRA) and the UK (NDA).

ESDRED was focused on technology to demonstrate, at an industrial scale, the technical feasibility of some very specific activities related to the construction, operation and closure of a deep geological repository for high level radioactive waste. The work was organized inside four 'Technical Modules' and essentially involves the conception, design, fabrication and demonstration of equipment or products for which relevant proven industrial counterparts (mainly in the nuclear and mining industry) do not exist today. At all times this work had to be carried out within the framework of compliance regarding the requirements for operational safety, long term safety, retrievability and monitoring.

Within the technical module #4 'Temporary Sealing Technology' for construction of sealing plugs and for rock support using shotcrete techniques, various low pH cement have been developed to build plugs or used as rock support in galleries. The target was to devise low pH cements to be used as shotcrete for rock support as well as to build plugs in tunnels (Alonso et al., 2008).

The development of a low-pH shotcrete formula for rock support for conditions in Sweden (field tests at the Äspö HRL) and in Switzerland (at the Hagerbach test facility) was based on a binary mix CEM I/Silica Fume. Mixes 50/50 and 60/40 CEM I/SF have been tested. With a different behaviour compared to 'classical shotcrete', low pH shotcretes have been adapted and successfully used both in Sweden and Switzerland. It appeared that such blends are difficult to prepare and to use mainly due to the viscosity of the blends.
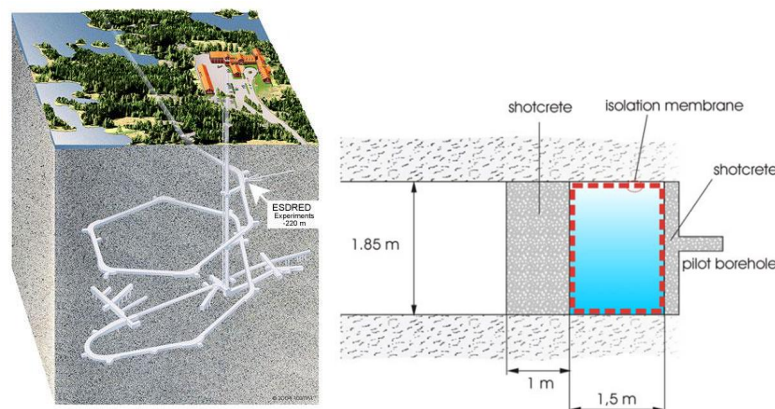


*Figure 4.1.9. Äspö URL -Sweden ; global layout of the short plug test.*

To build the plugs, 14 materials have been tested (two reference cements -OPC and CAC- and 12 blends using SF and FA) prior to construction. To fulfill the chemical requirement, for binary mixes, a substitution level above 40% with SF is needed and the pH decrease is more significant with ternary blends with SF and FA (Alonso et al., 2008).

Based on the binary blends (to prepare 'simple' low pH shotcretes as to have a compressive strength above 20 MPa), a short plug (Äspö-Sweden) and a long plug (Grimsel URL - Switzerland) were constructed. The short plug was loaded to failure and then sampled prior to dismantling. As the plug was monitored during the entire process, it constituted a significant database to design the second test performed in Grimsel URL. The full-scale longer plug was loaded using the swelling pressure created by bentonite blocks which are being artificially hydrated. This is a much slower loading process more closely related to what would happen in reality. The information of the performance of the long-plug test, has been followed through the MoDeRn project (7th Framework Programme EURATOM), in which most of the ESDRED members are involved.

*Table 4.1.5. Nominal compositions of the low pH concretes (Alonso et al., 2008).*

| Cement formulation | Short Plug (aggregate from the excavation) | | | Long Plug (conventional aggregates) |
|---|---|---|---|---|
| | 70%CAC+20%SF+10%FA | 60%OPC+40%SF | 35%OPC+35%SF+30%FA | 60%OPC+40%SF |
| Water (kg/m$^3$) | 262 | 277 | 237 | 230 |
| Binder (kg/m$^3$) | 310 | 307 | 316 | 275 |
| Water/Binder | 0.85 | 0.9 | 0.75 | 0.84 |
| Filler (kg/m$^3$) | - | - | - | 70 |
| Gravel (kg/m$^3$) | 621 | 615 | 635 | - |
| Fine Gravel (kg/m$^3$) | 201 | 200 | 205 | 588 |
| Sand (kg/m$^3$) | 825 | 818 | 843 | 1045 |
| Superplasticizer (kg/m$^3$) | 5.58 | 5.5 | 5.7 | 5.7 |
| Air-entraining Admixture (kg/m$^3$) | - | 0.6 | 0.6 | |
| | | | | |
| Static Elasticity modulus (GPa) | 15.8 ± 0.5 | 21.7 ± 2.5 | 18.3 ± 1.6 | |
| Compressive Strength (MPa) | 18.7 ± 0.3 | 37.5 ± 0.3 | 29.3 ± 0.2 | |

*Table 4.1.6. Low pH mix proportion for the short plug (Alonso et al., 2008).*

| Components | kg/m$^3$ |
|---|---|
| Water | 277.2 |
| Ordinary Portland Cement: CEM I 42.5 R/SR | 184.3 |
| Silica Fume | 122.9 |
| Coarse aggregate (5–12) | 615.6 |
| Medium aggregate (2–5) | 199.7 |
| Fine aggregate (0–2) | 818.1 |
| Superplastizer "Sikament TN-100" | 5.5 |
| Air entrapper "Sika Aer 5" | 0.6 |
| Accelerant "Sigunita L-53 AF S" | 18.5 |

*Table 4.1.7. Low pH mix proportion for the long plug (Alonso et al., 2008).*

| Components | kg/m$^3$ |
|---|---|
| Water | 230 |
| Ordinary Portland Cement: CEM I 42.5 R/SR | 165 |
| Silica Fume | 110 |
| Limestone filler | 70 |
| Fine size aggregate (0–4) | 1045 |
| Medium size aggregate (4–8) | 590 |
| Superplastizer "Sikament TN-100" | 2.8 |
| Accelerant "Sigunita L-53 AF S" | 16.5 |

*DOPAS*

DOPAS (Demonstration of Plugs And Seals - http://www.posiva.fi/en/dopas) is a European project involving six waste management agencies and eight R&D organizations or universities from Czech Republic (SURAO, CVUT FSv, UJV), Finland (POSIVA, VTT, B+Tech), France (Andra), Germany (GRS, DBE Tech), the Netherlands (NRG), Sweden (SKB), Switzerland (NAGRA) and the UK (NDA, Galson Science Ltd).

The global objective of this project is to test and to assess the feasibility of sealing and plugging tunnels in deep geological structures, within the nuclear waste management context.

*FSS*

Full Scale Sealing (FSS) is a full scale experiment of seal performed within the DOPAS European project.

Within the WP3 "Design and technical construction feasibility of the plugs and seals", Andra has to design and realize a full scale seal, made with a bentonite core, surrounded by two concrete plugs. The two elements have been built with a low pH concrete, one with a self-compacted concrete and the other with a shotcrete (Bosgiraud et al., 2014).
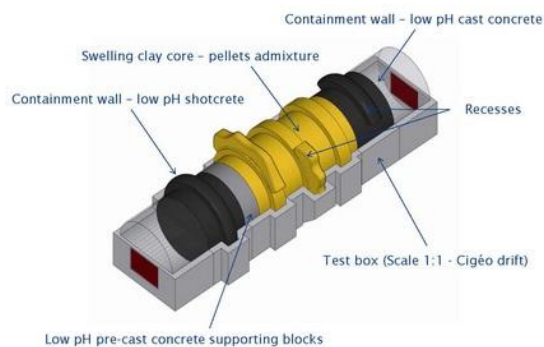


FSS data:
Full length 35 m
Internal diameter 7.6 m (up to 9 m into recesses)
Low pH cast concrete: 5 m thick; 240 m$^3$; ~500 t
Low pH shotcrete: 5 m thick; 267 m$^3$; ~614 t
Low pH pre cast wall: 2 m thick; 90 m$^3$; ~210 t
Swelling clay core: 13.5 m thick; 620 m$^3$; 1 050 t

*Figure 4.1.10. FSS global lay out (Bosgiraud et al., 2014).*

Both of these concretes have the same specifications:

Low hydration heat: $\Delta T < 20$ °C in semi-aidabatic conditions;

Low pH: pH≤11 after 2 months;

Workability > 2hours.

Two types of concrete have been formulated: a shotcrete and a self compactiong concrete. The shotcrete is based on a binary blend CEM I/SF and the SCC is based on a "*binary*" blend CEM III/SF, in fact a ternary blend CEM I/BFS/SF as a CEM III is a mix clinker/BFS.

Both of these materials succeeded in having a pH pore solution value below 11 after three months. The mechanical properties measured after three months give Rc ~51MPa and E ~ 28 GPa for the SCC. In both cases the temperature increase in each plug is below 15°C in the central part of the plugs, satisfying the specifications.

Table 4.1.8. Low pH mix proportion for the FSS shotcrete.

| Components | kg/m$^3$ |
|---|---|
| Water | 200 |
| Ordinary Portland cement CEM I | 190 |
| Silica Fume | 190 |
| Medium aggregate (4–8) | 408 |
| Sand (0–4) | 1 347 |
| Superplastizer "glénium SKY537" | 14 |
| Accelerant "masterRoc HCA 10" | 2.7 |

Table 4.1.9. Low pH mix proportion for the FSS Self Compacting Concrete.

| Components | kg/m$^3$ |
|---|---|
| Water | 204 |
| Slag Cement CEM III/A 52.5 | 130 |
| Silica Fume | 130 |
| Limestone filler | 408.4 |
| Sand (0–4) | 699 |
| Medium size aggregate (5-12.5) | 682 |
| Superplastizer "Glenium SKY537" | 14.7 |
| Retardant "Prelom 510" | 2 |

*POPLU*

POPLU is an acronym for POSIVA PLUG. It has been designed in Finland and two low pH concretes have been formulated (Holt et al., 2014).
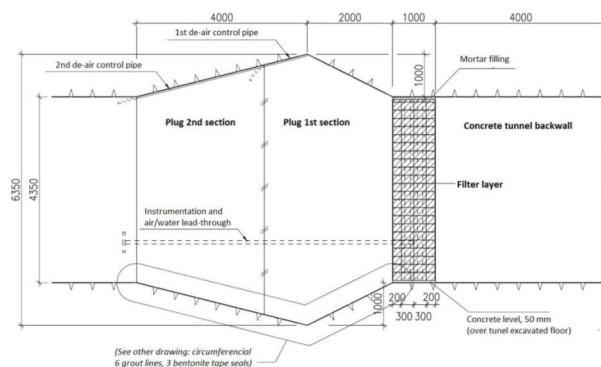


*Figure 4.1.11. Posiva's design for the deposition end tunnel plug (POPLU) (Holt et al., 2014).*

This plug is a 6 m length structure with a diameter of 4.35 m to 6.35 m.

Two mixes were developed: a binary and a ternary blend based on a mix CEM I/SF, with/or without FA. The compressive strength has to be over 50 MPa and pH < 11. The temperature increase of such blends is close to 5 °C.

*Table 4.1.10. Final mix designs of POSIVA's low pH concretes.*

|  | Ternary mix design (kg/m$^3$) | Binary mix design (kg/m$^3$) |
|---|---|---|
| CEM I 42.5 MH/SR/LA | 105 | 120 |
| Silica | 91 | 80 |
| Fly Ash | 84 | |
| Quartz filler | 114 | 256 |
| Aggregate | 1 840 | 1 805 |
| Water | 126 | 125 |
| W/B | 0.45 | 0.60 |

*Table 4.1.11. Final mix designs of POSIVA's low pH concretes properties.*

|  | Ternary mix design (kg/m$^3$) | Binary mix design (kg/m$^3$) |
|---|---|---|
| Compressive strength (MPa) | 79.5 | 91.5 |
| Modulus of elasticity (GPa) | 34.2 | 37.4 |
| pH of leachate after 90 days (reference water / groundwater) | 11.4/10.3 | 11.4/10.3 |

**Other possible chemical systems**

Most of the developments dealing with low pH cements use Calcium/Silica chemical systems. Other raw materials are possible candidates, mainly involving alumina chemical systems. These other hydraulic binders are mainly dedicated to chemically reactive waste immobilization but not to build large structures such as seals (Cau-dit-Coumes, 2013).

Alumina cements used in different studies present weaknesses that do not allow using it alone (George, 1983; Goni et al., 1991; Capmas et al., 1992):

- Too alkaline to reach pH < 11; most of the tests give a pH of the pore water in the range 11.5/12.5;

- Important high hydration heat;

- Decrease of the mechanical properties due to the conversion of the alumina hydrates.

Blended with pozzolanic compounds could change these properties to fulfill some of the requirements, but still with an important lack of knowledge regarding the long term behaviour (Hidalgo et al., 2003; Garcia Calvo et al., 2011). Calcium Alumina Cements (CAC) have been tested within the ESDRED project but even blended with SF or FA, pH of the pore solution remained above 11.3 (Alonso et al., 2008).

Sulfo-alumina cements are close to the previous one but differ in composition with a high sulfate amount. Then after hydration, the chemical characterization exhibits a pH range from 10.5 to 11.0, the hydration kinetics and the hydration heat lead to high temperature increase during the setting (Winnefeld & Lotenbach, 2010; Péra & Ambroise, 2004).

Another types of cement involve phosphate compounds. In this "category" apatitic cements and phosphor-magnesia cements are the main known materials. High strength apatitic cements are

mainly developed for medical application (i.e. sealing/repairing bones). At a larger scale, these cements could be interesting due to their very low hydration heat and the (bio compatible) pH of the hydrated material (range from 7 to 9) (Cau-Dit-coumes, 2002). Recent works in the medical field, present high strength apatitic cements but without any information about a possible use at a cubic meter scale.

Phospho-magnesia cements are well known to have a brief setting period and then to develop high mechanical resistance at a very short time scale. Due to the high chemical stability of the phosphate compounds, these cements are resistant to the main chemical degradations and after hydration have a pore solution pH in the range 7 to 8 (Seehra et al., 1993; Wagh et al., 1993; Yang & Wu, 1999; Soudée & Péra, 2000). However, the availability of the raw materials is one of the main problems related to the use of such cements. Moreover, as these materials have a significant hydration heat, an important thermal shrinkage could lead to cracks in massive structure.

# References

Alonso J., Garcia-Siñeriz J.L., Bàrcena I., Alonso M.C., Fernàndez Luco L., Garcià J.L., Fries Th., Petterson S., Bodén A. & Salo J.P. (2008) ESDRED WP4.Temporary sealing technology. Final technical report. Cont. N° FI6W-CT-2004-508851.

Andra (2015) http://www.andra.fr/international/index.html and http://www.cigeo.com/en/.

Bach T.T.H. (2010) Evolution physico-chimique des liants bas pH hydrates – Influence de la température et mécanisme de rétention des alcalins. Thèse de doctorat de l'Université de Bourgogne, 236 p.

Bosgiraud J.M., Foin R. & Bethmont S. (2014) "Full Scale Demonstration of Plugs and Seals" DOPAS - Work Package 3. Deliverable D3.11: "Report on FSS cast concrete plug construction".

Capmas A., Dumas T. & Letourneux J.P. (1992) Durabilité spécifique des bétons de ciment alumineux - dans la durabilité des bétons. Sous la direction de J. Baron et J.P. Ollivier, Presses de l'ENPC, Paris, 429–453.

Cau-Dit-Coumes C. (2002) Etude bibliographique des ciments phospho-calciques pour une application au blocage du combustible irradié en situation de stockage direct. Note Technique CEA-SEP 02/173.

Cau-Dit-Coumes C., Courtois S., Nectoux D., Leclercq S. & Bourbon X. (2006) Formulating a Low-Alkalinity, High Resistance and Low-Heat Concrete for Radioactive Waste Repositories. Cem. Concr. Res., 36, 2152–2163.

Cau-dit-Coumes C. (2013) Alternative binders to ordinary Portland cements for radwaste solidification and stabilization. In Cement based materials for nuclear waste storage. Eds Bart F., Cau-dit-Coumes C., Frizon F. & Lorente S., Springer, Berlin, 171–193.

Chandler N., Cournut A., Dixon D., Fairhurst C., Hansen F., Gray M., Hara K., Ishijima Y., Kozak E., Martino J., Masumoto K., McCrank G., Sugita Y., Thompson P., Tillerson J. & Vignal B. (2002) The five year report on the tunnel sealing experiment: An international project of aecl, jnc, andra and wipp. AECL-12127.

Codina M. (2007) Les bétons bas pH, formulation, caractérisation et étude à long terme. Thèse de doctorat de l'INSA de Toulouse, 167 p.

Codina M., Cau-Dit-Coumes C., Le Bescop P., Verdier J. & Ollivier J.P. (2008) Design and characterization of low-heat and low-alkalinity cements. Cem. Concr. Res., 38, 437–448.

ECOCLAY II (2005) Effect of cement on clay barrier performance. European Report EN 21921.

El-Bitouri Y., Buffo-Lacarrière L., Sellier A. & Bourbon X. (2016) Modelling a chemo-mechanical behaviour of low pH concretes. Cem. Concr. Res., 81, 70–80.

Fries T., Weber H. & Wetzig V. (2007) Low pH shotcrete field tests on opalinus clay samples. Proc. 3rd workshop R&D on low pH cement for a geological repository, Paris, June 13-14, 107–115.

Garcia Calvo J.L., Alonso M.C., Hidalgo A. & Fernandez Luco L. (2007) Design of low-pH cementitious materials based on functional requirements. Proc. 3rd workshop R&D on low pH cement for a geological repository, Paris, June 13-14, 48–51.

Garcia Calvo J.L., Alonso M.C., Hidalgo A. & Fernandez-Luco L. (2011) Low pH cements based on CAC for underground repositories of HLW: long term hydration and resistance against ground water aggression. Proc. NUWCEM 2011, Avignon, France, October 11-14.

Garcia V. & Verdier J. (2009) Optimisation des formulations de bétons bas pH. Rapport Andra C.RP.FSCM.10.0021, 101 p.

George C.M. (1983) Industrial Aluminous Cements. Structure and Performance of Cements, P. Barnes Ed., Appl. Sci. Publishers, London, 422.

Goni S., Andrade G. & Page C.L. (1991) Corrosion behaviour of steel in high alumina cement mortar samples : effect of chloride. Cem. Concr. Res., 21, 635–646.

Gray M.N. & Shenton B.S. (1998) For Better Concrete, Take Out Some of the Cement. Proc. 6th ACI/CANMET

Symposium on the Durability of Concrete, Bangkok, Thailand, 5–31.

Hidalgo A., LlorenteE I. & Andrade C. (2003) Preliminary physico-chemical characterization of some low-ph concretes using silica fume and aluminous cement. Proc. Workshop on Qualification of Low-pH Cement for a Geological Repository, Stockholm, Suède, 15-16 October.

Holt E., Leivo M. & Vehmas T. (2014) Low pH concrete developed for tunnel end plugs used in nuclear waste containment. Concrete Innovation Conference 2014, Oslo, 11-13 june.

Kobayashi Y., Yamada T., Matsui H., Nakayama M., Miahara M., Naito M. & Yui M. (2007) Development of low-alkali cement for application in a JAEA URL. Proc. 3rd workshop R&D on low pH cement for a geological repository, Paris, June 13-14, 98–106.

Leung Pah Hang Thierry (2015) les bétons bas pH : comportement initial et différés sous contraintes externes. Thèse de l'université de Toulouse 3 – Université Paul Sabatier. 334 p. (in french).

Lotenbach B., Wieland D E., Schwyn B., FigiI R. & Rentsch D. (2008) Hydration of low-pH cements. Proc. international workshop on the mechanisms and modelling of cement / waste Interactions, Le Croisic, France, October 12-16.

Martino J., Dixon D., Stroes-Gascoyne S., Guo R., Kozak E.T., Gascoyne M., Fujita T., Vignal B., Sugita Y., Masumoto K., Saskura T., Bourbon X., Gingras-Genois A. & Collins D. (2008) The Tunnel Sealing Experiment 10 Year Summary Report. URL-121550-REPT-001.

Martino J.B. (2007) Low heat high performance concrete used in a full scale tunnel seal. Proc. 3rd workshop R&D on low pH cement for a geological repository, Paris, June 13-14, 89–97.

Martino J.B., Dixon D.A., Kozak E.T., Gascoyne M., Vignal B., Sugita Y., Fujita T. & Masumoto K. (2007) The tunnel sealing experiment: An international study of full-scale seals. Physics and Chemistry of the Earth, Parts A/B/C, Volume 32, Issues 1–7, 93–107.

Mattus C.H. & Dole L.R. (2007) Low pH concrete for use in the US High-Level Waste repository: Part II – Formulation and tests. 3rd workshop R&D on low pH cement for a geological repository, Paris, June 13-14, 72–82.

Nishiuchi T., Yamamoto T., Hironaga M. & Ueda H. (2007) Mechanical properties of low pH concretes, LAC, HFSC and SAC. Proc. 3rd workshop R&D on low pH cement for a geological repository, Paris, June 13-14, 62–71.

Seehra S.S., Gupta S. & Kumar S.S. (1993) Rapid setting magnesium phosphate cement for quick repair of concrete pavements. Characterisation and durability aspects, Cem. Concr. Res., 23, 254–266.

Soudée E. & Péra J. (2000) Mechanism of setting reaction in magnesia-phosphate cements. Cem. Concr. Res., 30, 315–321.

Péra J. & Ambroise J. (2004) New applications of calcium sulfoaluminate cements. Cem. Concr. Res., 34, 671–676.

Vuorinen U. & Lehikoinen J. (2005) Low pH grouting cements – Results of leaching experiments and Modelling. Proc. 2nd workshop R&D on low pH cement for a geological repository, Madrid June 15-16.

Wagh A.S., Cunnana J.C., Singh D., Reed D.T., Armstrong S., Subhan W. & Chawla N. (1993) Chemically phosphate ceramics for radioactive and mixed-waste solidification and stabilization. Proc. conference technology and programs for radioactive waste management and environmental restoration, WM'93, Tucson, USA 2, 1613–1617.

Winnefeld F. & Lothenbach B. (2010) Hydration of calcium sulfoaluminate cements — Experimental findings and thermodynamic modeling. Cem. Concr. Res. 40, 1239–1247.

Yang Q. & Wu X. (1999) Factors influencing properties of phosphate cement-based binder for rapid repair of concrete. Cem. Concr. Res., 29, 389–396.

# 5 Phenomenological approaches

## 5.1 Diffusion of species through cement materials

*V. Havlova, P. Večernik*

*ÚJV Řež, a.s., Hlavni 130, Rez, 250 68 Husinec, Czech Republic*

Concrete will be used in the repository as barrier material, backfill and construction material. Except using fibre concrete containers for HLW, plugs, seal and grouts are considered be used. The evolution of these structures toward their desirable achievements of their function will depend on the time and rate at which processes occur. A number of variables can affect the nature and rate of these evolution processes as radiation intensity, heat, water content, material composition, hydrovariables, groundwater composition, mechanical properties, stress etc. (Posiva 2007)

Basically, ordinary Portland Cement (OPC, pH>13) is used, with low pH cement (LPC, pH<11) for some specific purposes.

The major concern of cementitious material chemical degradation due to reaction with groundwater is the generation of hyperalkaline leachate that could potentially interact with bentonite and dimish its swelling properties. Therefore LPC material is recommended in order to decrease the impact of OPC leaching in contact with groundwater.

Generally, OPC degradation generates high-alkaline gradient, with pH > 13, being rich in $K^+$, $Na^+$, $Ca^{2+}$ in the first period (pH around 13). In the second period pH is governed namely by portlandite transformation with pH around 12.4. The last period will be influenced by CSH (Calcium Silica Hydrates) with pH around 10 (e.g. Gaucher and Blanc 2006; Savage D., 2003; Sánchez etal., 2006; Dolder et al., 2014)

Assessing long-term performance of cement material for radionuclide encasement requires knowledge of the radionuclide-cement migration, interaction and mechanisms of retention (i.e., sorption or precipitation). This understanding will enable accurate prediction of radionuclide fate when the waste forms come in contact with groundwater (Szántó et al., 2002).

In the case of a release of radionuclides from the waste matrix the transport will be influenced by a series of chemical and physico-chemical processes: diffussion, sorption, ion exchange, precipitation occurring at the inner and outer surface area of the rock matrix (Szántó et al., 2002). Diffusion is considered to be one of the most important retardation processes, leading to slowing down the speed of the species in comparison with main ground water flow in the fractures.

The diffusion process is governed by Fick´s laws, reported elsewhere (Eriksen and Locklund, 1989; Ohlssons and Neretnieks, 1995; Bradbury and Green, 1986; Vilks et al., 2004; Löfgren and Neretnieks 2003, 2004, 2006):

$$\frac{\delta C_p}{\delta t} = \frac{D_p}{R_p}\frac{\delta^2 C_p}{\delta z^2} \ (Equation\ 1.)$$

where $C_p$ is the concentration in pore water (mol $m^{-3}$), $D_p$ the pore diffusion coefficient (diffusivity, $m^2 s^{-1}$), R the retardation factor in the rock matrix ($m^{-3} \cdot kg^{-1}$), t is time (s) and z is coordinate of movement

The effective diffusion coefficient $D_e$ ($m^2 \cdot s^{-1}$) is defined as

$$D_e = \varepsilon \frac{\delta_D}{\tau^2} D_w = \varepsilon D_p = F_f D_w \quad (Equation\ 2.)$$

where $\varepsilon$ is porosity, $\delta_D$ is the constrictivity, $\tau^2$ the tortuosity, $D_w$ the diffusivity in free water ($m^{2 \cdot} s^{-1}$) and $D_p$ the pore diffusivity in pores ($m^{2 \cdot} s^{-1}$). $F_f$ is called the formation factor.

Extensive literature review on Fickian diffusion of radionuclides for engineering barriers was reported in the paper of Shackelford and Moore (2013).

The authors usually point out the importance of porosity, tortuosity, pore structure and geometry of the geological material (Bajja et al, 2015). Moon et al. (2006) states that chlorine diffusivity increases with the average pore diameter.

Diffusion is an important mechanisms, influencing (Posiva 2007):

    a) transport of substances that influence degradation of cement material (e.g. chlorine, sulphate)

    b) radionuclide migration through these materials.

Bentz (1997) presented that concrete diffusivity depends on water-to-cement ratio (W/C), degree of hydration and aggregate volume fraction. The other variables that will affect the transport of radionuclides and other substances through cementitious materials are temperature, material composition, hydrovariables and groundwater composition (Posiva, 2007).

In civil engineering specie diffusion, namely Cl, is a subject of number of studies, studying namely its corrosive impact on reinforcement and structures of cementitious materials - so called chloride induced corrosion (ČSN, 2010; ASTMC 1202, 1997; Concrete Q & A, 2006; NT Build 492, 1999; Bentz D., 2007; Chaussadent T. a Arliguie G., 1999; NT Build 443, 1995; Elfmarkova et al., 2015).

Techniques influded migration test, immersion tests (e.g. Bentz D., 2007; Chaussadent T. a Arliguie G., 1999; NT Build 443, 1995; Elfmarkova et al., 2015 etc.), electrical methods (e.g. Yang, 2006; Moon 2006 etc.) followed also by conventional through-diffusion tests (Szántó et al., 2002; Bajja et al., 2015; Wellman et al., 2007 etc.).

Studies are basically focused on different radionuclide/specie diffusion through cement samples, resembling defined properties. However, it is clear that most of the data are available for ordinary portland cement. Low pH cement diffusive properties are almost not available.

Diffusivity data for radionuclides through cementitious materials (mostly concrete) have been obtained in the field of cementitious repositories for low- and intermediatelevel nuclear waste. In the Data report for short lived radioactive waste (SFR; SKB 2014) in Sweden those are defined on the bases of wide literature review. In the same time the rate of cement degradation is considered, resulting into $D_e$ values, ranging from $3.5 \cdot 10^{-12}$ $m^2/s$ for construction concrete in time period 0–100 years up to $1 \cdot 10^{-10}$ $m^2/s$ for period of 20,000–100,000 years (SKB, 2014). Chloride diffusion was usually considered in the literature sources and expert judgement.

Furthermore, some of the studies do not exhibit information detailed enough. For example Szántó et al. (2002) did not present neither cement material porosity, nor the procedure of solution equilibration and its final composition. The composition of the solution in contact with cement material can be a key parameter, influencing radionuclide migration. If grounwater exhibiting pH 7.52 and low mineralisation (Szántó et al. 2002), gets into contact with cement sample, both pH and total dissolved solid content (TDS) increases. None of this is reported in the paper.

The similar deficiency can be found in Bajja et al (2015), looking into diffusion of $^3$H, Li and Cl. Neither pH development, nor final value and solution composition are reported.

Some of the papers looked into more detailed problems, as for example influence of cement carbonation and metallic iron content on radionuclide diffusion, as for example in Wellman et al, (2007) or Mattigod et al. (2012). Carbonation was induced by immersion in sodium carbonate solution. The highest Tc and I diffusivities were observed in all uncarbonated Fe-free concrete specimens (Mattigod et al., 2012). Specific technique was used in Wellman et al. (2007) that seems to be a predecessor of Mattigod et al. (2012), however not being fully compatible. They use a combination of dynamic and leaching techniques (leaching of contaminated soil in contact with cement material) in order to determine diffusion coefficients of Re, I and Tc. However, the technique is not fully clear. Some of the values presented are to be too low after recalculation from $cm^2/s$ to $m^2/s$ (e.g. $10^{16}$ $m^2/s$ for I) that the measurement seems to be almost impossible (according to the experience with granitic low porosity rock).

In the work of Fan et al. (2014) effects of kaolinite clay on the mechanical properties and chloride diffusivity in cement paste, mortar and concrete were investigated. Ordinary Portland cement was partially replaced by kaolinite clay at 0%, 1%, 3%, 5%, 7% and 9% by weight of cement. The test results showed that the addition of clay improved the micro-pore structure in the cement paste and limited, e.g. to decrease diffusion, for chloride ions. The chloride diffusion coefficient of cement concrete decreases exponentially with the clay addition. The reduction of chloride diffusion coefficient of cement concrete is 8.68% and 18.87% at 1% and 5% clay, respectively. However, eventhough the decrease in porosity is reported in the paper, exact values can be found here.

The paper of Caré (2008) is devoted to the effect of temperature on cement porosity and Cl diffusion, presuming heat transfer from radioactive waste. Rise of temperature leads to cracking and modification of porosity characteristics. Chloride migration was studied using penetration technique and colorimetric method allowing to distingush the different cannels for cloride transport. Chloride ingress increased with water/cement ratio and with heating temperature.

However, Albinsson et al,. (1993) studied several cement type samples, ranging from ordinary portland cement throutgh sulphate resistant paste, fly ash paste, high alumina paste etc and so as in cement/bentonite combined system where radionuclides from spiked cement were diffusing into bentonite. The apparent diffusion coefficients $D_a$ ($m^2/s$) for radionuclide diffusion from spiked cement into bentonite were following for Na $6 \cdot 10^{-11}$ $m^2/s$, for Ca $3 \cdot 10^{-11}$ $m^2/s$ and finally Cs $3 \cdot 10^{-12}$ $m^2/s$.

Results of through-diffusion experiment for cement samples showed that Da values for Cs reached $10^{-12}$ to $10^{-13}$ $m^2/s$. On the other hand no movement for Am and Pu was detected.

A specific theoretical approach is taken in Windt et al. (2004), where a rigorous model has been developed using reactive transport code HYTEC to assess the geochemical evolution of clay rock due to interaction with cement material. The impact of precipitation and dissolution of minerals on porosity and diffusion is studied. The study is interesting by specifying basic parameters for

ordinary Portland cement with porosity 20%, $D_p = 1.0 \cdot 10^{-10}$ m$^2$/s and $D_{eff} = 1.0 \cdot 10^{-11}$ m$^2$/s, however not specifying the source. All the radionuclides here (Cs, Ra, Tc and U) are considered to have the same diffusion coefficients in cement, being influenced namely via solution composition and mineralogical changes in the system. Eventhough the results are rather possitive - buffering capacity of clay seems to play an important role resulting into $K_d$ and solubility limit changes of one order of the magnitude that is in the range of commonly found uncertainties - the study is only a theoretical one, not being confirmed by direct experimental tests.

**Conclusions**

Data for diffusive properties for cement materials are available, however being mostly available for OPC and based on Cl diffusion. Studies for other elements that can be expected e.g. in the case of release from NPP decommissioned waste, C-14, Ca-41, Tc-99, Ni-63, or even actinides, are rare.

Studies are mostly driven by different requirements, focused on chloride corrosion observation. The boundary conditions have not been described properly or not included at all. On our opinion, both cement material equilibration and pH development during experiments are not tackled enough and not evaluated in appropriate detail. Dependence of diffusion rate on cement degradation stages are rarely determined as well.

*Table 5.1.1. Diffusion coefficients of radionuclides/other species in cement materials.*

| Reference | Material type | Solution | Other properties | Method | Solution pH | Porosity (%) | RN/ Specie | De x $10^{12}$ m$^2$/s |
|---|---|---|---|---|---|---|---|---|
| **Bajja et al. (2015)** | CEM I | Saturated lime water | Sand CEN (SN) 0–60% | TD | Not reported | 31 - 14 | [3]H | 2.56 - 3.39 |
| **Bajja et al. (2015)** | CEM I | Saturated lime water | Sand CEN (SN) 0 | TD | Not reported | 31 | Li | 1.15 - 1.70 |
| **Bajja et al. (2015)** | CEM I | Saturated lime water | Sand CEN (SN) 0 | TD | Not reported | 31 | Cl | 2.18 - 2.68 |
| **Szántó et al. (2002)** | Paks NPP cement Details not reported | GW | Not reported | TD | Not reported | Not reported | [3]H | 54.9 |
| **Szántó et al. (2002)** | Paks NPP cement Details not reported | GW | Not reported | TD | Not reported | Not reported | [125]I | 26.0 |
| **Szántó et al. (2002)** | Paks NPP cement Details not reported | GW | Not reported | TD | Not reported | Not reported | [36]Cl | 30.0 |
| **Elfmarková et al. (2015)** | M1-OPC | NaOH | | RCM | Not reported | 14,64 | Cl | 8.03; 8.94 |
| **Mattigod et al. (2012)** | Portland I or II. | Destilled water (not fully clear) | Non carbonated | TD | Not reported | Not reported | Tc | 0.17 |
| **Mattigod et al. (2012)** | Portland I or II. | Destilled water (not fully clear) | Non carbonated | TD | Not reported | Not reported | I | 0.14 |
| **Mattigod et al. (2012)** | Portland I or II. | Destilled water (not fully clear) | Carbonated | TD | Not reported | Not reported | Tc | 0.53 |
| **Mattigod et al. (2012)** | Portland I or II. | Destilled water (not fully clear) | Carbonated | TD | Not reported | Not reported | I | 0.54 |
| **Mattigod et al. (2012)** | Portland I or II. | Destilled water (not fully clear) | Non carbonated, Fe 12% | TD | Not reported | Not reported | Tc | 0.023 |
| **Mattigod et al. (2012)** | Portland I or II. | Destilled water (not fully clear) | Non carbonated Fe 12% | TD | Not reported | Not reported | I | 0.040 |
| **Mattigod et al. (2012)** | Portland I or II. | Destilled water (not fully clear) | Carbonated Fe 12% | TD | Not reported | Not reported | Tc | 0.011 |
| **Mattigod et al. (2012)** | Portland I or II. | Destilled water (not fully clear) | Carbonated Fe 12% | TD | Not reported | Not reported | I | 0.013 |
| **Caré (2008)** | CEM I (different water/cement ratios) | Non-saturated | T initial; w/C = 0.35–0.6) | PT | | Not reported | Cl | $D_a$ = 1.86 - 42.0 |
| **Caré (2008)** | CEM I (different water/cement ratios) | Non-saturated | T = 45 °C; w/C = 0.35–0.6) | PT | | 22.9 | Cl | $D_a$ = 6.54 - 42.0 |
| **Caré (2008)** | CEM I (different water/cement ratios) | Non-saturated | T = 80 °C; w/C = 0.35–0.6) | PT | | 26.9 | Cl | $D_a$ = 1.41 - 46.5 |

| Reference | Material type | Solution | Other properties | Method | Solution pH | Porosity (%) | RN/ Specie | De x $10^{12}$ m$^2$/s |
|---|---|---|---|---|---|---|---|---|
| **Caré (2008)** | CEM I (different water/cement ratios) | Non-saturated | T = 105 °C; w/C = 0.35–0.6) | PT | | 31.2 | Cl | $D_a$ = 2.62 - 61.5 |
| **Fan et al (2014)** | OPC PO42.5R cement | KOH | Kaoline 0% | RCM | | Not reported | Cl | 9.42 |
| **Fan et al (2014)** | OPC PO42.5R cement | KOH | Kaoline 1% | RCM | | Not reported | Cl | 9.19 |
| **Fan et al (2014)** | OPC PO42.5R cement | KOH | Kaoline 3% | RCM | | Not reported | Cl | 7.46 |
| **Fan et al (2014)** | OPC PO42.5R cement | KOH | Kaoline 5% | RCM | | Not reported | Cl | 8.09 |
| **Fan et al (2014)** | OPC PO42.5R cement | KOH | Kaoline 7% | RCM | | Not reported | Cl | 8.87 |
| **Fan et al (2014)** | OPC PO42.5R cement | KOH | Kaoline 9% | RCM | | Not reported | Cl | 8.71 |
| **SKB (2014)** | Construction concrete (OPC presumed) | Expert judgement | 0–100 years after closure | | | | (based on Cl) | 3.5 |
| **SKB (2014)** | Construction concrete (OPC presumed) | | 100–10 000 years after closure | Expert judgement | | | (based on Cl) | 11 |
| **SKB (2014)** | Construction concrete (OPC presumed) | | 10 000–20 000 years after closure | Expert judgement | | | (based on Cl) | 50 |
| **SKB (2014)** | Construction concrete (OPC presumed) | | 20 000–100 000 years after closure | Expert judgement | | | (based on Cl) | 100 |
| **Albinsson et al. (1993)** | OPC | Artificial GW- not reported | | TD | Not reported | Not reported | Am, Pu | No movement |
| **Albinsson et al. (1993)** | OPC | Artificial GW- not reported | | TD | Not reported | Not reported | Cs | 0.1 - 1 |

Abbreviations

TD - through diffusion

RCM - rapid chloride migration test (Elfmarkova et al., 2015)

GW - groundwater

PT - penetration technique (Caré, 2008)

W/C - water/cement ratio

NPP - nuclear power plant

OPC - ordinary Portland cement

LPC - low pH cement

*Durability of concrete*

Durability and resistance of cement mixtures is mainly affected by the internal chemical composition and microstructure of the concrete. In the pure Portland cement concrete the total volume is contributed by two types of porosity. Isolated pores are completely sealed in concrete by hydration products and material transfer into and out of the pore is very limited. Open/transfer porosity is that through which there is a path between two areas of the material. This connected porosity often, but not always, connects the entire volume of the cementitious material with the surrounding environment and thus aggressive chemicals can penetrate into the concrete and degrade the material from inside. Concrete resistance includes both the effect of mechanical damage (e.g. abrasion, thermal expansion), but more often is associated with resisting chemical attack, e.g. sulfate effect, corrosion of steel reinforcement, whether general or supported by chlorides, alkaline aggregates reaction etc.

Sulfate attack - a reaction takes place between $C_4ASH_{12}$ (monosulfate) and $SO_4^{2-}$ in the presence of calcium ions (gypsum) in an aqueous medium and is formed a new mineral phase, ettringite (Atahan & Dikme, 2011). The conversion of the high density phase into a low density mineral phase may cause material expansion and cracking. Cracks could increase the porosity and thus accelerate the transport of sulfate ions in the cement matrix and its degradation.

Carbonation - due to the reaction between the dissolved $CO_2$ and calcium containing matrix phase is reduced the pH of the matrix. Carbonation is formed on the surface area and carbonation product penetrates into the concrete matrix, the distance to which the products penetrate corresponds to the porosity. Carbonation may consume $Ca(OH)_2$ and CSH (calcium silica hydrates) and produce $CaCO_3$ (Chang & Chen, 2006). The degradation of CSH can lead to progressive decalcification and to very small Ca/Si ratios and finally to the silicate gels formation. Degradation of the basic structural phases can lead to loss of material strength. Another factor is the loss of the higher pH of concrete with steel reinforcement. At pH > 10.5 a film of passivation products that prevents further corrosion of steel is formed at the surface of the steel reinforcement, the loss of higher pH increase the risk of corrosion.

The influence of chloride - is harmful for its corrosion of steel reinforcement, when is disturbing passivation film on steel surface. The pitting and facet corrosion on steel occurs.

Alkali aggregate reaction (AAR) - some rocks contain silicon in a slightly reactive form, generally flint, opal, chert, pressure-metamorfed quartz, have high reactivity in the concrete. The reaction is controlled by the high pH of pore fluids and silicon available for reaction with sodium gives rise to silica gels which contain very small amount of calcium. Gels absorb the water, swell and increases in volume and then thereby cause cracks in the concrete (Fournier & Bérubé, 2000).

*Cement-bentonite interactions*

Cementitious materials when interacting with water form a leachate with high pH (~ 12–13). These highly alkaline water may affect other parts of the engineered barrier system or host environment. The most relevant interactions are concrete and bentonite or other clay material (see Figure 5.1.1) used as a buffer, which may cause significant degradation of the properties of this backfill material (Alexander et al., 2008).
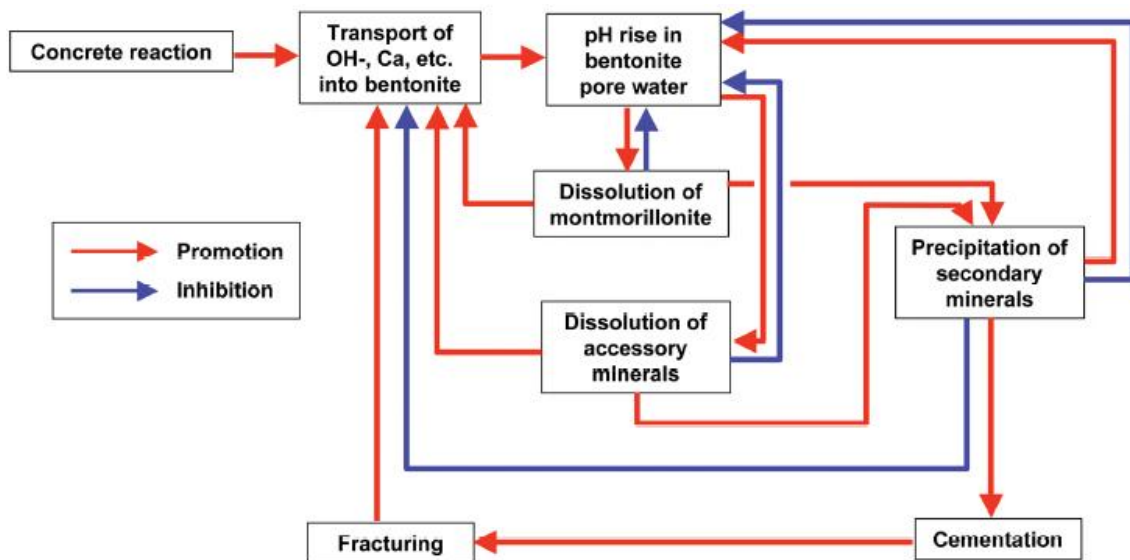
*Figure 5.1.1. Cement-bentonite interactions: Some of the important processes involved in bentonite alteration (Alexander et al., 2008).*

However bentonite has a very high ability to buffer the pH, so the effect of alkaline plumes are likely to be only near the of concrete - bentonite interface (Gaucher et al., 2004). For the development of pH in bentonite affected by alkaline solution in the long time scale are used computer simulations (see Figure 5.1.2).
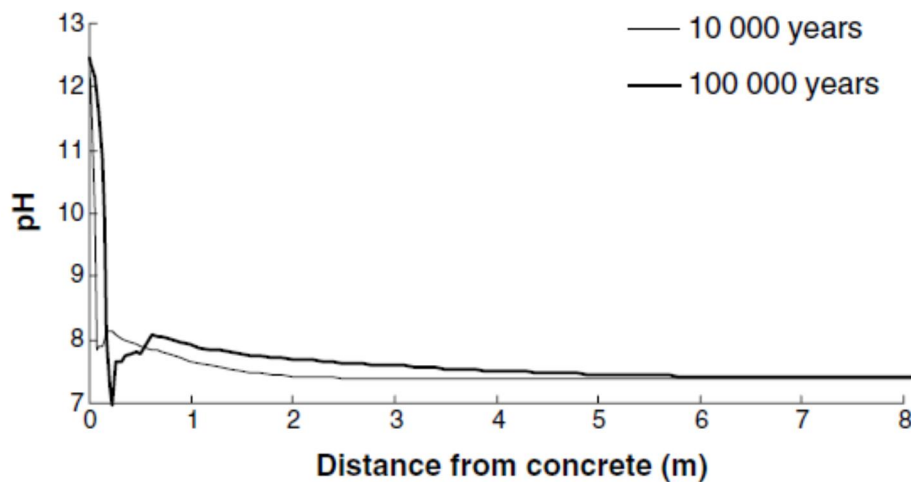


*Figure 5.1.2. Model of the change in the pH of the barrier (MX80) pore water (Gaucher et al., 2004).*

As the alkali solutions react with bentonite the formation of new mineral phases can occur (Savage et al., 2007), see Figure 5.1.3. To avoid as much possible alteration of bentonite, it is proposed to use low-alkaline cements or concretes with a low pH (where a low is considered to pH ~ 11). Reducing the pH of the concrete can be achieved by appropriate selection of the cement and by the ratio of additive to the cement content in the concrete batch. The pH value can be significantly reduced in particular by the addition of silica fume and other additives.
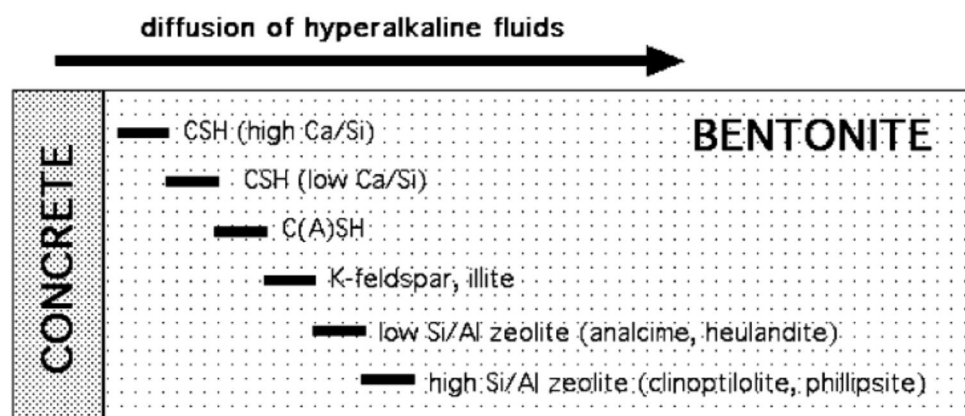
*Figure 5.1.3. Schematic diagram of the potential sequence of secondary minerals due to the migration of hyperalkaline pore fluids through bentonite (Savage et al., 2007).*

Although computer models and codes are used in long-term assessment, experimental results are needed as input parameters and also for the functional verification of models. The great advantage can also shows the data obtained from measurements archaeological analogues and especially natural analogues of cement in locations Maqarin and Khushaym Matruk in Jordan and other of natural analogues and sites of the interaction of alkaline waters with clays (bentonites): Cyprus, Oman, California, China, Japan and the Philippines (Alexander et al., 2008).

**References**

[1]     AASHTO T 277-93, Standards Specifications for Transportation Materials.
[2]     ASTMC 1202 (1997): Standard Test Method for Electrical Indication of Concrete's Ability to Resist Chloride Ion Penetration -1997, USA, 1997.
[3]     Albinsson, Y., Andersson, S., Börjesson, S. & Allard, B. 1993. Diffusion of radionuclides and concrete-bentonite systems. SKB Technical report TR 93 - 29. SKB, Stockholm, Sweden.
[4]     Alexander, W. R., Arcilla, C. A., McKinley, I. G., Kawamura, H., Takahashi, Y., Aoki, K., Miyoshi, S. (2008): A new natural analogue study of the interaction of low-alkali cement leachates and the bentonite buffer of a radioactive waste repository. In MRS Proceedings (Vol. 1107, p. 493). Cambridge University Press.
[5]     Atahan, H. N., Dikme, D. (2011): Use of mineral admixtures for enhanced resistance against sulfate attack. Construction and Building Materials, 25(8), 3450–3457.
[6]     Bajja Z., Dridi W., Larbi B., Le Bescop P. (2015): The validity of the formation factor concept from through-out diffusion tests on Portland cement mortars. Cement and Conrete Composites, 63, 76–83.
[7]     Bentz D. (2007): A virtual rapid chloride permeability test, Cem. Concr. Comp. 29, 723–731.
[8]     Bentz, D.P., Garboczi, E.J. & Lagergren, E.S. 1998. Multi-scale microstructural modelling of concrete diffusivity: Identification of significant variables. Journal of Cement, Concrete, and Aggregates 20, 129–139.
[10]    Bradbury M. J. and Green A. (1986): Investigation into the factors influencing long range matrix diffusion rates and pore space accessibility at depth in granite. Journal of Hydrology, 89, 123–139.
[11]    ČSN (2010): CEN P/TS 12390-11: Zkoušení ztvrdlého betonu - Část 11: Stanovení chlorozivzdornosti betonu, jednosměrná diúfúze. Předběžná česká norma.
[12]    Caré S. (2008): Effect of temperature on porosity and on chloride diffusion in cement pastes. Construction and Building Material, 22, 1560–1573.
[13]    Chang, C. F., Chen, J. W. (2006): The experimental investigation of concrete carbonation depth. *Cement and Concrete Research*, *36*(9), 1760–1767.
[14]    Chaussadent T., Arliguie G. (1999): AFREM test procedures concerning chlorides in concrete: extraction and titration methods, Mat. Struct. 32 (1999) 230–234.
[15]    Concrete Q & A (2006): Rapid chloride permeability tests, Concr. Int. 28 (8) (2006) 98–100.
[16]    De Windt L., Pellegrini D., van der Lee J. (2004): Coupled modeling of cement/claystone interactions and radionuclide migration. Journal of Contaminant Hydrology, 68, 165–182.
[17]    Dolder F., Mäder U., Jenni A., Schwendener N. (2014): Experimental characterization of cement-

bentonite interaction using core infiltration techniques and 4D computed tomography, Physics and Chemistry of the Earth 70-71, 104–113

[18] Elfmarkova V., Spiesz P., Brouwers H.J.H. (2015): Determination of the chloride diffusion coefficient in blended cement mortars. Cement and Concrete Research 78 (2015) 190–199.

[19] Eriksen, E., Locklund, B. (1989): Radionuclide sorption on crushed and intact granitic rock. Volum and surface effects. SKB Technical Report TR 89-25.

[20] Fan Y., Zhang S., Kawashima S., Shah S. (2014): Influence of kaolinite clay on the chloride diffusion property of cement-based materials. Cement & Concrete Composites 45 (2014) 117–124.

[21] Fournier B., Bérubé M.-A. (2000): Alkali-aggregate reaction in concrete: a review of basic concepts and engineering, Canadian Journal of Civil Engineering, 27(2): 167–191.

[22] Gaucher C. E., Blanc P., Matray J.-M., Michau N. (2004): Modeling diffusion of an alkaline plume in a clay barrier, Applied Geochemistry 19, 1505–1515.

[23] Gaucher C. E., Blanc P. (2006): Cement/clay interactions – A review: Experiments, natural analogues and modeling, Waste Management 26, 776–788.

[24] Johnston, H.M. & Wilmot, D.J. 1992. Sorption and diffusion studies in cementitious grouts. Waste Management 12, 289–297.

[25] Löfgren M., Neretnieks I. (2003): Formation factor logging by electrical methods – Comparison of formation factor logs obtained in situ and in the laboratory. J. of Contam. Hydrol. 61, 107–115.

[26] Löfgren M., Neretnieks I. (2004): A conceivable technique of measuring sorption coefficients in intact rock using an electrical potential gradient as the driving force for migration. Scientific Basis for Nuclear Waste Management XXVII, vol. 807, 683–688.

[27] Löfgren M., Neretnieks I. (2006): Through electromigration: A new method of obtaining formation factors and investigating connectivity. J. of Contam. Hydrol. 87, 237–252.

[28] Marchand J. (2001): Modeling the behavior of unsaturated cement based systems exposed to aggressive chemical environments, Mater. Struct. 34 (2001) 195–200.

[29] Mattigod S.V., Wellman D., Bovaird Ch., Parker Ch., Recknagle K., Clayton L., Wood M. (2002): Diffusion of Radionuclides in Concrete and Soil. In Rahman R., A. (2002): Radioactive waste. InTech, DOI: 10.5772/1859.

[30] Methods of Sampling and Testing, sixteenth ed., 1993, p. 876. Washington DC,

[31] NT Build 443 (1995): Nordtest Method NT Build 443, Concrete, Hardened: Accelerated Chloride Penetration, 1995.

[32] NT Build 492 (1999): Concrete, Mortar and Cement-based Repair Materials: Chloride Migration Coefficient from Non-steady-state Migration Experiments,Nordtest Method, 1999.

[33] Ohlssons Y. (2000): Studies of ionic diffusion in crystalline rock. Doctoral thesis. KTH Stockholm, Sweden.

[34] Ohlssons, Y., Neretnieks, I. (1995): Literature survey of matrix diffusion theory and of experiments and data including natural analogues. SKB Technical Report TR 95-12.

[35] Posiva (2007): Process report FEPs and scenarios for spent fueld repository in Oikiluoto. Miller B. and Marco N. Eds. Report Posiva 2007-12. Posiva, Eurojaki, Finland.

[36] Sánchez L., Cuevas J., Ramírez S., Riuiz De León D., Fernández R., Vigil Dela Villa R., Leguey S. (2006): Reaction kinetics of FEBEX bentonite in hyperalkaline conditions resembling the cement-bentonite interface, Applied Clay Science 33 (2006), 125–141.

[37] Savage, D., Walker, C., Arthur, R., Rochelle, C., Oda, C., Takase, H. (2007): Alteration of bentonite by hyperalkaline fluids: A review of the role of secondary minerals. Physics and chemistry of the Earth, Parts A/B/C, 32(1), 287–297.

[38] Savage D. (2013): Constraints on cement-clay interaction, Proceeding Earth and Planetary Science 7, 770–773.

[39] Shackelford Ch. and Moore S. (2013): Fickian diffusion of radionuclides for engineering containment barriers: Diffusion coefficients, porosities and complicating issues. Engineering Geology, 152, 133–147.

[40] SKB (2014): Data for safety assessment SR-PSU. SKB Technical report TR 14-10. SKB, Stockholm.

[41] Szántó Z., Svingor É., Molnár M., Palcsu L., Futó I., Szucs Z. (2002): Diffusion of 3H, 99Tc, 125I, 36Cl and 85Sr in granite, concrete and bentonite. Journal of Radioanalytical and Nuclear Chemistry, Vol. 252, No. 1.

[42] Vilks, P., Miller, N.H. and Stanchell F. W. (2004): Phase II. In situ diffusion experiment. Rep. AECL No. 06819-REP-01200-10128-R00.

[43] Wellman D.M., Mattigold S.V., Powers L., Parker K.E., Clayton L.N., Wood M.I. (2007): Concrete property and radionuclide migration tests. US department of Energy, PNNL-17676. Pacific Northwest Laboratories, Batelle.

## 5.2 Conventional studies of diffusion cell test method with cementitious materials

*Naila ait Mouheb, Vanessa Montoya, Thorsten Schäfer*

*Karlsruhe Institute of Technology (KIT), Institute for Nuclear Waste Disposal, Germany*

It is well known that the degradation process of cementitious materials involves diffusion of internal and external ions, interaction between these ions and re-deposition of the interacted products. The diffusion coefficient is a highly important parameter as an assessment criterion in the domain of nuclear waste disposal. Radionuclides are transported by diffusion in the cement matrix and can be described by Fick's laws. If we consider diffusion in the steady state, the first Fick's law can be applied to these systems:

$$J = -D\frac{\partial C}{\partial x} \quad (1). \ (1^{st}\ Fick's\ law\ in\ 1D)$$

where J is the substance flux [kg/m$^2$·s]; $\frac{\partial C}{\partial x}$ is the concentration gradient [kg/m$^4$]; and D is the diffusion coefficient [m$^2$/s]. However, transport processes in cementitious materials can be time dependent since the pore structure of this materials can change with time. In that case the Fick´s first law is not applicable and diffusion can be explained with the Fick´s second law which states that the change in concentration per time is equal to the change of the flux per unit of length.

Although diffusion processes play an important role in the deterioration process, there is lack of reliable data on ion diffusion coefficient in cement materials. In the literature, it is described different methods to study diffusion processes in these materials including the determination of diffusion coefficients under steady state or transient state conditions, which are listed below:

- Through diffusion
- Leaching test/Out diffusion
- Electrochemical migration (acceleration method)

Chloride diffusion processes through concrete has been one of the dominant studies described in the literature. However, diffusion studies with low pH cements are very scarce which makes difficult to predict the migration of radionuclides in this solids. For example, it is well know from previous studies that the addition of silica fume or fly ash (main additives to obtain low pH cement) in ordinary Portland cement paste considerably reduces the diffusion rate for chloride (Byfors et al. 1987) which will affect to the transport properties.

Bellow it is given a summary of through and out-diffusion experiments in saturated porous materials indicating the experimental setup used by the different groups and the type of cement used and the approximation follow to determine the diffusion coefficient. Not description of the leaching test of the electrochemical migration is given is this section as more information can be found in the contribution of Alonso and Garcia Calvo (this report).

### 5.2.1 Through diffusion experiments

Diffusion coefficients in cementitious systems can be determined by **through-diffusion** cells where two compartments (up-stream and down-stream cell) are filled with solutions characterized by different salt concentrations and are separated by a cylindrical cement paste sample with cross-sectional area $A_{(sample)}$ and thickness $t_{(sample)}$ (Figure 5.2.1.1). The transport mechanism in this technique is very similar to the one that takes place in real structures but one of the biggest inconvenient is the long time needed to perform the experiments and the need of use thin samples to reduce the experimental time.
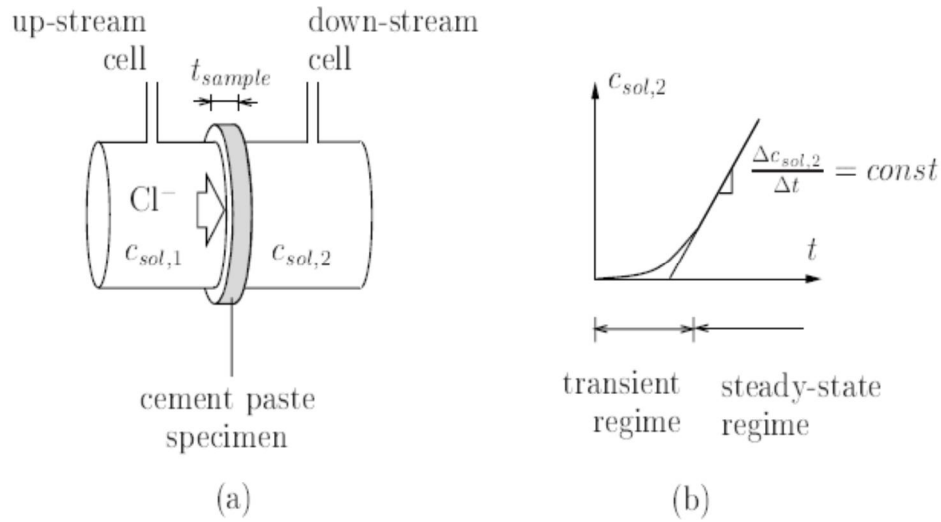


*Figure 5.2.1.1. Schematic representation of a through diffusion cell (Pivonka et al. 2004), b) time-dependent evolution of chloride concentration in down-stream cell.*

In order to arrive at an adequate description and interpretation of the diffusion experiments, it is needed to solve the diffusion equation with appropriate initial and boundary conditions consistent to the designed experiments. In most of the experiments described in the literature the boundary conditions are considered as constant (Figure 5.2.1.2). For this reason the downstream solution is normally renewed each day (to maintain concentration equal to zero in this compartment) and the upstream activity is changed each three day and conserved at the initial value of the tracer studied.
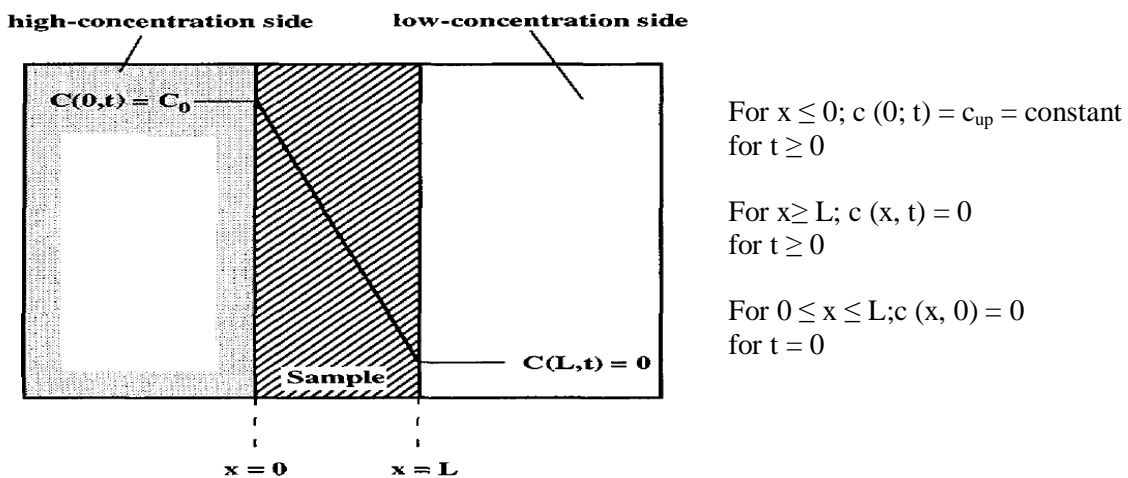


For $x \leq 0$; $c\,(0; t) = c_{up} = $ constant for $t \geq 0$

For $x \geq L$; $c\,(x, t) = 0$ for $t \geq 0$

For $0 \leq x \leq L$; $c\,(x, 0) = 0$ for $t = 0$

*Figure 5.2.1.2. Sketch of a cross-section through the diffusion cell (Jakob et al., 1999).*

In order to determine the diffusion coefficient of the studied species, the concentration in the downstream cell is measured as a function of time. In Figure 5.2.1.3 and Figure 5.2.1.1b, a general evolution tendency of the activity cumulated (concentration) in the downstream compartment and the flux as a function of time is represented. As can be seen from this plot (Figure 5.2.1.3), there are two different regimes:

1) The transient regime, where the flux increases while the porosity is filled with the diffusing species and

2) The steady state regime where the concentrations in the liquid and on the solid come into equilibrium and the flux remind constant.
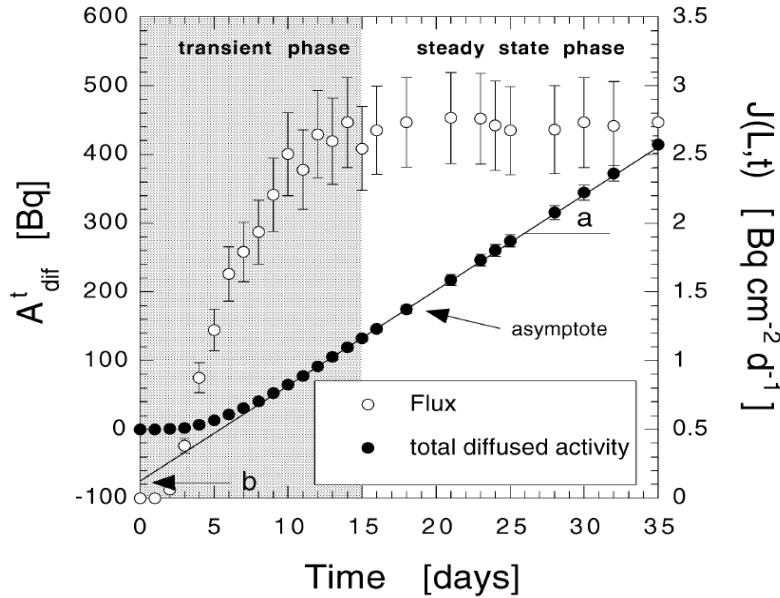


*Figure 5.2.1.3. Evolution tendency of the flux and total diffused mass as a function of time during a through diffusion experiment (van Loon et al. 2004).*

Diffusion experiments are normally running until the steady state is reached (constant flux). In the steady state the slope between the concentration in the downstream cell vs time becomes constant which means the diffusive flux across the sample is also constant. Fick's first law can then be applied to calculate the cumulative quantity Q(t) [mol] of diffusing species passed through a sample with a cross-sectional area A [$m^2$]. In this case the effective diffusion coefficient (De) can be calculated from the slope of the total diffused activity curve and the porosity of the system ($\varepsilon$) from the intercept with the y-axis.

There is an analytical solution to be applied to diffusion experiments performed under constant boundary conditions. (Crank, 1979) where the evolution of the radioactivity in the downstream compartment with a thick sample "L" (i.e. x max = L) can be calculated, by the following expression:

$$A_{dif}^t = S.L.C_0 \left( \frac{D_e.t}{L^2} - \frac{\alpha}{6} - \frac{2.\alpha}{\pi^2} \sum_{n=1}^{\infty} \frac{(-1)^n}{n^2} \, exp \left\{ -\frac{D_e.n^2.\pi^2.t}{L^2.\alpha} \right\} \right) \qquad (1)$$

And:

Where:
$A_{diff}^t$  the cumulative activity of tracer in the downstream compartment (Bq),
$C_0$  the activity of the solution in the high concentration container (cpm.$cm^{-3}$),

102

*L*     the thickness of the sample,
$D_e$     the effective diffusion coefficient (m$^2$/s),
$D_a$     the apparent diffusion coefficient (m$^2$/s),
*t*     time (s),
$\alpha$     the rock capacity factor. $\alpha = \varepsilon + \rho \cdot K_d$ ($\varepsilon$ = porosity),
$K_d$     equilibrium distribution coefficient (m$^3$/kg), $K_d = 0$ for no-sorbing tracers.
$\rho$     the dry bulk density of the rock (kg/m$^3$),
*S*     the cross sectional area of the exposed surface (m$^2$).

As time increases, the exponential term reduces towards zero and the equation 2 approximates:

$$A_{dif}^{\Delta t} = S \cdot L \cdot C_0 \left( \frac{D_e \cdot t}{L^2} - \frac{\alpha}{6} \right) \tag{2}$$

This equation can be expressed as a linear equation:

$$A_{dif}^{t} = a \times t + b$$

Where:

$$a = \frac{S \cdot C_0 \cdot D_e}{L}, \quad -b = \frac{S \cdot L \cdot C_0 \cdot \alpha}{6}$$

The flux $J_{dif}^{\Delta t}$ at time $t_i$ is calculated by:

$$J_{dif}^{\Delta t} = \frac{A_{dif}^{\Delta t}}{S \cdot \Delta t_i} \tag{3}$$

*Determination of the effective diffusion coefficients described in the literature*:

Atkinson et al. 1984 studied the diffusion of I$^-$ and Cl$^-$ ions and the tracer diffusion of Cs$^+$ ions in water saturated Ordinary Portland Cement as a function of water/cement ratio at cement manufacturing by through diffusion experiments. The diffusion cell is schematically shown in Figure 5.2.1.1. The concentration of the diffusing specie in the low concentration side of the cell as a function of time was measured and the boundary conditions was kept constant. The authors observed that diffusion was strongly influenced by the water/cement ratio in an approximately exponential manner. Cs was significantly less mobile than the other ions. Diffusion measurements were also made as a function of temperature, but not temperature effects will be discussed in this report.

Byfors et al. 1986 studied the diffusion of chloride ions through the cement paste by means of the 2-chamber method as illustrated in Figure 1. The cement discs were mounted in diffusion cells to measure the rate of diffusion. The upstream reservoir was filled with 1 M NaCl/ saturated Ca(OH)$_2$ solution (pH = 12.5) and the downstream was filled with saturated Ca(OH)$_2$ solution only. At the beginning, very little Cl$^-$ diffuses through the disc due to the fact that the cement paste binds chlorides chemically in the hydration products. After a few days, equilibrium is achieved between free and bound chloride ions and a steady state flow occurs on condition that the concentration of Cl$^-$ in both chambers is kept constant all the time. Constants boundary conditions by replacing the solutions during the experimental period was performed. The determination of the diffusion parameters method is based on following the increase in the Cl concentration by ion-selective electrode in the downstairs

reservoir as a function of the time. Chloride diffusion through the paste disc was calculated by means of Fick's 1st law in the steady state and is shown in Table 5.2.1.1. The experimental results show that an addition of silica fume of fly ash with the same water-binder ratio gives a lower rate of diffusion compared with a pure Portland cement paste. The results also show that the diffusion constant decreases with a decrease in the water-binder ratio.

*Table 5.2.1.1. Diffusion coefficients determined by Byfors et al. 1986 in different cement pastes.*

| Cement | Diffusivity for Cl⁻ (cm²/s)x10⁻⁹ | | | |
|---|---|---|---|---|
| | w/b = 0.40 | w/b = 0.50 | w/b = 0.60 | w/b = 0.70 |
| OPC | 18 | 68 | 187 | |
| OPC+SP | 34 | | | |
| OPC/10% CSF | 18 | 24 | 99 | |
| OPC/10% CSF+SP | 20 | 23 | | |
| OPC/20% CSF | 3.2 | 5.9 | 31 | 63 |
| OPC/20% OPC+SP | 3.0 | 21 | | |
| OPC/15% PFA 1 | 6.3 | 32 | 26 | |
| OPC/15% PFA 2 | | 36 | | |
| OPC/40% PFA 1 | 0.79 | 1.3 | 17 | |
| OPC/40% PFA 2 | | 3.2 | | |

Johnston et al. 1992 determined the diffusion coefficients for tritiated water (HTO) and [36]C1 under simulated saline groundwater ($CaCl_2$ solution at 1 M) conditions at pH = 12.5 for six mixtures of Sulphate Resistant Portland Cement containing Silica Fume at two water to cement ratios. Superplasticizer (naphthalene sulphonate formaldehyde condensate) was also included. The schematic representation of the diffusion cell is shown in Figure 5.2.1.4. The basic cell consists of two 125 mL reservoirs separated by the sample disc (0.59 mm); one reservoir contained the active solution (spiked with HTO and [36]C1⁻) while the other reservoir contained the non-active solution. Detailed information regarding its construction and the cell filling and sampling procedure is given in Johnston and Wilmot (1988).

To ensure constant boundary conditions and constant tracer concentration at the upstream reservoir, the active solution was circulated from a central stock reservoir by a peristaltic pump at a rate of 0.65 to 0.75 mL/min. For obtaining the diffusion coefficient, it is assumed steady state and homogeneous sample.

The results of the diffusion experiments show both HTO and [36]C1 to behave as reactive tracers in cement-based materials. The water to cement ratio was shown to have a significant effect on the retardation capabilities of the grout mixes with retardation factors increasing as the water to solid ratio was reduced from 0.35 to 0.25.

Diffusion coefficient for [37]Cs and [85]Sr were calculated by the authors using the diffusion coefficient determined for HTO and using the distribution coefficient determined by the same authors in batch experiments. Tortuosity factors were calculated from the results of the diffusion tests. The results also showed the addition of silica fume to have impact on the

potential migration rates of both [37]Cs and [85]Sr, however, under saline conditions, a similar reduction in the effective diffusion coefficients could be achieved through a decrease in the water to cement ratios.
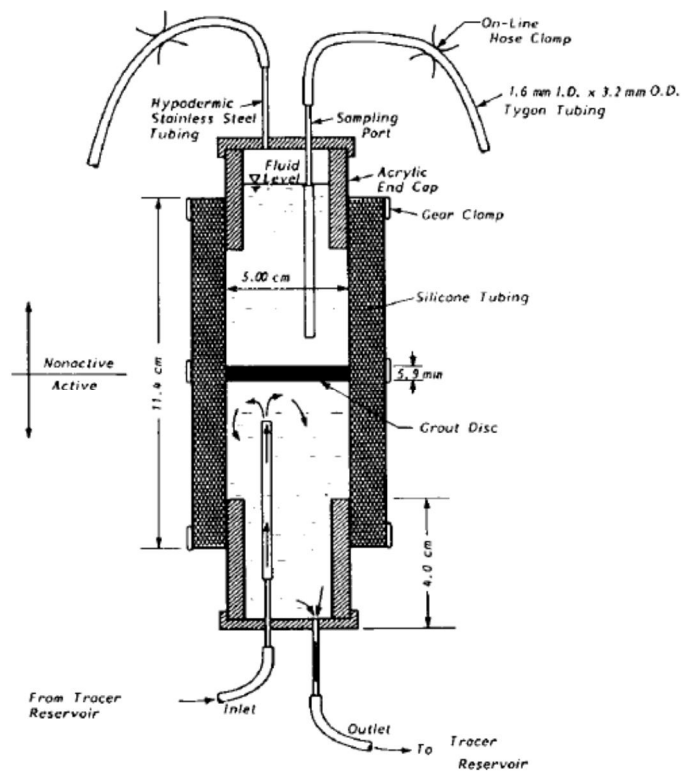


*Figure 5.2.1.4. Schematic representation of the diffusion cell used in Johnston et al. 1992.*

Nugue et al. (2007) propose a new method for testing molecular diffusion in concrete containing normal Portland cement, sand and gravel at a solid/iquid ratio of 0.4. A saturated specimen of porous material of 15 mm thick was placed between two compartments containing an alkaline solution with NaOH (1g/L) and KOH (4.65 g/L). The upstream compartment contained tritiated water (HTO) at an initial concentration of $37 \times 10^9$ Bq m$^{-3}$ and the downstream compartment a solution without HTO. The boundary conditions were maintained constant. Usually, the flux of HTO was repeatedly measured by analysing the content of the downstream cell in the steady state by liquid phase scintigraphy. In this work, a theoretical study based on Fick's laws is used to show that it is possible to determine the diffusion coefficient $D_{Fick1}$ by considering only two measurements obtained in the non-steady state, in the downstream compartment of a diffusion cell. A significant saving of time (approximately half) was obtained.

Bajja et al. 2015 performed through-diffusion studies of HTO, Li$^+$ and Cl$^-$ in 6 different mortar compositions (see Table 5.2.1.2) to identify the diffusion coefficients as a function of the selected solid materials. Lithium and Chloride were included as a LiCl salt at low concentration (41 mmol/L) to neglect the effect of the electrical interaction. The initial concentration for HTO was 3.2 x10$^6$ Bq/L. Mortars were manufactured by mixing Portland cement with standardized siliceous sand, water and super plasticizer (Glenium 27). The microstructure and porosity of the studied materials was investigated by free water porosity and by Mercury Intrusion Porosimetry measurements (see Figure 5.2.1.4).

*Table 5.2.1.2. Proportions of the materials tested by Bajja et al. 2015.*

| Mixtures ID | SN. 0% | SN. 10% | SN. 30% | SN. 50% | SN. 55% | SN. 60% | SN. 65% |
|---|---|---|---|---|---|---|---|
| W/C | 0.4 | 0.4 | 0.4 | 0.4 | 0.4 | 0.4 | 0.4 |
| $C_{ag}$ | 0% | 10% | 30% | 50% | 55% | 60% | 65% |
| Gle-27 (%) | — | — | — | — | — | 0.5 | 1.5 |

W/C is the water-to-cement ratio.
$C_{ag}$ is the relative aggregate volume content.
Gle-27 (%) is the mass of Glenium 27 relative to mass of cement.

The through diffusion set-up consists in a cell with the mortar sample of 6 mm length between two compartments (upstream and downstream), as it is shown schematically in Figure 5.2.1.1. The solid sample is sealed into position using an epoxy adhesive. Each compartment have a volume of 111 ± 1 ml and is filled with saturated lime water (pH ~12.5).
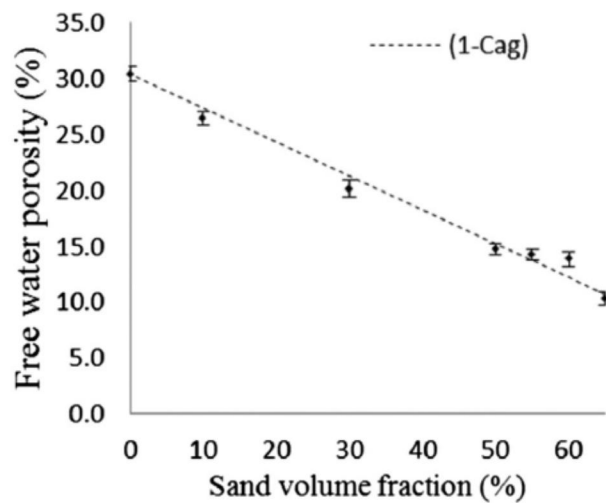


*Figure 5.2.1.4. Effective diffusion coefficient De of HTO vs the sand content in mortars (Bajja et al. 2015).*

Experimental measurements were performed until a stationary state was reached. During the diffusion test, the upstream and downstream concentrations were maintained at nominally constant values. The concentration at the downstream compartment was set to not reach 3% of the upstream concentration.

The amount of tracer accumulated in the downstream compartment was measured and the effective diffusion coefficient was determined by the analytical solution proposed in Nugue et al. 2007. Calculated diffusion coefficients are shown in Table 5.2.1.3.

*Table 5.2.1.3. Diffusion coefficients determined by Bajja et al. 2015.*

| Mixtures ID | $D_e^{HTO}$ (m²/s) | $D_e^{Li}$ (m²/s) | $D_e^{Cl}$ (m²/s) |
|---|---|---|---|
| SN. 0% | $2.56 \cdot 10^{-12} \pm 1.40 \cdot 10^{-14}$ | $1.149 \cdot 10^{-12}$ | $2.18 \cdot 10^{-12}$ |
| SN. 10% | $2.40 \cdot 10^{-12} \pm 2.70 \cdot 10^{-13}$ | $1.01 \cdot 10^{-12}$ | $1.93 \cdot 10^{-12}$ |
| SN. 30% | $1.96 \cdot 10^{-12} \pm 4.00 \cdot 10^{-14}$ | $8.55 \cdot 10^{-13}$ | $1.64 \cdot 10^{-12}$ |
| SN. 50% | $1.45 \cdot 10^{-12} \pm 6.00 \cdot 10^{-14}$ | $5.69 \cdot 10^{-13}$ | $1.15 \cdot 10^{-12}$ |
| SN. 55% | — | $5.90 \cdot 10^{-13}$ | $1.28 \cdot 10^{-12}$ |
| SN. 60% | $3.39 \cdot 10^{-12} \pm 2.99 \cdot 10^{-13}$ | $1.70 \cdot 10^{-12}$ | $2.68 \cdot 10^{-12}$ |
| SN. 65% | — | $8.24 \cdot 10^{-13}$ | $1.79 \cdot 10^{-12}$ |

According to this results can be concluded that the presence of nonporous sand grains tend to decrease the diffusivity, however, the presence and the interconnectivity in the interfaces are the origin of the appearance of larger pores and probably the cause of the increase of the diffusion coefficient (in the SN. 60% mortar).

The work carried out in PSI research center (Jakob et al. 1999, 2002, Sarott et al. 1992, Tits et al. 2003) described the diffusion of HTO, Cl^{-}, I[-], $^{22}Na^+$, $Cs^+$ and $Ni^{2+}$ in a Sulphate Resisting Portland Cement (SRPC) equilibrated with an artificial pore water at pH = 13.3. Very recently, the same group (Wieland et al. 2016) has studied the diffusion of small organics by the same type of cement at different hydration time and using the same diffusion cell. The diffusion experiments were performed in a globe box with nitrogen in order to avoid carbonation of the sample.
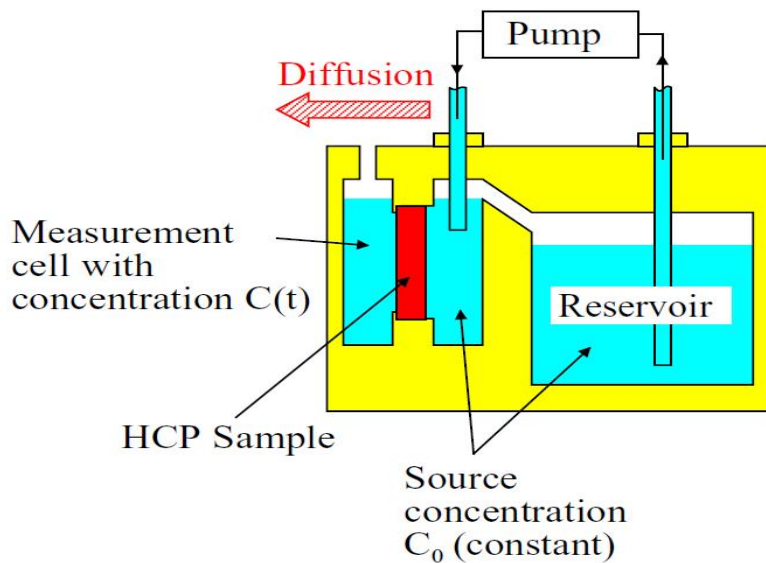


*Figure 5.2.1.5. Schematic representation of the set-up used for the through-diffusion experiments (Jakob et al. 1999).*

The set-up used in the through-diffusion experiments of Jakob et al. 1999 and Sarott et al. 1992 is shown in Figure 5.2.1.5. The whole apparatus is constructed modularly and consists of transparent polystyrene allowing an easy check of the height of the solutions. The samples are sealed by two component synthetic resin (Epoxy resin), into a sample holder which formed part of the diffusion cell.

The pipes consist of PTFE, having a total length of about 0.7 m and an inner diameter of about 4 mm; the wetted parts of the pump are covered with PVDF, and the pump rate is about 12–15 ml/min. The dimensions of the apparatus are given in Table 5.2.1.4.

*Table 4. Some geometrical aspects of the apparatus (A. Jakob et al., 1999 and Sarott et al., 1992).*

| V$_{reservoir}$ (mL) | V$_{Low concentration}$ (mL) (Measurement cell) | V$_{High concentration}$ (mL) (Smaller part of the reservoir) | Reference |
|---|---|---|---|
| 540.0 | 47.0 | 45.0–50.0 | Jakob et al., 1999 |
| 500.0 | / | / | Sarott et al., 1992 |

The sample was glued into a sample holder made of polystyrene which itself was part of the diffusion apparatus. The sizes of the cement sample used in these studies is shown in Table 5.2.1.5 and compare with the sample size of other authors.

The two compartments (Source concentration or upstream and the measurement cell or downstream) contain an alkaline solution in order to limit the leaching of the pore solution alkalis. In the case of hardened cement pastes "HCP" from the work of Tits et al 2003 [28], this alkaline solution consists to an Artificial Cement Water (ACW) with a composition of 0.18M KOH; 0.114M NaOH; $1.7.10^{-3}$ $Ca(OH)_2$ and pH = 13.3.

*Table 5.2.1.5. Geometrical parameters of the cement samples.*

| Experimental time (days) | Sample thickness $10^2$ [m] | Sample Diameter $10^2$ [m] | Reference |
|---|---|---|---|
| 60 | 0.3 | 3.2 | Atkinson et al., 1984 |
| 60 | 0.3 | 1.9 | Byfors et al., 1986 |
| 200 | 0.59 | 5.0 | Johnston et al., 1992 |
| 208 | 1.0 | 4.0 | Sarott et al., 1992 |
| 180 | 0.5 | 4.1 | Jakob et al., 1999 |

In Table 5.2.1.6 is included a summary on the effectives diffusion coefficient determined by different authors including the porosity of the sample, the ratio water/solid (W/C) of the samples, the type of tracer used and their initial concentration $C_0$ in the high concentration reservoir and the equilibrium distribution coefficient ($K_d$) determined in the same work if possible.

*Table 5.2.1.6. Literature review of the effectives diffusion coefficient values, given during through-diffusion experiments.*

| Sample type | Porosity[b] | w/c | Tracer[c] | time (days) | $C_0$ (mol/L) | $D_e$ ($m^2$/s) | Source |
|---|---|---|---|---|---|---|---|
| HCP (Type 50-SRPC[e]) | 0.63±0.05 | 1.3 | $^{36}Cl$ | 176 | $2.79\ 10^{-5}$ | $1.56 \cdot 10^{-10} \pm 0.07$ | Jakob et al., [25] |
| | | | $^{125}I$ | 84 | $3.61\ 10^{-8}$ | $2.86 \cdot 10^{-11} \pm 0.07$ | |
| | | | $^{134}Cs$ | 87 | $3.82\ 10^{-8}$ | $1.12 \cdot 10^{-11} \pm 0.4$ | |
| HCP (Type 50-SRPC[e]) | 0.63±0.05 | 1.3 | $^{36}Cl$ | | $2.9\ 10^{-5}$ | $1.6\ 10^{-10\ (a)}$ | Sarott et al., 1992 |
| | | | $^{125}I$ | 170 | $3.9\ 10^{-8}$ | $3.0\ 10^{-11\ (a)}$ | |
| | | | $^{134}Cs$ | | $3.6\ 10^{-8}$ | $1.4\ 10^{-10\ (a)}$ | |
| 85% Type 50-SRPC[e] +15% silica fume | 0.198 | 0.35 | $^{137}Cs$ | 200 | $2.75\ 10^{-7}$ | $4.9 \cdot 10^{-13}$ | Johnston et al., [30] |
| | | | $^{85}Sr$ | | $4.0\ 10^{-4}$ | $2.3 \cdot 10^{-13}$ | |
| Concrete | 0.086[f] | 0.4 | HTO | 160 | $37.10^9$ Bq $m^{-3}$ | $8.06 \cdot 10^{-13}$ | Nugue et al., 2007 |
| | | | | | | $7.94 \cdot 10^{-13}$ | |
| | | | | | | $7.51 \cdot 10^{-13}$ | |
| HCP (Type 50-SRPC[e]) | 0.63±0.05 | 1.3 | HTO | 42 | $74\ 10^{10}$ Bq $m^{-3}$ | $2.8 \cdot 10^{-10}$ | Tits et al. 2003 |
| | | | $^{22}Na$ | | | $1.1 \cdot 10^{-10}$ | |

[a] Errors in De and Rd are estimated to be ± 10%. [b] Porosity determined by mercury intrusion porosimetry. [e] SRPC = Sulphate Resisting Portland Cement. [f] Calculated porosity. Capacity factor calculated by the authors but we assumed that the $K_d$ of HTO is 0.

### 5.2.2 Out diffusion experiments

Out-diffusion experiments are considered a crucial test of the predictive quality of a given data from the through-diffusion experiments. However, in the literature there are very few authors using this technique to determine the diffusion coefficient of tracers in cement (Jakob et al. 1999, 2002, Tits et al. 2003, Wieland et al. 2016).

Tits et al. 2003 (Jakob et al. 2002) studied the diffusion of tritiated water (HTO) and $^{22}Na^+$- in non-degraded Hardened Cement Pastes. Jakob et al. 1999 perform the same kind of experiment with $^{63}Ni$ in the same kind of cementitious materials. The particular method using the samples loaded with tracer from the previous through-diffusion phase was novel allowing measuring independent values for the diffusive tracer flux differing at both boundaries (both reservoirs). The experimental set-up is very similar than the one described for the through diffusion experiments (see Figure 5.2.2.1). As soon as the steady-state is achieved in the through- diffusion experiments at time $t_i$, the solid sample is removed from the through diffusion cell and placed between two containers filled with the same synthetic pore water in equilibrium with the sample and the same volume (101mL) but without containing the tracer. After regular time, the solutions are replaced by a new solution (synthetic pore water) and their activities are measured until all the activity was diffused out of the samples.
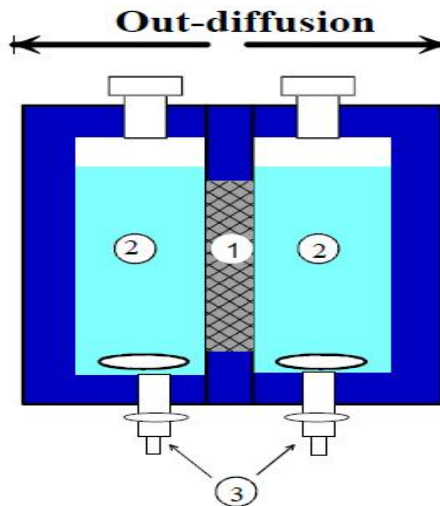


*Figure 5.2.2.1. Schematic representation of the set-up used for the out-diffusion experiment [(1): cement disk, (2): downstream compartment and (3): outlet (picture from Wieland et al. (2016)).*

For the calcultation of the effective diffusion coefficients, it is needed to solve the 1D diffusion equation with an initial (steady-state) tracer distribution from the through-diffusion phase as explained by Jakob et al. 2002 taking into account the correct boundary conditions of the system:

$C (x = 0, t) = C(x = L ,t) = 0; t > 0.$

To give an example of results from out-diffusion experiments, Figure 5.2.2.2 shows an evolution tendency of the flux to both compartments. as a function of time.
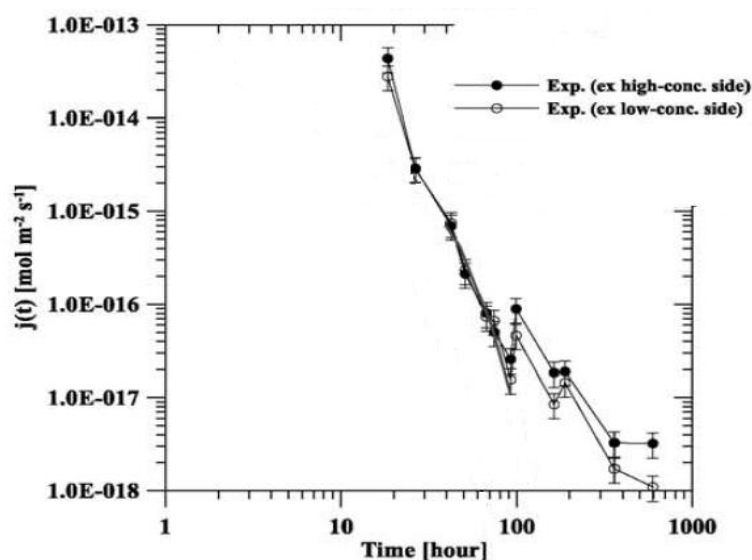
*Figure 5.2.2.2. Evolution tendency of the flux as a function of time during an out-diffusion experiment (Tits et al. 2003).*

In Table 5.2.2.1, the diffusion coefficient determined with this technique is given. Some geometrical aspects of the hardened cement pastes (HCP's), the diffusion cells, the values for the porosity and the dry bulk density, (pis the dry solid phase density.

*Table 5.2.2.1. Diffusion coefficients determined by out-diffusion experiments, determined in the literature.*

| Sample type | Porosity[a] [-] | w/c | Tracer | time (days) | $K_d.10^3$ $(m^3/kg)^c$ | $D_e$ $(m^2/s)$ | Reference |
|---|---|---|---|---|---|---|---|
| HCP (Type 50-SRPC[b]) | 0.63±0.05 | 1.3 | HTO | 42 | 0.8±0.2 | $2.72 \times 10^{-10}$ | J. Tits et al. 2003 |
| | | | $^{22}$Na | | 0.5±0.1 | $1.04 \times 10^{-10}$ | |
| HCP (Type 50-SRPC) | 0.63±0.05 | 1.3 | $^{63}$Ni | 556 | 36.7 | $2.52 \times 10^{-11}$ | Jakob et al., 1999 |

[a] Porosity experimentally determined by mercury intrusion porosimetry. SRPC = Sulphate Resisting Portland Cement, c: sorption determined by separately sorption batch experiments.

### 5.2.3 In diffusion experiments

There is another type of experiments to determine the diffusion coefficients in cementitious materials based on measuring concentration profiles in the solid.

Albinsson, et al. 1993 used this technique to study the diffusion of Cs, Am and Pu into 5 different types of concretes which composition is described in Allard et al. 1984. The samples have an inner diameter of 20 mm and a length of 25 mm. No results could be obtained for Am and Pu, because after 2.5 and 5 years contact, respectively, as Pu and Am only move 0.2 mm in the concrete.

The apparent diffusion coefficient determined by the authors for the different concrete mixtures is shown in Table 5.2.3.1. In this case for determining the diffusivity, the concentration of the studied species is measured on the solid at different distances from the interface. Constant boundary conditions were keep it in the experiments. As can be seen, the

apparent diffusion coefficient for cesium in the concretes with Standard Portland, Sulphate Resistant, Blast furnace slag, and fly ash paste are of the same order of magnitude. The lower diffusivity is obtained in the concrete with silica fume and it is explained by the different density of the solid. The higher diffusivity obtained for the cement with high aluminium content is explained by the low content of silica.

*Table 5.2.3.1. Diffusion coefficients of Cs in different concretes determined by Albinsson et al. 1993).*

| Sample type (days) | Experimental time (days) | $D_e$ (m$^2$/s) |
|---|---|---|
| SPB | 231 | 7.9 10$^{-14}$ |
| SRB | 231 | 1.0 10$^{-13}$ |
| MB | 260 | 2.5 10$^{-13}$ |
| FAB | 260 | 1.6 10$^{-13}$ |
| SIB | 260 | 7.9 10$^{-15}$ |
| ALB | 260 | 1.3 10$^{-12}$ |

Standard portland paste (SPB), Sulphate resistant paste (SRB), Blastfurnace slag paste (MB): SPB + blastfurnace slag, Fly ash paste (FAB): SPB + 30% fly ash, Silica paste (SIB): SPB + 20% silica fume + 3.2% naphthalene, High aluminia paste (ALB).

Additionally, the sorption of Cs was determined by the same authors observing a very low sorption in all the used materials. In several cases, especially for cement paste no measurable sorption was observed. The highest distribution coefficient observed was 0.25 m$^3$/kg for one sample of Standard Portland concrete. The major part of the values were in the range between 0.001 and 0.01 m$^3$/kg.

# References

Albinsson, Y., Andersson, S., Börjesson, S. and Allard, B. (1993). Diffusion of radionuclides and concrete-bentonite systems. SKB Technical report TR 93 - 29. SKB, Stockholm, Sweden.

Allard, B., Eliasson, L., Höglund, S., and Andersson, K. (1984). Sorption of Cs, I and Actinides in Concrete Systems", KBS-TR 84-15, Svensk, Kärnbränsleförsörjning AB, Stockholm 1984.

Atkinson A., and Nickerson, K (1984). The diffusion of ions through water-saturated cement, J. Mater. Sci., 19, 9, 3068–3078.

Bajja, Z., Dridi, W., Larbi, B., and Le Bescop, P. (2015). The validity of the formation factor concept from through-out diffusion tests on Portland cement mortars. Cement and Conrete Composites, 63, 76–83.

Byfors, K. (1987). Influence of silica fume and fly ash on chloride diffusion and pH values in cement paste. Cem. Concr. Res., 17, 1, 115–130.

Crank, J. (1979). The Mathematics of Diffusion. Clarendon Press.

Jakob, A. (1999). Diffusion and Sorption on Hardened Cement Pastes – Experiments and Modelling Results. PSI Report 99-05.

Jakob, A. (2002). Diffusion of Tritiated Water (HTO) and 22Na+-Ions through Non-Degraded Hardened Cement Pastes II. Modelling Results, PSI report Nr. 02-21.

Johnston, H.M. and Wilmot, D.J. (1992). Sorption and diffusion studies in cementitious grouts. Waste Management 12, 289–297.

Johnston, H. M. and Wilmot, D. J. (1988). Sedimentary sequence study: results of laboratory sorption and diffusion experiments. Ontario Hydro Research Report No. 88-85-K, Ontario Hydro Research Division, Toronto, Ontario, Canada.

Nugue, F., Yssorche-Cubaynes, M.-P., and Ollivier, J. P. (2007). Innovative study of non-steady-state tritiated water diffusion test. Cem. Concr. Res., 37, 8, 1145–1151.

Pivonka, P., Hellmich, Ch, and Smith D.W. (2004). Microscopic effects on chloride diffusivity of cement pastes - a scale transition analysis. Cement and Concrete Research, 34, 12, 2251–2260.

Sarott, F.-A., Bradbury, M. H. Pandolfo, P. and Spieler, P. (1992). "Diffusion and adsorption studies on hardened cement paste and the effect of carbonation on diffusion rates," Cem. Concr. Res., 22, 2, 439–444.

Tits, J., Jakob, A. Wieland, E., and Spieler, P. (2003). "Diffusion of tritiated water and $^{22}$Na$^+$ through non-degraded hardened cement pastes," J. Contam. Hydrol., 61, 1, 45–62.

van Loon L.R, and Soler J.M., (2004). Diffusion of HTO, 36CI-, 125I- and 22Na+ in opalinus clay: effect of confining pressure, sample orientation, sample depth and temperature. PSI report 04-03.

Wieland, E., Jakob, A., Tits, J., Lothenbach, B., and Kunz, D. (2016). "Sorption and diffusion studies with low molecular weight organic compounds in cementitious systems," Appl. Geochem., 61, 101–117.

## 5.3 Experimental studies of hydromechanical behavior of concrete fractures: a state-of-the art

*J. Shao*

*University of Lille, Laboratory of Mechanics of Lille*
*59655 Villeneuve d'Ascq, France*

**Context**

In the context of geological disposal of nuclear waste, ordinary and high performance concretes are used either as supporting material for underground structures and engineered barrier. In both cases, they are subjected to mechanical, hydraulic and thermal solicitations as well as chemical degradation. Among various aspects related to performance of concrete structures, damage induced by microcracks is an essential mechanism of inelastic deformation and failure of concrete. In many cases, the failure of concrete structures is resulted by the coalescence of microcracks leading to localized fractures. The description of transition from diffused damage to localized fracture remains so far the most important challenge of durability analysis of concrete structure. Many previous investigations have been performed on experimental characterization of mechanical and transport properties of concretes in relation with damage evolution. It is found that the microcrack induced damage not only affect mechanical behaviors but also transport and diffusion properties. The main consequences include deterioration of elastic properties, induced anisotropy, unilateral effects, friction-damage coupling, irreversible deformation and hysteretic response, significant evolution of permeability and thermal conductivity (Kermani 1991; Sugiyama et al. 1996; Wang et al. 1997; Abbas et al. 1999; Baroghel-Bouny et al. 1999; Picandet et al. 2001; Choinska et al. 2007; Hoseini 2009; Yurtdas et al. 2011, just to mention some representative works on concrete permeability). These works have clearly shown inherent relationships between concrete permeability evolution and microcrack growth. However, most existing works are limited to concrete materials with diffused microcracks or no fully connected localized cracks. There are very few works devoted to hydromechanical characterization of individual concrete fractures, in particular when such fractures are subjected to both normal and shear stresses. Such experimental data are obviously necessary for modeling of progressive propagation of localized fractures, the key phenomenon of failure process in concrete structures (Bourgeois et al. 2002; Chen et al. 2011). On the other hand, in the context of geological disposal of radioactive waste, concrete components are also in contact with engineered clay barrier and claystone as geological barrier. It is a crucial issue to study hydromechanical behaviors of interfaces between concrete and rocks. Unfortunately very few studies have been so far performed on this feature. In this state of the art, we present a summary of experimental studies of hydromechanical behaviors of a fresh concrete fracture, realized in the PhD thesis of He (2011, 2012) at the University of Lille. This work serves as the background for the ongoing works in the Cebama project.

**Experimental studies**

The experimental studies have been performed on the CEM I concrete specifically chosen by ANDRA (French National Agency for Nuclear waste management) for potential use in underground structures for nuclear waste disposal. The University of Lille developed a specific device in order to investigate hydromechanical behaviors of fractures and interfaces, as shown in Figure 5.3.1. Fractures are created in cylindrical samples with the help of two

cylindrical discs with the same diameter as the sample. Each disc is composed of two semi discs made of materials with different stiffness. The two semi discs are placed in an opposite way at the top and bottom surfaces of the sample. Due to the stiffness difference between two semi discs, the application of an axial force allows the generation of a shear stress along the diameter plane. This shear stress is at the origin of fracture creation and allows direct searing tests of the fracture under different confining pressures.
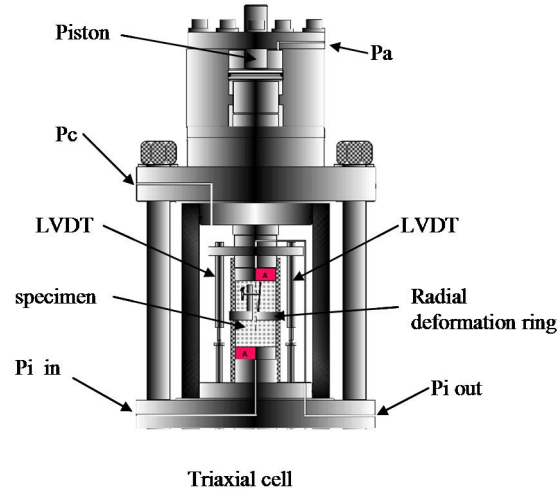


*Figure 5.3.1. Illustration of the specific triaxial cell for hydromechanical testing of fractures and interfaces.*

Using the device, four series of mechanical and hydromechanical tests are performed:

- ✓ Hydrostatic compression test; the main objective here is to establish the relationship between fracture opening (and closure) and applied normal stress.

- ✓ Direct shear test under confining pressure; the objective of this test is to characterize the tangential shear strain and normal strain of fracture versus shear stress for different values of confining pressure.

- ✓ Hydraulic flow test; the purpose of this test is to determine the relationship between hydraulic flow rate and injection pressure inside the fracture under different confining pressures.

- ✓ Shear test with constant fluid pressure; this test is complementary to the direct shear test and its objective is to identify influences of fluid pressure inside the fracture on its mechanical behavior.

Some typical results obtained from the different series of tests are presented below.

In Figure 5.3.2a, typical curves of radial strain versus hydrostatic stress are presented respectively for the sound sample (without fracture) and fractured sample. The difference between the two samples is mainly attributed to the progressive closure of fracture as a function of confining pressure, as shown in Figure 5.3.2b. It is found that the fracture closure occurs essentially in the range of 0 and 5 MPa of hydrostatic stress. After this stage, the variation of radial strain becomes nearly constant and its slope is quasi identical to that of the sound sample. Therefore, the closure pressure of concrete fracture can be identified as around 5 MPa in the present case.
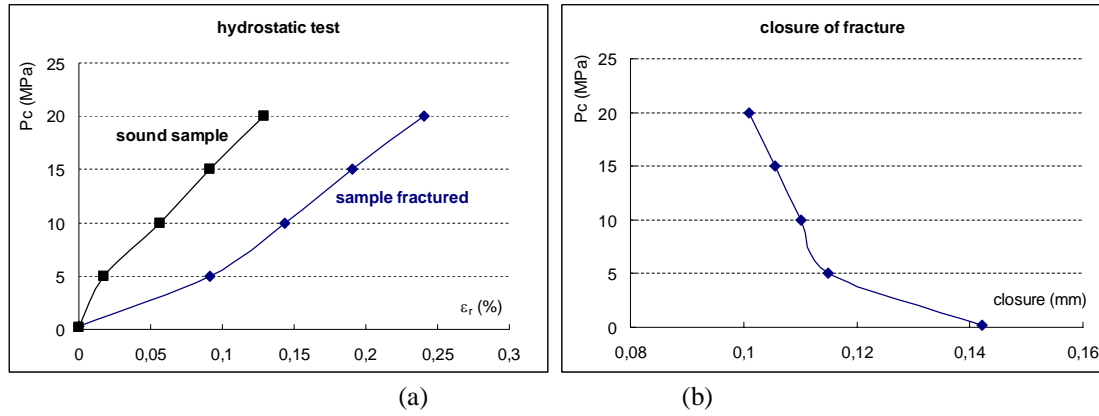
*Figure 5.3.2. Comparison of radial strain curve between sound and fractured samples (a) and evolution of fracture closure versus confining pressure in fractured sample.*

In Figure 5.3.3, we present typical results obtained from three direct shear tests performed with confining pressures of 5, 10 and 15 MPa. Shear and radial strains are expressed as functions of shear stress. Like the mechanical behaviors of rock joints (Bandis et al. 1983; Barton and Choubey 1998; Bart et al. 1984), the peak shear stress significantly increases with the confining pressure while the shear modulus remains nearly constant. For all confining pressures, a softening response is obtained after the peak stress. This behavior is generally related to the progressive destruction of asperities on the fracture surfaces leading to significant decrease of surface friction angle. However, due to the relatively high values of confining pressure used in the present work, we obtain a quite smooth softening regime which could become sharper under lower confining pressures. On the other hand, the radial strain represents fracture opening or closure generated by direct shearing of fracture. Obviously this strain plays an essential role in the evolution of mechanical and hydraulic properties of fracture. We observe that the radial strain remains relatively small under low shear stress and is as smaller as the confining pressure is lower. In some case under low confining pressure, a compressive radial strain can be obtained due to progress matching of fracture asperities. When the shear stress approaches to the peak value, the radial strain quickly increases indicating significant opening of fracture. The latter is depending on the roughness of fracture.
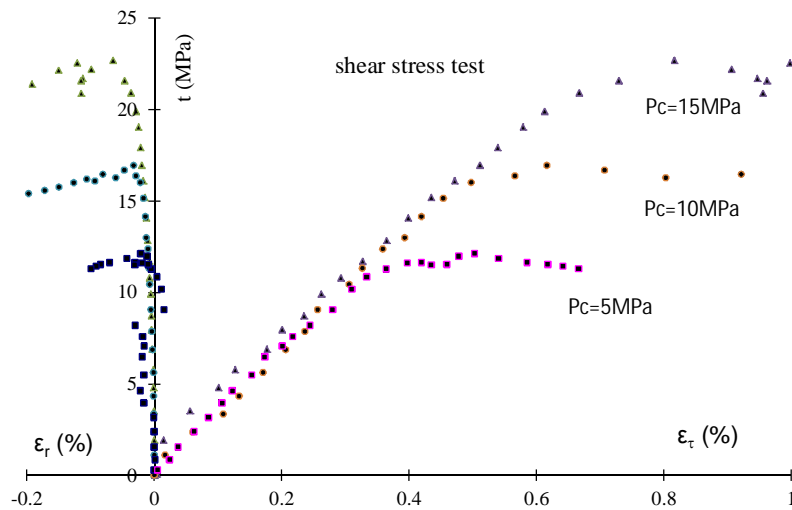


*Figure 5.3.3. Typical shear and radial strains versus shear stress during direct shear tests with different confining pressures.*

115

In Figure 5.3.4, we present the evolution of hydraulic transmissibility of fracture under different confining pressures and with different injection pressures in hydraulic flow tests. It is found that the overall permeability of fracture is higher when the injection pressure is higher. With the help of measured radial strain of fracture during water injection, the fracture opening is evaluated. Therefore, the variation of overall permeability can be expressed as a function of fracture opening as shown in Figure 5.3.5. It is very interesting to observer there is a nearly unique relationship between the permeability and fracture opening for all confining pressures. As a conclusion, the fracture overall permeability is inherently controlled by the fracture opening and closure.
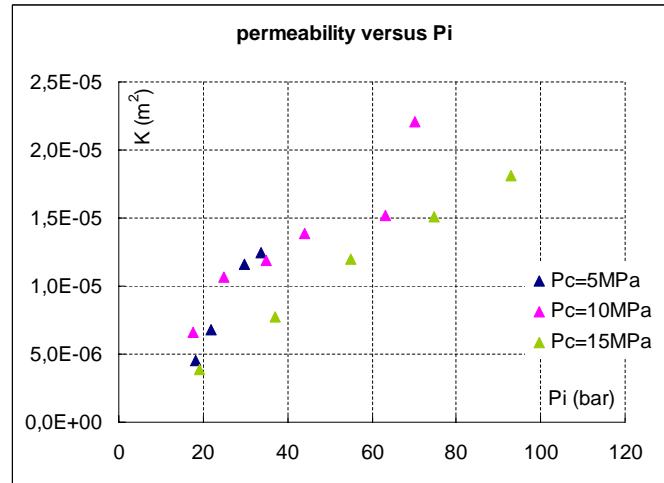


*Figure 5.3.4. Relationships between overall permeability and injection pressure for different confining pressures.*
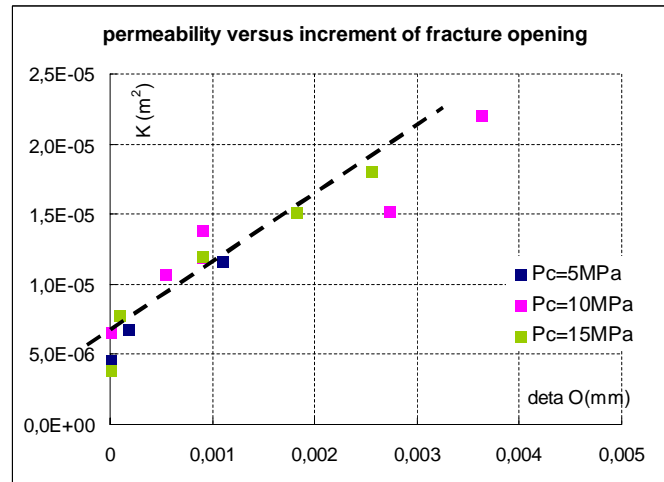


*Figure 5.3.5. Relationships between overall permeability and fracture opening for different confining pressures.*

In Figure 5.3.6, we present stress-strain curves of two complementary shear tests. The first one is performed without fluid pressure inside the fracture. And in the second test, a constant fluid pressure is prescribed inside the fracture so that the effective confining pressure is equal to that of the first test, say 5 and 10 MPa. The objective here is to compare the results between the two tests and to verify the validity of Terzaghi's effective stress concept for the fractures or interfaces. One can see that the results issued from the two tests are very close in terms of the peak shear stress and radial strain. The shear modulus in the elastic zone is slightly

smaller for the test with fluid pressure. These results seem to indicate that the effective stress defined according to Terzaghi's concept can be used for poromechanical coupling in concrete fractures studied in the present work.
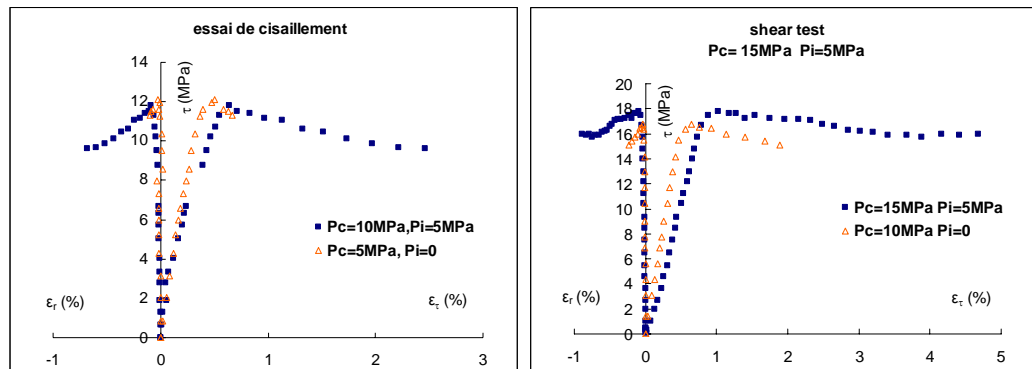


*Figure 5.3.6. Comparison between results respectively from shear tests with and without fluid pressure.*

## Conclusions

Original mechanical and hydromechanical tests on concrete fractures have been performed at the University of Lille with the help of a specific testing device. It is found that the concrete fracture exhibit a nonlinear and inelastic behavior under hydrostatic compression. The mechanical behavior of fracture under shear stress is strongly affected by confining pressure. The shear strength increases with the confining pressure. The fracture exhibits a softening response after the peak stress due to progressive destruction of asperities. The overall permeability of fracture is inherently controlled by its opening and closure. It is possible to define an effective normal stress for poromechanical coupling of fracture according to classical Terzaghi's concept. This previous study serves as the starting background for the ongoing investigations in the Cebama project. The objective is to characterize mechanical and hydromechanical behaviors of interfaces between low pH concrete and the Callovo-Oxfordian claystone.

## References

[1]     Abbas A, Carcasses M, Ollivier JP (1999), Gas permeability of concrete in relation to its degree of saturation, Materials and Structures 32, 3–8.
[2]     Bandis SC, Lumden AC, Barton N (1983), Fundamentals of Rock Joint Deformation, Int. J. Rock Mech. Min. Sci. & Geomech. Abstr. 20(6), 249–268.
[3]     Bart M, Shao JF, Lydzba D (2004), Coupled hydromechanical modeling of rock fractures under normal stress, Canadian Geotechnical Journal 41(4), 686–697.
[4]     Barton N, Choubey V (1998), The shear strength of rock joints in theory and practice, Rock Mechanics 10(1), 1–54.
[5]     Baroghel-Bouny V, Mainguy M, Lassabatere T, Coussy O (1999), Characterization and identification of equilibrium and transfer moisture properties for ordinary and high-performance cementitious material. Cement and Concrete Research 29, 1225–1238.
[6]     Bourgeois F, Burlion N, Shao JF (2002), Modelling of elastoplastic damage in concrete due to desiccation shrinkage, Int. J. Numerical and Analytical Methods in Geomechanics 26, 759–774.
[7]     Chen L, Duveau G, Shao JF (2011), Modelling of plastic deformation and damage in cement-based material subjected to desiccation, International journal for numerical and analytical methods in Geomechanics 35, 1877–1898.
[8]     Choinska M, Khelidj A, Chatzigeorgiou G, Pijaudier-Cabot G (2007), Effects and Interactions of Temperature and Stress level Related Damage on Permeability of Concrete, Cement and Concrete Research 37, 79–88.
[9]     Kermani A (1991), Permeability of stressed concrete, Building research and information 19(6).

[10]    Hoseini M (2009, The effect of mechanical stress on permeability of concrete: A review, Cement & Concrete Composites 31, 213–220.

[11]    Picandet V, Khelidj A, Bastian G (2001), Effect of axial compressive damage on gas permeability of ordinary and high-performance concrete, Cement and Concrete Research 31, 1525–1532.

[12]    Sugiyama T, Bremner TV, Holm TA (1996), Effect of stress on gas permeability in concrete, ACI Materials Journal 93(5), 234–241.

[13]    Wang K, Jansen DC, Shah SP, Karr AF (1997), Permeability study of cracked concrete, Cement and Concrete Research 27(3), 381–393.

[14]    Yang H (2011), Hydromechanical behaviour of concrete under low and high confining pressure, PhD thesis, University of Lille, France.

[15]    Yang H, Xie SY, Secq J, Jia Y, Shao JF (2012), Hydromechanical behaviour of concrete fracture subjected to compressive and shear stresses, Proceedings of First International Conference on Performance-based and Life-cycle Structural Engineering, 5-7 December 2012, Hong Kong, China.

[16]    Yurtdas I, Xie SY, Burlion N, Shao JF, Saint-Marc J, Garnier A (2011), Deformation and permeability evolution of petroleum cement paste subjected to chemical degradation under temperature, Transport in Porous Media 86(3), 719–736.

## 5.4 Chemical degradation of concrete with emphasis on Ca-leaching and carbonation

*Q.T. Phung, N. Maes*

*Belgian Nuclear Research Centre (SCK•CEN), Belgium*

### General introduction

Many environments to which concrete is exposed are highly aggressive due to various chemical components. In such environments, concrete is subjected to processes of chemical degradation. Chemical degradation is typically the result of alteration of the cement matrix mineralogy caused by interacting with severe environment. The interaction disturbs the equilibrium between the pore solution and the solid phases of the cement matrix which results in dissolution and/or precipitation of minerals. The chemical degradation of cementitious materials is mostly followed by a weakening of the material and the alteration of the microstructure. Changes in the microstructure thereby affect the transport properties.

Depending on the roles of structures, the expected life span and the environments to which the concrete structures are exposed, different chemical degradation processes are considered (Figure 5.4.1). Carbonation and leaching are extremely slow processes but very important for long-term durability assessment [1] and have been identified as the most important degradation mechanisms in waste disposal facilities. In this section, the consequences of exposure of cementitious materials to carbon dioxide and calcium leaching are reviewed.
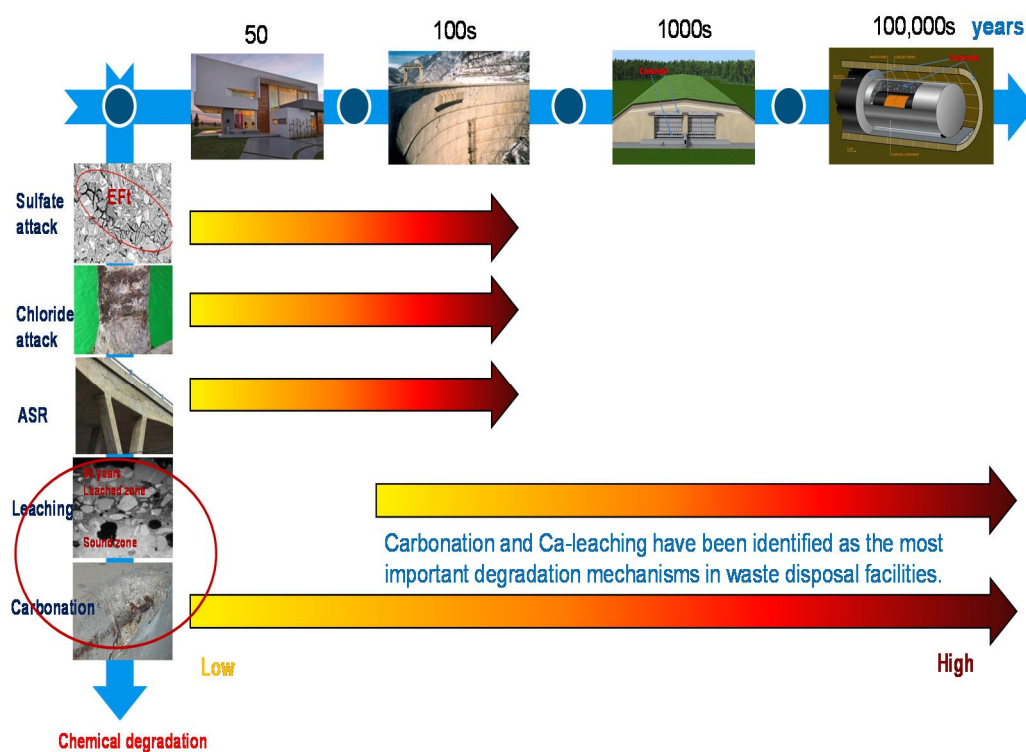


*Figure 5.4.1. Common chemical degradation processes of concrete structures with different life span requirements.*
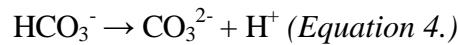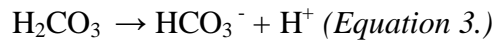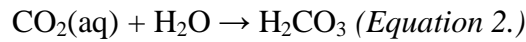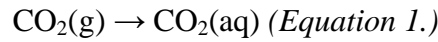
## Carbonation

*Introduction*

The carbonation process in cement-based materials is a deterioration phenomenon. Carbonation results in a pH decrease. The development of lower alkaline environment accelerates the corrosion of reinforcing bars in concrete because of dissolution of the thin oxide passive layer protecting the steel bars from corrosion [2]. Another effect of carbonation is shrinkage which is less serious and not commonly considered in practice. The mechanism of carbonation shrinkage is not yet fully understood. It is probably caused by reorganization of the microstructure due to carbonation, or by polymerization and dehydration of the hydrous silica product from the carbonation of C-S-H. Further explanations of carbonation shrinkage can be found elsewhere [3, 4]. On the other hand, carbonation also results in beneficial effects. It is generally believed that carbonation decreases transport properties and refines pore structure of Portland cement-based materials. Furthermore, in recent years, there is considerable interest in applying carbonation of cement-based materials for solidification and stabilization of radioactive waste. The technique often used to carbonate radioactive waste-forms is supercritical carbonation by applying a high $CO_2$ pressure in a reactor to accelerate the carbonation [5].

*Mechanism of carbonation*

Carbonation is a chemical degradation process through the reaction between $Ca^{2+}$ and $CO_3^{2-}$ ions. However, the carbonation process is a complex physicochemical phenomenon. In most cases, it is believed that the driving force behind the carbonation is diffusion of $CO_2$ [6–8]. When concrete is exposed to environmental conditions containing carbon dioxide, $CO_2$ penetrates into the concrete pore network system and dissolve in the pore water.

$$CO_2(g) \rightarrow CO_2(aq) \text{ (Equation 1.)}$$

$$CO_2(aq) + H_2O \rightarrow H_2CO_3 \text{ (Equation 2.)}$$

$$H_2CO_3 \rightarrow HCO_3^- + H^+ \text{ (Equation 3.)}$$

$$HCO_3^- \rightarrow CO_3^{2-} + H^+ \text{ (Equation 4.)}$$

Bicarbonate ion $HCO_3^-$ is unstable in high alkaline environment (about 12.8 in concrete). Therefore it dissociates and forms carbonate ion $CO_3^{2-}$. The carbonate ions then react with available $Ca^{2+}$ ions in pore solution to precipitate as $CaCO_3$.

$$Ca^{2+} + CO_3^{2-} \rightarrow CaCO_3 \text{ (Equation 5.)}$$

Portlandite (solid state) formed during hydration of $C_3S$ and $C_2S$ will start dissolving because of the decrease of the $Ca^{2+}$ concentration in the pore water resulted from the $CaCO_3$ precipitation, sustaining the reaction of portlandite dissolution and calcite precipitation (Eq. (5)). A schematic representation of the process is presented in Figure 5.4.2.
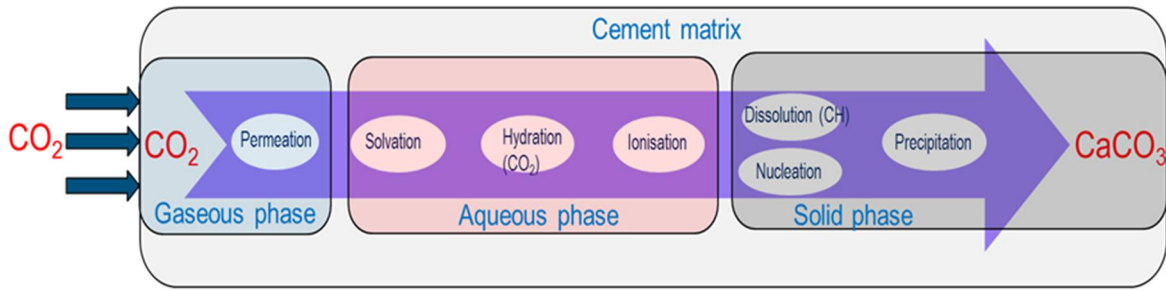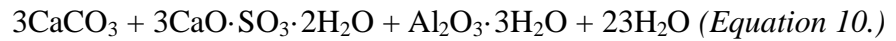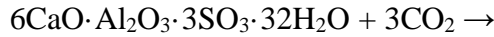
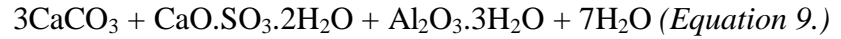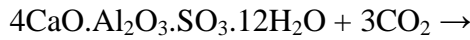$$Ca(OH)_2(s) \rightarrow Ca^{2+} + 2OH^- \text{ (Equation 6.)}$$
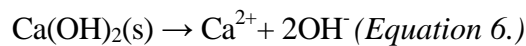
*Figure 5.4.2. Summary of carbonation process in cement-based materials.*

As long as portlandite is present, the pH is buffered. After depletion of portlandite, the pH drops by approximately 3 units [9] when not buffered by other cement minerals. Thus, other solid hydration products (Calcium-silicate-hydrate (C-S-H), Monosulphate (AFm), Ettringite (AFt)) become unstable. C-S-H starts dissolving at pH of 12.5, AFm at pH of 11.6, while AFt decomposes at pH of below 10.6 [10, 11]. Carbonation will reduce the Ca/Si ratio of C-S-H. The carbonation reactions of C-S-H, AFm and AFt are summarized in Eqs. (7) to (10), respectively [12, 13].

$$\text{C-S-H}_1 + CO_2 \rightarrow \text{C-S-H}_2 + CaCO_3 + H_2O \text{ (Equation 7.)}$$
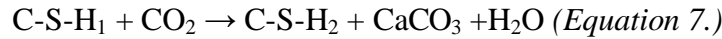
where Ca/Si in C-S-H$_1$ is higher than in C-S-H$_2$. If $CO_2$ still remains, the carbonation reaction continues until the C–S–H$_1$ is completely decalcified and finally forms calcium carbonate.

$$3CaO.2SiO_2.3H_2O + 3CO_2 \rightarrow 3CaCO_3 + 2SiO_2 + 3H_2O \text{ (Equation 8.)}$$

$$4CaO.Al_2O_3.SO_3.12H_2O + 3CO_2 \rightarrow$$

$$3CaCO_3 + CaO.SO_3.2H_2O + Al_2O_3.3H_2O + 7H_2O \text{ (Equation 9.)}$$

$$6CaO \cdot Al_2O_3 \cdot 3SO_3 \cdot 32H_2O + 3CO_2 \rightarrow$$

$$3CaCO_3 + 3CaO \cdot SO_3 \cdot 2H_2O + Al_2O_3 \cdot 3H_2O + 23H_2O \text{ (Equation 10.)}$$

Carbonation also occurs with unhydrated products (e.g. C$_3$S, C$_2$S) of hardened cementitious materials as shown in reactions (11) to (14). Actually, C$_3$S and C$_2$S may slowly hydrate to release Ca(OH)$_2$, and carbonate ions will react with calcium ions to form calcium carbonate afterwards. These processes can occur in the carbonated zone.

$$2(3CaO.SiO_2) + 6H_2O \rightarrow 3CaO.2SiO_2.3H_2O + 3Ca(OH)_2 \text{ (Equation 11.)}$$

$$2(2CaO.SiO_2) + 4H_2O \rightarrow 3CaO.2SiO_2.3H_2O + Ca(OH)_2 \text{ (Equation 12.)}$$

$$3CaO.SiO_2 + 3CO_2 + xH_2O \rightarrow 3CaCO_3 + SiO_2.xH_2O \text{ (Equation 13.)}$$

$$2CaO.SiO_2 + 2CO_2 + xH_2O \rightarrow 2CaCO_3 + SiO_2.xH_2O \text{ (Equation 14.)}$$

Calcium carbonate exists in three crystallographic forms: the stable form of calcite and two metastable forms of aragonite and vaterite [14].

In general, it is thought that the carbonation mechanism is determined by the inward diffusion of $CO_2$ [6–8] in normal conditions. However, it depends on the conditions of carbonation: whether the concrete is fully or partially saturated; the $CO_2$ concentration, the relative

humidity; and the $CO_2$ pressure gradient. In the case of carbonation of unsaturated materials, $CO_2$ gas will diffuse in the concrete through the connected pore network. The $CO_2$ gas then dissolves into the aqueous phase and precipitates with $Ca^{2+}$ ions. Because the rates of dissolution and reaction are much faster than the rate of diffusion, the diffusion of $CO_2$ gas becomes the rate-limiting process of carbonation. Nevertheless, in the case of concrete used for underground waste disposal purposes, concrete is almost fully saturated and subjected to a high hydrostatic pressure and the surrounding environment may contain a high bicarbonate concentration, for example clay rock in Callovo-Oxfordian formation [15] or Boom clay in Mol site [16]. Therefore, a combination of diffusion and advection should be taken into account when one considers the carbonation mechanism. This is also the case in accelerated carbonation by applying a high gradient pressure in which advection has a significant contribution to the carbonation process. However, so far as the author is aware, none of published studies considers the contribution of advection to carbonation of cementitious materials.

*Factors influencing carbonation*

There are many factors influencing carbonation: chemistry of hydration products, free water content, internal relative humidity (RH), pore structure, $CO_2$ partial pressure and external conditions where carbonation occurs (e.g. ambient relative humidity, temperature, $CO_2$ concentration and applied pressure).

In general, the higher the $CO_2$ concentration, the quicker the carbonation proceeds. However, up to a certain concentration, the carbonation may not increase because the retention process resulting from porosity reduction and releasing water overwhelms the effect of higher concentration. Increasing temperature will speed up the carbonation process because the reaction and penetration of $CO_2$ occurs faster. The core reaction in carbonation is the reaction between $CO_2$ and portlandite. Therefore, the more portlandite present in the hydration products, the higher the degree of carbonation [17]. Note that a higher carbonation degree is not necessarily synonymous with larger carbonation depth. As an example, the depth of carbonation in concrete produced by cement with a certain replacement of other pozzolanic materials (fly ash, silicafume) may be greater than one produced by ordinary Portland cement (OPC) [10]. However, the carbonation degree may be lower because the amount of portlandite in pozzolanic materials is less than those in OPC due to pozzolanic reaction consuming $Ca(OH)_2$. $CO_2$ still remains after carbonation at outer layer and it can penetrate more deeply to inner layer of concrete. Also, $CO_2$ can diffuse more easily through less dense carbonated layer in this case.

Water plays an important role in the carbonation process. Carbonation does not occur without water. It is a catalyst in carbonation reaction even though this reaction releases water. However, water can fill the pores and prevent $CO_2$ gas to penetrate into the concrete pore network. In fact, carbonation reaches the highest efficiency at an internal relative humidity between 50–70% [10]. It is worth noting the difference between relative humidity and degree of saturation when carbonation is considered. The degree of saturation is the fraction of the pore volume filled with water while internal RH is the fraction of the ambient vapour pressure to the saturation vapour pressure in pore system. The effect of the former on carbonation is more significant than the latter.

*Methods to carbonate cement-based materials and examine its carbonation products*

To some extent, the main goal of a carbonation study is to predict the rate of carbonation depth propagation and the service lifetime of reinforced concrete structures. However, carbonation of concrete under atmospheric conditions (low $CO_2$ concentration) is extremely slow because it is a diffusion-controlled process. The reaction conditions (temperature, RH) may vary due to climate change during carbonation process. Due to the long duration, it is very difficult to study the carbonation and a comparative study is almost impossible to perform due to the inconsistency in carbonation conditions. Therefore, in order to study carbonation a number of accelerated carbonation methods have been proposed.

A standard way is to put concrete samples in a controlled chamber with a specific $CO_2$ concentration and optimized relative humidity to speed up carbonation [17–19]. This method takes weeks or months to get a carbonation front of several millimetres depending on the $CO_2$ concentration. A common range of partial pressure of carbon dioxide is from 1% to 10% [20–22]. However, a higher $CO_2$ concentration [23–25] has been extensively applied to accelerate the carbonation despite the criticism that phenomena would be different from natural carbonation [26, 27] in terms of the chemical composition and the microstructure of carbonated cement-based materials. In order to conclude whether carbonation at different $CO_2$ concentrations results in different changes in microstructure and mineralogy, one should perform the carbonation experiments until a stable endpoint at which the carbonation process is completely finished. This condition is difficult to reach for natural carbonation in a limited experimental timeframe or even with low $CO_2$ concentration. Therefore it still needs more quantitative experiments to answer the question about difference in natural and accelerated carbonation with high $CO_2$ concentration. Nevertheless, it is widely accepted that the moisture evolution during carbonation plays a key role. In accelerated conditions, a large amount of released water due to the fast reaction may not have sufficient time to leave the sample which reduces the carbonation rate. In contrast, less water is released and it has enough time to diffuse and leave the sample in natural carbonation. For this reason, accelerated carbonation with high $CO_2$ concentration might not be suggested for kinetic studies.

An alternative method is based on applying a high pressure gradient (tens to hundreds of bar). Concrete samples can reach full carbonation in few hours or even in few minutes. However, the samples can be damaged by micro cracks (elevated pressure) and heat generation (exothermic reaction). The method is mostly applied for $CO_2$ sequestration or heavy metal immobilization [28–32]. Additionally, accelerated carbonation during curing is found to have great benefits in terms of increasing the mechanical properties and reducing transport properties [33, 34].

Recently, Phung et al. [35, 36] developed a new carbonation method to investigate the effects of limestone filler replacement on microstructural alterations and permeability changes after carbonation. The proposed method allows for studying the carbonation under accelerated conditions in which an elevated $CO_2$ pressure gradient is applied. The setup allowed for easy connecting to other setups before and after carbonation to measure diffusivity [37] or water permeability [38]. An elevated pure $CO_2$ pressure gradient is applied on a partially saturated sample which is embedded in a special carbonation cell. The penetration of $CO_2$ into the cement paste sample occurs via two ways: i) $CO_2$ gas transports through connected pores under a pressure and concentration gradient, and ii) dissolved $CO_2$ transports with the movement of water under a pressure driving force (when initial saturation degree of sample is high). The amounts of $CO_2$ flowing in and out of the carbonation cell are precisely measured with mass flow meters allowing for quantification of the amount of carbon dioxide reacting with the cement.
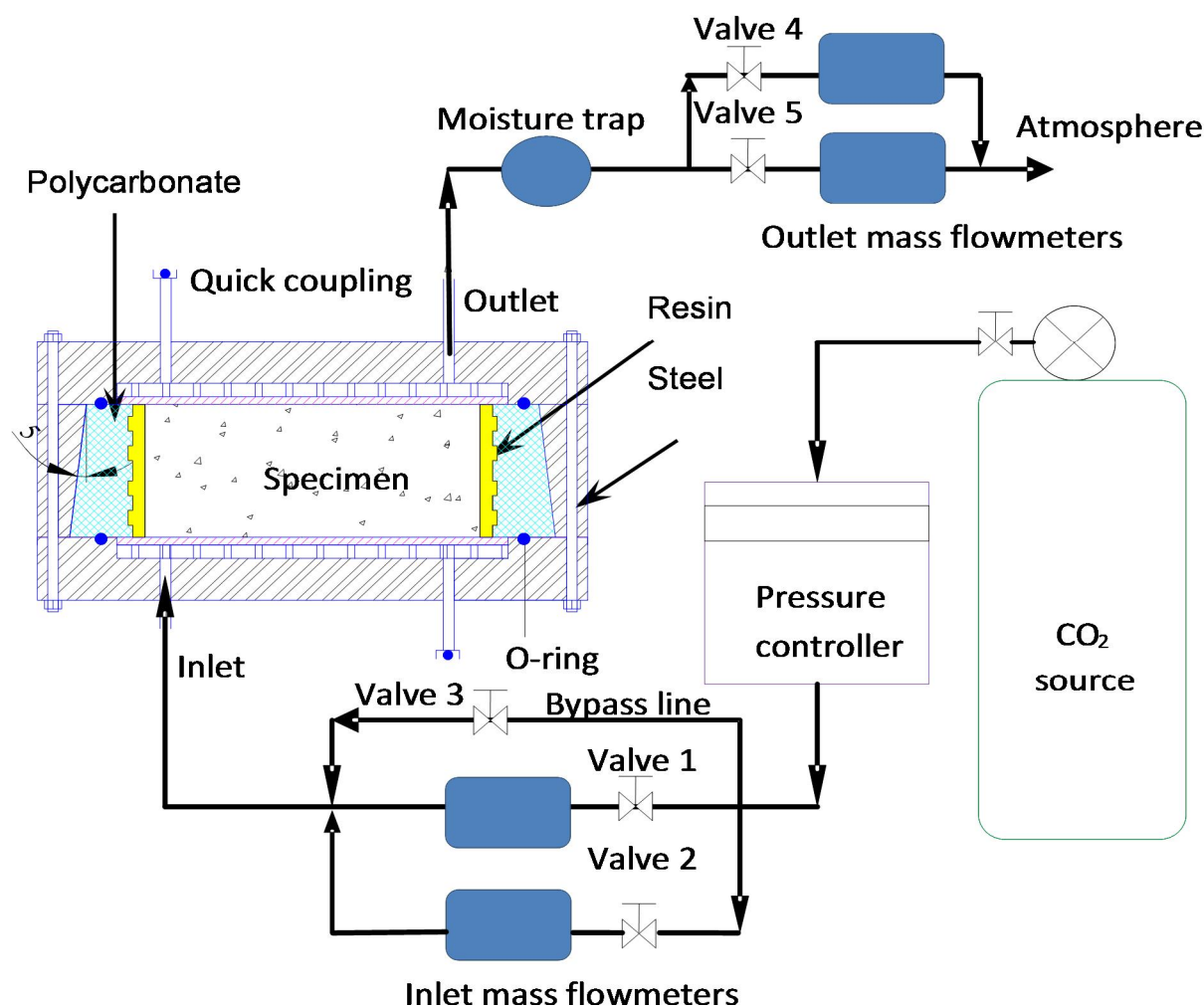
*Figure 5.4.2. Novel carbonation setup using pressurized $CO_2$ and recording of the $CO_2$ in- and out-flows [36].*

In order to characterize the carbonation products, a number of experimental techniques can be used, including methods of mass gain, Thermo-gravimetric analysis (TGA), X-ray diffraction (XRD), chemical analysis, and infrared spectroscopy. Mass gain is a simple method by determining the percentage of mass change of specimen due to carbonation [8, 39]. However, the most common method consists of determining the carbonation depth by phenolphthalein indicator. By observing the colour change of phenolphthalein (pink changes to colourless in carbonated zone because of change in pH), one can quantitatively determine the carbonation depth. Nevertheless, it is not always easy to define clearly where the border is in the case of a non-sharp front. This method cannot detect carbonated area with pH values of higher than 9 [40, 41]. To overcome this problem TGA, gammadensimetry [42], XRD and infrared spectroscopy [41] are more suitable methods. However, these methods are quite complex and time consuming, and require specialized equipment. The principle of TGA is to determine changes in weight of a sample according to temperature changes while gammadensimetry is based on measuring density variations due to the evolution of the water content gradient over time. With the assumption that no water moves out by drying during the carbonation process, the $CO_2$ profile can be drawn based on the density increase. This method also provides water content profiles, which is important input data for modelling [43]. XRD is a destructive technique to identify crystalline phases. This method can detect portlandite and amorphous hydrated products [44]. Infrared (IR) spectrometry is used to identify the different forms of

124

calcium carbonate (calcite, aragonite, vaterite) [45] by its characteristic infrared absorption wavelengths. Optical microscopy or/and scanning electron microscopy (SEM) are other useful approaches to study how the microstructure changes after carbonation.

*Influence of carbonation on microstructure and transport properties*

It is generally believed that carbonation decreases transport properties (permeability, diffusivity) [35, 46, 47], and refines pore structure (porosity, pore size) [22, 35] of Portland cement-based materials. However the extent of modification in transport properties and microstructure significantly depends on carbonation conditions (RH, $CO_2$ concentration, etc.) and cement types. The reduction of permeability and diffusivity is the result from the precipitation of carbonation products (mainly calcite) in the pore structure. This leads to a significant reduction of the total porosity (molar volume of portlandite is smaller than molar volume of calcite), and thereby transport properties.

In blended cement systems (containing ground granulated blast-furnace slag – BFS or fly ash – PFA), the carbonation depth propagation can be faster than in OPC system due to lower portlandite content. The modifications in microstructure are also expected to occur in different ways. Kinoshita *et al*. [23] investigated the carbonation of blended cement systems with a very high replacement level of OPC with BFS or PFA in accelerated conditions (15% $CO_2$, 50–60% RH). It is observed that in the BFS:OPC = 9:1 system, the space of C–S–H gel is occupied by grain-like products after carbonation, leaving a distinctive pore structure of up to several micrometres, while not observed in the microstructure of the OPC and PFA:OPC = 3:1 systems. The porosity increase in BFS/OPC paste was also reported by Borges *et al*. [48] despite accelerated or natural carbonation, and was attributed to the carbonation of C-S-H gel. However, Borges also observed a porosity increase in PFA/OPC pastes but with higher replacement (40–75%).

In lower puzzolanic additive replacement systems (30% PFA, 65% BFS), Ngala *et al*. [49] found that there is not only a reduction in the total porosity in both OPC and blended pastes with carbonation, but also a redistribution of the pore sizes. The proportion of large pores (diameter > 30 nm) is increased slightly for OPC pastes but much more significantly for the BFS and PFA pastes. This is in line with the findings of Pihlajavaara [50] who stated that the carbonation seems to affect more the larger pores (20–100 nm) than the smaller ones.

Liwu Mo *et al*. [51] studied the effects of accelerated carbonation on the microstructure of Portland cement pastes containing reactive MgO in accelerated condition with mostly pure $CO_2$ (99.9%) and high RH (98%). It has been found that the degree of porosity reduction is larger with the increase of reactive MgO content.

Most published studies report a decrease in specific surface area after carbonation [52–55]. The decrease is due to both a decrease in total porosity and a shift in a pore size distribution towards smaller pore sizes. Houst [53] showed that specific surface area is significantly reduced after carbonation. For cement paste with w/c ratio of 0.3, that specific surface area of carbonated material is 70% of the non-carbonated material. The decrease is higher with an increase in w/c ratio, down to 43% for sample with w/c ratio of 0.8. Pihlajavaara [50] observed the same phenomenon in which cement paste with w/c ratio of 0.3 exhibits a smaller specific surface area decrease (44%) compared to one with w/c ratio of 0.45 (50%). Chen *et al*. [54] also found a decrease in specific surface area of low heat carbonated Portland cement paste, but only for samples with pre-curing in water. The specific surface area sharply decreases by about 50% after 21 day carbonation. For those without pre-curing, the specific

surface areas vary in narrow range regardless the carbonation time (up to 70 days). Johannesson *et al.* [55] reported that the specific surface area of OPC paste is slightly decreased after carbonation. The specific surface area of well-carbonated paste is 29.4 $m^2/g$ compared to 31.8 $m^2/$ of non-carbonated paste.

Specific surface area of carbonated cementitious materials is sometimes increased as shown by You *et al.* [56]. The specific surface area of carbonated waste cement (from a recycling process to recover coarse aggregate from waste concrete) increases linearly with the increase of the carbonation degree. The observation is explained due to the formation of highly polymerized silica gel.

Carbonation in OPC systems normally results in a decrease in the transport properties, but carbonation under supercritical conditions (high pressure) or in blended cement systems with high additive replacements could sometimes increase the transport properties. Borges *et al.* [22] showed that permeability increases for composite cement pastes containing high amounts of BFS (BFS:OPC = 3:1 and 9:1) subjected to accelerated carbonation, due to carbonation shrinkage and cracking during testing. Although carbonation has resulted in an overall density increase and overall porosity decrease, OPC pastes, however, do not show a significant change in permeability after carbonation.

For the Nirex reference vault backfill (NRVB) cement pastes (containing 6% Portland cement, 28.6% limestone powder, 9.8% lime, and 35.6% water) which have high porosity, Rochelle *et al.* [57] showed that the carbonation under high pressure (4 and 8 MPa) decreases 3 orders of magnitude for water permeability and 2 orders of magnitude for gas permeability. Even higher permeability decrease has been observed for cement grout as reported by Dewaele *et al.* [58]. The carbonation of cement grouts (w/c ratios of 0.4 and 0.47) under high pressure decreases the permeability in carbonated layer from two to six orders of magnitude. Carbonated samples exhibit a smaller average pore size and an increased specific surface area compared to non-carbonated samples.

Liteanu *et al.* [46] measured the permeability changes in wet mature Class A wellbore cement exposed to supercritical $CO_2$ (30 MPa confining pressure, 10 MPa $CO_2$ pressure, 80 °C). Water permeability measurements of unfractured cement show a continuous and significant decrease during exposure to static $CO_2$ rich-fluids. The intrinsic permeability is decreased from $1.8 \times 10^{-16}$ $m^2$ down to $5.2 \times 10^{-17}$, $3.8 \times 10^{-17}$ and $8.3 \times 10^{-18}$ $m^2$ after one, two and three months of exposure, respectively. For fractured samples, permeability decrease is not strong despite the fact that the fractured samples showed heavy carbonation in the fracture plane. The permeability is decreased from $3.9 \times 10^{-14}$ $m^2$ to $1 \times 10^{-14}$ $m^2$ after one month reaction and remained constant afterwards. In case of accelerated carbonation under atmospheric pressure, the degree of permeability reduction is much lower than carbonation under high pressure. Under accelerated carbonation (65% RH, 5% $CO_2$, 25 °C), Song *et al.* [59] showed that the permeability of carbonated concretes are 3.2 and 2.7 times lower compared to reference concretes after 4 month carbonation for w/c ratios of 0.65 and 0.55, respectively. In the same carbonation conditions, Claisse *et al.* [47] showed there is only a small increase in the impermeability index. After 140 days of exposure to $CO_2$, carbonation leads to an approximately 37 percent and 4 percent increase in the impermeability index (defined as $\log_{10}(1/k)$) for concretes with w/c ratios of 0.6 and 0.45, respectively.

On the other hand, Lesti *et al.* [60] reported a permeability increase of cement-based materials exposed to supercritical $CO_2$. Most of the samples exhibit gas permeability increases of 2 to 4 orders of magnitude after 6 month exposure, except for the fly ash containing cementing

system which shows no increase after one month exposure and only a slight increase in permeability after six month exposure. The authors attributed the increase in permeability to crack formation as a consequence of expansion during $CaCO_3$ crystallization. This statement is in line with the findings of Fabbri *et al*. [61] who showed that micro crack formation during supercritical $CO_2$ induces not only an increase of its permeability but also a degradation of the mechanical properties of cement-based materials.

Studies on changes in diffusivity due to carbonation are rare, perhaps due to long experimental time needed to measure the diffusion coefficient of carbonated materials. Ngala *et al*. [49] concluded that carbonation of cement pastes has a large effect on diffusion. The effects are more significant for the blended pastes than for plain OPC pastes. It is surprising that the effective chloride diffusion coefficient in blended pastes increases by two orders of magnitude while oxygen diffusion coefficient increases by one order of magnitude. The reasons could be attributed to larger capillary porosity observed in carbonated sample despite smaller total porosity. The coarsening of the pore structure is attributed to the formation of additional silica gel due to the decomposition of the C-S-H gel.

Portlandite is the main phase to carbonate in most cases, however, under accelerated conditions other phases may be carbonated, especially C-S-H. When C-S-H is carbonated, a decalcification occurs, leading to a C-S-H with a smaller molar volume and a smaller Ca/Si ratio compared to non-carbonated C-S-H as shown by Morandeau *et al*. [20]. If the pore volume created by C-S-H carbonation is not compensated by formed calcium carbonation, the carbonation of C-S-H will result in a porosity increase.

**Calcium leaching**

*Introduction*

Leaching is a process of ion extraction from solid compounds by dissolution. In cement based-materials, leaching of calcium, also called decalcification, is of utmost importance because of the high calcium (Ca) content in cement compared to other potentially leachable ions ($Fe^{2+}$, $Al^{3+}$, $Mg^{2+}$, etc.) and the high solubility of the aqueous Ca-controlling phase portlandite. Ca-leaching is one of the most serious degradation processes in concrete and reinforced concrete structures for the very long-term (nuclear waste disposal system) or in hydro structures (dam, bridge, water tank) but it has only been studied since the 1980s despite the long history of concrete. The reason is that leaching of concrete is an extremely slow process under normal conditions (few mm leaching front in a hundred years [62]). However, the lifetime of civil concrete structures is normally under one hundred years and that is too short to see the effects of leaching degradation. Leaching of cement-based materials changes its properties such as a reduction in pH, an increase in porosity and transport properties and detrimental effects on properties related to long-term durability.

*Chemical and physical leaching process*

Ca-leaching is a dissolution-diffusion process of dissolved Ca ions in the pore solution. This happens when the cement matrix is in contact with a low pH or low alkaline solution. The typical pH value of the pore solution of concrete is about 12.5–13, therefore, any solution with pH below this range (e.g. water) is considered as an aggressive environment to concrete. During leaching, dissolution is much faster than diffusion; hence the solid-liquid equilibrium curve of calcium has been commonly used for understanding different stages of leaching. Berner [63] is the first researcher who proposed the solid-liquid equilibrium curve by

compiling experimental solubility data available in literature. The curve is composed out of three almost linear parts characteristic for the different leaching stages.

In the first stage, where the Ca concentration in the aqueous phase is higher than 20 mol/m$^3$, portlandite is quickly dissolved. Portlandite has the highest solubility amongst all calcium containing solid phases in cement matrix. Portlandite is entirely dissolved and does not re-precipitate like C-S-H. In the second stage, where the Ca concentration in aqueous phase is higher than 2 mol/m$^3$ and lower than 20 mol/m$^3$, C-S-H is partially dissolved. Sulfoaluminates are also dissolved in this stage [64]. The dissolution of C-S-H is incongruent, in which C-S-H with higher Ca/Si ratio completely dissolves and re-precipitates at a lower Ca/Si ratio C-S-H [65]. In the third stage, where the Ca concentration in the aqueous phase is lower than 2 mol/m$^3$, the partially leached C-S-H continues dissolving at a faster rate to form silica gel which is the end product of leaching.

When dissolved in pore solution, calcium ions will leach out by advection or diffusion. Advective removal of Ca is governed by the water flow and is the quickest leaching degradation of a concrete structure. However, it is not common in reality except in some special structures like dams or water tanks. Diffusive removal of Ca is much slower but more common and is controlled by the Ca concentration gradient. Both diffusion and advection are governed by the microstructure of concrete which is changed during leaching.

*Factors influencing leaching*

There are many factors influencing the leaching of cementitious materials. Among them, the main factors are listed below:

- Diffusivity and permeability (in case of flowing water) are the most important factors. These factors determine how easy Ca ions are transported out of the cement matrix.

- Surrounding solution: the lower the pH of the solution, the higher the leaching rate. Leaching in flowing solution is faster than in static solution. Solutions with the ability to increase the solubility of calcium containing solid phases (e.g. ammonium nitrate) can significantly accelerate the leaching process. Leaching in deionized water occurs quicker than in hard water.

- An electrical field could accelerate the leaching process because of the increasing Ca ion movement in the pore solution towards electrode of opposite charge [66].

- Saturation degree: partially saturated concrete can undergo leaching, but with much slower rate compared to saturated concrete.

- Initial amount of Ca in solid phases: the higher the total amount of Ca in concrete (especially the amount of portlandite), the higher the potential of leaching.

*Experimental methods to study leaching*

Considering the slow degradation process but the need to study long-term durability of concrete, accelerated testing is a relevant approach to better understand the effect of leaching on the alteration of microstructure and transport properties. A variety of accelerated methods have been proposed such as applying an electrical field [66], using deionized water [67, 68], using low pH solutions [69, 70]; applying flow-through conditions [71] or using high concentration ammonium nitrate ($NH_4NO_3$) solutions [72–75]. Among them, using an ammonium nitrate solution to accelerate the leaching kinetics is one of the most popular methods because it results in faster degradation compared to other methods under diffusive-

transport conditions while it results in the same end-products. The mechanism of acceleration is not only due to the lower pH of $NH_4NO_3$ solution but primarily because of the increase in the solubility of the leachable phases in cementitious matrix induced by $NH_4NO_3$.
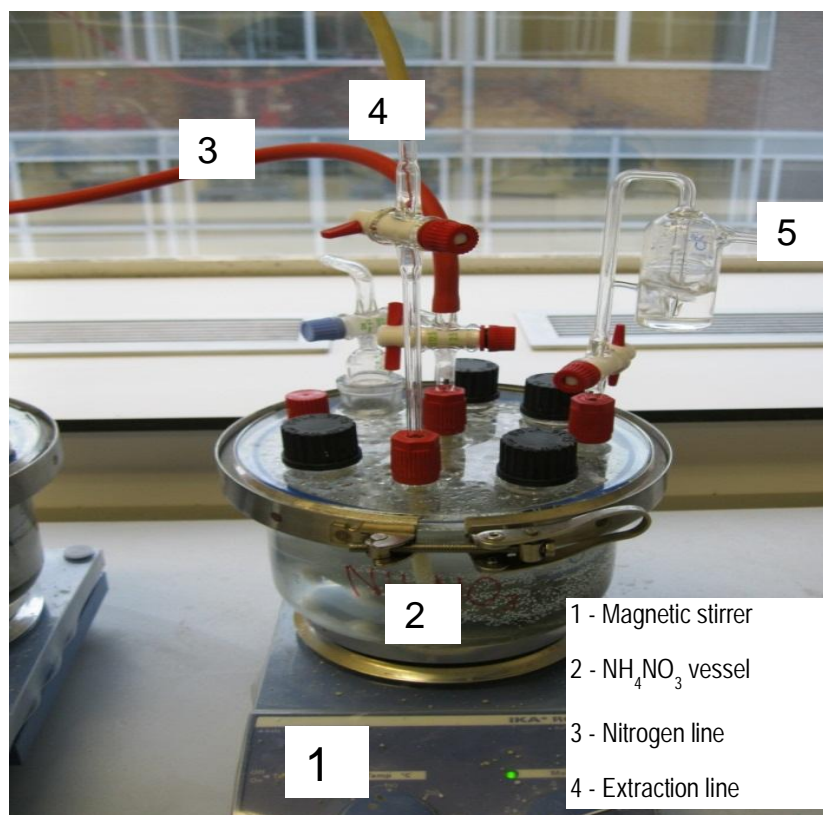


*Figure 5.4.3. Accelerated leaching setup using $NH_4NO_3$ solution [75].*

Many studies quantify the propagation of degraded depth of leached materials and characterize its mechanical behaviour [76, 77]. However, there are only a few studies that discuss the modification of the microstructure after leaching [78–80] and the effects of leaching on transport properties [81, 82]. The post-analysis techniques used for characterizing carbonated materials are also applied to study leached materials. However, care must be taken while preparing samples of leached cement-based materials. Due to significant loss in mechanical properties, the samples must be handled in a proper way to preserve the integrity of leached materials.

*Influence on microstructure and transport properties*

One might intuitively presume that leaching alters the cementitious materials to a material with coarser microstructure and higher transport properties. And this presumption is confirmed by literature. However, to what extent the microstructure and transport properties are modified, is still questionable.

With regard to accelerated leaching in ammonium nitrate solution, most studies report an increase in porosity and coarser pore size distribution. Nevertheless, the level of modifications strongly depends on the compositions of the native materials. In general, cementitious materials with less portlandite content exhibit a better leaching resistance, and the same trend is observed for materials having pozzolanic activity.

Berra *et al.* [83] showed that adding 3.8% nanosilica could slightly reduce the porosity increase due to accelerated leaching of cement paste CEM I, however, the decrease of compressive strength of the leached specimens is significantly retarded. Porosity even decreases for mortars with cement CEM III (blast-furnace slag) and CEM IV (fly ash +limestone filler) due to precipitation, as reported by Segura *et al.* [84]. However, porosity still increases for long time (more than 2-week leaching). A maximum porosity increase of about 30% has been observed for CEM I mortars after 32-day leaching regardless the w/c ratio. The pore surface area significantly increases, but critical pore diameter and threshold pore diameter (the largest pore size at which pore volume is significantly increased) are almost unchanged for CEM III and CEM IV mortars. However, the critical and threshold pore diameters increases for CEM II and CEM I mortars, respectively. The effect of slag admixture to cement mortar in the reduction of porosity increase was also found by Cheng *et al.* [85]. The porosity increase is a function of degraded depth as pointed out by Poyet *et al.* [79]. A huge porosity increase from 26% to 80% has been reported at the surface directly in contact with ammonium nitrate solution for cement paste with w/c of 0.5 and 18.5% fly ash replacement.

In an attempt to assess the influence of cement type on transport properties and Ca-leaching, Perlot [81] performed accelerated leaching in ammonium nitrate solution on two mortars made from CEM I and CEM V/A (22% fly ash and 22% blast furnace slag). The fly ash and blast furnace slag addition not only improves the microstructure of sound mortar, but also increases the resistance against leaching. Even while having a similar porosity, the chloride diffusivity is 5 times lower for sound CEM V/A mortar. After leaching, the porosity and specific surface area are doubled and tripled, respectively, in both leached mortars. The alterations of transport properties are similar for both mortars regardless its difference in initial transport properties (and microstructure): gas permeability increases more than one order of magnitude while chloride diffusivity increases less than one order of magnitude. Agostini *et al.* [86] confirmed that the degree of gas permeability is the same for CEM II/B-M mortars despite its difference in w/c ratios (0.5 and 0.8). The permeability in the leached zone in which portlandite is completely dissolved and C-S-H is partially leached increases more than two orders of magnitude under ammonium nitrate leaching. However for both mortars tested, major variations in permeability (and microstructure) are thought to be linked to portlandite leaching, minor alteration is attributed to C-S-H decalcification.

Sometimes, as in the study of Yurtdas *et al.* [87], a reduction in permeability for leached material is observed. The water permeability of the degraded material is lower than that of sound material during triaxial compression tests, although ammonium nitrate leaching leads to significant increase of porosity of cement paste (approximately 50%). This is due to the plastic deformation of the leached material which allows a compaction without cracking. However, under measuring conditions without confining pressure, the permeability of the degraded material is about 2.4 times higher than that of the sound material.

Gallé at el. [82] investigated the leaching behaviour of a CEM I cement paste and of a concrete prepared with almost similar w/c ratios (0.45 and 0.43, respectively). Until the complete dissolution of portlandite, water porosity is doubled for both cement paste and concrete, respectively from 33% to 61% and 10% to 19%. The authors observed that C-S-H is also significantly affected by leaching in ammonium nitrate solution which contributes about 13% porosity increase. A significant increase in water permeability is observed, more than two orders of magnitude for both leached cement paste and concrete in which all the portlandite is completely dissolved. Note that confining pressure was also applied to measure permeability like the case of Yurtdas *et al.* [87], but a decrease in permeability of the leached

130

materials was not observed. The permeability increase is assumed to be related to the newly created porosity which is mainly due to portlandite dissolution.

In order to investigate diffusivity changes at different degradation stages, Bernard *et al*. [88] performed the leaching tests on CEM I cement paste and mortar with the same w/c of 0.4. The authors showed that at the degradation stage at which porlandite, hydrated aluminates and sulfoaluminates disappear, the effective diffusivity of HTO is increased 118 times for either cement paste or mortar. While only portlandite is disappearing, the diffusivity is only increased 31 times for both cement paste and concrete.

Instead of using ammonium nitrate solution, Saito *et al*. [66] applied an electrochemical method to accelerate the leaching. A potential gradient of 10 V/cm is applied on a mortar with and without pozzolanic admixture replacement (blast furnace slag and silica fume). The porosity is increased two times in OPC mortars while it is only increased by 40% to 50% in the pozzolanic admixture replacement mortars. This results in a large difference in water permeability alterations. The water permeability in the degraded region increases by about two orders of magnitude in the OPC mortars, but only by one order of magnitude in the pozzolanic replacement mortars regardless the same starting permeability.

The number of studies on leaching using deionized water is limited due to long experimental time. Jain *et al*. [68] investigated the leaching of plain paste (CEM I/II), pastes with 10% replacement of cement by fly ash and glass powder, and paste with 6% replacement of cement by silica fume. All pastes have the same w/c of 0.4. The porosity of all the cement pastes increases with leaching duration. The plain pastes show the highest increase, up to 11% after 90 days of leaching. The glass powder modified pastes show the lowest porosity increase, only 5% because the presence of NaOH in its pore solution reduces the solubility of portlandite. The silica fume/fly ash modified pastes show a similar porosity increase of about 8%. Porosity increase is mainly caused by portlandite dissolution, although C–S–H decalcification also contributes to porosity increase for long leaching duration. After 90 days of leaching, C-S-H contributes almost 3%, while portlandite contributes 8% to the total porosity enhancement. Haga *et al*. [89] performed leaching experiments on OPC cement paste with high w/c of 0.7 using ion-exchanged water. The pore size distribution after leaching for 56 weeks shows an increase in the pore volume in the pore size range between 0.05 and 0.5 µm. The total pore volume of the sample is increased 22% after 56 weeks of leaching. C-S-H leaching is also observed and contributes about 6% of the porosity increase which is determined by comparing experimental total porosity results and the calculation of porosity increase resulting from portlandite dissolution.

In a comparison study, Carde *et al*. [72] performed the leaching tests on the same CEM I cement paste with w/c of 0.5 using ammonium nitrate solution and deionized water. The pH of deionized water is lowered to 4.5 by nitric acid addition in order to increase the leaching kinetics. Results show that both environments lead to total portlandite dissolution in the degraded zone and to a progressive decalcification of C-S-H, but the kinetics is much faster when using of ammonium nitrate (2 orders of magnitude). At the same leaching degree, the porosity increase is the same for both conditions.

**Concluding remarks**

Leaching and carbonation of cement-based materials are slow processes but relevant for assessment of long-term (reinforced) concrete durability. Many experimental approaches exist to understand the behaviour of degraded materials at different degradation stages. Most of the

approaches rely on accelerated techniques by making the environmental conditions more aggressive. However, there is still on-going discussion regarding whether the degradation mechanism in accelerated conditions is the same to natural conditions. If it is, it is still not generally validated how to extrapolate the accelerated testing conditions to real performance. To answer this key question, one has to validate the accelerated methodologies against natural testing conditions in detail in which the changes in mineralogy and microstructure at certain degradation stages should be identical or mostly similar for both conditions.

One important thing that cannot be captured in accelerated tests is the continuous hydration of cement-based materials. Under natural conditions there is still evolution of the hydrated cement matrix structure, while under accelerated conditions the continuous hydration is not taken into account due to shortened experimental time. It is generally assumed that accelerated tests can be used for the characterization of degraded materials and its resistance to chemical degradation. However, it is not fully recommended to use accelerated testing for the kinetic study in term of predicting the degradation rate under natural conditions.

There is an agreement in literature that carbonation and leaching change the transport properties of cement-based materials, but to what extent is still questionable. The confusion comes from the unclear definition of what exactly is a leached material; whether it concerns complete/partial portlandite dissolution or complete portlandite dissolution + partial C-S-H dissolution. To better understand how far the transport properties are altered due to chemical degradation, changes in mineralogy and microstructure should be intensively examined.

## References

[1] Jacques D, Maes N, Perko J, Seetharam SC, Phung QT, Patel R, et al. Concrete in engineered barriers for radioactive waste disposal facilities - phenomenological study and assessment of long term performance. 15th International Conference on Environmental Remediation and Radioactive Waste Management - ICEM2013. Brussels, Belgium2013. p. 1–10.

[2] Glasser FP, Marchand J, Samson E. Durability of concrete - Degradation phenomena involving detrimental chemical reactions. Cement and Concrete Research. 2008;38(2):226–246.

[3] Houst YF. Carbonation Shrinkage of Hydrated Cement Paste. Proc 4th CANMET/ACI International Conference on Durability of Concrete. CANMET, Ottawa, Canada1997. p. 481–491.

[4] Swenson EG, Sereda PJ. Mechanism of the carbonatation shrinkage of lime and hydrated cement. Journal of Applied Chemistry. 1968;18(4):111–117.

[5] Hidalgo A, Domingo C, Garcia C, Petit S, Andrade C, Alonso C. Microstructural changes induced in Portland cement-based materials due to natural and supercritical carbonation. J Mater Sci. 2008;43(9):3101–3111.

[6] Papadakis VG, Vayenas CG, Fardis MN. Experimental Investigation and Mathematical-Modeling of the Concrete Carbonation Problem. Chem Eng Sci. 1991;46(5-6):1333–1338.

[7] Papadakis VG, Vayenas CG, Fardis MN. Fundamental Modeling and Experimental Investigation of Concrete Carbonation. Aci Mater J. 1991;88(4):363–373.

[8] Reardon EJ, James BR, Abouchar J. High Pressure Carbonation of Cementitious Grout. Cement and Concrete Research. 1989;19(3):385–399.

[9] Fernandez Bertos M, Simons SJR, Hills CD, Carey PJ. A review of accelerated carbonation technology in the treatment of cement-based materials and sequestration of CO(2). J Hazard Mater. 2004;112(3):193–205.

[10] Lagerblad B. Carbon dioxide uptake during concrete life cycle: State of the art: Swedish Cement and Concrete Research Institute; 2005.

[11] Chen JJ, Thomas JJ, Taylor HFW, Jennings HM. Solubility and structure of calcium silicate hydrate. Cement and Concrete Research. 2004;34(9):1499–1519.

[12] Venhuis MA, Reardon EJ. Vacuum method for carbonation of cementitious wasteforms. Environ Sci Technol. 2001;35(20):4120–4125.

[13] Papadakis VG, Fardis MN, Vayenas CG. Fundamental Concrete Carbonation Model and Application to Durability of Reinforced Concrete. Durability of Building Materials and Components. 1991:12.

[14] Zdeněk Š. Carbonization of porous concrete and its main binding components. Cement and Concrete Research. 1971;1(6):645–662.

[15] Dauzeres A, Le Bescop P, Sardini P, Cau Dit Coumes C. Physico-chemical investigation of clayey/cement-based materials interaction in the context of geological waste disposal: Experimental approach and results. Cement and Concrete Research. 2010;40(8):1327–1340.

[16] Craen MD, Wang L, Geet MV, Moors H. Geochemistry of Boom Clay pore water at the Mol site. SCK•CEN-BLG-990 SCK•CEN, Mol, Belgium2004.

[17] Atis CD. Accelerated carbonation and testing of concrete made with fly ash. Constr Build Mater. 2003;17(3):147–152.

[18] Deceukelaire L, Vannieuwenburg D. Accelerated Carbonation of a Blast-Furnace Cement Concrete. Cement and Concrete Research. 1993;23(2):442–452.

[19] Fernández-Carrasco L, Torréns-Martín D, Martínez-Ramírez S. Carbonation of ternary building cementing materials. Cement and Concrete Composites. 2012;34(10):1180–1186.

[20] Morandeau A, Thiéry M, Dangla P. Investigation of the carbonation mechanism of CH and C-S-H in terms of kinetics, microstructure changes and moisture properties. Cement and Concrete Research. 2014;56(0):153–170.

[21] Lollini F, Redaelli E, Bertolini L. Effects of portland cement replacement with limestone on the properties of hardened concrete. Cement and Concrete Composites. 2014;46(0):32–40.

[22] Borges PHR, Costa JO, Milestone NB, Lynsdale CJ, Streatfield RE. Carbonation of CH and C-S-H in composite cement pastes containing high amounts of BFS. Cement and Concrete Research. 2010;40(2):284–292.

[23] Kinoshita H, Circhirillo C, SanMartin I, Utton CA, Borges PHR, Lynsdale CJ, et al. Carbonation of composite cements with high mineral admixture content used for radioactive waste encapsulation. Miner Eng. 2014;59(0):107–114.

[24] Ji Y-s, Wu M, Ding B, Liu F, Gao F. The experimental investigation of width of semi-carbonation zone in carbonated concrete. Constr Build Mater. 2014;65(0):67–75.

[25] Younsi A, Turcry P, Aït-Mokhtar A, Staquet S. Accelerated carbonation of concrete with high content of mineral additions: Effect of interactions between hydration and drying. Cement and Concrete Research. 2013;43(0):25–33.

[26] Castellote M, Andrade C, Turrillas X, Campo J, Cuello GJ. Accelerated carbonation of cement pastes in situ monitored by neutron diffraction. Cement and Concrete Research. 2008;38(12):1365–1373.

[27] Castellote M, Fernandez L, Andrade C, Alonso C. Chemical changes and phase analysis of OPC pastes carbonated at different $CO_2$ concentrations. Mater Struct. 2009;42(4):515–525.

[28] Huntzinger DN. Carbon dioxide sequestration in cement kiln dust through mineral carbonation [Geological Engineering]: Michigan Technological University; 2006.

[29] Huntzinger DN, Gierke JS, Kawatra SK, Eisele TC, Sutter LL. Carbon Dioxide Sequestration in Cement Kiln Dust through Mineral Carbonation. Environ Sci Technol. 2009;43(6):1986–1992.

[30] Rendek E, Ducom G, Germain P. Carbon dioxide sequestration in municipal solid waste incinerator (MSWI) bottom ash. J Hazard Mater. 2006;128(1):73–79.

[31] Venhuis MA, Reardon EJ. Carbonation of cementitious wasteforms under supercritical and high pressure subcritical conditions. Environ Technol. 2003;24(7):877–887.

[32] Hartmann T, Paviet-Hartmann P, Rubin JB, Fitzsimmons MR, Sickafus KE. The effect of supercritical carbon dioxide treatment on the leachability and structure of cemented radioactive waste-forms. Waste Manage. 1999;19(5):355–361.

[33] Rostami V, Shao Y, Boyd A. Carbonation Curing versus Steam Curing for Precast Concrete Production. J Mater Civil Eng. 2012;24(9):1221–1229.

[34] Kashef-Haghighi S, Ghoshal S. CO2 Sequestration in Concrete through Accelerated Carbonation Curing in a Flow-through Reactor. Ind Eng Chem Res. 2009;49(3):1143–1149.

[35] Phung QT, Maes N, De Schutter G, Jacques D, Ye G. A methodology to study carbonation of cement paste and its effect on permeability. 4th International Conference on Accelerated Carbonation for Environmental and Materials Engineering (ACEME-2013)2013. p. 459–463.

[36] Phung QT, Maes N, Jacques D, Bruneel E, Van Driessche I, Ye G, et al. Effect of limestone fillers on microstructure and permeability due to carbonation of cement pastes under controlled CO2 pressure conditions. Constr Build Mater. 2015;82(0):376–390.

[37] Jacops E, Volckaert G, Maes N, Weetjens E, Govaerts J. Determination of gas diffusion coefficients in saturated porous media: He and $CH_4$ diffusion in Boom Clay. Applied Clay Science. 2013;83–84(0):217–223.

[38] Phung QT, Maes N, De Schutter G, Jacques D, Ye G. Determination of water permeability of cementitious materials using a controlled constant flow method. Constr Build Mater. 2013;47(0):1488–1496.

[39] Hills CD, Johnson DC, MacLeod CL, Carey PJ. Solidification of stainless steel slag by accelerated carbonation. Environ Technol. 2003;24(6):671–678.

[40] RILEM. CPC-18 Measurement of hardened concrete carbonation depth. Mater Struct. 1988;21(6):453–455.

[41] Chang CF, Chen JW. The experimental investigation of concrete carbonation depth. Cement and Concrete Research. 2006;36(9):1760–1767.

[42] Villain G, Platret G. Two experimental methods to determine carbonation profiles in concrete. Aci Mater J. 2006;103(4):265–271.

[43] Villain G, Thiery M. Gammadensimetry: A method to determine drying and carbonation profiles in concrete. Ndt&E Int. 2006;39(4):328–337.

[44] Slegers PA, Rouxhet PG. Carbonation of the hydration products of tricalcium silicate. Cement and Concrete Research. 1976;6(3):381–388.

[45] Vagenas NV, Gatsouli A, Kontoyannis CG. Quantitative analysis of synthetic calcium carbonate polymorphs using FT-IR spectroscopy. Talanta. 2003;59(4):831–836.

[46] Liteanu E, Spiers CJ. Fracture healing and transport properties of wellbore cement in the presence of supercritical CO2. Chem Geol. 2011;281(3–4):195–210.

[47] Claisse PA, El-Sayad H, Shaaban IG. Permeability and pore volume of carbonated concrete. Aci Mater J. 1999;96(3):378–381.

[48] Borges P, Milestone N, Costa J, Lynsdale C, Panzera T, Christophoro A. Carbonation durability of blended cement pastes used for waste encapsulation. Mater Struct. 2011:1–16.

[49] Ngala VT, Page CL. Effects of carbonation on pore structure and diffusional properties of hydrated cement pastes. Cement and Concrete Research. 1997;27(7):995–1007.

[50] Pihlajavaara SE. Some results of the effect of carbonation on the porosity and pore size distribution of cement paste. Mat Constr. 1968;1(6):521–527.

[51] Mo L, Panesar DK. Effects of accelerated carbonation on the microstructure of Portland cement pastes containing reactive MgO. Cement and Concrete Research. 2012;42(6):769–777.

[52] Thomas JJ, Hsieh J, Jennings HM. Effect of carbonation on the nitrogen BET surface area of hardened portland cement paste. Advanced Cement Based Materials. 1996;3(2):76–80.

[53] Houst YF. The role of moisture in the carbonation of cementitious materials. Internationale Zeitschrift für Bauinstandsetzen und Baudenkmalpflege. 1996;2:49–66.

[54] Chen D, Sakai E, Daimon M, Ohba Y. Carbonation of low heat portland cement paste precured in water for different time. Journal of University of Science and Technology Beijing, Mineral, Metallurgy, Material. 2007;14(2):178–184.

[55] Johannesson B, Utgenannt P. Microstructural changes caused by carbonation of cement mortar. Cement and Concrete Research. 2001;31(6):925–931.

[56] You KS, Lee SH, Hwang SH, Ahn JW. Effect of CO2 Carbonation on the Chemical Properties of Waste Cement: CEC and the Heavy Metal Adsorption Ability. Mater Trans. 2011;52(8):1679–1684.

[57] Rochelle CA, Purser G, Milodowski AE, Noy D, Wagner D, Butcher A, et al. CO2 migration and reaction in cementitious repositories: a summary of work conducted as part of the FORGE project. Nottingham, UK2013.

[58] Dewaele PJ, Reardon EJ, Dayal R. Permeability and Porosity Changes Associated with Cement Grout Carbonation. Cement and Concrete Research. 1991;21(4):441–454.

[59] Song HW, Kwon SJ. Permeability characteristics of carbonated concrete considering capillary pore structure. Cement and Concrete Research. 2007;37(6):909–915.

[60] Lesti M, Tiemeyer C, Plank J. $CO_2$ stability of Portland cement based well cementing systems for use on carbon capture & storage (CCS) wells. Cement and Concrete Research. 2013;45(0):45–54.

[61] Fabbri A, Corvisier J, Schubnel A, Brunet F, Goffe B, Rimmele G, et al. Effect of carbonation on the hydro-mechanical properties of Portland cements. Cement and Concrete Research. 2009;39(12):1156–1163.

[62] Yokozeki K, Watanabe K, Sakata N, Otsuki N. Modeling of leaching from cementitious materials used in underground environment. Applied Clay Science. 2004;26(1–4):293–308.

[63] Berner UR. Modeling the Incongruent Dissolution of Hydrated Cement Minerals. Radiochim Acta. 1988;44-5:387–393.

[64] Pichler C, Saxer A, Lackner R. Differential-scheme based dissolution/diffusion model for calcium leaching in cement-based materials accounting for mix design and binder composition. Cement and Concrete Research. 2012;42(5):686–699.

[65] Heukamp FH. Chemomechanics of calcium leaching of cement-based materials at different scales: the role of CH-dissolution and C-S-H degradation on strength and durability performance of materials and structures [PhD thesis]: Massachusetts Institute of Technology; 2003.

[66] Saito H, Deguchi A. Leaching tests on different mortars using accelerated electrochemical method. Cement and Concrete Research. 2000;30(11):1815–1825.

[67] Haga K, Sutou S, Hironaga M, Tanaka S, Nagasaki S. Effects of porosity on leaching of Ca from hardened ordinary Portland cement paste. Cement and Concrete Research. 2005;35(9):1764–1775.

[68] Jain J, Neithalath N. Analysis of calcium leaching behavior of plain and modified cement pastes in pure water. Cement and Concrete Composites. 2009;31(3):176–185.

[69] Bertron A, Duchesne J, Escadeillas G. Accelerated tests of hardened cement pastes alteration by organic acids: analysis of the pH effect. Cement and Concrete Research. 2005;35(1):155–166.

[70] De Windt L, Devillers P. Modeling the degradation of Portland cement pastes by biogenic organic acids. Cement and Concrete Research. 2010;40(8):1165–1174.

[71] Butcher EJ, Borwick J, Collier N, Williams SJ. Long term leachate evolution during flow-through leaching of a vault backfill (NRVB). Mineralogical Magazine. 2012;76(8):3023–3031.

[72] Carde C, Escadeillas G, François AH. Use of ammonium nitrate solution to simulate and accelerate the leaching of cement pastes due to deionized water. Magazine of Concrete Research. 1997;49(181):295–301.

[73] Chen JJ, Thomas JJ, Jennings HA. Decalcification shrinkage of cement paste. Cement and Concrete Research. 2006;36(5):801–809.

[74] Phung QT, Maes N, Jacques D, Schutter GD, Ye G. Decalcification of cement paste in $NH_4NO_3$ solution: Microstructural alterations and its influence on the transport properties. In: Bastien J, Rouleau N, M. Fiset, Thomassin M, editors. 10th fib International PhD Symposium in Civil Engineering. Québec, Canada. 2014 p. 179–187.

[75] Phung QT. Effects of Carbonation and Calcium Leaching on Microstructure and Transport Properties of Cement Pastes [PhD thesis]. Belgium: Ghent University; 2015.

[76] de Larrard T, Poyet S, Pierre M, Benboudjema F, Le Bescop P, Colliat J-B, et al. Modelling the influence of temperature on accelerated leaching in ammonium nitrate. Eur J Environ Civ En. 2012;16(3-4):322–335.

[77] Nguyen VH, Colina H, Torrenti JM, Boulay C, Nedjar B. Chemo-mechanical coupling behaviour of leached concrete: Part I: Experimental results. Nucl Eng Des. 2007;237(20–21):2083–2089.

[78] Yang H, Jiang L, Zhang Y, Pu Q, Xu Y. Predicting the calcium leaching behavior of cement pastes in aggressive environments. Constr Build Mater. 2012;29(0):88–96.

[79] Poyet S, Le Bescop P, Pierre M, Chomat L, Blanc C. Accelerated leaching of cementitious materials using ammonium nitrate (6M): influence of test conditions. Eur J Environ Civ En. 2012;16(3-4):336–351.

[80] Phung QT, Maes N, Jacques D, Schutter GD, Ye G. Microstructural and permeability changes due to accelerated Ca leaching in ammonium nitrate solution. In: Grantham M, Basheer PAM, Magee B, Soutsos M, editors. Concrete Solutions - 5th International Conference on Concrete Repair: CRC Press; 2014 p. 431–438.

[81] Perlot C, Verdier J, Carcasses M. Influence of cement type on transport properties and chemical degradation: Application to nuclear waste storage. Mater Struct. 2006;39(5):511–523.

[82] Gallé C, Peycelon H, Bescop PL. Effect of an accelerated chemical degradation on water permeability and pore structure of cementbased materials. Adv Cem Res. 2004;16(3):105–114.

[83] Berra M, Carassiti F, Mangialardi T, Paolini AE, Sebastiani M. Leaching behaviour of cement pastes containing nanosilica. Adv Cem Res2013. p. 352–361.

[84] Segura I, Molero M, Aparicio S, Anaya JJ, Moragues A. Decalcification of cement mortars: Characterisation and modelling. Cement and Concrete Composites. 2013;35(1):136–150.

[85] Cheng A, Chao SJ, Lin WT. Effects of Leaching Behavior of Calcium Ions on Compression and Durability of Cement-Based Materials with Mineral Admixtures. Materials. 2013;6(5):1851–1872.

[86] Agostini F, Lafhaj Z, Skoczylas F, Loodsveldt H. Experimental study of accelerated leaching on hollow cylinders of mortar. Cement and Concrete Research. 2007;37(1):71–78.

[87] Yurtdas I, Xie SY, Burlion N, Shao JF, Saint-Marc J, Garnier A. Deformation and Permeability Evolution of Petroleum Cement Paste Subjected to Chemical Degradation Under Temperature. Transport Porous Med. 2011;86(3):719–736.

[88] Bernard F, Kamali-Bernard S. Performance simulation and quantitative analysis of cement-based materials subjected to leaching. Comp Mater Sci. 2010;50(1):218–226.

[89] Haga K, Shibata M, Hironaga M, Tanaka S, Nagasaki S. Change in pore structure and composition of hardened cement paste during the process of dissolution. Cement and Concrete Research. 2005;35(5):943–950.

## 5.5  Geochemical and physical evolution of cementitious materials in an aggressive environment

*A. Dauzeres*

*Institute for Radiological Protection and Nuclear Safety IRSN/PRP-DGE/SRTG/LETIS, Fontenay-aux-Roses Cedex, France*

**Impact of aqueous ionic or multi-ionic aggressive environments on the physical-chemical evolution of cementitious materials**

In the context of deep geological disposal, over the long term, groundwater, more or less concentrated with aggressive chemical ions, is the main driving factor for cementitious materials deterioration. Porewater in equilibrium with the argillaceous surrounding rock of either the Callovo-Oxfordian (France) (COX), the Toarcian argillite of Tournemire (France), or the Opalinus clay of Mont Terri (Switzerland) exhibits a multi-ionic composition (HCO3-, Cl⁻, $SO_4^{2-}$, $Mg^{2+}$, neutral pH) that may disturb cementitious materials. In fact, the concentrations of sulfate, chloride and magnesium carbonate, and the neutral pH (Table 5.5.1), are the main factors of aggression. This type of solution is classified as XA-2 according to the AFNOR standard (Table 5.5.2) which classifies the aggressiveness of environments depending on the concentrations and the pH of the natural solution in regard to the concrete. It can generate a moderate attack of cementitious materials. This classification is primarily related to the concentration of sulfate; other aggressive agents are either classified as XA-1 or unclassified.

*Table 5.5.1. Chemical composition of the porewater of three clayey rocks at 25 °C (in mmol/L).*

|  | **Na** | **K** | **Ca** | **Si** | **Mg** | **SO₄** | **Cl** | **HCO₃** | **pH** |
|---|---|---|---|---|---|---|---|---|---|
| **Callovo-Oxfordian (France)** *Gaucher et al., 2007* | 45.6 | 1 | 7.4 | 0.2 | 6.7 | 15.6 | 41 | 3.3 | 7.1 |
| **Toarcian (France)** *Tremosa et al., 2012* | 23.5 | 0.8 | 1.5 | 0.03 | 0.7 | 9.5 | 4.5 | 4.6 | 7.4 |
| **Opalinus (Switzerland)** *Pearson et al., 2003* | 250 | 2 | 23 | 0.1 | 39 | 18 | 340 | 1.6 | 7.2 |

*Table 5.5.2. Classification of aggressive environments with respect to concretes (AFNOR-NF EN 206) [AFN 04].*

| Degree of aggression | XA-1 | XA-2 | XA-3 |
|---|---|---|---|
|  | **Concentration (mg/l)** | | |
| **pH** | 6.5–5.5 | 5.5–4.5 | 4.5–4 |
| **SO₄** | 200–600 | 600–3000 | 3000–6000 |
| **Mg** | 300–1000 | 1000–3000 | >3000 |
| **CO₂ agressif** | 15–40 | 40–100 | >100 |
| **NH₃** | 15–30 | 30–60 | 60–100 |

To better understand the mechanisms controlling the reactive evolution of concrete placed in contact with clays, it is possible to learn from studies having chemical analogies. Numerous studies have been carried out on the chemical behavior of concrete placed in aggressive environments. The stresses to which cementitious materials can be exposed vary due to the involved concentrations of aggressive agents. Cementitious materials can become exposed to pure water, acid water, sea water, water rich in sulfates, nitrates or chlorides, or wastewater.

The natural solution in equilibrium with the COX argillite, due to its ionic species, may also induce alteration mechanisms identical or similar to those identified in, for example, concrete placed in seawater or freshwater.

For this reason, the following state of the art review provides a synthesis of the chemical degradation mechanisms identified in previous studies. It mainly focuses on cementitious materials subjected to leaching, carbonation, and sulfate and magnesium attacks. Many natural or experimental conditions are described, such as sea water or deep water. Directly related to the initial composition of the solution of the COX, this part is devoted exclusively to experimental work on the impact of such waters on cementitious materials. The objective is to identify the evolution of primary phases and the nature of secondary phases precipitated in environments close to clayey rock. Lastly, this section presents a few studies on synthetic water representative of clay or granitic porewater.

Concrete is almost always in balance with the environment, the latter being in most cases acid or neutral, as the concrete has a very basic character. Water is the vector allowing the arrival of aggressive ions in the material. Ions transport in the concrete, diffusive or convective, is reactive. Species transported in the porosity of the material continuously interact with the pore solution of the concrete and with hydrates. These interactions cause imbalances that generate dissolutions or precipitation possibly influencing the structure of the material (mechanical damage, clogging...).

Regourd (Regourd et al., 1981) produced a balance sheet diagram showing the three mechanisms behind and the effects of concrete deterioration, as a basis for the understanding of the identifiable disturbances in a cementitious material.

The selection of studies, illustrating each theme in this part, depends on the relevance to the issue of the cementitious material's durability in a clayey environment. The list is certainly not exhaustive, but it highlights the important points that are useful for the progress of future work.

**Cementitious material evolution in pure water**

"It is considered for the chemical degradation of CEM I type concretes in saturated medium, that the mineralogical evolution of the cementitious system is governed by the dissolution of the portlandite and C-S-H" (Gallé et al., 2006).

*Mineralogical evolutions*

In the case of pure water or freshwater, the major phenomenon controlling the chemical evolution of the cementitious material is the leaching. This mechanism is a result of the material's solid state chemistry and porosity. The contact with pure water creates a chemical imbalance due to the concentration gradient between the surface and the core of the material. The local solid chemistry tries to adjust to this disturbance. To correct the concentration

gradient, ions diffuse through the porosity of the cement paste. This migration creates local chemical imbalances resulting in a process of dissolution/precipitation.

The work of Adenot (Adenot, 1992) on the behavior of cementitious materials for the storage of radioactive waste enables us to precisely identify the mechanisms of attack by a pure solution at pH 7 at 20 °C. The tests carried out consisted in leaching cement paste specimens by using continuously deionized water.

Note that tests on cement pastes are a simplification of tests on concrete. Transport in the concrete is concentrated in the cementitious matrix, which is much more permeable than the aggregates. Working on cement pastes is representative of the mechanisms that concrete placed in the same conditions would experience, aggregates being not reactive, while it overcomes post-experimental difficulties for the solid characterization. The degradation process is fully controlled by the hydrated cement paste.

Two experimental options are carried out. The first consists in maintaining a pure solution throughout the experiment by imposing permanent circulation of the aggressive solution through an ion exchange resin and regular renewals. Furthermore, in order to avoid the presence of carbonates in the solution, and thus the carbonation of the cementitious material, continuous nitrogen bubbling is imposed in the solution.

The second experimental option consists in maintaining the aggressiveness by adding acid solution (no ion exchange resins) (Revertegat et al., 1992). This acid addition enables continuous monitoring of the amount of hydroxide ions leached. From a certain quantity of acid addition, the solution is renewed and the calcium concentrations in the leachate measured. Note that in both options, the loss of mass of the material is also monitored continuously by hydrostatic weighing. The perturbation consists in the dissolution of the cement paste hydrates into the material in the form of dissolution fronts.

At constant degradation conditions, the hydrates dissolution order is the following: portlandite, C-S-H, AFm, ettringite. Note that the C-S-H decalcification takes place gradually.

The calcium and silicon concentrations in solution impose changes of the equilibrium phases in the CaO-SiO2-H2O system. For calcium concentrations around 22 mmol/kg, the mineral assemblage at equilibrium is portlandite-C-S-H (IIC) or C-S-H-□. From the time when the calcium concentration is less than 22 mmol/kg, portlandite is out of balance and is dissolved. By reducing the calcium concentration in the solution, successive C-S-H are formed and dissolved gradually reducing the CaO/SiO2 ratio in their structure until reaching the amorphous silica stage.

Portlandite acts as a chemical buffer vis-à-vis external aggressions. Silicates and aluminates are not dissolved until all of the portlandite is leached. The solution of the cementitious material, previously in equilibrium with the portlandite, then rebalances with a new mineral assemblage: C-S-H, AFm, AFt. As to the continuation of the perturbation, the CaO/SiO2 ratio of C-S-H gradually decreases accompanied firstly by the AFm dissolution. This dissolution, in the case of hydrated calcium monosulfoaluminate, releases calcium, but also aluminum and sulfates. This mechanism may generate, without the addition of external sulfates in the material, the precipitation of ettringite or secondary AFm phases in the dissolving zone of portlandite (Faucon, 1997).

The continued leaching causes ettringite dissolution. The system is in equilibrium with C-S-H (low C/S) and at the final stage, the C-S-H are totally decalcified; the system is then in equilibrium with amorphous silica.

By placing cement pastes made from C3S into demineralized water, Faucon shows the evolution of the Ca/Si ratio in the solid with the progress of the degraded area (Faucon et al., 1997).

The dissolution fronts evolve linearly with the square root of time, confirming that the kinetics of decalcification is controlled by diffusive phenomena (Adenot, 1992).

A degraded mortars study by Bourdette (Bourdette et al., 1994) showed no influence of the presence of aggregates on the zonation of the disturbance, thus confirming the work by Adenot et al on cement paste and validating their model.

*Temperature influence*

The impact of temperature on the leaching of cementitious materials is studied by Peycelon et al. (2006). The tests, very similar to those of Adenot, consist in plunging a cement paste (OPC-type) into a solution at different temperatures: 25 °C, 50 °C and 85 °C. The temperature increase accelerates the degradation process of the solid. However, the solubility of portlandite decreases with increased temperature and should slow down or stop the alteration. This is explained by the fact that the degradation is controlled by diffusion. When the temperature increases, the diffusion coefficient increases. The viscosity of water decreases with increased temperature and the diffusion coefficient increases according to the Stokes-Einstein law.

$$D = \frac{kT}{6\Pi r\mu} \ (Equation \ 1).$$

With:
- k = Boltzmann constant ($1,3806.10^{-23}$ J.K$^{-1}$)
- T = Temperature (° Kelvin)
- r = The radius of the diffusing molecule assumed spherical.
- μ = The fluid viscosity.

By increasing the temperature and decreasing the viscosity of the fluid (water in this case), the diffusion coefficient increases.

The thicknesses affected by leaching according to the temperatures used are summarized in Table *5.5.3*.

*Table 5.5.3. Experimental data of the leaching evolution of OPC cement paste immerged in pure water at 25 °C, 50 °C et 85 °C (Peycelon et al., 2006).*

| Temperatures (°C) | Experimental times (days) | Leached thickness (mm) | Velocities of perturbations (mm/square root of days) |
|---|---|---|---|
| 25 | 85 | 1.8 | 0.19 |
| 50 | 88 | 2.85 | 0.3 |
|  | 109 | 2.96 |  |
| 85 | 62 | 4.47 | 0.56 |
|  | 72 | 5.2 |  |
|  | 134 | 5.95 |  |

The alteration rate of an OPC cement paste leached in pure water is 1.6 times greater at 50 °C than at 25 °C.

> **To summarize, a Portland cement paste immerged in pure water is exposed to dissolution of its hydrates, mainly the portlandite and the C-S-H (C/S ratio decrease) and also ettringite and AFM. The perturbation is characterized as multiple dissolution fronts corresponding to new mineral equilibriums. Decalcification causes a leaching of Ca2+ and OH- ions and alkali to the outside environment. This mechanism is controlled by the diffusion and is temperature-dependent despite the retrograde solubility of portlandite. The impact on the microstructure is strong because the successive dissolutions generate porosity opening that increases the diffusion coefficient and thus degradation. This theme has been studied extensively and now allows for benchmarks on the evolution of perturbations over time.**

## Cementitious material evolution in carbonated water

### Origin of carbonates

The calcium ion leaching of concrete in our environment often appears visually. Indeed, drips or whitish concretions are often identified on the concrete surface. The mechanism responsible for these courses is the precipitation of calcium carbonate due to carbon dioxide (CO2) from the atmosphere (gas) or carbonates species in solution (aqueous). Studies about carbonation are overwhelmingly made in an unsaturated environment. Parrot (quoted by Badouix, 2000) and Chaussadent (Chaussadent, 1997) provide summaries of the results associated with the carbonation.

Carbonate in natural waters may have three origins: the atmosphere, the mineral phases or bacterial activity in soils or effluents. Waters, from surface or underground, present equilibrium with a range of CO2 partial pressures, leading to some carbonate concentration in the solution, which can be estimated from Henry's Law.

$$[H_2CO_3]^* = \alpha.pCO_2 \text{ with } \alpha = 10^{-1.46} \text{ at } 25 \text{ °C at } 1 \text{ atm } (\textit{Equation 2.})$$

with $[H_2CO_3]^*$ representing the total concentration in dissolved carbonates.

The groundwater in the COX argillite, for example, is in equilibrium with a CO2 partial pressure 30 times bigger than the atmospheric pCO2 (pCO2 (COX) = 1.3.10-2 atm) (Girard et al., 2005) (Gaucher et al., 2006b) imposing a hydrogen ion concentration of about 3.3 mmol/L (Gaucher et al., 2007). The water, in this case, is in equilibrium with carbonate sediments of the natural formation. It is the dissolution of rocks that brings the carbonates in the solution.

Carbon dioxide dissolved in water results in the formation of carbonic acid H2CO3 (or CO2 (aq)). The ion HCO3- is the main carbonate species in the water of the COX and in many natural waters with a pH close to neutrality. For more acid water (rainwater or water in contact with acid rock), carbonic acid is the main species. A speciation diagram of carbonates species in function of pH is shown in Figure 1.

A detailed description of the chemical equilibrium between the different ionic species of the carbonates is provided by Michard (Michard, 1989).
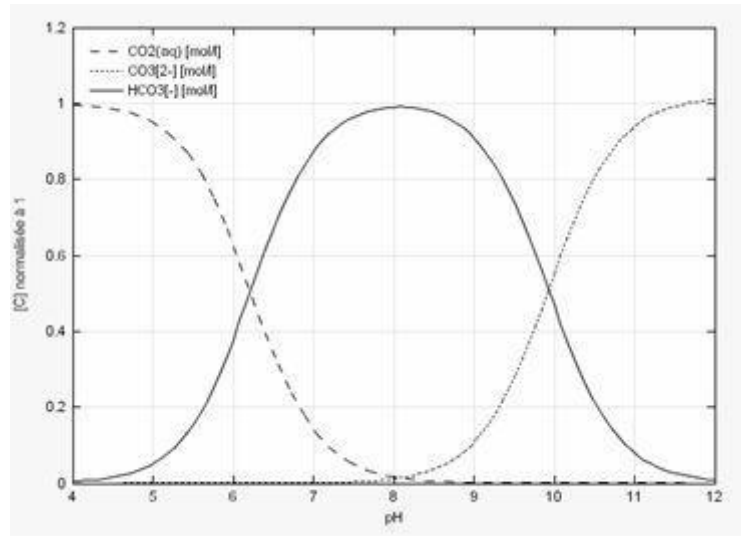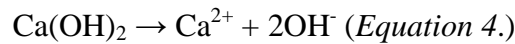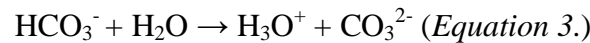
*Figure 5.5.1. Speciation diagram of ions carbonates in function of the solution pH; carried out with JCHESS (database: chess.tdb).*

*Carbonation mechanisms of a cementitious matrix under water*

Carbonation of cementitious material is the introduction of carbonates in a chemical system in permanent evolution. Under water, during the portlandite leaching, and to a lesser extent C-S-H, a calcium and hydroxides flux migrates from the most concentrated area (the healthy zone of the concrete) into the less concentrated area in these elements (the surface). In the case of aggressive water rich in carbonates, the meeting with the calcium ions causes precipitation of a low soluble mineral phase: the calcium carbonate.

$$HCO_3^- + H_2O \rightarrow H_3O^+ + CO_3^{2-} \text{ (\textit{Equation 3.})}$$

$$Ca(OH)_2 \rightarrow Ca^{2+} + 2OH^- \text{ (\textit{Equation 4.})}$$

$$CO_3^{2-} + Ca^{2+} \rightarrow CaCO_3 \text{ (\textit{Equation 5.})}$$

Damidot (Damidot et al., 1995b) provides a stable phase diagram of the CaO-SiO2-CO2-H2O system at 25 °C (Figure 5.5.2). Compared to the CaO-SiO2-H2O diagram presented above, a new mineralogical phase appears, namely calcite. The diagram contains three invariant points:

Point 1 : calcite + C-S-H (SII) (or C-S-H-γ)+ CH + H$_2$O

Point 2 : calcite + C-S-H (SI) (or C-S-H-β)+ C-S-H (SII) (or C-S-H-γ)+ H$_2$O

Point 3 : calcite + SH + C-S-H (SI) (or C-S-H-α)+ H$_2$O

Carbonation of cementitious material in a solution can be summarized in the following two balance equations:

$$Ca(OH)_2 + CO_3^{2-} \rightarrow CaCO_3 + 2OH^- \text{ (\textit{Equation 6})}$$

$$1,7CaO.SiO_2.1,7H_2O + 1,7CO_3^{2-} \rightarrow SiO_{2(am)} + 1,7CaCO_3 + 3,4\ OH^- \text{ (\textit{Equation1})}$$
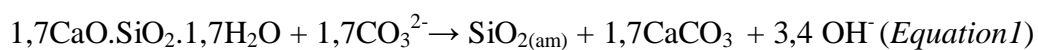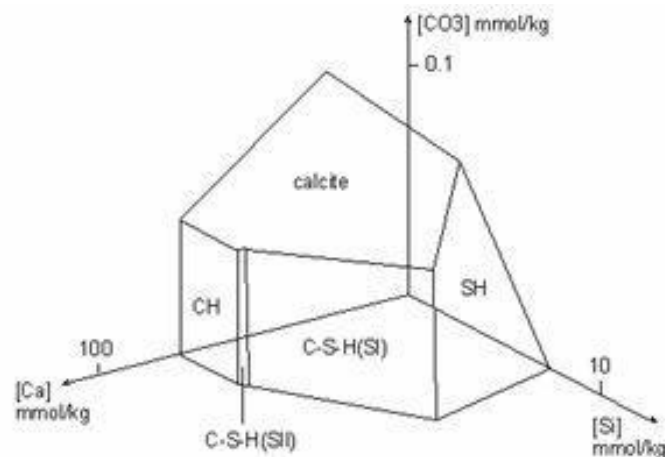
*Figure 5.5.2. Diagram of stable phases in the CaO-SiO2-CO2-H2O system at 25 °C (Damidot et al., 1995b).*

If the state of the art on the carbonation is well documented, it especially covers carbonation in an unsaturated environment (or atmospheric). The carbonation in saturated medium is indeed presented as negligible compared to atmospheric carbonation (Parrot and Killoh 1989). However, with the problem of nuclear waste disposal in deep geological layers, leading to more or less long-term arrival of carbonated water in contact with the concrete structure of cells, the study of the carbonation materials based on hydraulic binders becomes essential for modeling the long-term physical and chemical perturbation of concrete cells. Therefore, many experiments were carried out in the early 1990s.

Sets of experiments have been carried out on cement pastes immerged in solutions of different pH (Revertegat et al., 1992). One test is particularly interesting here: an OPC cement paste is immerged in a solution at pH = 4.6, in equilibrium with a very high pCO2 in the atmosphere of the reactor. Calcium concentration profiles are measured over test durations of 3 months and 2 years (Figure 3). The sound zone of the sample is richer in calcium (composed of portlandite and C-S-H and located above the horizontal bar in Figure 5.5.3). The gradual decrease of the calcium content until the surface is very clear. The peaks under the crossbar correspond to the calcite.
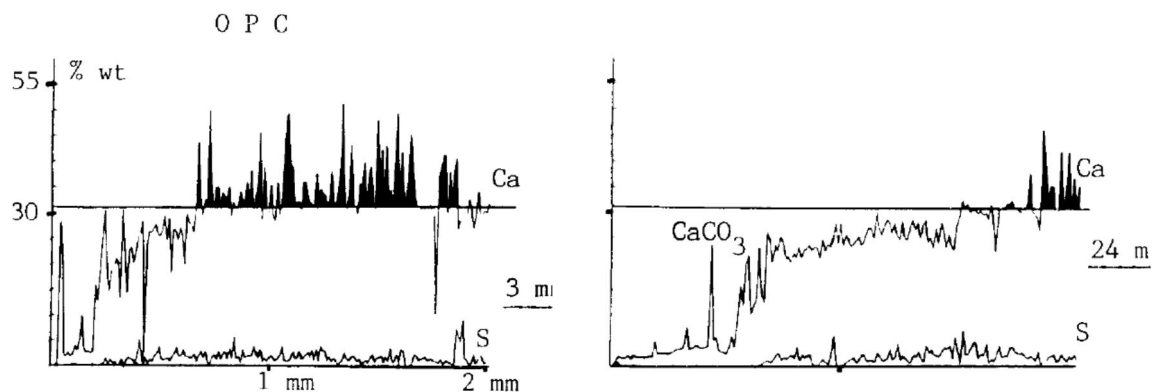


*Figure 5.5.3. Microprobe profiles of calcium and sulfur for an OPC cement paste immerged for 3 months in a carbonated solution at pH 4.6 (Revertegat et al., 1992).*

These experiments were complemented 5 years later with new tests of cement paste carbonation in solution. This time, the carbonate ion concentration is controlled in the

aggressive solution ([C] = 0.01 mmol/L) (Revertegat et al., 1997). This study helps to highlight the role of the diffusion barrier related to the formation of calcium carbonate in the cementitious material.

This notion of diffusion barrier is studied by Badouix (Badouix, 2000). Figure 5.5.4 illustrates the effect of carbonate introduction in the aggressive solution on the hydroxides and calcium diffusion.
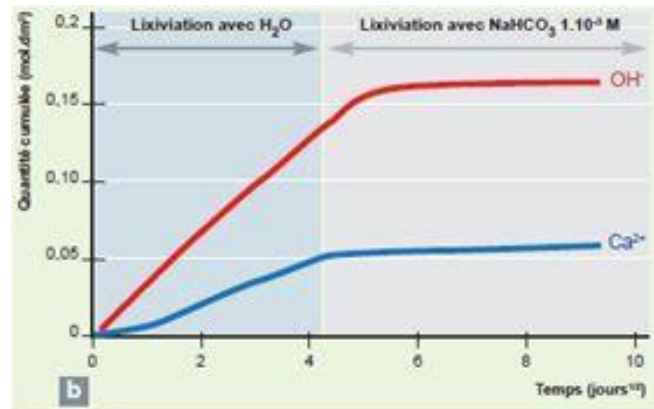


*Figure 5.5.4. Evolution of released calcium and hydroxyl ions during the leaching period in pure water and a second leaching period in a carbonated solution (1.10-3 mol/L) (Badouix et al., 2000).*

It is very clear that ions diffusion is slowed or stopped, after the introduction of carbonates in the system. The precipitation of calcium carbonate clogs the porosity and decreases the effective diffusion coefficient of the material in the affected area. In order to model the long-term deterioration of concrete, Badouix produces cement pastes from leaching tests in carbonated water (NaHCO3 2,5.10-3 mol / L) at 25 °C. The test involves placing the cement paste sample into a thermostated reactor of 500 mL. A magnetic agitator assures homogenization of the solution. A titrator containing nitric acid regulates the pH value to 8.5. The solution is renewed regularly to maintain constant external chemical conditions. The system is very similar to that used by Revertegat et al. (Revertegat et al., 1992). After 200 days, calcite is the only identifiable compound on the first 7 microns. It seems that a clogging layer of calcite forms on the surface exposed to the solution. Between 7 microns and 40 microns, ettringite seems carbonated. At 75 microns, the portlandite content is very low and disappears totally at 40 microns. Between 75 and 175 microns, the ettringite precipitation is authenticated by DRX (increased signal). Disruption extends to 250 microns with the return to the nominal concentration of portlandite at this depth (Figure 5.5.5 and Figure 5.5.6).
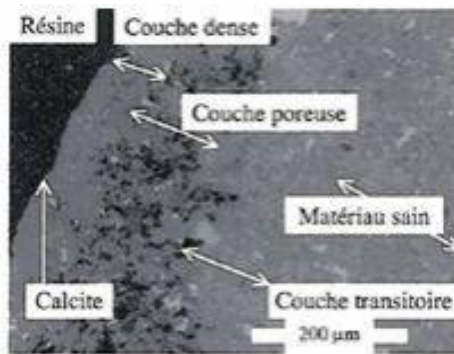
*Figure 5.5.5. SEM picture of a CEM I cement paste immerged 7 months in a carbonated solution (NaHCO₃ = 2.5 mmol/l) (Badouix, 2000).*
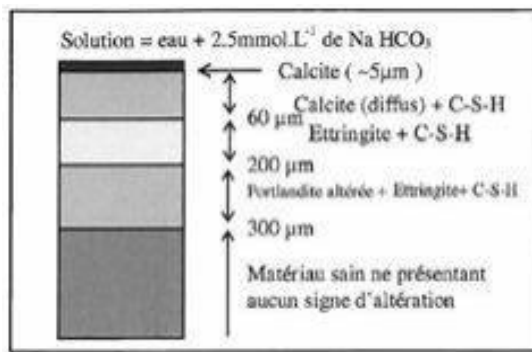
*Figure 5.5.6. Zonation of a CEM I cement paste (w/c = 0.4) immerged 7 months in a carbonated solution (NaHCO₃ = 2.5 mmol/l) (Badouix, 2000).*

**Badouix explains the degradation in carbonated water with five separate zones:**

- **Zone 1: A dense surface layer (5 μm-thick) with a very low porosity composed of calcite.**

- **Zone 2: A dense layer below the surface layer until 60 μm depth composed of diffuse calcite and C-S-H.**

- **Zone 3: A high porous zone composed of ettringite and C-S-H.**

- **Zone 4: A zone composed of altered portlandite, ettringite and C-S-H.**

- **Zone 5: The sound zone composed of portlandite, ettringite and C-S-H.**

The superficial surface layer is described as consisting of rhombohedral calcite microcrystals. Their size ranges from 400 nm to 1 micron. The porous layer of a hundred microns presents perfectly crystallized ettringite.

An experimental study identifies the influence of carbonation on the leaching of cementitious materials (Kurashige et al., 2007). In the same paper, the authors also show the influence of chlorides associated with carbonates.

OPC cement pastes (at different w/c) are immerged in various aggressive solutions (pure water, representative synthetic solution of groundwater and sea water). Our focus here is on the interaction between the solutions containing carbonates (sea water, groundwater) and the cementitious material. As in Badouix's research, the degradation is carried out in one dimension through the protection of the faces on the periphery with Epoxy resin to simplify the understanding of the degradation mechanisms.

Calcite precipitation is identified by XRD and SEM at the material surface and inhibits the leaching process of the cementitious material. The greater the carbonate concentration is in the solution, the greater the degradation becomes low.

The degradation appears to be less significant in the case of the representative solution of sea water than in the case of the representative solution of groundwater after 1 year. The authors attribute this finding to the development of a layer of calcite at the sample surface in the case of sea water (Figure 5.5.7).
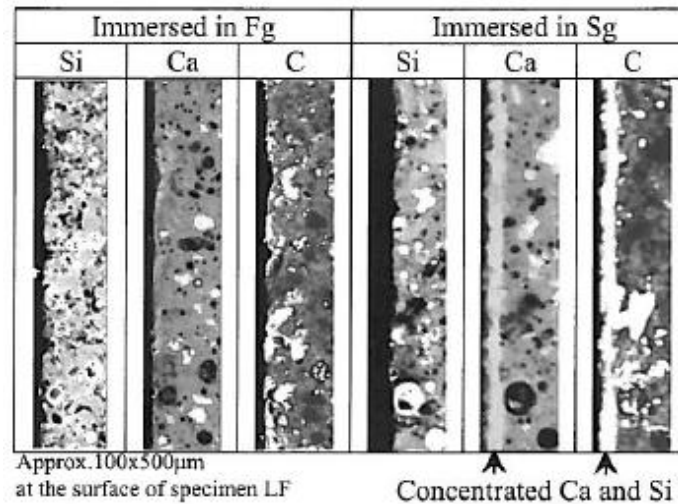
*Figure 5.5.7. Elementary mappings of an OPC cement paste after 1 year of immersion in solutions representative of ground water (Fg) and sea water (Sg) (Note that a mistake is observed in this figure: C enrichment is observed in the surface of the sample and no Si-enrichment) (Kurashige et al., 2007).*

In regards to the identical concentrations of carbonates in groundwater and seawater in this study, the formation of a clogging layer in sea water can be explained by the large amount of calcium already present in the solution (which is not the case in groundwater), which in the vicinity of the material is exposed to an abrupt increase in pH, allowing calcite precipitation on the substrate which is the surface of the material. The growth is very rapid. Figure 5.5.8 shows the mechanisms at work in the formation of this layer of calcium carbonate.
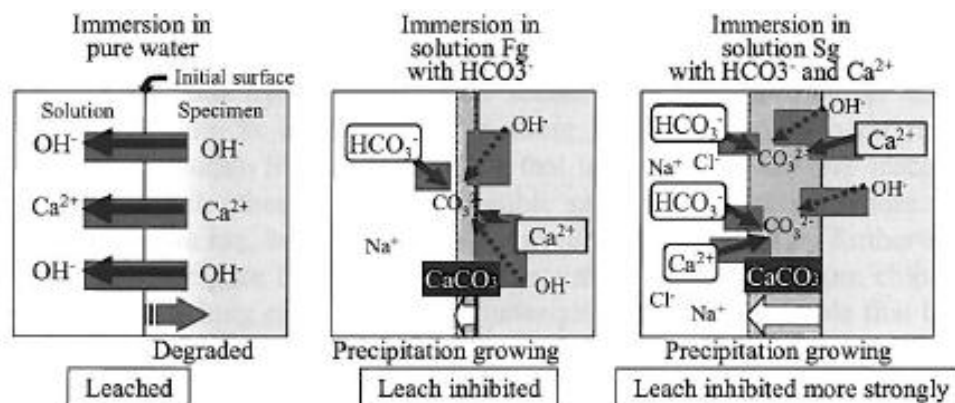


*Figure 5.5.8. Simplified representations of the inhibition mechanisms linked to the leaching of a cementitious material in carbonated solutions (Kurashige et al., 2007).*

**Portland cement-based materials immerged in solutions containing carbonates undergo two main mechanisms of aggression: leaching and carbonation. During the leaching of portlandite, the calcium released reacts with carbonate from the external solution to form calcium carbonate, mainly calcite. This carbonation causes the development of a clogging layer within the first micron of the material. This layer can inhibit the alteration mechanisms implemented in the case of alteration in pure water. The development of this layer is not perfectly located. It is certain that it occurs on the surface of the material, but is it internal to it (primary dissolution/precipitation phases), or is it an exogenous crust that develops over the surface of the material? No**

> **experimental data exists on the porosity of this layer because of its very thin size. In any case, this carbonation plays a protective role of the cementitious material in aggressive environments and its presence or not is an important issue in predicting the long-term behavior of the cementitious material in such environments. Is this protective crust formed when the cementitious material is put in contact with a solid material in the same chemical conditions?**

## Cementitious material evolution in solution rich in sulfates

This part is divided into two separate paragraphs. The first paragraph is dedicated to the physical and chemical evolution of a cementitious material immerged in pure sulfate solutions. The second is devoted to sulfate attack in natural environments, combined with other ionic species, such as chloride or magnesium. This last paragraph is illustrated in particular by the case of attack by sea water and also by a solution representative of porewater of clayey or granitic rocks.

*Evolution with pure sulfate solution*

Portland cement-based materials placed in contact with solutions containing sulfates, even at low concentrations, are subject to physical and chemical reactions. The sulfate ions penetrating into the material can locally modify the mineralogy of the material, with a significant impact on the mechanical properties.

According to Bogue (Bogue, 1952), the study of the influence of sulfates on cementitious materials has a history of more than 250 years, starting with the work of Smeaton in 1756 who sought the most suitable cement for the construction of the Eddystone lighthouse in England. Bogue reported an excellent bibliography, compiled in 1925 by the United States Department of Agriculture, listing 700 references on the resistance of cements hydrated with sulfates. Study of the behavior of cementitious materials in saturated environments rich in sulfates is still relevant today. There are many publications trying to provide answers concerning the understanding of the mechanisms involved.

In 1991, Cohen and Mather (Cohen and Mather, 1991) pointed out that the mechanisms of sulfate attack were not yet well understood. Le Bescop and Solet (Le Bescop and Solet, 2006) note that the difficulty of prediction and validation is mainly due to the phenomenology involved, associating closely chemistry, mechanical and diffusive transport. The importance of the initial and boundary conditions is also emphasized.

Damidot (Damidot et al., 1993) provides a stable phase diagram for $CaO-Al_2O_3-CaSO_4-H_2O$ system at 25 °C (Figure 5.5.9).
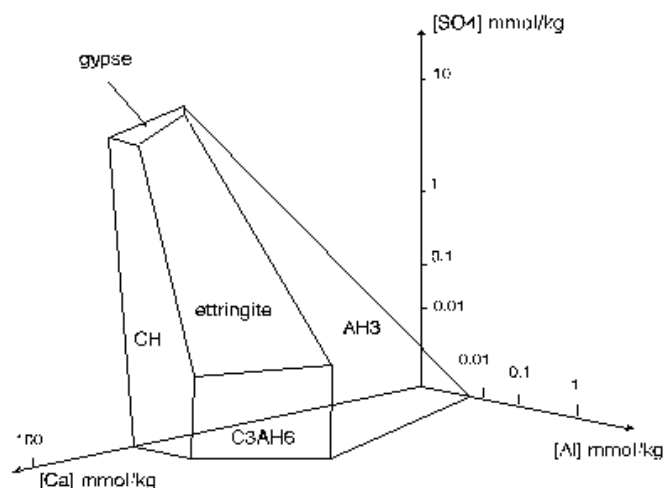
*Figure 5.5.9. Phases diagram of the system CaO-Al$_2$O$_3$-CaSO$_4$-H$_2$O at 25 °C (Damidot et al., 1993).*
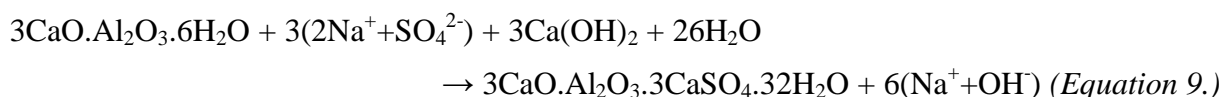
This system contains 5 stable phases: hydrogarnet, gibbsite (AH3), ettringite, portlandite and gypsum. With the increase of the sulfate concentration, four invariant points exist, giving the following four mineralogical associations: ettringite/hydrogarnet/gibbsite (low concentrations of sulfate and calcium); ettringite/hydrogarnet/portlandite (high concentrations of calcium and low in sulfate); ettringite/portlandite/gypsum (high concentrations of calcium and sulfate) and ettringite/gypsum/AH3 (high concentrations of sulfate and low calcium). Hydrogarnet and gypsum phases cannot coexist, as the stability domain of ettringite separates the areas of stability of these two minerals. At 25°C, ettringite has the wider stability range in this system: only a few micromoles of aluminum sulfate suffice to form it. During sulfate attacks, ettringite is therefore one of the minerals which will form regularly.

In regard to the CaO-Al2O3-CaSO4-H2O diagram, some authors, such as Matschei (Matschei et al., 2007), by considering a revised solubility constant for C3AH6, obtain a small area of monosulfoaluminate solubility, leading to 6 invariant points instead of 4.

The mineralogical association related to this system in a hydrated portland cement at 25 °C contains portlandite, ettringite and hydrogarnet. The calculation of the thermodynamic stability for this mineralogical association provides a sulfate concentration of less than 30 micromoles per liter in the absence of alkali. In the case of contact with a solution rich in sulfates, secondary ettringite precipitates to the detriment of hydrogarnet according to the chemical equation:

$3CaO.Al_2O_3.6H_2O + 3(Ca^{2+}+SO_4^{2-}) + 26\ H_2O \rightarrow 3CaO.Al_2O_3.3CaSO_4.32H_2O$ *(Equation 8.)*
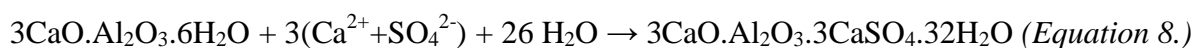
In presence of alkaline (Na$^+$ or K$^+$), the same system is described following the chemical equation:

$3CaO.Al_2O_3.6H_2O + 3(2Na^++SO_4^{2-}) + 3Ca(OH)_2 + 26H_2O$

$$\rightarrow 3CaO.Al_2O_3.3CaSO_4.32H_2O + 6(Na^++OH^-)\ \textit{(Equation 9.)}$$

If monosulfate is the aluminum source a similar chemical equation may be written (3CaO.Al$_2$O$_3$.CaSO$_4$.12H$_2$O) (Le Bescop and Solet, 2006).

During a sulfate attack, the ettringite precipitation, due to the stability of this phase, is the predominant phenomenon (Damidot and Glasser, 1993). Ettringite is sometimes associated with the deterioration of the cementitious material bonded to an expansion mechanism.

147

However, the precipitation of ettringite may not be expansive and it is necessary to emphasize that the presence of this compound in the concrete is not automatically a sign of aggression (Escadeillas and Hornain, 2008).

The AFGC-RGCU working group (AFNOR 2004) defines three categories of ettringite: 1) Primary ettringite which is the formation product of the reaction between the C3A of the clinker and the gypsum. This mineral does not alter the cementitious material if it is gypsum. In case of an overdose, there is a risk of delayed ettringite formation (DEF); 2) Secondary ettringite which is derived from the reaction with external sulfates. This generates ettringite expansion phenomena on concrete, heavily altering it by replacing the primary mineral phases (cracks and porosity opening); 3) Secondary ettringite causing no expansion phenomena. This phenomena result from dissolution / precipitation. The ettringite is formed in the cracks or the porosity generated by ettringites of the second type.

**There are numerous experimental works on the sulfate attack. The objective is to identify the behavior of the cementitious materials used in contact with solutions at different concentrations of sulfates.**

In an experimental system similar to the system used by Badouix (Badouix, 2000), Planel (Planel et al., 2006) immerges an OPC cement paste disk with a w/c of 0.4 in a solution of $Na_2SO_4$ at 15 mmol / L at 25 °C (equilibrium concentration with the same COX argillite). The solution is maintained at pH 7 throughout the duration of the test through regulation by nitric acid when the pH exceeds the setpoint (Figure 5.5.10).
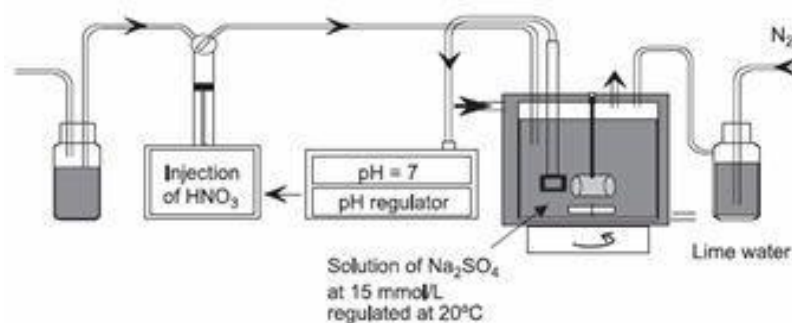


*Figure 5.5.10. Experimental device of a sulfate attack experiment on a cement paste (Planel et al., 2006).*

These works highlight a zonation in the degraded zone after 12 months of interaction with sulfates (15 mmol/l) (Figure 5.5.11):

- Zone 1 (from the surface until 0.9 mm in depth): zone composed by ettringite and C-S-H with a low C/S ratio.
- Zone 2 (from 0.9 mm until 1.3 mm in depth): zone composed by ettringite, gypsum and portlandite.

The degraded thickness changes proportionally to the square root of time, which shows a control by diffusion processes. The calcium leaching rate in this type of environment is similar to that in pure water. Zone 2 (+ gypsum + portlandite ettringite) is highly cracked.
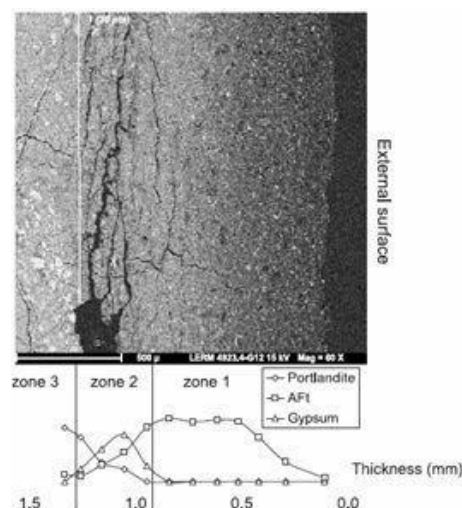
*Figure 5.5.11. SEM picture and XRD profile of a cement paste altered for 1 year in a Na2SO4 solution (15 mmol/L) (Planel, 2006).*

A study very similar to that of Planel was conducted by Le Bescop (Le Bescop and Solet, 2006). In this study, the sulfate concentration in the attack solution is reduced: 10 mmol/L of Na2SO4 (similar to the concentration in the Toarcian or the Callovo-Oxfordian clayey rock). The experiments are performed on two cement pastes: a portland cement paste rich in C3A and a SRPC-type (Sulfate Resisting Portland Cement) portland cement paste with a very low C3A content.

The mechanisms for the two types of materials and the disturbed depth are very similar (Figure 5.5.12). In the two cases, precipitation of ettringite, gypsum and dissolved portlandite are identified. The major difference is the amount of precipitated phases, which is much larger for the OPC paste rich in C3A compared to the SRPC OPC paste, particularly for the gypsum precipitation.
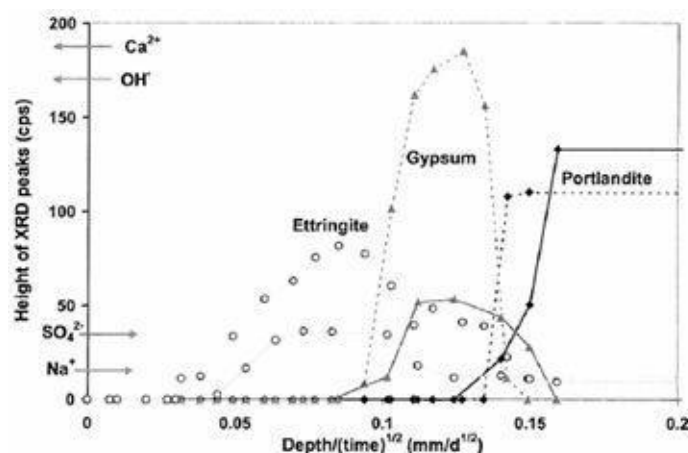


*Figure 5.5.12. Mineralogical distribution in the calcium depleted zone of OPC cement pastes immerged in a solution of Na2SO4 (10 mmol/L) (dotted lines: OPC rich in C3A, full lines: OPC/SRPC-type) (Le Bescop et al., 2006).*

In order to understand the behavior of the Portland cement-based materials in very aggressive environments, Maltais (Maltais et al., 2004) carried out leaching tests in solutions rich in sulfate (Na2SO4 = 50 mmol/l) on Portland cement pastes (w/c = 0.4 and 0.6). The experimental setup consists of placing a first sample in unsaturated conditions: one half of the

149

sample is immersed in the solution and the other half is exposed to the gas overhead (nitrogen atmosphere + 65% relative humidity). Another sample is completely immersed in the solution (saturated test) (Figure 5.5.13).
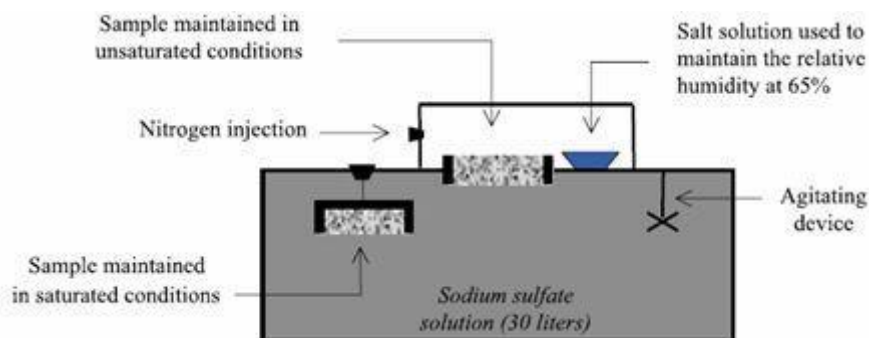


*Figure 5.5.13. Experimental device used for the alteration solution (Na2SO4 = 50 mmol/L) in saturated and unsaturated solution (Maltais et al., 2004).*

In this second test, the precipitations of ettringite and gypsum are observed in all samples exposed to the sodium sulfate solution. The analyses are carried out by SEM and microprobe, and show a systematic band of sulfur enrichment in the material. The influence of the w/c is demonstrated. To increase the durability of the cementitious material vis-à-vis the chemical attack, it is necessary to use a as low as possible w/c ratio. After 3 months of degradation, the calcium leaching front extends between 1 and 1.2 mm for a w/c of 0.4.

Recently, exposures of concretes with additions (Liu et al., 2012) to solutions charged with sodium sulfate have also been studied. For cements with additives, in particular fly ash, intense changes were noted after only 3 months.

*Evolution with multi-ionic solutions containing sulfates*

Attack by sulfates is often linked to sea water attack, where sulfate concentrations are substantial, as well as chlorides, carbonates and magnesium. The first recorded test of concrete resistances in seawater was carried out by Vicat in 1812 (Candlot, 1897). Candlot discusses and highlights the great synthesis work by Thurninger and Viennot on the observations carried out on mortar specimens immersed in La Rochelle harbor (France) since 1856. These tests were performed on several cement-based mortars (Ponilly, Vassy...) with pozzolan. Candlot wrote about the results: "Almost all specimens have lost their cohesion after a shorter or longer period. Only a few specimens have been characterized on the whole, and the English cement-based mortars, Portland cement from Dauphiné and Portland cement from Boulogne remained in very good condition."

In 1891, Michaelis (Michaelis, 1897) published a study entitled "The influence of sea water on the hydraulic binders-based materials." In order to identify the evolution of different mortars, Michaelis manufactured several synthetic sea water-based solutions of sodium chloride, magnesium sulfate, magnesium chloride and calcium sulfate. Through macroscopic observations and mechanical characterizations, he highlighted the influence of the type of cement used on the resistance to seawater.

If sulfate attack is one of the main mechanisms of concrete degradation in seawater, it is certainly not the only one. To sulfate attack one must add carbonation, leaching, and attacks by chlorides and magnesium. Excluding extreme cases like the Caspian, Dead, and Red Seas

(very high salinities), and the Baltic Sea (low salinity), the salinity of the oceans and seas on the planet varies between 30 and 36 g/L, imposing a very high concentration of chloride ions.

Concrete structures built in a marine environment are subject to a number of areas of degradation as Mehta shows (Mehta, 1986). There is the zone of sea spray (no direct contact with sea water), followed by the spray zone (above the high tide level, subject to splashing waves), the tidal zone (subject to the sway of the tides), and the permanent immersion zone. It is particularly the latter type of environment that interests us here.

Moskvin (Moskvin et al., 1980) suggests a scheme of the preferential localization of the multi-ionic attack to which a concrete structure continuously immerged in seawater is subject (Figure 5.5.14).
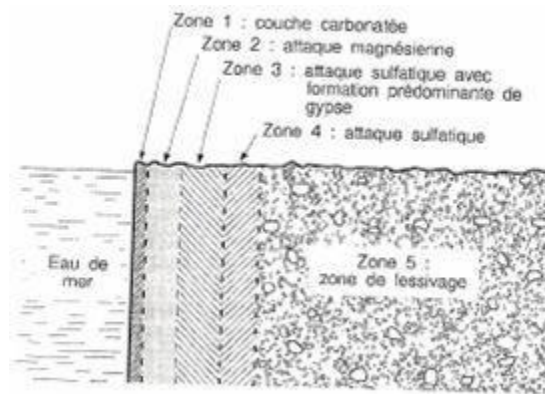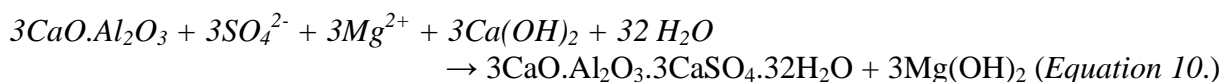


*Figure 5.5.14. Scheme of the different zones in the cement paste after immersion in sea water (Moskvin et al., 1980).*

The system is described in five separate zones, where 4 are characteristic of various degrading mechanisms: zone 1 results from the action of carbonate on the concrete, zone 2 from the attack by magnesium, zones 3 and 4 from the attack by the sulfate ions and finally zone 5 which is subject to single leaching. It appears that the ion action is not cumulative. The aggressiveness of sea water seems to be lower than that of sulfated water. According Regourd (Regourd et al., 1976), the carbonation within the framework of a multi-ionic attack can provide a beneficial effect on the stability of the concrete, later confirmed by, among other studies, Kurashige (Kurashige et al., 2007) who highlighted the precipitation of a carbonated layer, with a low porosity, at the surface of the cementitious material.

Escadeillas and Hornain (Escadeillas and Hornain, 2008) emphasize the influence of the cation associated with the sulfate in the intensity of the concrete alteration. In the case of a combination with magnesium during the attack, the magnesium is substituted for the calcium of the portlandite to form brucite and the calcium reacts with sulfate to form gypsum or ettringite. Gypsum being very soluble, ettringite formation is more likely in the presence of an aluminate phase (C3A, to illustrate, is selected from the following chemical equation).

$$3CaO.Al_2O_3 + 3SO_4^{2-} + 3Mg^{2+} + 3Ca(OH)_2 + 32\ H_2O$$
$$\rightarrow 3CaO.Al_2O_3.3CaSO_4.32H_2O + 3Mg(OH)_2\ (\textit{Equation 10.})$$

When all the portlandite is consumed to form gypsum and brucite, the C-S-H phase is degraded by the formation of brucite and gypsum, but also by that of M-S-H (hydrated magnesium silicate):

$$C\text{-S-H} + Mg^{2+} + SO_4^{2-} + 2H_2O \rightarrow Mg(OH)_2 + CaSO_4.2H_2O + (C,M)\text{-S-H} \ (\textit{Equation 11.})$$
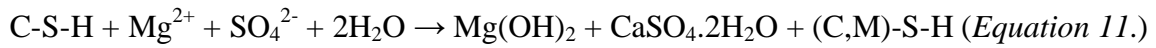
Several studies have been made on the action of magnesium sulfate (Brown and Badger, 2000; Brown and Doerr, 2000; Brown and Hooton, 2002; Brown et al., 2003). The tests and the results are discussed in the section dedicated to examples of experimental work on multi-ionic attacks. These tests are carried out with solutions containing small amounts of CaSO4 similar to those found in the groundwater and not in marine environments (from 1 to 15 mmol/l).

The action of chlorides on the concrete is relatively well known. The degradation mechanisms involved can be summarized as follows:

- The attack by sodium or potassium chloride solution leads to leaching of the portlandite and C-S-H and to precipitation of the calcium monochloroaluminate (source of Al: aluminum hydrate, calcium monosulfoaluminate for example)

- Under the form of $MgCl_2$, the mechanisms are identical plus Brucite precipitation.

Moranville (Moranville et al., 2004) and Kamali (Kamali et al., 2008) immerge a set of OPC cement pastes with different w/c ratios for 114 days in one liter of solution of Ca (11.5 mg/l) Mg (8 mg/l), Na (11.6 mg/l), K (6.2 mg/l), Cl (13.5 mg/l), SO3 (8.1 mg/l) and HCO3 (71 mg/l) to a pH equal to 7, to generate a multi-ionic attack representative of groundwater. The solution and the sample are placed in a container and a thermostatic chamber at 26°C. The solution is renewed continuously with a 1 l/day flow rate.

The results obtained in this experiment are compared with tests in pure water. The difference in behavior is very significant. In pure water under the same conditions, the material was decalcified about 1.5 mm. In synthetic groundwater, as observed previously in the attack by carbonated solution, the decalcification is limited to the extreme cement paste surface. The authors explain this by the beneficial effect of carbonation due to the development of a protective layer. Calcite microcrystals cover the sample surface and reduce the porosity of the material, thus reducing the diffusion of aggressive ions. A decrease in the sulfur content is recorded on the cement paste surface.

In other studies (Brown et al., 2002; Brown et al., 2003), samples from California homes were immerged in solutions of MgSO4 at different concentrations (50 mg/L) for a period of 21 years as part of a study on the resistance to sulfate of slag cement. The temperature ranged between 16 °C and 30 °C.

Precipitations of brucite, M-S-H, ettringite and thaumasite can be observed (Figure 5.5.15).

Gypsum and brucite precipitation from Portlandite:

$$Ca(OH)_2 + Mg^{2+} + SO_4^{2-} + 2H_2O \rightarrow CaSO_4.\ 2H_2O + Mg(OH)_2 \ (\textit{Equation 12})$$
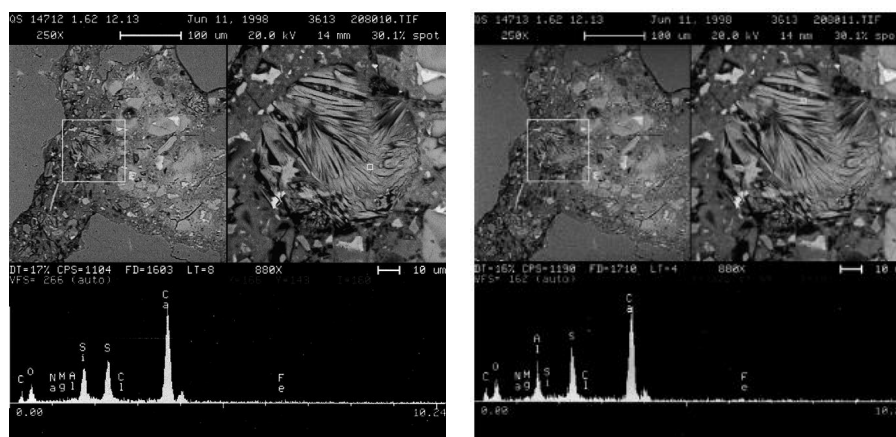
*Figure 5.5.15. SEM pictures and EDS spectra of thaumasite (left) and ettringite (right) precipitations in concretes placed in a sulfate-rich environment (Brown et al., 2002)*

Ettringite precipitation conditions have been discussed previously. The reactant path leading to the precipitation of Thaumasite is:

1- dissolution of portlandite
2- gypsum precipitation (or ettringite)
3- decalcification of C-S-H
4- ingress of carbonates and thaumasite precipitation ($CaO.SiO_2.CaSO_4.CaCO_3.14H_2O$).

The thaumasite precipitation is known to occur in cold climates ($< 15$ °C). However, the tests conducted here indicate precipitation at temperatures around 23 °C. These formations generate an intense swelling in the cement matrix and cause it to break up.

In the domain of multi-ionic attacks, the study of the cement matrix degradation by rainwater and sulfated waters can also be cited (Albert, 2002). The protocol used for studying sulfate attack is similar to the work of Le Bescop and Solet (Le Bescop and Solet, 2006) and Maltais (Maltais et al., 2004), with the preparation of Na2SO4 aggressive solutions. It also highlights the gypsum precipitation in the veins of the material and non-expansive secondary ettringite.

*Studies with multi-ionic solutions representative of rock porewaters*

Since 2010, with the development of deep radioactive waste disposal projects, some new projects have been carried out. The goal is to try to understand the possible physico-chemical evolution of cementitious materials immerged in synthetic or natural rock porewaters.

Two studies in particular may be cited. Firstly the studies by Garcia-Calvo (Garcia Calvo et al., 2010 and Garcia Calvo et al., 2013) focusing on the chemical durability of a low-pH cementitious material in granitic water from the Aspö site (Sweden). After 14 months of interaction, the results show good strength of the cementitious materials. An alteration front is still observed at the surface in all samples. In concretes containing fly ash, magnesium incorporation is detected in the C-A-S-H matrix, composing the starting material, as well as ettringite.

In the second study (Dauzeres et al., 2014), a comparison is made between the different physicochemical changes in two cement pastes: an OPC-type and a low-pH-type. The two cement pastes were immerged in a solution representative of porewater of Callovian-Oxfordian clayey rock respecting the partial pressure of CO2. The results show a chemical

and mechanical destabilization of low-pH material through intense decalcification of C-S-H to the amorphous silica stage, carbonation in the material, and M-S-H-type magnesium silicate precipitation (Figure 16). The OPC cement paste perturbation is lower due to the formation on the surface of an exogenous Mg-calcite crust already observed in previous studies. This crust clearly protects the material from leaching and sulfate attack.
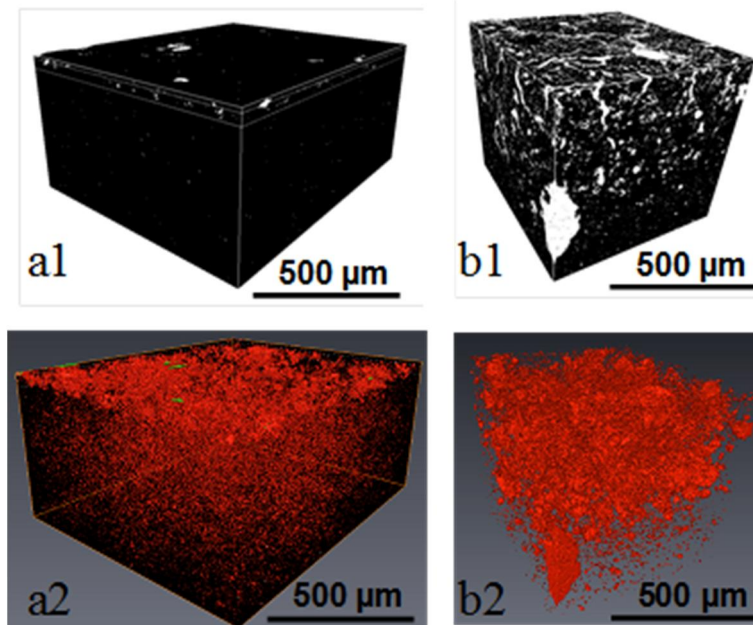


*Figure 5.5.16. Comparison of the macropore networks between CEM I and low-pH cement paste after 5 months in COX solution (COX solution put in contact with the top face of the samples). Based on the microtomography analyses: a1) The macroporosity in the CEM I cement paste defined by image analysis; a2) 3D view of the macroporosity network in the CEM I cement paste; b1) The thresholded macroporosity in the low-pH cement paste; b2) 3D view of the macropore network in the low-pH cement paste (Dauzeres et al., 2014).*

**Cementitious materials immerged in a more or less sulfate-rich solution are exposed to heavy precipitation linked mainly to the ettringite and gypsum precipitation. The sulfate attack generates, as in the case of the attack in pure water or carbonated water, the leaching of the calcium hydrates composing the cementitious matrix: dissolution of the portlandite and decalcification of C-S-H. In natural systems, the presence of sulfate is often associated with an aggressive cation. In the presence of magnesium, the degradation is very high: brucite, ettringite, M-S-H (non-binding phase) and gypsum precipitation. In the case of an association with carbonates, possible thaumasite precipitation is added to the usual mechanisms; thaumasite is a very harmful mineral species for the cohesion of concrete (break-up).**

**This synthesis offers important information about the behavior of cementitious materials based on portland cement in sulfate environments: the sulfate concentration in the aggressive solution does not need to be high (10–15 mmol/l) to precipitate gypsum and ettringite or damage the material. The precipitation of ettringite is not systematically synonymous of mechanical alteration. Finally, a multi-ionic attack, with sulfates, does not necessarily generate a very significant degradation. This synthesis highlights some studies showing that the deterioration in seawater (multi-ionic environment) causes less degradation than a pure attack by sulfate ($Na_2SO_4$) to**

concentrations equivalent in sulfates. In studies of interactions with groundwater, with compositions close to the solution of the COX, carbonation is characterized by the development of a dense surface layer, composed of calcite microcrystals, which greatly limits the action of other aggressive species and thus plays a role in protecting the material. Sulfate attack, carbonation and magnesium attack are all processes that may occur in the concrete/clay system. The issue of identifying and studying their influence is at the heart of the present work.

Finally, some studies on representative solutions of environments encountered in future geological disposals, mainly in clayey-type rock, show that some cementitious materials, including those with siliceous additions to achieve so-called "low pH" cements, may present a chemical fragility that can lead to substantial mechanical disturbances in contact with this type of environment; in contrast, OPC-type materials seem to be very stable in this type of environment due to the development of a protective exogenous carbonate layer. However, one must not forget that this type of test is not necessarily representative of the direct contact (interface) with the materials tested. Studies at the interface between the cementitious materials and the clayey rock must be compared.

## Geochemical and microstructural evolution of cementitious material in contact with clayey rock

*Experiments*

The experiments carried out on the physico-chemical evolution of cementitious material in contact with argillaceous rocks try to reproduce the aging of structures such as might occur in the natural environment. Almost all studies are conducted in order to characterize the mechanisms involved in the storage of radioactive waste in deep geological layers.

Until the mid-2000s, work on concrete/clay interfaces was mainly dedicated to the study of the clayey rock's reactivity vis-à-vis the alkaline plume in order to qualify the clayey rock for disposal. Over the past ten years, with the precision of disposal concepts, new research has sought to also study the physical and chemical behavior of cementitious materials in this type of environment.

In the early 2000s, the first series of experiments conducted on the development of cementitious materials in contact with a clay material were performed by Read (Read et al., 2001) in the HADES Underground Research Laboratory (Mol, Belgium) over periods of 12 and 18 months. The laboratory is located at 220 m depth in the formation of Boom Clay. Seven formulations of cementitious materials are tested: portland cement; portland cement and fly ash; portland cement and slag; cemented ion exchange resins; aluminous cement paste; cemented waste from research reactors; gallery filling mortar (reference NIREX (UK)). Each sample is stored for 28 days at 20 °C. Manufactured cylinders are then deposited in holes between 4.5 and 5 m in distance from the wall of the gallery.

Tests are carried out at temperatures of 25 °C and 85 °C. Some of the samples are taken after 12 months of interaction and the remaining ones after 18 months. Each sampling allows the extraction of a cement paste/Boom clay interface. The portland cement samples show a considerable deterioration after 12 months of interaction as well as the clay in contact. At 85 °C, well-defined zonation appears on each side of about 100 microns to 250 microns-depth from the interface (Figure 5.5.17):

- Zone I: non-degraded clay (quartz, illite, smectite, mixed-layer, chlorite, feldspar).

- Zone II: altered clays, decreasing concentrations of Al, Si and Mg and calcium enrichment.

- Zone III: altered cement, calcium concentration decrease and enrichment of Mg, S, Al and Si.

- Zone IV: unaltered cement paste.

Precipitation of Si-Mg and Al-Mg gels were identified in the cementitious material in the first ten microns, as hydrotalcite, and sepiolite.
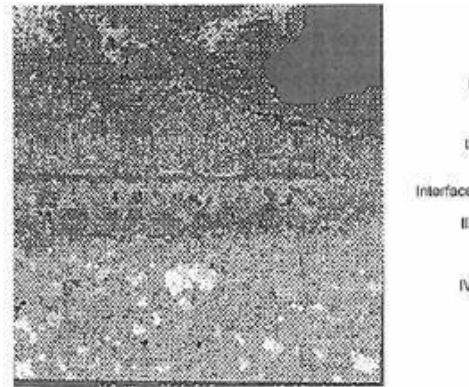


*Figure 5.5.17. Elementary mapping of calcium distribution in a portland cement-based material (Read et al., 2001).*

Research has focused on the aging of OPC-type concrete with limestone additions in contact with the Toarcian argillite Tournemire (Aveyron, France), an argillite composition that is very close to the argilite of the Callovo-Oxfordian (Bonin et al., 1998). Exploratory drilling in the 1990s was resealed with CEM II cement pastes and concrete under environmental conditions imposing a saturated area. After 15 years of interaction, the interfaces were over cored. The transformations are significant (Tinseau et al., 2006): precipitation of gypsum to the interface, punctual observation of Na-zeolite (morphologically observed by SEM and analyzed by EDS), that is questionable, precipitation of calcite and dolomite. As the cementitious material in this study was not really characterized out of the contact area, two new studies on these contacts were carried out: isotopic fractionation around the interface (Techer et al., 2012) and evolution of the microstructure (Gaboreau et al., 2011).

With the isotopic technology including the 87Sr/86Sr, it is clearly shown the material thicknesses affected by the disturbed clay. Thus the changes in the cementitious material reach up to 10–15 mm deep after 15 years. These transformations are mainly calcite formation, dissolution of the portlandite and partial decalcification of C-S-H. These mineralogical changes cause a porosity opening in the cementitious material which is perfectly characterized by autoradiography. Carbonation is very low compared to decalcification (Figure 5.5.18). These results were confirmed a few years later on older interfaces (20 years), where the same mechanism causing the same evolution of porosity was observed (Bartier et al., 2013), as well as on concrete placed in contact with the Mont Terri argillite (Jenni et al., 2014).
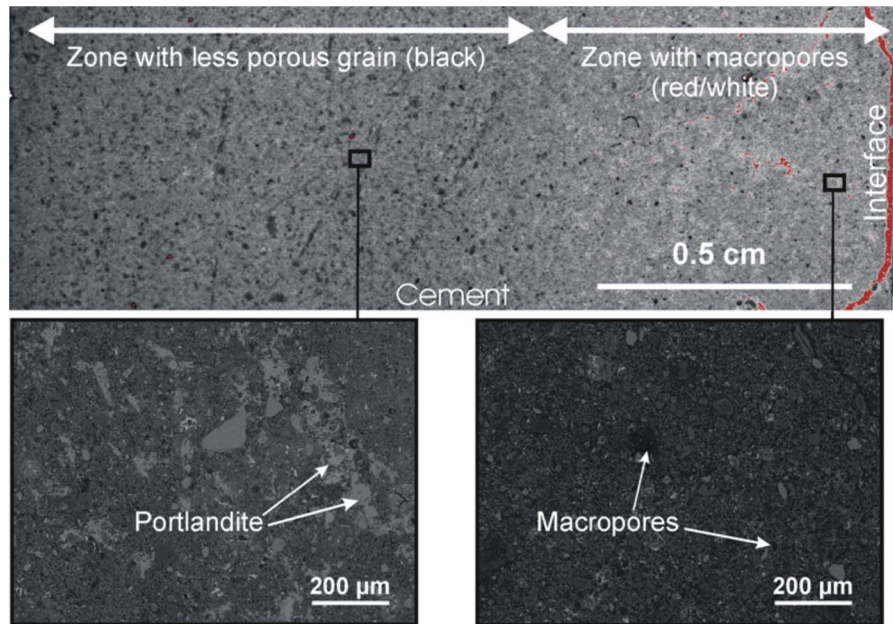
*Figure 5.5.18. Porosity map of cement paste obtained by autoradiography (top) and BSE-SEM images (bottom).*

Yamaguchi (Yamaguchi et al., 2009) also presents results of characterizations of argillite/concrete from Tournemire interfaces. In addition to the findings of Tinseau et al, it appears that the nature of the carbonates precipitated at the interface is threefold: aragonite, calcite and vaterite. The authors state that the precipitation of these minerals is observed on both sides of the interface, as is the precipitation of C-S-H and ettringite. Contrary to the work of Tinseau, there is no precipitation of zeolites, while the observed interfaces are the same.

Fernandez (Fernadez et al., 2006), in addition to bentonite disturbance tests with alkaline fluids, performed tests at the interfaces between the FEBEX bentonite and OPC-based mortar (w/c = 0.45, hydrated 28 days). The composition of the mortar hydrates is: C-S-H, portlandite, AFm and AFt. The test consists in contacting a bentonite disc of 2.2 cm in height and 7 cm in diameter with a mortar disc of 0.7 cm high and 5.5 cm in diameter in a Teflon cell. A stream of alkaline solution (NaOH 0.25 mol/l) is sent from the upper base of the mortar. The fluid passing through the composite is recovered for analysis (Figure 5.5.19).
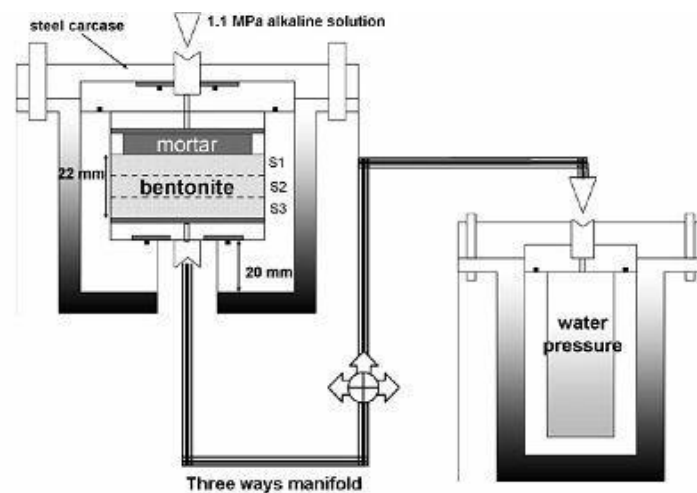


*Figure 5.5.19. Device for experiments between mortar and bentonite under pressure gradient of alkaline solution (Fernandez et al., 2006).*

157

The experimental times are 1, 6 and 12 months to test temperatures of 25 °C, 60 °C and 120 °C. Only the first few millimeters around the mortar/bentonite interface are disturbed at 25 °C and 60 °C. The disturbance is characterized by the precipitation of C-S-H and brucite. At 120°C, the degradation in the bentonite is more significant: tobermorite precipitation at the interface, then Mg-saponite up to 10 mm in the clay and also zeolites such as analcime in the rest of the material. Cuevas et al. [CUE 06], completing the synthesis of the research group on the FEBEX bentonite under alkaline conditions, present analcime and calcium phases precipitation at the interface of both materials.

The first laboratory experiments on connecting OPC hardened cement paste or low-pH (OPC + silica fumed + fly ash) paste with argillaceous rock (remolded COX argillite) in pure diffusive transport were published in 2010 (Dauzeres et al., 2010; Dauzeres, 2010). These experiments are carried out at 25 °C and 50 °C and show the same mechanisms as those previously observed for portland cementitious materials: very low carbonation, decalcification creating opening of macropores, precipitation of non-destructive ettringite… However, concerning the low-pH hardened cement paste, Si-Mg phases are identified inside the cementitious material in contact with argillite, as was observed for the same materials immerged in the synthetic COX pore solution (Dauzeres et al., 2014) and was observed a few years later on low-pH/Opalinus clay interfaces from the Mont Terri Underground Research Laboratory (Dauzeres et al., 2016) (Figure 5.5.20). However, the impact of the magnesium perturbation on the low-pH cement paste matrix in contact with a clay material is incomparable with what had been observed under water: the matrix presents no particular modification of the porosity or mechanical alteration.
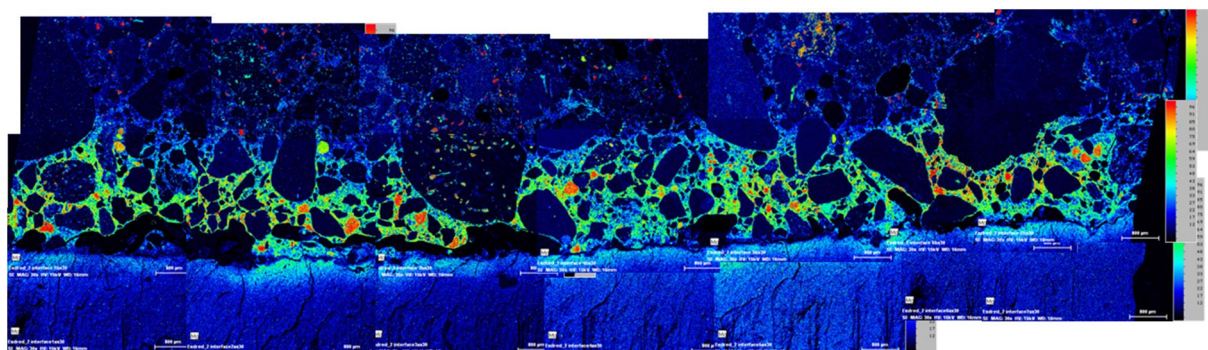


*Figure 5.5.20. SEM picture and EDS mappings of Mg and Ca at the OPA (bottom) /ESDRED (top) interface after 5 years of interaction (Dauzeres et al., 2016).*

Lastly, the origin of sulfates at the OPC/COX contact (Lerouge et al., 2014) and the influence of sulfate from argillaceous rocks (at high concentrations) (Abubaker et al., 2013) have been studied. The latter in particular to identify the precipitation or not of thaumasite in OPC subjected to temperatures ranging from 5 °C to 20 °C. It particularly highlights the influence of the composition of the clay on the precipitation of thaumasite, which in some cases forms at a temperature of 20 °C.

> **Before 2010, there were few or no representative experiments concerning concrete placed in a clayey environment in the context of deep geological disposal of radioactive waste. The number of studies exploring the physico-chemical evolution of cementitious materials has multiplied since 2010.**
>
> **At present, the numerous research results, consistent with each other, offer good understanding of the chemical and pore structure evolutions of cement placed in a clay**

**environment.**

**An OPC material is likely be exposed to two main mechanisms when systems are resaturated: leaching (portlandite dissolution and decalcification of C-S-H) and carbonation (mainly calcite precipitation). Placed in contact with clayey rocks rich in sulfates, ettringite precipitation is also likely to be observed without undergoing sulfate attack that would damage the structure. These chemical changes seem to cause a slight porosity opening but no mechanical altering of the cementitious material.**

**The low-pH materials (based on OPC and siliceous additions), of which there are currently numerous formulations still approved by the Waste Management Organization, seem to present very similar behaviors whatever their formulation. The three main mechanisms governing the chemical system seem to be: decalcification of CSH, carbonation, and magnesium disturbance. Although the perturbation does not cause any mechanical damage when this type of material is put directly in contact with clayey rock, one must keep in mind the very poor chemical and mechanical behavior of this material when the clayey rock is substituted with its synthetic pore solution (Part Impact of aqueous ionic or multi-ionic aggressive environments on the physical-chemical evolution of cementitious materials).**

**Despite the real progress made over the past 5 years concerning the knowledge of the chemical and microstructural evolution of cementitious structures in a clayey environment, several issues remain to be investigated: What is the impact of chemical and microstructural changes on the mechanical behavior of the structure? What are its properties of transport? Are the reaction mechanisms identical for temperatures above 60 °C (a temperature likely to be encountered in the course of the future geological disposal)?**

## Numerical simulations

The literature review on modeling works reproducing the concrete/clay interfaces has multiple objectives. The first is to identify all the necessary input data to models. The second objective is to identify the physico-chemical mechanisms associated with different models. The general objective of course is to identify the possible chemical evolutions of the cementitious material, planned by the thermodynamic databases, when the cement is placed in contact with a clayey rock.

This part of the state of the art review refers only to models having been made on interfaces between cementitious materials and clayey rock. All the simulations are obtained from computer codes coupling chemistry (based on thermodynamic equilibria sometimes with the inclusion of kinetic data including dissolution) and diffusive transport.

Like the section devoted to experimental tests, this section is organized according to the type of environment (or material) placed in contact with the cementitious material.

Trotignon works on two types of models (Trotignon et al., 2006; Trotignon et al., 2007). The objective of the first model is to simulate the evolution of two interface types after 25,000 years: i) OPC/argillite; ii) CEM V/argillite. The geometry of the system is modeled in 1D: 5.5 m of concrete are put in contact with 12 m of argillite (Figure 21). It is noteworthy that another modeling conducted here consists of simulating the evolution of the same concrete in direct contact with the porewater solution (without argillite).
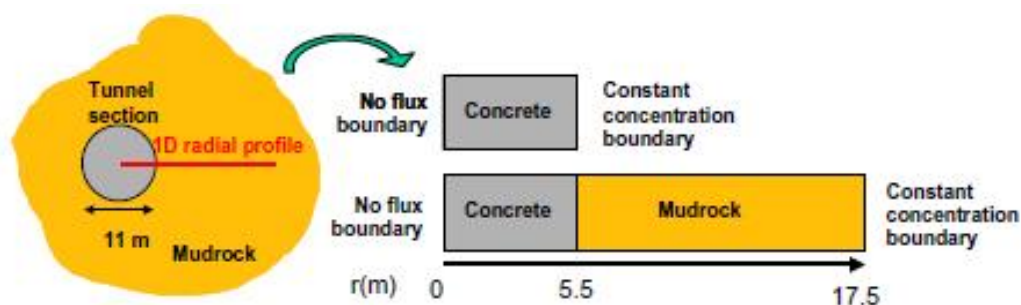
*Figure 5.5.21. Representation of a waste disposal cell (left) and the 1D geometry used for the modeling of concrete/water interactions and the concrete/argillite interface (Trotignon et al., 2006).*

For the OPC concrete, the mineralogy is: portlandite, jennite, ettringite monosulfoaluminate, hydrotalcite. The mineralogy of the argillite considered in this study is: quartz, calcite, illite, montmorillonite, Ca, kaolinite. The uncertainty of the solution sulfate levels forced the author to offer each simulation two types of solutions in argillite: first with 10 mmol/l of sulfate and a second with 25 mmol/l sulfate. All simulations are performed with the chemistry of the reactive transport code HYTEC (Van der Lee et al., 2003). The results are shown in Figure 5.5.22.
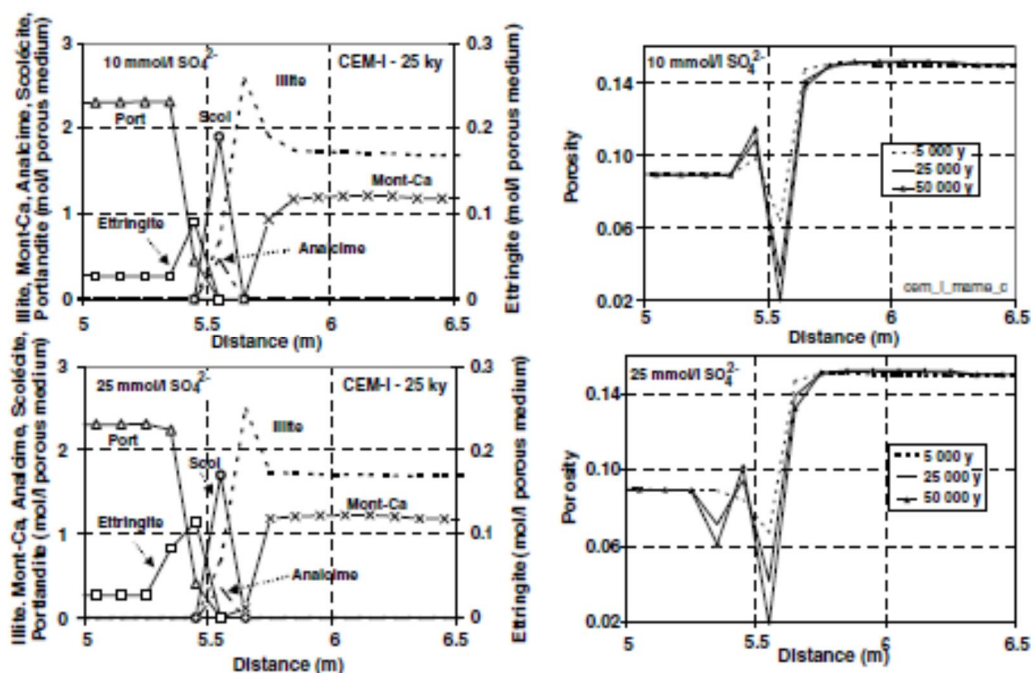


*Figure 5.5.22. Numerical simulations after 25,000 years of a CEM I concrete in contact with the argillite at 25 °C (Trotignon et al., 2006).*

Simulations after 25,000 years for the OPC material in contact with argillite predict portlandite dissolution and ettringite precipitation in the cementitious material (more intense with 25 mmol/l of $SO_4^{2-}$). In both cases, two zeolites are formed in the argillite: scolecite and analcime. The alteration of argillaceous phases results in the dissolution of montmorillonite and precipitation of illite. The formation of zeolites at the interface causes the abrupt drop in porosity, reflecting a blockage. In the cementitious material, it is clear that the precipitation of ettringite has some impact on the porosity. However, the opening of the porosity is higher on the side of the cementitious material.

The CEM V material presents a deeper disturbance, with the precipitation of ettringite and brucite along the interface. Zeolites are always present (scolecite) and precipitation of Na-montmorillonite is present at the interface. In another study, Trotignon (Trotignon et al., 2007) perform the same simulations, but over a much longer time (up to 100,000 years) (Figure 5.5.23).
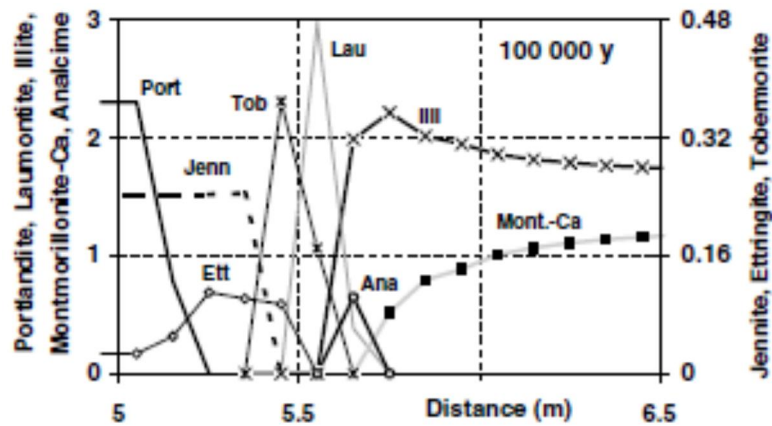


*Figure 5.5.23. Results of an OPC / argillite interface simulation after 100,000 years (Trotignon et al., 2007).*

The cementitious material in these conditions undergoes a decalcification which results in the dissolution of portlandite and jennite and in the precipitation of a C-S-H with a lower C/S ratio: tobermorite. The sulfate ingress in the material causes precipitation of ettringite. Two zeolites are formed on the surface of the argillite: analcime and laumontite. The illitization of the illite/smectite mixed-layer continues. Note that tobermorite is also formed on the surface of the argillite.

The ALLIANCES simulation platform was used to simulate the evolution of gallery disposal, including concrete/clay interactions, in deep geological rock (Montarnal et al., 2007). These simulations are performed with a 2D system with 3 materials: argillite / concrete / bentonite (Figure 5.5.24).
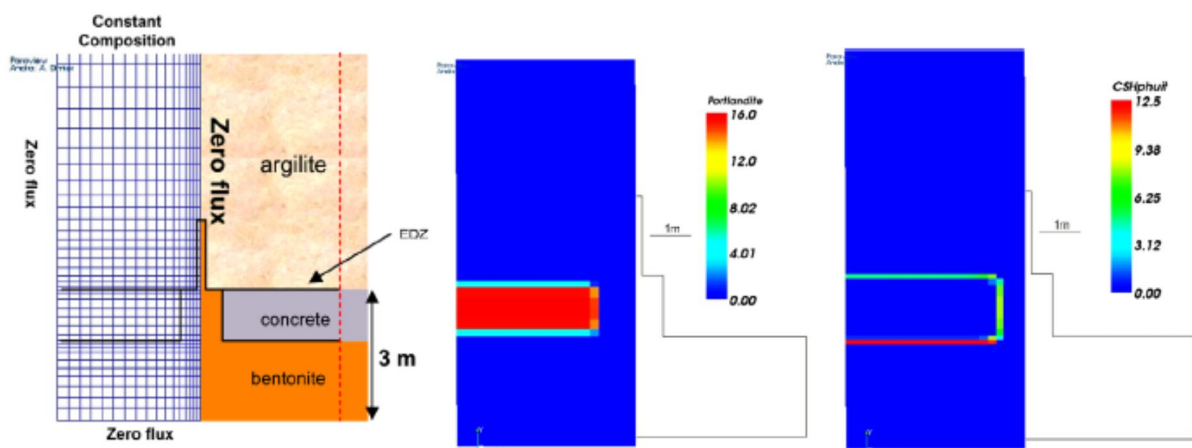


*Figure 5.5.24. Geometry of the bentonite/concrete/argillite interfaces system and of the associated meshing considered (left), portlandite (center) and C-S-H 0.8 (right) evolutions after 100,000 years of interaction – calculations carried out with the ALLIANCES reactive transport code (Montarnal et al., 2007).*

161

After 100,000 years, the dissolution of portlandite and precipitation of C-S-H with a C/S ratio = 0.8 is simulated. The dissolution of the portlandite is similar on both interfaces of the cementitious material. The C-S-H precipitation is more pronounced for contact with bentonite.

Other numerical simulations of argillite/concrete interactions are made with argillites of the Tournemire site (De Windt et al., 2004; 2008; Yamaguchi et al., 2009). De Windt, using the HYTEC code, carried out simulations over 1,000, 10,000 and 100,000 years. The considered concrete is an OPC whose mineralogical composition after hydration is: C-S-H (C/S = 1.8), portlandite and ettringite. The argillite is represented by a mineral assemblage: illite, smectite, dolomite, calcite. In these simulations, the authors consider two assemblages on the clay mineralogical phases:

- Hypothesis 1: The illite evolution is controlled by the thermodynamic equilibrium and the smectite precipitation is not allowed.

- Hypothesis 2: The illite and the smectite are involved at thermodynamic equilibrium.

The results show clearly that the pH at the interface is buffered to 11.5. The extension of the alkaline plume depends on the hypothesis used. With the first hypothesis (Figure 5.5.25), C-S-H (C/S = 1.1) and brucite abundantly precipitate at the interface. The dolomite dissolution and the calcite precipitation are results observed by Adler (Adler et al., 1999).

For the second hypothesis of calculation, zeolites are formed. Scolecite is the thermodynamically most stable zeolite for this calculation, whereas the most experimentally observed zeolites are phillipsite and analcime. Zeolites at the interface are less stable than the C-S-H, because of the high pH and high calcium concentration. Sepiolite is more stable than brucite and precipitates at the interface.
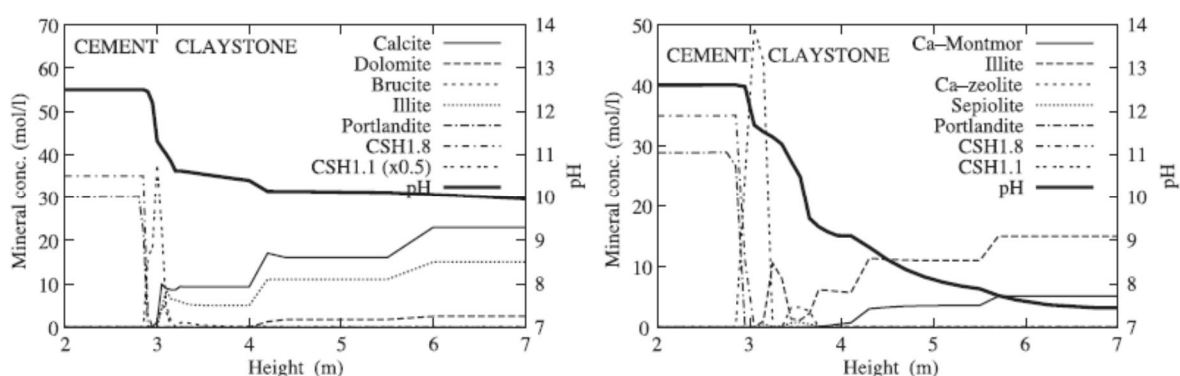


*Figure 5.5.25. Profiles of the mineralogical perturbations and the pH after 10,000 years at the concrete/argillite depending on the hypotheses chosen: hypothesis 1 (left) hypothesis 2 (right) (De Windt et al., 2004).*

To reproduce the interactions observed in the Tournemire Underground Research Laboratory (Tinseau et al., 2006), numerical simulations are performed on the concrete/clay interfaces over a period of 15 years (De Windt et al., 2008) using the HYTEC code. First, calculations are performed at the thermodynamic equilibrium, then with the kinetics of dissolution and precipitation in a second time. The authors compare the results at thermodynamic equilibrium with those taking into account the kinetic by separating the main mineral phases from the minor phases by first processing the evolution of the cementitious material and the argillite (Figure 5.5.26). The nature of the main phases precipitated or dissolved is the same with or without kinetic data. Concrete undergoes a leaching of portlandite and of C-S-H. A new C-S-

162

H with a lower C/S ratio is formed at the interface, accompanied by carbonation. The zone at the interface is in equilibrium with C-S-H and calcite. Argillite is exposed to dissolution of the clay phases (mainly montmorillonite). The main effect observed when the kinetics is taken into account in the calculations is the smoothing of the mineralogical fronts. Based on the model, the thickness of the degraded cementitious material after 15 years is approximately 5 mm, when using the portlandite dissolution as a marker for degradation.
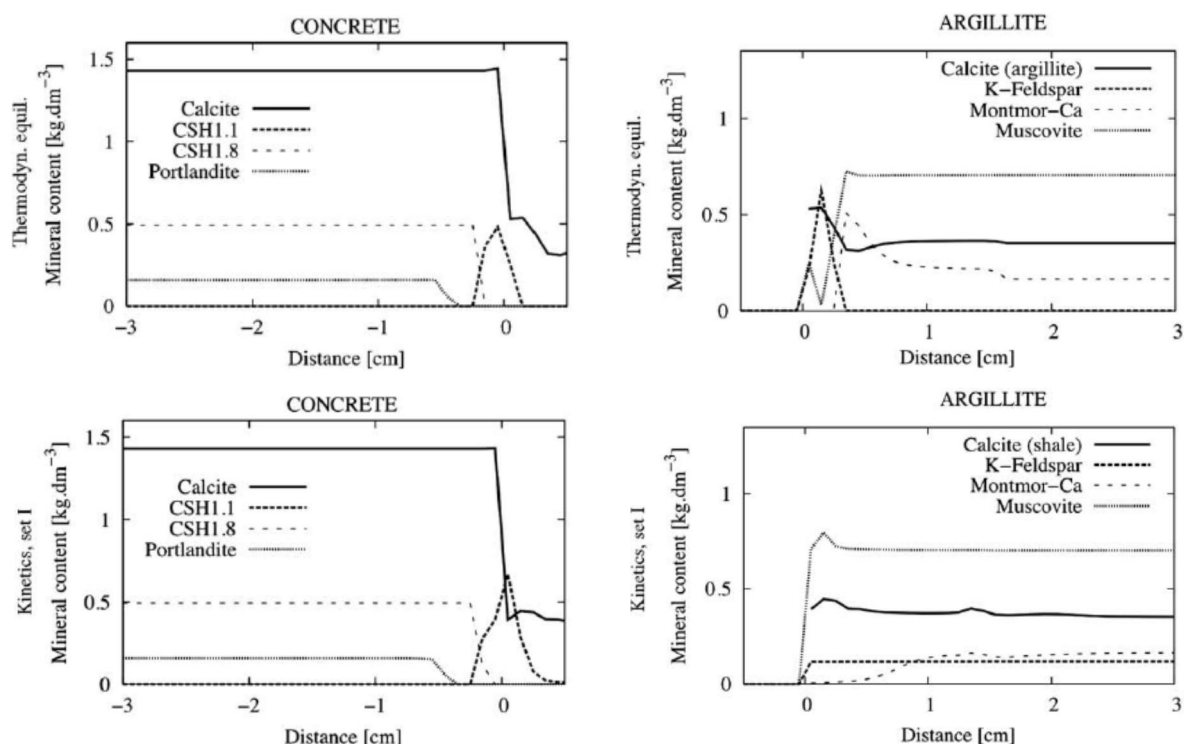


*Figure 5.5.26. Mineralogical profiles modeled of the main phases for a concrete/argillite interface after 15 years of interaction in the Tournemire URL; calculation at the thermodynamic equilibrium compared to the calculations with the kinetic data (De Windt et al., 2008).*

The experimental results on the concrete/Tournemire argillite interface are also subject to other comparisons with numerical simulations (Yamaguchi et al., 2009). This work is done with the reactive MC-BENT transport code (Yamaguchi et al., 2007). The geometry of the system considered in 1D is 5.5 cm of concrete in contact with 5.5 cm of argillite. The results on the main phases are similar to those reported previously. The interface is dominated by the precipitation of C-S-H and calcite (Figure 5.5.27).
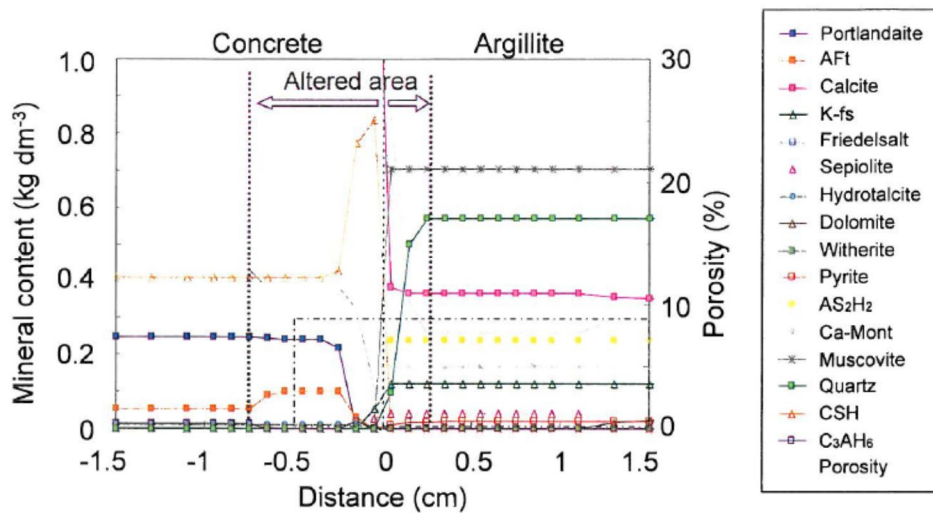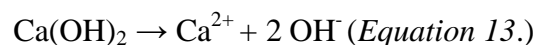
*Figure 5.5.27. Simulation result of a concrete/Tournemire argillite interface after 15 years of reaction (Yamaguchi et al., 2009).*
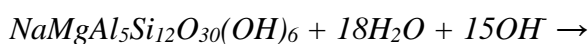
Please note that the author does not discriminate C-S-H according to their stoichiometry in this work, which makes it difficult to quantify the decalcification of concrete. The cementitious material is degraded deeper than the argillite.

The portlandite dissolution and the ettringite precipitation are again highlighted. The results of this calculation still raise some questions. The alteration front in the argillite is measured relative to the quartz dissolution. It is quite unlikely to see the quartz dissolve in these conditions while other mineralogical phases are stable. In addition, the dissolution of quartz causes a significant release of silicon, which the calcium from the leaching of the cementitious material uses to precipitate C-S-H. The amount of C-S-H formed at the interface is probably overestimated, and this model is unlikely that unrepresentative of the concrete/argillite interactions.

A comparison between numerical simulation and experimental results is achieved (Read et al., 2001). Beyond simulations that lead to results close to those already presented (dissolution of montmorillonite and portlandite, calcite precipitation and porosity drop in the interface), modeling is used to explain the reactive mechanisms that occur in the tests. Initially, interstitial solutions are in equilibrium with the mineralogical assemblage of each material. After contact, the reactive processes begin: the diffusion of elements in solution caused by the concentration gradient induces sub-saturation of the system over several mineral phases. This is the case of the portlandite, which dissolves. This dissolution releases calcium into the solution and the hydroxyl ions migrate to the clay. The diffusion of these elements, combined with the distribution of sodium and potassium (initially present in the pore solution of the cementitious material), causes an increase in the pH in argillite. The presence of carbonates in the clay associated with increasing pH and the arrival of calcium ions allows the calcite precipitation as the alkaline plume moves.

$$Ca(OH)_2 \rightarrow Ca^{2+} + 2\ OH^- \text{ (\textit{Equation 13}.)}$$

$$OH^- + Ca^{2+} + HCO_3^- \rightarrow CaCO_3 + H_2O \text{ (\textit{Equation 14}.)}$$

The hydroxide excess causes the dissolution of montmorillonite:

*NaMgAl$_5$Si$_{12}$O$_{30}$(OH)$_6$ + 18H$_2$O + 15OH$^-$ →*

164

The aluminum source from the dissolution of montmorillonite may cause, in the presence of calcium, precipitation of katoite (Read et al., 2001) and/or, in the presence of sulfate, precipitation of ettringite (Trotignon et al., 2006; 2007; De Windt et al., 2004; 2008) in the concrete.

Some authors focus more specifically on the degraded thicknesses of the cementitious materials and bentonite as a function of time (Yokoseki et al., 2004) and depending on the w/c ratio used to prepare the cement paste (Figure 5.5.28). According to the model, after 100 years, the altered thickness in the concrete extends up to 2.1 cm, against 7.5 cm in the bentonite. After 2,000 years, the altered thickness in the concrete extends up to 8.5 cm, against more than 30 cm in the bentonite.

The concrete-bentonite interfaces are subject to other simulations with other tools. The CrunchFlow reactive transport tool is used for these applications (Fernandez et al., 2009). The goal is to simulate the interactions between montmorillonite FEBEX and a portland cement-based concrete tested for 1 year at 25 °C then at 120 °C in laboratory. Four cases are modeled: Case 0: test at 25 °C; Case 1: test at 120 °C; Case 2: Idem to case 1 with porosity divided by 2; Case 3: identical to case 1 by increasing the reaction constant of the bentonite to an order of magnitude. At 25 °C, the changes are limited to the clay material with the precipitation of analcime and brucite. At 120 °C, regardless of the input data, ettringite is dissolved and precipitated at slightly greater depth in the concrete, and the interface is occupied by a C-S-H phase (C/S 0.8). The dissolution of montmorillonite is substantial, and it accompanied by analcime, brucite and tobermorite-11 Å precipitations in clay.
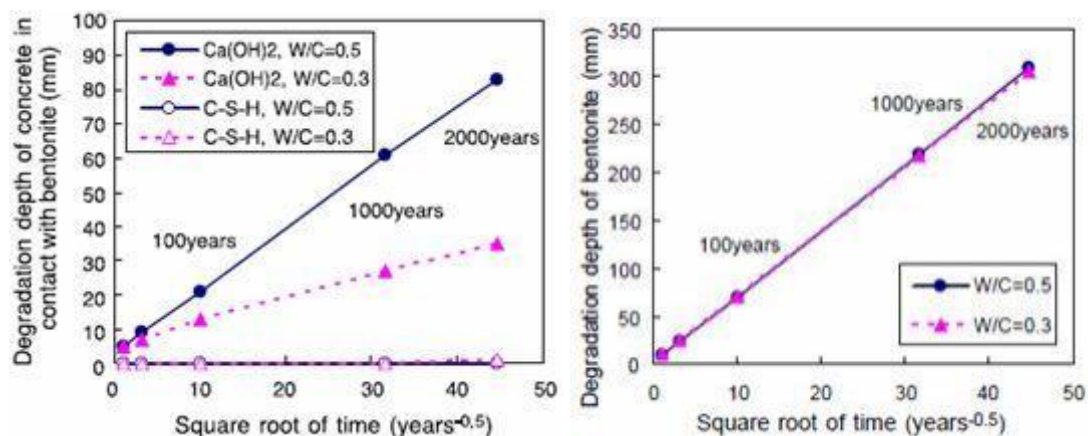


*Figure 5.5.28. Evolutions of altered depths of concrete and bentonite in function to the square root of time (Yokoseki et al., 2004).*

The TOUGHREACT code is used to simulate the interactions between concrete/argillite (Marty et al., 2009). Beyond the simple modeling of interactions, this work allows to highlight the influence of kinetics reaction and the refinement of the mesh. This work highlights the existence of a delay between the extension of the alkaline plume and the clogging of the porosity by calcite precipitation described previously. The results show the precipitation of calcite in the cementitious material, and the dissolution of portlandite, the precipitation of ettringite and the reduction of C/S in the C-S-H. The perturbation extension in the cementitious material is highly heterogeneous. Clogging at the interface may be very substantial, due to the carbonation and zeolites precipitation, or it may be zero. The clogging is totally dependent of the kinetic parameters used and is subject to strong variations.

More recent modeling exercises focused on the physicochemical behavior of low-pH concrete in contact with the Opalinus clay (Berner et al., 2013; Dauzeres et al., 2016). Berner provides a 1D numerical simulation of the physicochemical evolution of a bentonite/ESDRED concrete/OPA system with the reactive OpenGeoSys-GEM transport code (Figure 5.5.29).
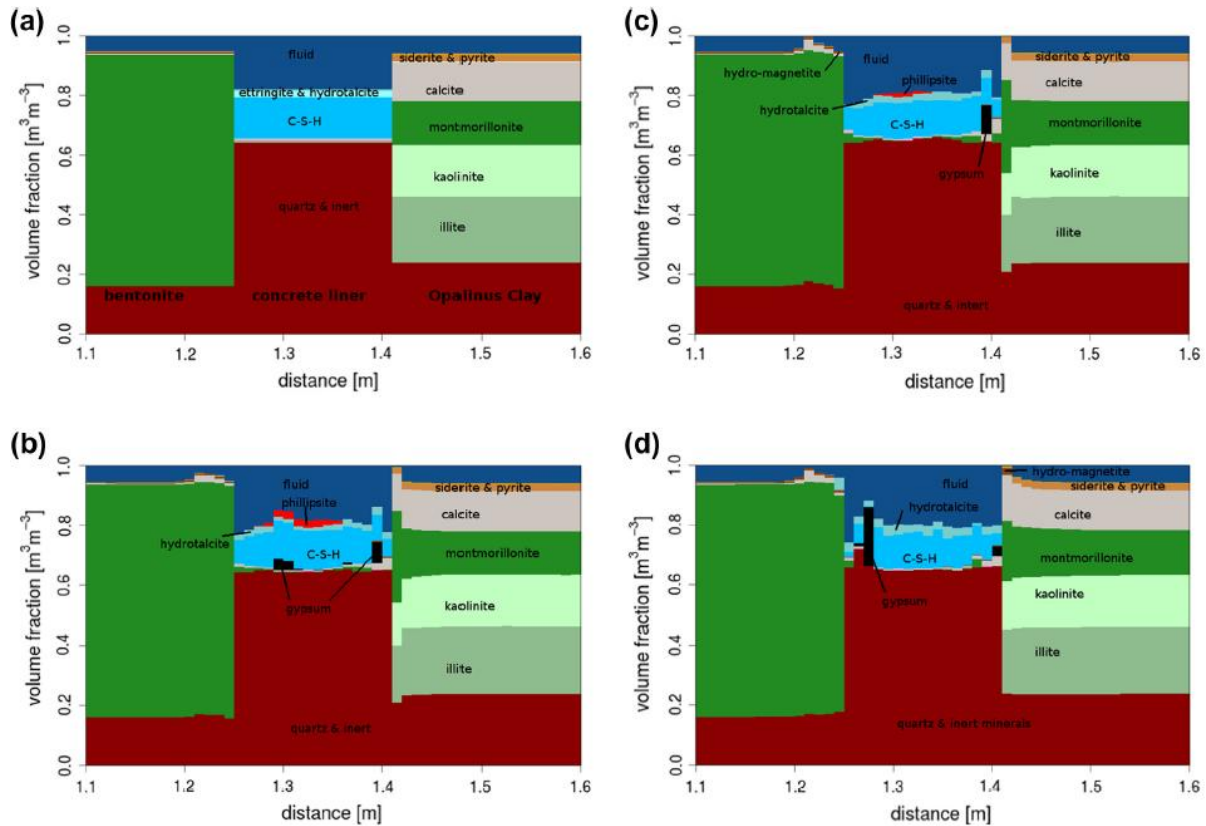


*Figure 5.5.29. Mineralogical profiles across the concrete liner layer considering full (porosity) feedback on transport: initially (a), after 10,000 years (b), after 30,000 years (c) and after 30,000 years with kinetic control of clay minerals and quartz (d) (Berner et al., 2013).*

These calculations are conducted at room temperature to represent interactions between a bentonite plug, a concrete liner and the surrounding clayey rock. The calculations carried out over 10,000 years and 30,000 years highlight mechanisms already identified previously in the concrete, namely: decalcification of C-S-H, and clogging of the interface due to calcite hydrotalcite and zeolite precipitations.

A recent study provides a paper coupling experimental results of two low-pH concretes placed in contact with the clayey rock at Mont Terri as part of the CI experiment and reactive transport modeling with the HYTEC code. Based on the experimental data and calculated for new M-S-H phases, the study highlighted the precipitation and the stability of these phases in the low-pH concretes. The precipitation of magnesium silicates, systematically placed by the code in the low-pH concrete in contact with argillaceous rocks containing magnesium, is accompanied by the well-known decalcification of C-S-H and carbonation (Figure 5.5.30). In both of the studied concretes types (ESDRED and LAC), the code places the precipitation of M-S-H as it is observed experimentally.
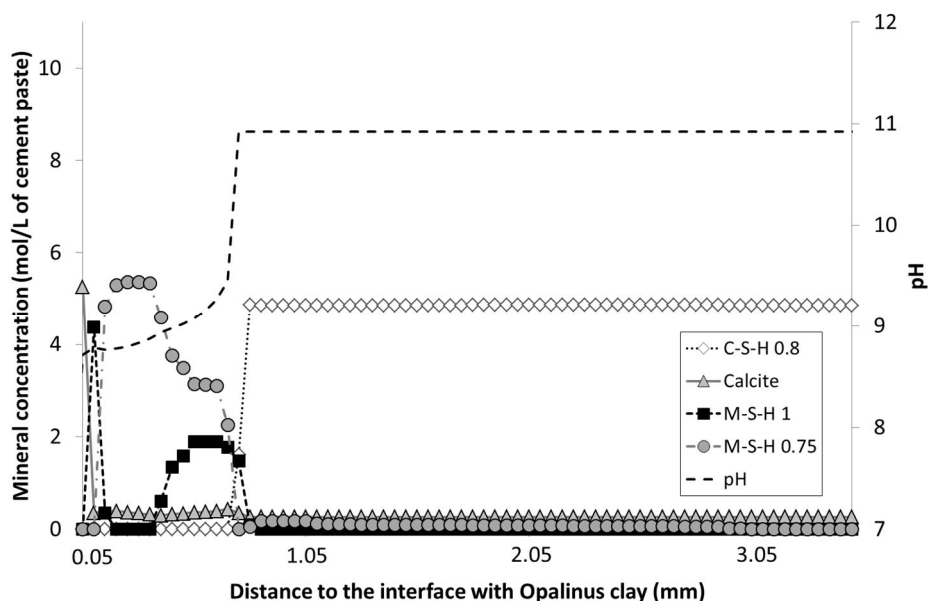
*Figure 5.5.30. Modeling of the ESDRED concrete evolution after 5 years of interaction with the clayey rock - with M-S-H in the thermodynamic database (Dauzeres et al., 2016).*

This section on numerical simulations focuses on concrete placed in contact with clayey rock. Numerous studies have also been carried out on simulations of alkaline plumes interacting with clays, but they are not discussed here. The purpose of this literature review is to identify the state of research on the physicochemical mechanisms controlling the development of concrete placed in clayey environments. Simulation results vary greatly. Some results mention concrete carbonation, while others do not. Over the same time frames, the thicknesses of the disturbed concrete fluctuate significantly depending on the models (dependence on kinetic parameters). The existence of clogging is not clear. Some models suggest precipitation of zeolites... There are many uncertainties. However, there are recurring results, such as decalcification of the cementitious material (portlandite dissolution, decrease of the C/S ratio in C-S-H), precipitation of ettringite in the presence of sulfates, and carbonation (although the location and intensity are not well known). The extension speed of the disturbance induced by the clay into the cementitious material is dependent on the porosity evolution, the kinetics and the law controlling the porosity/diffusion feedback. The significant differences in results show that more work is required on short- and medium-term modeling before we can achieve proper predictive modeling over the long and very long term.

Tables 5.5.4 and 5.5.5 summarize all the experimental and modeling studies discussed previously on the cementitious materials placed in contact with a clayey rock.

*Table 5.5.4. Summary of modelings of cementitious material evolutions in contact with clayey rock.*

| | Cement-material | Clay-material | T (°C) | Duration | Cement-material results | Clay-results | Calculation tools | References |
|---|---|---|---|---|---|---|---|---|
| **Simulations** | CEM I and CEM V concretes | Callovian-Oxfordian Argillite | 25 °C | 25 000 y | Portlandite dissolution, C/S decrease in C-S-H, ettringite precipitation. | Zeolites précipitation (scolecite et analcime), Montmorillonite dissolution and illite precipitation, interface clogging to the zeolites precipitation. | HYTEC | Trotignon et al., 2006 |
| | CEM I and CEM V concretes | Callovian-Oxfordian Argillite | 25 °C | 100 000 y | Decalcification and tobermorite precipitation in surface, ettringite precipitation. | Analcime and Laumontite precipitation. C-S-H precipitation and illitisation. | HYTEC | Trotignon et al., 2007 |
| | CEM I concrete | Argillite/bentonite | 25 °C | 100 000 y | Portlandite dissolution | C-S-H C/S 0.8 precipitation. Precipitation ++ in contact with bentonite. | ALLIANCES | Montarnal et al., 2007 |
| | CEM I concrete | Tournemire Argillite | 25 °C | 1000, 10 000 and 100 000 y | Decalcification | C-S-H and brucite precipitation, dolomite dissolution and calcite precipitation, illitisation et Ca-zeolite formation. | HYTEC | De Windt et al., 2004 |
| | CEM I concrete | Tournemire Argillite | 15 °C | 15 y | Portlandite leaching, C/S deacrease in C-S-H + calcite preciptation. The thickness concerned by the perturbation is equal to 5 mm. | C-S-H precipitation at the interface with calcite, montmorillonite and muscovite dissolution. | HYTEC | De Windt et al., 2008 |
| | CEM I concrete | Tournemire Argillite | - | 15 y | AFt precipitation, portlandite dissolution and C-S-H precipitation. Interface clogging linked to the carbonation. | C-S-H precipitation + calcite, quartz dissolution. Very low perturbation | MC-BENT | Yamaguchi et al., 2009 |
| | CEM I concrete | Bentonite | 25 °C | 100-1000-2000 y | Degradation evolution of the cementitious material in square root of time: 21 mm after 100 years, 85 mm after 2000 years | Degradation evolution of the bentonite in square root of time : 75 mm after 100 years, 300 mm after 2000 years | - | Yokoseki et al., 2004 |

| | | | | | | | |
|---|---|---|---|---|---|---|---|
| CEM I concrete | FEBEX bentonite | 25 and 120 °C | 1 y | Dissolution in contact of the argillite and precipitation in depth. C-S-H precipitation at the interface (C/S 0.8) | Analcime and brucite precipitation. Dissolution of montmorillonite et tobermorite precipitation. | CrunchFlow | Fernandez et al., 2009 |
| Portlandite, afwillite, katoite | Boom clay | 25 °C | 18 months | Portlandite dissolution and calcite. Interface clogging. | Montmorillonite dissolution and calcite precipitation. | - | Read et al., 2001 |
| CEM I concrete | Callovian-Oxfordian Argillite | 25 °C | variable | Partial decalcification of the cementitious material, carbonatation fully dependant of the kinetic parameters chosen. Ettringite precipitation. | Precipitations of several zeolites, carbonation (calcite), dolomite dissolution. | TOUGHREACT | Marty et al., 2009 |
| ESDRED Low-pH concrete | Bentonite and Opalinus Clay | 25 °C | 10 000 y and 30 000 y | C-S-H decalcification, precipitations of hydrotalcite, zeolites, clay minerals, gypsum and calcite. | Higher alteration in the OPA vs Bentonite. Low alteration amount of clay-minerals. Decrease of porosity. Calcite and hydrotalcite precipitations. Kaolinite and illite dissolved to form Montmorillonite near the interface. | OpenGeoSys-GEM | Berner et al., 2013 |
| LAC and ESDRED concretes | Opalinus clay | 25 °C | 5 years | C-S-H decalcification, Carbonation and M-S-H precipitation. | No perturbation | HYTEC | Dauzeres et al., 2016 |

*Table 5.5.5. Summary of experiments of cementitious material evolutions in contact with clayey rock.*

| | Cement-material | Clay-material | T (°C) | Duration | Cement-material results | Clay-results | References |
|---|---|---|---|---|---|---|---|
| **Experiments** | CEM II concrete and Si-lime | Toarcian Argillite | Variations | 15 and 100 y | Carbonation (calcite/vaterite) | Gypsum, Na-zéolites and dolomite precipitation, chlorite and kaolinite leaching, highest mixed-layer phases recristallisation with the CEM II in contact | Tinseau et al., 2006 Devol Brown et al., 2008 |
| | CEM II concrete and Si-lime | Toarcian Argillite | Variations | 15 y | Carbonation (calcite/vaterite/aragonite) | Idem + calcite/vaterite/aragonite | Yamaguchi et al., 2009 |
| | CEM I mortar discs | FEBEX bentonite discs | 25, 60, 120 °C | 1, 6, 12 months | Perturbations over several millimeters | Perturbations over several mm, C-S-H gel and brucite precipitation at 25 and 60 °C. Degradation highest at 120 °C: tobermorite and Mg-saponite until 10 mm and analcime in the rest of the column (convective tests). | Fernandez et al., 2006 |
| | CEM I mortar discs | FEBEX bentonite discs | 25, 60, 120 °C | 1, 6, 12 months | Carbonation (convective tests) | Analcime precipitation | Cuevas et al., 2006 |
| | 7 formulations of cement pastes : CEM I; CEM I + FA;CEM I + Slag; cemented IER; Al-cement; NIREX mortar | Mol clay | 25 and 85 °C | 12 - 18 months | High alteration: decalcification, S, Al, Si and Mg-enrichments, precipitations of Mg-Si gel and Mg-Al gel near the interface. | (in situ tests) Ca-enrichment, Al, Si and Mg depletion. | Read et al., 2001 |
| | CEM I cement paste | Callovian – Oxfordian argillite | 25 °C | 2, 6 and 12 months | Alteration inferior to 1 mm after 1y. Low carbonation with diffuse calcite precipitation, portlandite dissolution, C-S-H decalcification and ettringite precipitation. | Illite/smectite mixed layer modification. | Dauzeres et al., 2010 |
| | Low pH cement paste | Callovian – Oxfordian argillite | 25 and 50°C | 2, 6 and 12 months | C-S-H decalcification and Mg-enrichment at the interface possibly linked to M-S-H precipitation. | Low Mg-enrichment near the interface. | Dauzeres, 2010 |
| | CEM II concrete | Toarcian Argillite | 15 °C | 15 y | Alteration over 10-15 mm. Portlandite dissolution, C-S-H decalcification and calcite precipitation. | Alteration over 18-20 mm, with mainly C-S-H precipitation into the argillite and calcite dissolution and new precipitation in the front of the alkaline plume. | Techer et al., 2012 |

| Cement-material | Clay-material | T (°C) | Duration | Cement-material results | Clay-results | References |
|---|---|---|---|---|---|---|
| CEM II concrete | Toarcian Argillite | 15 °C | 15 y | Porosity increasing over 1-1.5 cm | Porosity clogging over 2 cm | Gaboreau et al., 2011 |
| CEM I and CEM I + Filler concretes | Lower Lias Clay – rich in SO4 | 5 °C and 20 °C | 1 y | Very high deterioration of the both concretes, mainly at 5°C linked to the formation of Thaumasite. | Not characterized | Abubaker et al., 2014 (x2) |
| CEM II cement paste | Toarcian Argillite | 15 °C | 18 y | Alteration of few hundred microns. Decalcification (Portlandite dissolution and C/S deacrease in C-S-H) causing a porosity opening. | Alteration over 11-13 mm. Loss of the specific area in the black rim zone associated to C-S-H and calcite precipitation and to a suspicion of illitization. | Bartier et al., 2013 |
| CEM I, EDRED and LAC concretes (Low-pH type) | Opalinus clay | 20 °C | 2.2 years | Alteration on few hundred microns. Decalcification, Mg-enrichment possibly linked to MSH precipitation (strong near the interface) and carbonation. Ettringite precipitation. | No detection | Jenni et al., 2014 |
| CEM I with low addition of fly ash. | Callovian – Oxfordian argillite | 20 °C | 5 years | Gypsum precipitation in surface | Gypsum precipitation due to pyrite oxydation at the interface associated with the loss of cohesion in contact with the concrete. | Lerouge et al., 2014 |
| Cement analogue of Maqarin and concretes from CI experiment (Mont Terri) | Maqarin site and Opalinus clay | Ambient T° | 100 000 years and 2 years | μ-XRD testing | μ-XRD testing | Dähn et al., 2014 |
| ESDRED and LAC concretes (Low-pH type) | Opalinus clay | 20 °C | 2.5 and 5 y | Several mm of perturbation. High decalcification of C-S-H and Mg-enrichment probably linked to M-S-H precipitation. Carbonation is also observed. | Mg-enrichment detected | Dauzeres et al., 2016 |

# References

[1]  F. Abubaker, C. Lynsdale, J. Cripps, Investigation of concrete-clay interaction with regards to the thaumasite form of sulfate attack, Construction and Building Materials, 64: (2014) 130–140.

[2]  F. Abubaker, C. Lynsdale, J. Cripps, Investigation of concrete–clay interaction with regards to the thaumasite form of sulfate attack, Construction and Building Materials, Volume 67, Part A: (2014) 88–94.

[3]  F. Adenot, Caractérisation et modélisation des processus physiques et chimiques de dégradation du ciment, Thèse de l'Université d'Orléans, France, 239 p.

[4]  F. Adenot, M. Buil, Modeling of the corrosion of cement paste by deionized water, Cement and Concrete Research, 22 : (1992) p 489.

[5]  AFNOR, Norme FD P18-011, Béton-Définition et classification des environnements chimiquement agressifs-Recommandations pour la formulation des bétons, 2004.

[6]  B. Albert, Altération des matrices cimentaires par des eaux de pluie et des eaux sulfatées : approche expérimentale et thermodynamique, Thèse de l'Ecole Nationale Supérieure des Mines de Saint-Etienne, 2002.

[7]  F. Badouix, Modélisation de l'altération à long terme des bétons : prise en compte de la carbonatation, Thèse de doctorat de l'Ecole Nationale Supérieure de Cachan (2000).

[8]  D. Bartier, I. Techer, A. Dauzères, P. Boulvais, M.-M. Blanc-Valleron, J. Cabrera, In situ investigations and reactive transport modelling of cement paste/argillite interactions in a saturated context and outside an excavated disturbed zone, Applied Geochemistry, 31: (2013) 94–108.

[9]  U. Berner, D. A. Kulik, G. Kosakowski, Geochemical impact of a low-pH cement liner on the near field of a repository for spent fuel and high-level radioactive waste, Physics and Chemistry of the Earth, Parts A/B/C, 64 : (2013) 46–56.

[10]  R.H. Bogue, La chimie du ciment Portland, Editions Eyrolles (1952) 586 p.

[11]  B. Bonin, Deep geological disposal in argillaceous formations: studies at the Tournemire test site, Journal of Contaminant Hydrology, 35 : (1998) 315–330.

[12]  B. Bourdette, Durabilité du mortier : prise en compte des auréoles de transition dans la caractérisation et la modélisation des processus physiques et d'altération, Thèse de l'INSA Toulouse, (1994).

[13]  P.W. Brown, S. Badger, The distributions of bound sulfates and chlorides in concrete subjected to mixed NaCl, MgSO4, Na2SO4 attack, Cement and Concrete Research, 30: (2000) 1535–1542.

[14]  P.W. Brown, A. Doerr, Chemical changes in concrete due to the ingress of aggressive species, Cement and Concrete Research, 30: (2000) 411–418.

[15]  P. Brown, R.D. Hooton, Ettringite and thaumasite formation in laboratory concretes prepared using sulfate-resisting cements, Cement and Concrete Composites, 24 : (2002) 361–370.

[16]  P.W. Brown, R.D. Hooton, B.A. Clark, The co-existence of thaumasite and ettringite in concrete exposed to magnesium sulfate at room temperature and the influence of blast-furnace slag substitution on sulfate resistance, Cement and Concrete Composites, 25: (2003) 939-945.

[17]  E. Candlot, The influence of Sea Water on Hydraulic Mortars. In: Conclusions adopted by the French Commission in Reference to Tests of Cements by William Michaelis, 1897.

[18]  T. Chaussadent, Analyse des mécanismes de carbonatation des bétons, Journées techniques AFPC-AFREM Durabilité des bétons. Méthodes recommandées pour la mesure des grandeurs associées à la durabilité, Toulouse (1997).

[19]  M.D. Cohen, M.D. Mather, Sulfate attack on concrete: research needs. ACI materials journals, 88: (1991) 62–69.

[20]  J. Cuevas, R. Vigil De La Villa, S. Ramirez, L. Sanchez, R. Fernandez, S. Leguey, The alkaline reaction of FEBEX bentonite: a contribution to the study of the performance of bentonite/concrete engineered barrier systems, Journal of Iberian Geology 32 (2): (2006) 151–174.

[21]  R. Dähn, D. Popov, Ph. Schaub, P. Pattison, D. Grolimund, U. Mäder, A. Jenni, E. Wieland, X-ray micro-diffraction studies of heterogeneous interfaces between cementitious materials and geological formations, Physics and Chemistry of the Earth, Parts A/B/C, 70–71: (2014) 96–103.

[22]  D. Damidot, F.P. Glasser, Thermodynamic investigation of the CaO-Al2O3-CaSO4-H2O system at 25°C and the influence of Na2O, Cement and Concrete Research, 23: (1993) 221–238.

[23]  D. Damidot, F.P. Glasser, Investigation of the CaO-Al2O3-SiO2-H2O system at 25°C by thermodynamic calculations, Cement and Concrete Research, 25: (1995) 22–28.

[24]  D. Damidot, Description d'une méthode pour calculer les diagrammes de phases solides-liquide. Application à l'étude de parties du système CaO-Al2O3-SiO2-CaSO4-CaCO3-CaCl2-Na2O-K2O-H2O en relation avec l'hydratation du ciment. Habilitation à diriger des recherches de l'Université de Bourgogne, (1995).

[25]  A. Dauzeres, P. Le Bescop, P. Sardini, C. Cau Dit Coumes, Physico-chemical investigation of clayey/cement-based materials interaction in the context of geological waste disposal: Experimental approach and results, Cem Concr Res, 40 (2010) 1327–1340.

[26]  A. Dauzères, P. Le Bescop, C. Cau-Dit-Coumes, F. Brunet, X. Bourbon, J. Timonen, M. Voutilainen, L.

Chomat and P. Sardini, On the physico-chemical evolution of low-pH and CEM I cement pastes interacting with Callovo-Oxfordian pore water under its in situ CO2 partial pressure, Cement and Concrete Research, 58 (2014) 76–88.

[27]   A. Dauzeres, G. Achiedo, D. Nied, E. Bernard, S. Alahrache, B. Lothenbach,  Magnesium perturbation in low-pH concretes placed in clayey environment—solid characterizations and modeling, Cement and Concrete Research, 79 (2016) 137–150.

[28]   I. Devol-Brown, E. Tinseau, D. Bartier, D. Mifsud, D. Stammose, Interaction of Tournemire argillite (Aveyron, France) with hyperalkaline fluids : Batch experiments performed with powdered and/or compact materials, Physics and Chemistry of the Earth, 32 (2007): 320–333.

[29]   L. De Windt, D. Pellegrini, J. Van der Lee, Coupled modeling of cement/claystone interactions and radionuclide migration, Journal of Contaminant Hydrology 68: (2004) 165–182.

[30]   L. De Windt, F. Marsal, E. Tinseau, D. Pelligrini, Reactive transport modeling of geochemical interactions at a concrete/argillite interface, Tournemire site (France), Physics and Chemistry of the Earth 33: (2008) 295–305.

[31]   I. Devol-Brown, E. Tinseau, F. Marsal, D. Pelligrini, A. Mifsud, S. Lemius, D. Stammose, J. Cabrera, Argillite/concrete and argillite/steel interactions: Experiences gained from the Tournemire Underground Research Laboratory, In: Nuclear Waste Research: Siting, Technology and Treatment, ISBN 978-1-60456-184-5 (2008).

[32]   G. Escadeillas, H. Hornain, La durabilité des bétons vis-à-vis des environnements chimiquement agressifs, La durabilité des bétons Chapitre 12, Presses de l'Ecole Nationale des Ponts et Chaussées (2008) : 615–705.

[33]   P. Faucon, Durabilité du béton : physico-chimie de l'altération par l'eau, Thèse de l'Université de Cergy Pontoise, (1997) 260 p.

[34]   R. Fernandez, J. Cuevas, L. Sanchez, R. V. de la Villa, S. Leguey, Reactivity of the cement-bentonite interface with alkaline solutions using transport cells, Applied Geochemistry 21: (2006) 977–992.

[35]   R. Fernandez, J. Cuevas, U.K. Mâder, Modelling concrete interaction with a bentonite barrier, European Journal of Mineralogy, 21: (2009) 177–191.

[36]   S. Gaboreau, D. Prêt, E. Tinseau, F. Claret, D. Pellegrini, D. Stammose, 15 years of in situ cement–argillite interaction from Tournemire URL: Characterisation of the multi-scale spatial heterogeneities of pore space evolution, Applied Geochemistry, 26-12: (2011) 2159–2171.

[37]   C. Gallé, H. Peycelon, P. Le Bescop, S. Bejaoui, V. L'Hostis, B. Bary, P. Bouniol, C. Richet, Concrete long-term behaviour in the context of nuclear waste management : Experiment and modelling research strategy, Journal de Physique IV, 136 : (2006) 25–38.

[38]   J.L. Garcia Calvo, A. Hidalgo, C. Alonso, L. Fernandez Luco, Development of low-pH cementitious materials for HLRW repositories: Resistance against ground waters aggression. Cement and Concrete Research, 40, 8 : (2010) p. 1290.

[39]   J.L. Garcia Calvo, M.C. Alonso, A. Hidalgo, L. Fernández Luco, V. Flor-Laguna, Development of low-pH cementitious materials based on CAC for HLW repositories: Long-term hydration and resistance against groundwater aggression, Cement and Concrete Research, 51: (2013) 67–77.

[40]   E.C. Gaucher, P. Blanc, Cement/clay interactions-a review: Experiments, natural analogues, and modelling, Waste Management 26: (2006) 776–788.

[41]   E.C. Gaucher, P. Blanc, F. Bardot, G. Braibant, S. Buschaert, C. Crouzet, A. Gautier, J.-P. Girard, E. Jacquot, A. Lassin, G. Negrel, C. Tournassat, A. Vinsot, S. Altmann, Modelling the porewater chemistry of the Callovian-Oxfordian formation at a regional scale. Comptes Rendus Geosciences 338: (2006) 917–930.

[42]   E. Gaucher, C. Lerouge, Caractérisation géochimique des forages PAC et nouvelles modélisations THERMOAR. 2007, BRGM.

[43]   P. Gégout, E. Revertégat, G. Moine, Action of chloride ions on hydrated cement pastes : influence of the cement type and long time effect of the concentration of chloride, Cement and Concrete Research, 22 : (1992) 451–457.

[44]   J.-P. Girard, C. Flehoc, E. Gaucher, Stable isotope composition of CO2 outgassed from cores of argillites: a simple method to constrain [delta]18O of porewater and [delta]13C of dissolved carbon in mudrocks. Applied Geochemistry 20 : (2005) 713–725.

[45]   A. Jenni, U. Mäder, C. Lerouge, S. Gaboreau, B. Schwyn, In situ interaction between different concretes and Opalinus Clay, Physics and Chemistry of the Earth, Parts A/B/C, 70–71: (2014) 71–83.

[46]   S. Kamali, M. Moranville, S. Leclercq, Material and environmental parameter effects on the leaching of cement pastes: Experiments and modelling., Cement and Concrete Research 38: (2008), 575–585.

[47]   I. Kurashige, M. Hironaga, K. Niwase, Effects of hydrogencarbonate and chloride in groundwater on leaching of cementitious materials, CONSEC'07 Tours: (2007) 615–622.

[48]   P. Le Bescop, C. Solet, External sulfate attack by ground water, Revue Européenne de Génie Civil (2006).

[49]   C. Lerouge, F. Claret, C. Tournassat, S. Grangeon, S. Gaboreau, B. Boyer, D. Borschnek, Y. Linard, Constraints from sulfur isotopes on the origin of gypsum at concrete/claystone interfaces, Physics and Chemistry of the Earth, Parts A/B/C, 70–71 (2014) 84–95.

173

[50] Y. Maltais, E. Samson, J. Marchand, Predicting the durability of Portland cement systems in aggressive environments. Laboratory validation, Cement and Concrete Research, 34 : (2004) 1579–1589.

[51] N. Marty, C. Tournassat, A. Burnol, E. Giffaut, E. Gaucher, Influence of reaction kinetics and mesh refinement on the numerical modelling of concrete/clay interactions, Journal of Hydrology 364: (2009) 58–72.

[52] T. Matschei, B. Lothenbach, F.P. Glasser, Thermodynamic properties of Portland cement hydrates in the system CaO-Al2O3-SiO2-CaSO4-CaCO3-H2O, Cement and Concrete Research, 37, 10: (2010) 1379–1410.

[53] P.K. Mehta, Concrete: structure, properties and materials, Prentice Hall, Ed., (1986) 105–169.

[54] W. Michaelis, The influence of Sea Water on Hydraulic Mortars. In : Conclusions adopted by the French Commission in Reference to Tests of Cements by William Michaelis (1891), 1897.

[55] G. Michard, Equilibres chimiques dans les eaux naturelles, Publisud Ed., 1989.

[56] Ph. Montarnal, C. Mügler, J. Colin, M. Descostes, A. Dimier, E. Jacquot, Presentation and use of a reactive transport code in porous media, Physics and Chemistry of the Earth 32: (2007) 507–517.

[57] M. Moranville, S. Kamali, E. Guillon, Physicochemical equilibria of cement-based materials in aggressive environments-experiment and modeling, Cement and Concrete Research, 34: (2004) 1569–1578.

[58] V.M. Moskvin, F.M. Ivanov, S.N. Alekseyev, E.A. Suzeyev, Concrete and reinforced concrete deterioration and protection, Mir, Ed., Moscou, 1980.

[59] L.J. Parrot, D.C. Killoh, Carbonation in a 36 year old in-situ concrete, Cement and Concrete Research, 19 : (1989) 649–656.

[60] F.J. Pearson, D. Arcos, A. Bath, J.-Y. Boisson, A.M. Fernandez, H.-E. Gäbler, E. Gaucher, A. Gautschi, L. Griffault, P. Hernan and H.N. Waber, Mont-Terri Project – Geochemistry of Water in the Opalinus Clay Formation at the Mont Terri Rock Laboratory, Reports of the FOWG, Geology Series, 5, Bern 2003, 319 p.H. Peycelon, C. Blanc, C. Mazoin, Long term behavior of concrete: influence of temperature and cement binder on the degradation (decalcification/hydrolysis) in saturated conditions, Revue Européenne de Génie Civil, 10: (2006) 1107–1125.

[61] D. Planel, J. Sercombe, P. Le Bescop, F. Adenot, J.M. Torrenti, Long term performance of cement paste during combined calcium leaching-sulfate attack: kinetics and size effect, Cement and Concrete Research, 36: (2006) 137–143.

[62] D. Read, F.P. Glasser, C. Ayora, M.T. Guardiola, A. Sneyers, Mineralogical and microstructural changes accompanying the interaction of Boom Clay with ordinary Portland cement, Advances in Cement Research, 13, N°4, October 2001, 175–183.

[63] M. Regourd, Carbonatation accélérée et résistance des ciments aux eaux aggressives, Symposium international RILEM sur la carbonatation du béton, Slough, 5-6 April 1976, Cement and Concrete Association, Ed., 5, 5.3.

[64] M. Regourd, Resistance of concrete to chemical attack, Matériaux et Constructions 14, 80 : (1981) 130-137.

[65] E. Revertegat, C. Richet, P. Gégout, Effect of pH on the durability of cement pastes, Cement and Concrete Research, 22 : (1992) 259–272.

[66] E. Revertegat, F. Adenot, C. Richet, L. Wu, F.P. Glasser, D. Damidot, S.A. Stonach, Theoritical and experimental study of degradation mechanisms of cement in the repository environment, CEC contract n°F12W-CT90-0035, Final Report, ISBN 92-828-0394-5, 1997.

[67] I.Techer, I., Bartier, D., Boulvais, Ph., Tinseau, E., Suchorski, K., Cabrera, J., Dauzères, A., Tracing interactions between natural argillites and hyper-alkaline fluids from engineered cement paste and concrete: chemical and isotopic monitoring of a 15-years old deep-disposal analogue. Appl. Geochem. 27, 1384–1402.

[68] E. Tinseau, D. Bartier, L. Hassouta, I. Devol-Brown, D. Stammose, Mineralogical characterization of the Tournemire argillite after in situ interaction with concretes, Waste Management, 26: (2006) 789–800.

[69] L. Trotignon, H. Peycelon, X. Bourbon, Comparison of performance of concrete barriers in a clayey geological medium, Physics and Chemistry of the Earth 31: (2006) 610–617.

[70] L. Trotignon, V. Devallois, H. Peycelon, C. Tiffreau, X. Bourbon, Predicting the long term durability of concrete engineered barriers in a geological repository for radioactive waste, Physics and Chemistry of the Earth 32: (2007) 259–274.

[71] Y. van der Lee, L. De Windt, V. Lagneau, P. Goblet, Module-oriented modeling of reactive transport with HYTEC, Computers and Geoscience, 29 : (2003) 265–275.

[72] T. Yamaguchi, Y. Sakamoto, M. Akai, M. Takazawa, Y. Iida, T. Tanaka, S. Nakayama, Experimental and modeling study on long-term alteration of compacted bentonite with alkaline groundwater, Physics and Chemistry of the Earth 32: (2007) 298–310.

[73] T. Yamaguchi, Y. Mitsumoto, M. Kadowaki, S. Hoshino, T. Maeda, T. Tanaka, S. Nakayama, F. Marsal, D. Pellegrini, Verification of a reactive transport model for long-term alteration of cement-clay systems based on laboratory experiments and in-situ observations, CEA - JAEA meeting (2009).

[74] K. Yokoseki, K. Watanabe, N. Sakata, N. Otsuki, Modeling of leaching from cementitious materials used in underground environment, Applied Clay Science 26: (2004) 293–308.

## 5.6 Calcium-silicate-hydrates in low-pH concretes and deep geological nuclear waste repository environment

*T. Vehmas*

*VTT Technical Research Centre of Finland Ltd, Espoo, Finland*

### Introduction

Posiva Oy is constructing one of the world's first long-term nuclear waste repositories in Finland.[1] The safety of the nuclear waste repository is ensured with combination of natural and engineered barriers.[2]

Concrete plugs are used for closure and sealing of the repository and the deposition tunnels. Concrete plugs are utilized to assure mechanical and hydrological isolation of the compartments of the repository. Isolation is needed because compartments have different states in terms of water saturation and pressures. Such difference could potentially induce undesired mass redistributions. Besides concrete plugs, cementitious materials are used in shotcrete for tunnel wall rock supports, rock-bolting grouts and injection grouts for fissure sealing. Only some of the cementitious materials will remain in the repository after final closure. Shotcrete is removed before the final closure with assumed efficiency of 95%.[3]

The amount of cementitious materials in the repository will be significant although some of the materials are removed before final closure. Approximately half of the cementitious materials that will remain in the closed repository are located in the access tunnels and consists of grouts, shotcrete remnants and concrete constructions. In deposition tunnels, cementitious materials are present in grouted fractures, rock bolt mortars and deposition tunnel end plugs.

Total amount of cementitious materials including central tunnels are assumed 550 000–740 000 kg for grouts, 540 000–600 000 kg for shotcrete, 340 000–1 010 000 kg for rock bolt mortars and 16 500 kg for other constructions. Total mass of cementitious materials in access tunnels is approximately 1 446 000–2 367 000 kg. The mass of a single deposition tunnel end plug is 16 600 kg. Total mass of tunnel end plug concrete is 2 170 000 kg.

Cementitious materials will be in direct contact with backfill- and closure materials. It is assumed that cementitious leachates will interact with backfill and closure materials but not to an extent that it compromises the long-term safety of the barrier system. The bentonite buffer is not in direct contact with cementitious materials. However, the buffer may be affected due the migration of cementitious leachates through the bedrock fracture network. To meet the designed performance requirements during the lifecycle of the repository, the properties of the engineered barrier system should not alter due the presence of cementitious materials.[3]

Cementitious materials pore solution has naturally high pH of 13–14. Bentonite backfill and buffer properties are potentially altered in high -pH leachates. Nuclear waste managing organizations, Posiva (Finland), SKB (Sweden) and NUMO (Japan) have targeted a pH limit ≤11 for cementitious leachates. It has been suggested that more natural pH limit would be pH ≤10, as silicates aqueous behaviour changes. In pH <10, silicates are in neutral $SiO_2(aq)$ form in solution whereas in pH > 10 silicates dissociates to charged species $HSiO_3^-$. Correspondingly, the solubility of quartz increases by three orders of magnitude compared to the pH range 1–10.[4]

The highest tolerable pH of the leachate is 10 or 11 in the bentonite system. Otherwise the long-term stability of the engineered barrier system is endangered. Mix designs having a leachate lower pH than natural pH of 13–14 have been formulated[5][6][7][8]. The low-pH mix designs consist of low alkaline Portland cements mixed with large amounts of pozzolanic materials. Pozzolanic materials are known to react with the hydration products that control the pH of the cementitious materials pore solution. Low-pH materials are still highly basic but the pH value is significantly lower than in traditional Portland cements.

Another process that affects the pH of the cementitious materials in the repository is leaching.[9] Portland cement -based materials will be in contact with the groundwater in the repository. Hardened Portland cement is a soluble material that equilibrates with the pore solution. Solubilities of the hardened Portland cement phases will determine the composition of the pore solution. As pore solution is constantly changing with the external solution, leaching causes degradation of the hardened Portland cement matrix. The first phases that will dissolve are the alkalis that causes pH values above saturation pH of portlandite (pH >12.4). Second step is the dissolution of the portlandite, followed by the incongruent dissolution of calcium-silicate-hydrates. When congruently dissolving calcium-silicate-hydrates are formed, the pH will remain constant as long as calcium-silicate-hydrates are present in the Portland cement matrix. High pH leachate region in the groundwater, caused by the degradation of cementitious materials is usually referred as alkaline plume. Figure 5.6.1 presents the schematic evolution of the pore solution pH during the leaching pure water of Portland cement paste.
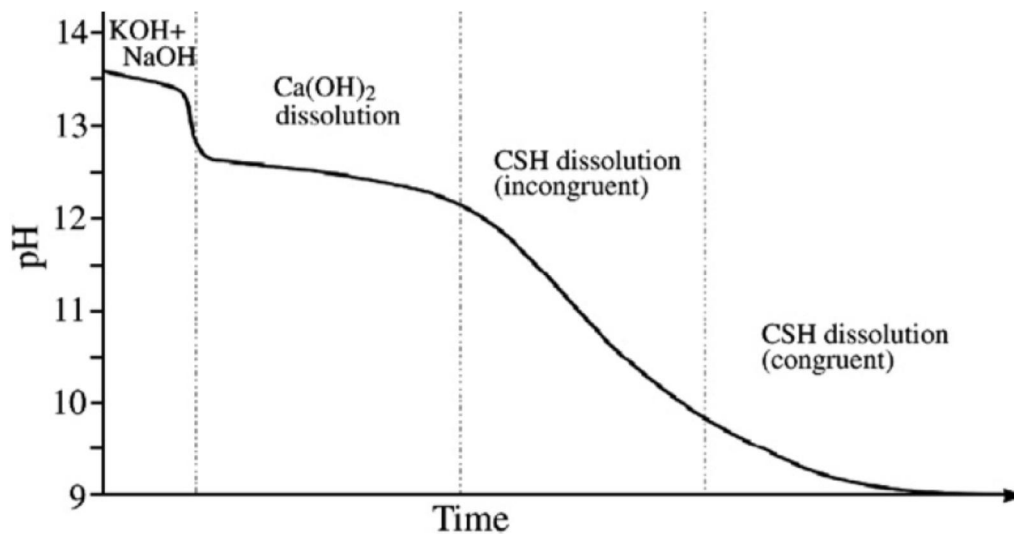


*Figure 5.6.1. Schematic evolution of pore solution pH during leaching of pure water of Portland cement.* [9][10]*[5]*

The third factor that controls the pH of the alkaline plume is the groundwater composition. Leaching of cementitious materials in distilled water has significantly higher pH than in saline groundwater due the common ion effects. Ions in groundwater will affect the composition of the alkaline plume and also the composition of the hardened Portland cement phases.

As a summary, pH of the alkaline plume of cementitious materials in the repository is controlled with three discrete processes:

1. Reaction of pozzolanic materials
2. Leaching of the cementitious materials
3. Common ion effect of groundwater leachate

Above mentioned discrete processes will affect simultaneously in the repository. pH development due to the dissolution of the crystalline phases is not a major problem as the compositions are known. Largest uncertainties are related to the calcium-silicate-hydrate-phases. Whatever the pH of the alkaline plume is affected by leaching, pozzolanic reaction or common ion effect, calcium-silicate-hydrate phases are responsible of the pH values of alkaline plume in the long-term. The long-term pH values are vital for the integrity of the buffer and backfill materials and therefore the safety of the whole engineered barrier system. The exact nature of the calcium-silicate-hydrate phases in hardened Ordinary Portland cement is not known and uncertainties related incongruent and congruent dissolution regions exists.

The focus of the current literature review is to summarize the state-of-the art knowledge of calcium-silicate-hydrates in respect of long-term safety of the nuclear waste repository. The basic knowledge of calcium-silicate-hydrates is summarized. Calcium-silicate-hydrates compositions in Ordinary Portland cement and low-pH cement are presented. The leaching process, groundwater effects and the long-term behaviour of calcium-silicate-hydrates in nuclear waste repositories is introduced.

**Calcium-silicate-hydrates**

Calcium silicate hydrates possess a remarkably level of structural complexity. More than thirty crystalline calcium-silicate-hydrates has been identified and their structures ranges from nearly amorphous to semi-crystalline.[11][12] The most important individual calcium-silicate-hydrates have been 1,4nm-tobermorite and jennite. A lot of current understanding of calcium-silicate-hydrates has been gained by studying these two crystalline forms of calcium-silicate-hydrate.

All of the calcium silicate hydrates are described by general term "C-S-H" according to abbreviation of cement chemistry (C = CaO, S = $SiO_2$, H = $H_2O$)[13]. Dashes indicate that no specific composition is implied. C-S-H is the essential "glue" of the cementitious materials and determines greatly the properties of hardened concrete. The nature of C-S-H has been studied experimentally since late 19th century but still major unsolved issues in C-S-H nature exist.[14] The biggest question relies in the structure(s) and amorphous nature of C-S-H encountered in Ordinary Portland Cement hydration in circumstances relevant to every-day construction.

*General Structure of C-S-H*

A lot of unanimous understanding of C-S-H structure and composition has been gathered during recent years. It is generally considered that C-S-H consists of composite layers of central calcium oxide sheets that are ribbed on either side with chains of silicate tetrahedrons (Figure 5.6.2). Two adjacent calcium oxide sheets are bound together, creating a lamellae structure. Interlayer of the silicate ribbed calcium oxide sheets is filled with counter-ions and physically bound water. Water is also adsorbed on the surfaces of individual C-S-H lamellae and lamellae interphases are filled with water. Typical method to characterize various C-S-H is performed by measuring calcium/silicon -ratio, water/silicon -ratio and polymerisation degree of silicate chains.
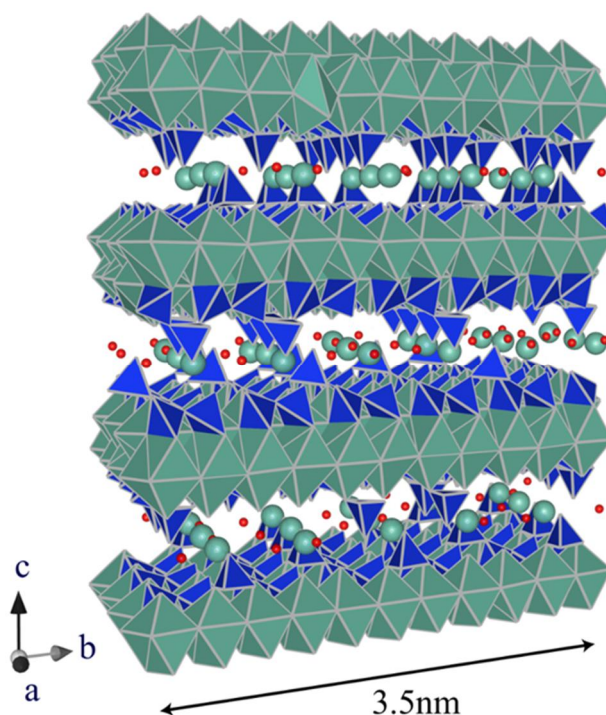
*Figure 5.6.2. General structure of C-S-H. Central calcium oxide sheets (green) are flanked with silicate chains (blue) and the interlayer is filled with water (omitted) and counter-ions (red and green spheres).* [15][16]

*Central calcium oxide sheet*

Central calcium oxide sheets consist of hepta-coordinated calcium oxides in pseudo octahedral conformation[17]. In crystalline 1.4 nm-tobermorite, central calcium oxide sheet does not have Ca-OH groups. All the calcium oxide bonds are shared either with the neighbouring calcium oxides or silicate tetrahedrons. Central calcium oxide sheet of crystalline jennite is more corrugated. Due the more corrugated structure, jennite has hydroxides in the central calcium oxide sheet. Approximately 33% of calcium oxide bonds are in hydroxyl form in crystalline jennite.[18]

*Silicate chains*

Central calcium oxide sheet is flanked with silicate tetrahedrons on either side. Theoretically, polymerisation of the silicate tetrahedrons can vary from monomeric to infinity. In practice, infinity long silicate chains are not encountered. Typical chain lengths vary from 2 to 5, whereas values over 30 are also reported[19][20]. Silicate tetrahedrons form single linear chains without branching.

Linear silicate tetrahedron chains repeat patterns of three. The pattern is often called "dreieketten". In dreieketten, two adjacent tetrahedrons are coordinated to calcium oxide sheet and the third tetrahedron binds two dimers together. Two coordinated tetrahedrons are called paired tetrahedrons and the third tetrahedron is called bridging tetrahedron. Paired tetrahedrons share two oxygens with the central calcium oxide sheet and the bridging tetrahedron share one oxygen with the central calcium oxide sheet (Figure 5.6.3). In every bridging tetrahedron exists one Si-OH. Because of the dreieketten structure, silicate chains have length according to formula (3n-1) where n is integer. [21][22][23]

Silicate chain structure can vary by omitting bridging tetrahedron, paired tetrahedron or whole dreiketten segment. For every missing bridging tetrahedron, one additional Si-OH and Ca-OH

groups are formed. Missing paired tetrahedrons and missing whole dreieketten segment increase Ca-OH content of C-S-H structure. Also Ca/Si -ratio of C-S-H increases with omitting silicate tetrahedrons. The silicate chain structure is in the key role when various qualities of C-S-H are explained.[24]
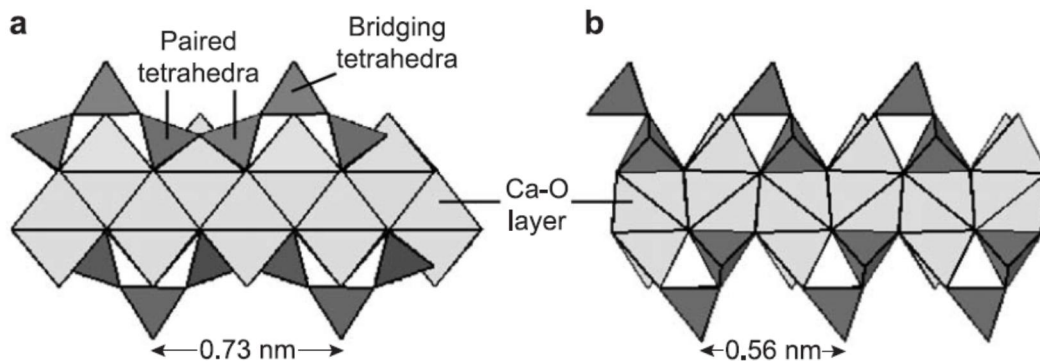


*Figure 5.6.3. The structure of silicate chains in C-S-H. Silicate "dreiketten" consist of two paired silicate tetrahedrons and one bridging silicate tetrahedron. At the left, illustration along the [210] plane and at the right along the [010] plane of C-S-H.* [11]

*Interlayer*

Interlayer of two adjacent silicate flanked central calcium oxide sheets contains physically bound water and counter-ions. Every bridging tetrahedron creates one Si-O⁻ -group into structure which charge must be balanced. It is usually assumed that in high calcium content environment ½ $Ca^{2+}$ creates the charge balance respect to Si-O⁻.[25]

*Nanostructure*

C-S-H is known to produce wide reflection peaks in x-ray diffraction measurements. Wide x-ray diffraction peaks are usually related to amorphous nature of the measured materials. C-S-H has been regarded as a three dimensional assemblage of C-S-H layers, which tend to form subparallel groups a few layers thick. Enclosed pore structure of such system ranges from interlayer spaces upwards. Three dimensional assemblage of C-S-H layers is presented in Figure 5.6.4.
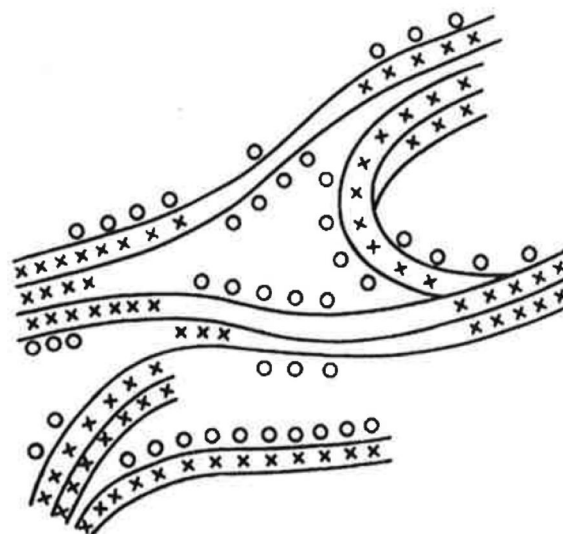


*Figure 5.6.4. Feldman-Serrera model of the structure of C-S-H. C-S-H layers are lines, interlayer water molecules are crosses and adsorbed water molecules are circles.* [13][26]

C-S-H has been also considered as a gel. According to Everett's definition, gel is a dispersion in which the attractive interactions between the elements of the disperse phase are so strong that the whole system develops a rigid network structure and under small stresses behaves elastically. According to gel definition, C-S-H consist small separate particles that are bounded together with surface forces. Wittmann described C-S-H as a xerogel. [27] Xerogel is a gel where the dispersion medium is absent and no particular internal structure of C-S-H particles is assumed.[24]

In last decade, Nonat considered that the C-S-H can be considered as gel-like, but it is not necessary amorphous. Broad x-ray reflections can originate from small coherent C-S-H domains and presence of the microdefects in the structure. Atomic force microscopy images have shown well-crystalline structure in individual C-S-H domains.[24] These domains are only size of 5 nanometers which corresponds only two crystalline cells of the lamellae structure. Figure 5.6.5 presents the atomic force microscopy images of hydrated cement paste. In Larger scale, heterogeneous distribution of C-S-H domains was observed whereas in the scale of nanometers well crystalline structure is observed. On the basis of 5nm C-S-H domains and well-crystalline nanoscale structure, X-ray diffraction peaks have been calculated with good correspondent to the measured x-ray diffraction patters.[24]
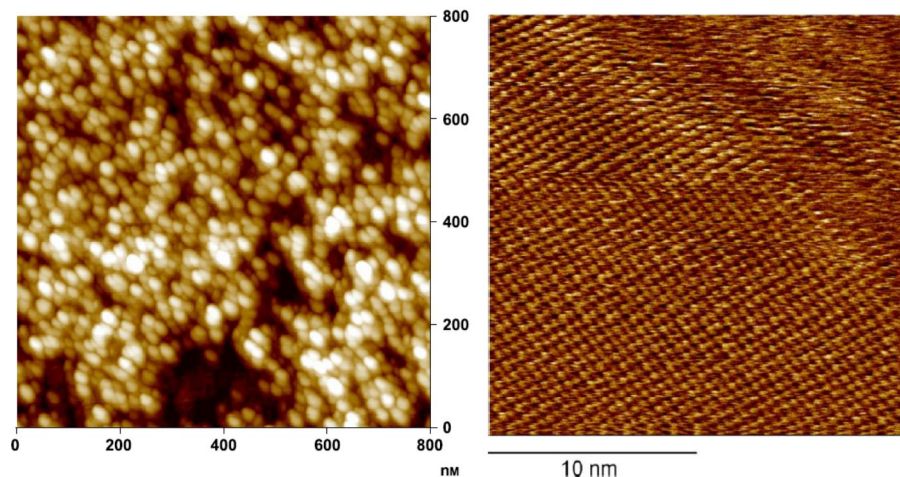


*Figure 5.6.5. Atomic force microscopy images of hydrated cement paste. At the left, heterogeneous distribution of C-S-H nanoparticles are observed in larger scale. At the right, well organized structure of C-S-H can be seen in the individual nanoparticles.* [24]

The difference between three dimensional assemblage of C-S-H layers and gel-type structure relies in the continuation of silicate chains. In three dimensional assemblage, silicate chains and central calcium oxide sheets connects throughout the structure, whereas in gel-type structure C-S-H forms particles and silicate chains do not connect the individual particles (Figure 5.6.6). In first case, the strength of the C-S-H matrix is determined by the internal forces of silicate flanked calcium oxide sheets whereas in the latter, the strength of the C-S-H matrix is determined by the surface forces of C-S-H particles.
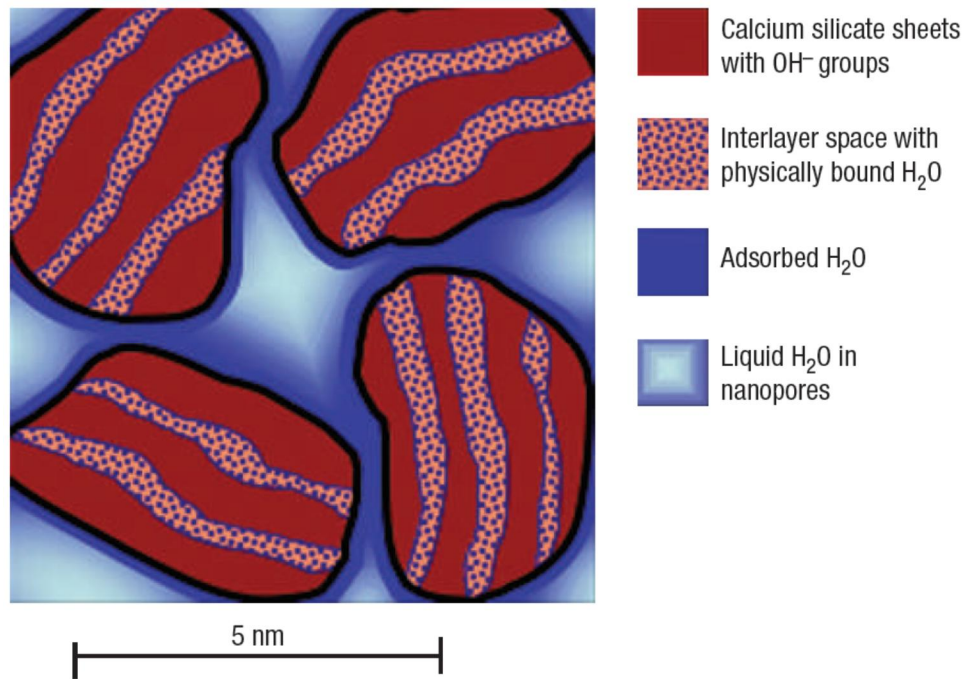
*Figure 5.6.6. Schematic presentation of C-S-H nanoparticles.*[28]

**Crystalline C-S-H phases**

Over thirty crystalline calcium-silicate-hydrate phases are known. The most important are 1.4 nm - tobermorite and jennite in the cement chemistry perspective. Other crystalline phases have been used to derive potential structures of C-S-H but as crystalline phases other calcium-silicate-hydrates do not have large role in cement chemistry.

*1,4nm-tobermorite and jennite*

The structure of 1.4 nm -tobermorite and jennite is presented in Figure 5.6.7. Both have a layered structure of calcium oxide sheets, flanked with silicate -chains in dreiketten -form.

Chemical formula of pristine 1.4 nm -tobermorite is $Ca_4H_4Si_6O_{18}*8H_2O$ and jennite $Ca_8H_4Si_6O_{18}(OH)_8*6H_2O$ with Ca/Si -ratios 0.66 and 1.33, respectively. Bridging tetrahedrons share one oxygen bond with calcium oxide sheet, leaving one of the silicates bond protonated. According to dehydration studies, the protons are substituted with ½ $Ca^{2+}$ leading to final formulae $Ca_5H_2Si_6O_{18}*8H_2O$ for 1.4 nm -tobermorite and $Ca_9H_2Si_6O_{18}(OH)_8*6H_2O$ for jennite.[29]

In 1.4 nm -tobermorite all oxygen atoms in main Ca-O layer are shared with silicate tetrahedrons or neighbouring calcium oxides, whereas in jennite only half is shared and the remainder exist in Ca-OH groups. There are no Si-OH bonds in well-crystallized Jennite, whereas no Ca-OH exists in the central calcium oxide sheet in 1.4 nm -tobermorite. Thus, a key difference between jennite and 1.4 nm -tobermorite is the presence of Ca-OH bonds in jennite's central calcium oxide layer.[18]
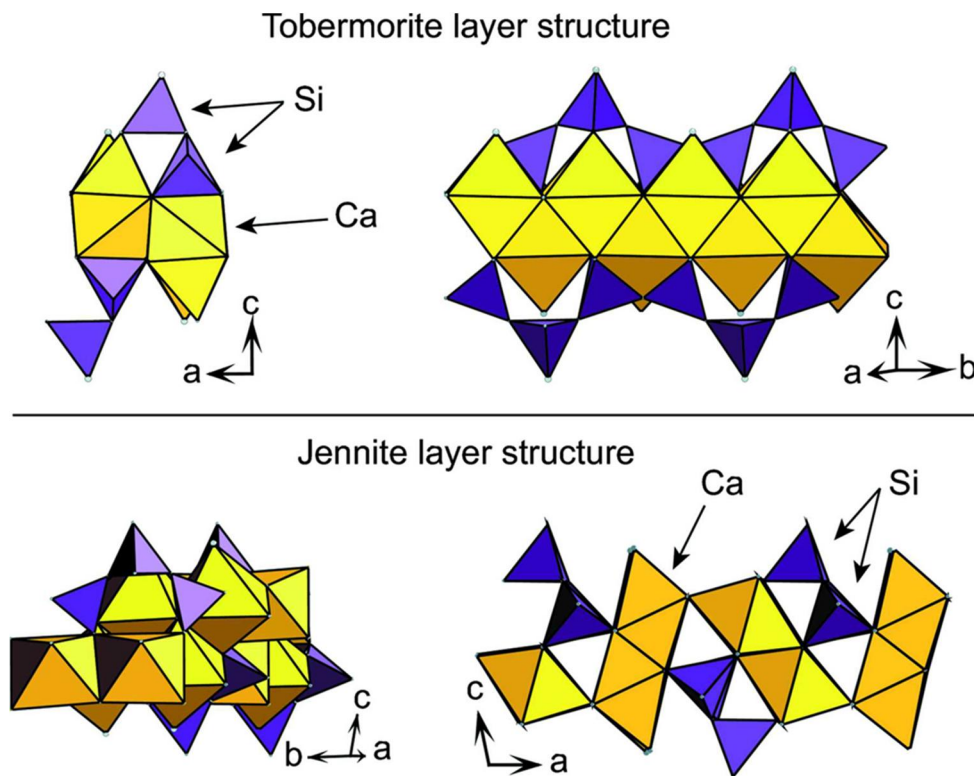
*Figure 5.6.7. Structures of Tobermorite and Jennite.* [30]

**General Properties of C-S-H**

Calcium silicate hydrates are usually characterized with solubility, calcium/silicate -ratio, water/silicate -ratio, length of the silicate chains and the amount of Ca-OH and Si-OH -sites. Comprehensive understanding of C-S-H structure requires and explanation of how above mentioned qualities are correlated.

*Ca/Si -ratio*

The Ca/Si -ratio defines the ratio of calcium atoms per silicon atom in the C-S-H structure. The Ca/Si -ratio of crystalline C-S-H structures are easily calculated and experimental measurement Ca/Si -ratio of the C-S-H is not difficult. Ca/Si -ratio has become valuable information as it can be compared to various structures and structural modifications. The Ca/Si -ratio of hydrated Portland cement does not correspond to the Ca/Si -ratio of any crystalline C-S-H phase and therefore various modifications of crystalline phases has been presented. Various qualities of the C-S-H have dependency with Ca/Si-ratio, such as silicate polymerisation degree and equilibrium pH (Figures 5.6.8, 5.6.9 & 5.6.10).
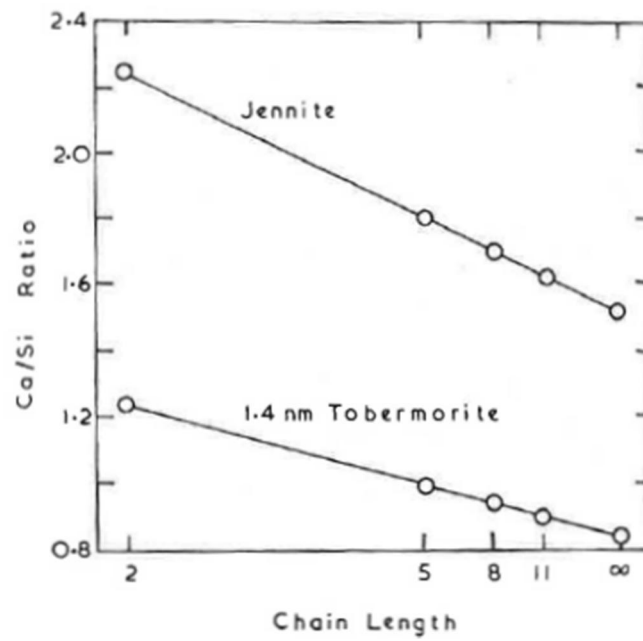
*Figure 5.6.8. Ca/Si -ratio of 1.4 nm –Tobermorite and Jennite in a function of silicate chain length. It is assumed that each bridging tetrahedron carries one H atom and one of the two end group tetrahedron of each anion also carries an H atom.* [25]
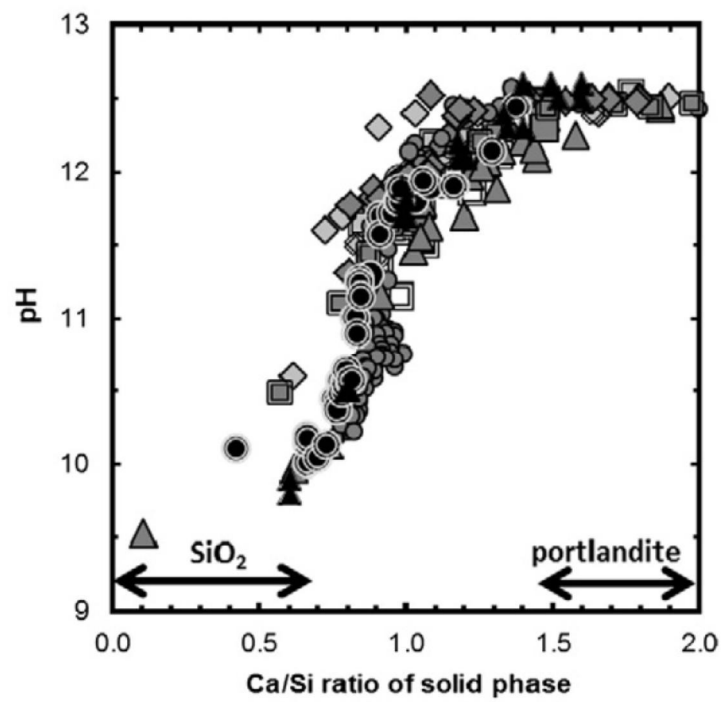


*Figure 5.6.9. Equilibrium pH and Ca/Si -ratio of solid C-S-H from various studies.* [20]
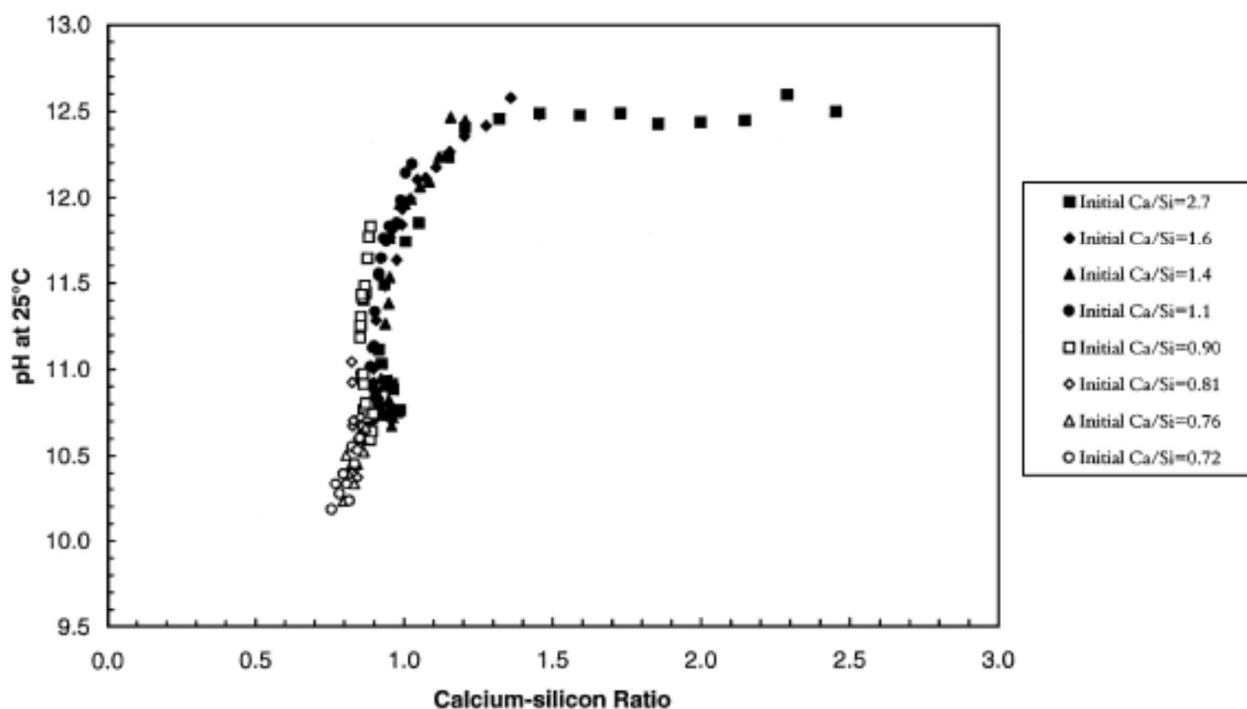
*Figure 5.6.10. Equilibrium pH in function of Ca/Si -ratio of solid phase from leaching studies.*[31]

*Ca-OH Si-OH*

Together with the Ca/Si ratio and the silicate structure, Ca-OH and Si-OH groups are important in the C-S-H structure. They are also likely the groups that will define the pH of the aqueous system. The content of Si-OH in C-S-H has been shown to decrease with the increasing Ca/Si -ratio. Si-OH groups are present in the C-S-H structures below Ca/Si -ratio 1.2–1.3. [32] [33] Above the Ca/Si-ratio 1.2–1.3, Si-OH -groups do not exist. According H-NMR studies, calcium ions replace the protons in Si-OH. Ca-OH bonds has been observed in C-S-H with Ca/Si -ratio higher than 1.[11] Various analysing techniques suggest that Ca-OH groups form in C-S-H only after all the protons in Si-OH groups have been replaced with calcium. Dipolar NMR correlation maps have shown that the protons in the Ca-OH groups are within 5 ångströms from the Si atoms, confirming that the Ca-OH and Si-OH are in the same structural unit. [34]

Si-OH sites are situated in the silicate tetrahedrons or surface sites. Bridging silicate tetrahedrons have one Si-OH -site. Also each end of silicate chain is one Si-OH site. Depending on the polymerisation degree of silicate chain, Si-OH -site can exist in each silicate tetrahedron (dimeric silicates) or every third silicate (infinitely long silicate chain).

Ca-OH bonds can occur in the central calcium oxide layer, at the charge balancing sites in the interlayer or at the surface sites. Current evidences cannot point out clearly preferred Ca-OH -sites.[24] However, it appears unlikely that surface sites would dominate the Ca-OH concentration. Ca-OH in interlayer and in central calcium oxide sheet has been provided as explanation of Ca/Si -variations.

*Solubility of C-S-H*

Solubility of C-S-H provides a systematic method to evaluate the structure of C-S-H because the structure and solubility are related according to laws of thermodynamics. Solubility also determines the reactivity and leaching properties of individual C-S-H phases. Kinetic ambiguities make the

analysis difficult but various methods have been developed to overcome the difficulties. By synthetizing C-S-H through various routes, at least metastable thermodynamic equilibrium has been reached, enabling reliable determination of metastable C-S-H composition. Metastable compositions can persist due the kinetic and energetic barriers that prevent the composition to reach the true thermodynamic equilibrium. C-S-H is a good example metastable material because various ill-crystallized C-S-H phases persist indefinitely although crystalline calcium-silicate-hydrate phases such as afwillite, tobermorite and jennite are the true thermodynamically stable phases. [11]

Calcium-silicate-hydrates aqueous solution is a three component system of calcium, silicon and water. If a single solid component is presence in the solution, the equilibrium concentrations should follow a single line which correspond the solubility product of the solid phase. In solubility measurements, Chen et al. has observed that C-S-H is able to attain various metastable phases that are stable at least for several weeks or months. Figure 5.6.11 presents the measurement data of Chen et al. together with previously published data from the literature.[11]

Chen et al. has developed a systematic way to interpret the composition of the metastable C-S-H phases according solubility equilibrium. The essential feature of their system is that variations in solubility varies from some variable structural feature of C-S-H and the curves labelled C, C' and C'' arise from the variations in the content of Ca-OH in C-S-H. Equilibrium solution compositions of C-S-H follow a single line in the Ca/Si -ratios below 1. According to Chen at al. higher Ca/Si -ratios can be theoretically attained by combination of small mean silicate chain length and low Ca-OH content or long mean silicate chain length and high Ca-OH content. They hypothesize that C-S-H structure which is equilibrium with the curve C in Figure 5.6.11, has a high mean silicate chain length and high Ca-OH content, corresponding jennite -type structures. Progressively lower mean silicate chain length and Ca-OH contents produce structures corresponding solubility equilibrium on the curves C', C'' and A. Curve A has no Ca-OH groups and the structure corresponds 1,4nm Tobermorite.

It has been stated that Si-OH and Ca-OH do not coexist in the C-S-H structure. The intersection of the curves A and C, C' or C'' corresponds to the situation where neither is present for a given silicate chain length. Chen et al. has also calculated the minimum Ca/Si -ratios for various silicate chain lengths were Ca-OH must form in the C-S-H structure. Calculated data corresponds quite well with experimentally measured.

Assuming that Ca-OH contents are accommodated by Jennite-like conformation, the family of solubility curves represents a spectrum of metastable phases, ranging from a purely tobermorite-like structure curve A to Jennite-like structure curve C.
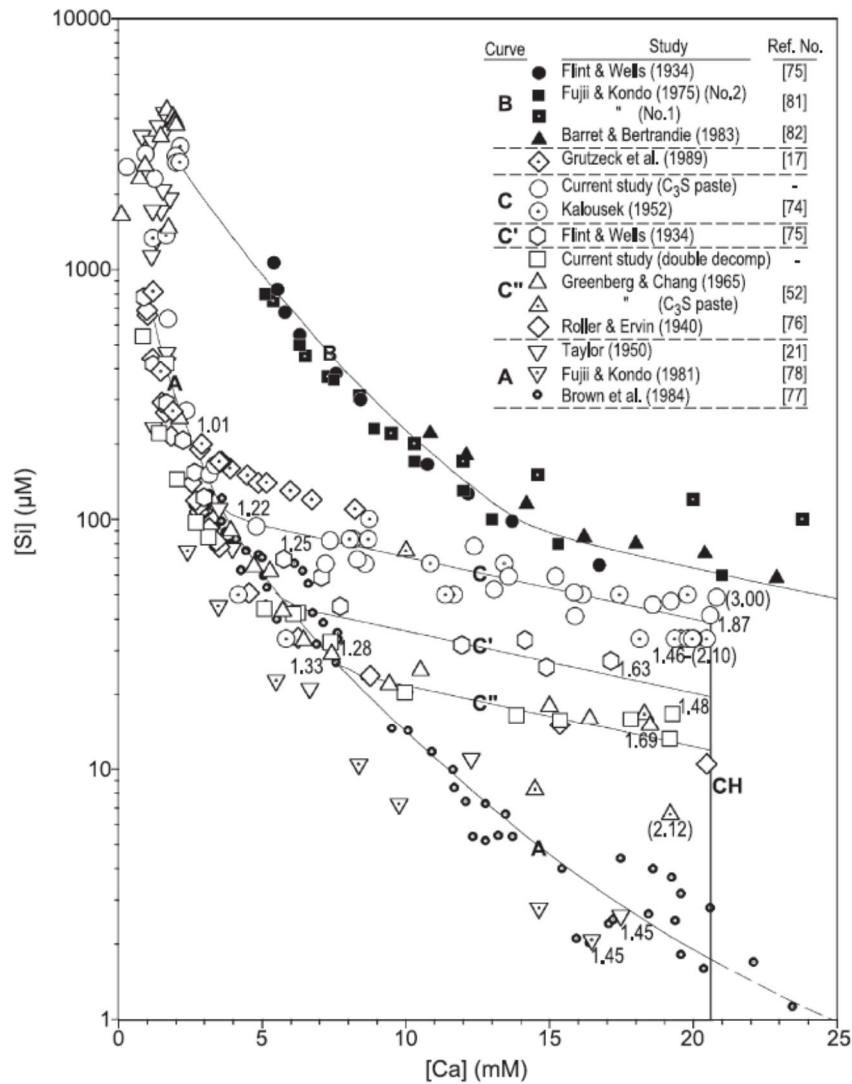
*Figure 5.6.11. Equilibrium concentrations of various C-S-H phases.* [11]

*pH*

The equilibrium pH of C-S-H depends on the Ca/Si -ratio of the C-S-H gel. Figure 5.6.12 presents the equilibrium pH of various synthetized C-S-H from the study of Chen et al. Although large variety of preparation methods, pH follows the Ca/Si -ratio of C-S-H.
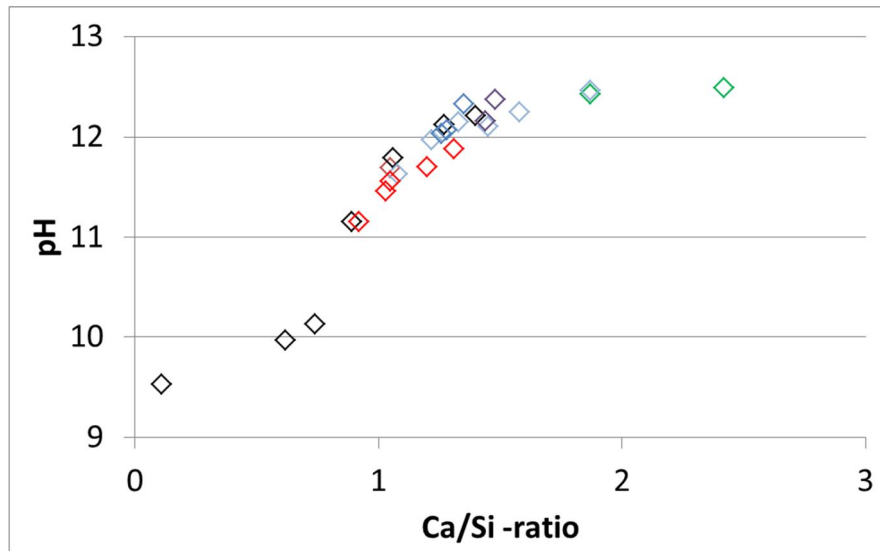
*Figure 5.6.12. Ca/Si -ratio of C-S-H and equilibrium pH. Data is replotted from* [11].

**Calcium-silicate-hydrates in Ordinary Portland Cement**

In Portland cements, calcium-silicate-hydrates co-exist with multiple crystalline phases. Typical main constituents of hydrated Ordinary Portland cement (OPC) are C-S-H, calcium hydroxide and aluminium ferrite phases, their respective proportions being roughly 70%, 20% and 10%. In respect of C-S-H, calcium hydroxide is the most important of the OPC crystalline phases. Calcium-silicate-hydrates in hydrated Portland cement are in equilibrium with crystalline CaOH which limits the potential C-S-H compositions. However, potential C-S-H composition has still great variations as can be seen from Figure 5.6.11. According to Figure of Chen et al. highly Jennite-like structures, Tobermorite with dimeric silicate chains and various mixtures of these two are metastable in presence of crystalline calcium hydroxide.

Other crystalline OPC phases will have an effect to C-S-H through introduction of foreign ions.[35][36][37] Multiple ions can replace C-S-H constituents in C-S-H structure. Aluminium replacement of silicate tetrahedrons forms various calcium-aluminate-silicate-hydrates (C-A-S-H) which are also metastable. C-S-H is also known to uptake large amount of alkalis in the C-S-H structure.

Another factor that complicates the chemistry of OPC hydration is the low amount of hydration water. Synthetic C-S-H are manufactured in excess amount of water, whereas OPC hydration takes place approximately water/OPC -ratios of 0.3–0.6. According to traditional calculations of Powers, approximately w/c -ratio of 0.45 is sufficient for full hydration of OPC.[13] The amount of free water is excessive in the beginning of the hydration but will lower during the hydration.

Also the free movement of water becomes restricted due solidification of the matrix. The environment in OPC hydration is largely heterogeneous due the dissolution of Portland cement minerals. Reaction conditions are significantly different in the vicinity of dissolving clinker particles than in the middle of particle interspaces. As a result, reaction conditions in OPC hydration differs greatly from the circumstances where laboratory research is conducted.

*C-S-H composition in OPC hydration*

C-S-H synthetized in excess water volume is typically an imperfect version of 1.4 nm -tobermorite which is called generally C-S-H(I). C-S-H(I) is known to form in reaction of alkali silicates and

calcium salts or in hydration of tri-calcium silicate and β-di-calcium silicate in dilute aqueous solutions.[11] The Ca/Si -ratio of C-S-H(I) can vary from 0.67–1.5 by omitting bridging tetrahedrons and variating the interlayer calcium content. The mean silicate chain length of C-S-H(I) increases with decreasing Ca/Si -ratio.

Prolonged reaction of tri-calcium silicate and β-di-calcium silicate are observed to produce unique phase called C-S-H(II). C-S-H(II) is characterized as imperfect form of jennite. The exact reaction conditions for C-S-H(II) formation has not been defined and multiple attempts to synthetize C-S-H(II) has failed.[19]

C-S-H which is formed in OPC hydration with w/c -ratios 0.3–0.6 has a broad x-ray diffraction spectrum covering the structures of C-S-H(I) and C-S-H(II).Because of the broad variety of the C-S-H which is formed in OPC hydration, it is usually described as C-S-H gel. In this context, term gel refers to non-defined chemical composition, not to exact nano-structural nature of C-S-H.

Two classifications of C-S-H gel have been adapted on the basis of microscopy. The C-S-H gel which has formed within the boundaries of original OPC grains is called Inner product. The C-S-H gel that fills the water filled spaces are called Outer product. These two C-S-H gel types are presented in Figures 5.6.13 and 5.6.14. Outer product has a fibrillary, directional morphology with high aspect ratio. Inner product has also directional aspect but the forming C-S-H fibrils are much finer. There is not necessarily an exact correspondence between the position of the Inner product and the original grains but the difference between Outer- and Inner product is clear. [12][38]
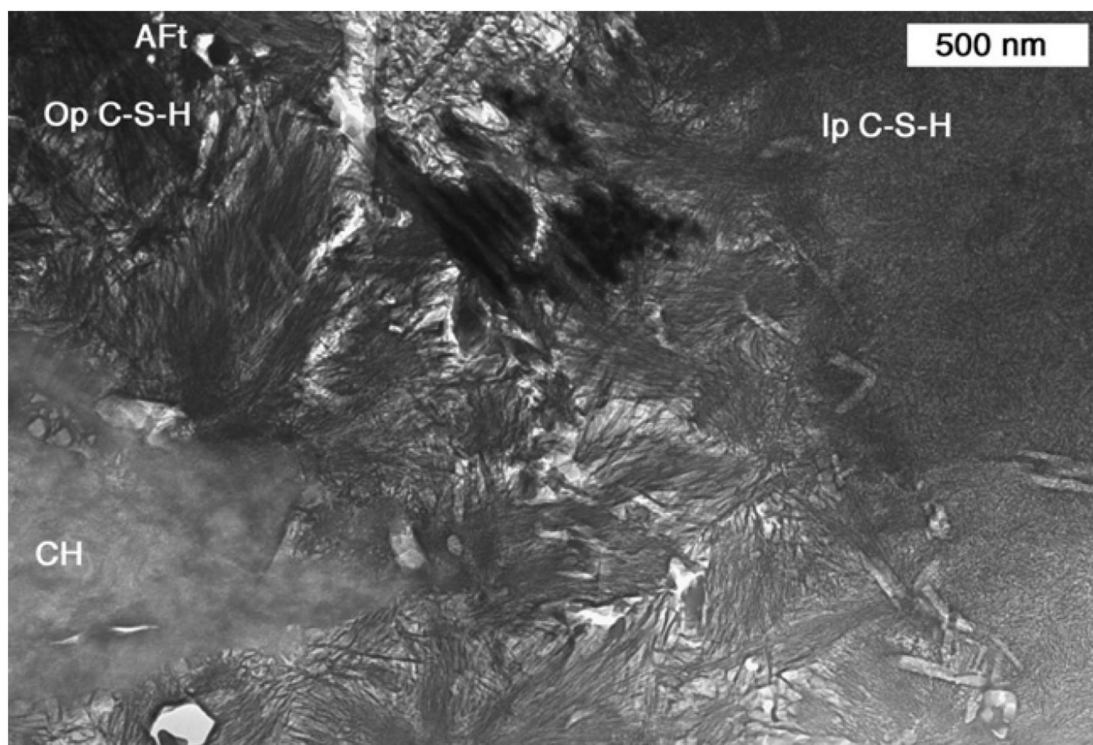


*Figure 5.6.13. Transmission electron microscope image of white Portland cement/fly ash (70%/30%) blend, hydrated for four years. Op = Outer product, Ip = Inner product, CH = portlandite.*
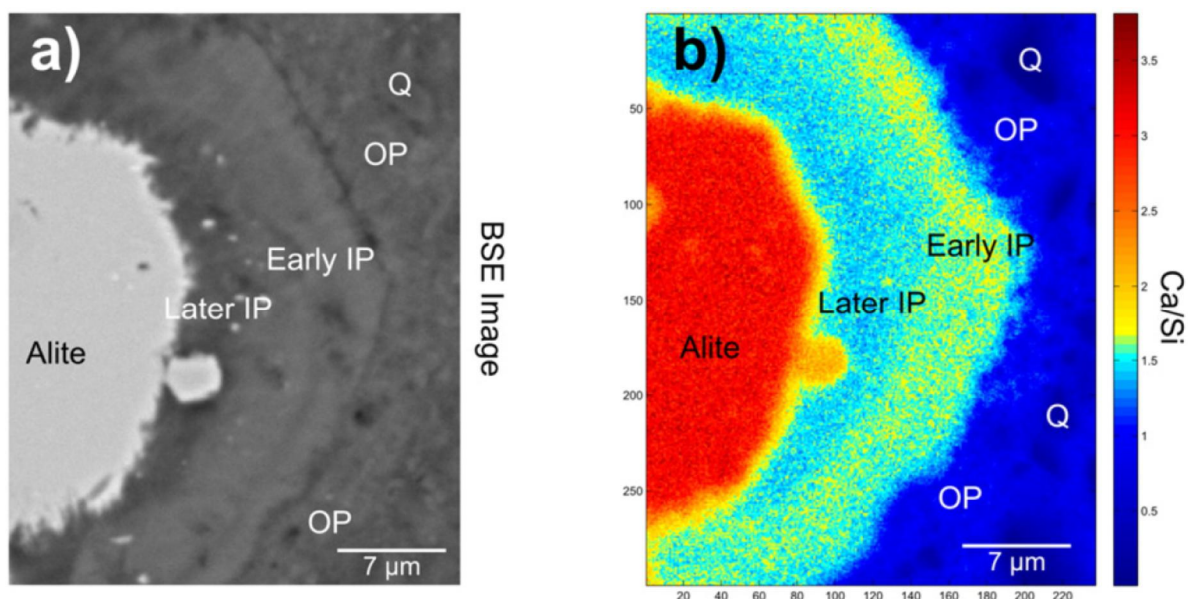
*Figure 5.6.14. a) Backscatter scanning electron microscope image of Inner and outer product. b) Ca/Si -ratio of the corresponding areas. Binder composition: 60% OPC, 20% SF and 20 Quartz.*[39]

*Ca/Si -ratio*

The mean Ca/Si -ratio in hardened OPC paste is typically 1.7–1.8.[38] This Ca/Si -ratio is higher than that of pristine jennite (1.5) and much higher than 1.4 nm -tobermorite (0.9). There is no significant variation of total Ca/Si -ratio with the hydration time. However, there is a large local variation at different ages. C-S-H gel has bimodal Ca/Si -ratio distribution in young OPC pastes. [21] As paste matures, the Ca/Si-ratio becomes unimodal.[40] Figure 5.6.15 presents the bimodal composition of $C_3S$ hydrated for 3.5 years.



*Figure 5.6.15. The Si/Ca -atom ratio frequency histogram from the mapping data from a 70*70µm region with 1µm increments in a $C_3S$ paste hydrated for three and half years.*[21]

*Silicate chain*

According to Si-NMR studies, first C-S-H formed in OPC hydration has dimeric silicate chain - structure. Within time silicate chains begins to polymerise (Figure 5.6.16). As hydration proceeds some of the dimers are linked by monomers to form pentamers.[22][23] Higher silicate chain lengths are not typically observed in hydration of pure OPC.
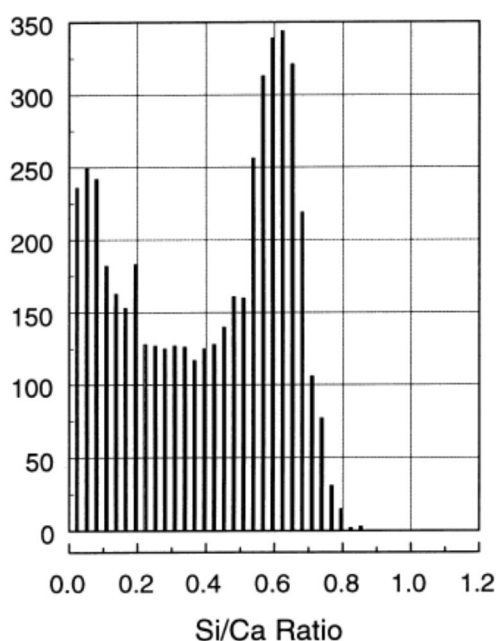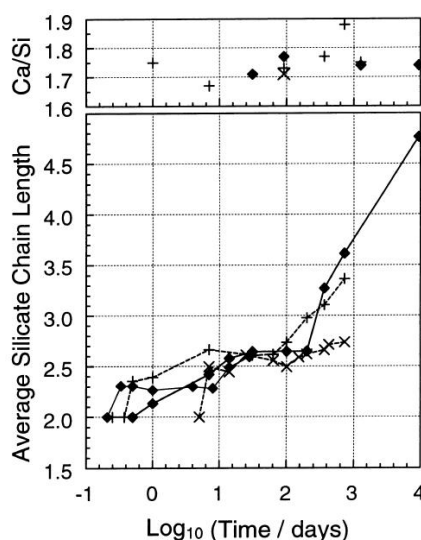


*Figure 5.6.16. Average silicate chain length of C-S-H gel and the mean Ca/Si -ratio.*

*CaOH SiOH*

Inelastic neutron scattering measurements has presented Ca-OH bonds in hydrated white OPC paste. According to measurements 33% of Ca-O bonds are balanced by protons in white OPC paste. The Ca/Si -ratio of the paste was 1.7. Value corresponds quite closely to the free Ca-OH bond of jennite.[18]

It is generally agreed that protonated Si-OH sites do not exist in the OPC hydration environment.

*Density of C-S-H gel*

The density of C-S-H gel, formed in the OPC hydration is 2.6–2.7 $g/cm^3$. This value is significantly higher than densities of 1.4 nm -tobermorite (2.2 $g/cm^3$) or jennite (2.32 $g/cm^3$).[41] [42] [20] [43] In order to explain the composition of C-S-H gel, the density difference must be accounted for. Any mechanism related to silicate chain elimination decreases the density of C-S-H as the volume of the crystal cell does not change significantly.[44] Vice versa, addition of atoms into silicate structure increases the C-S-H density.

*pH*

The pH of hydrated OPC is primary controlled by alkali content. If alkalis are not present, pH is controlled by crystalline calcium hydroxide which buffers the pH to value 12.4.

*Models for C-S-H gel*

Since 1952, various models for C-S-H gel structures in hydrated OPC have been presented.[14] Two most important parameters in these models are the basic structure of C-S-H gel and the polymerisation degree of silicate chains. Monomeric and dimeric silicate chain compositions have

been used in past years. However, silicate chain length 3n-1 is the most popular in up to date models due the experimental results. The biggest unsolved question in today's models is the structural composition of C-S-H gel in Ca/Si -ratio 1.7. Modified 1.4 nm -tobermorite and jennite has been proposed as the explanation of the C-S-H gel composition at the Ca/Si -ratio 1.7. Most important models for C-S-H gel are described and compared in the following sections.

*Taylor's model*

According to Taylor's model C-S-H in OPC can be derived from the 1.4 nm -tobermorite and jennite by eliminating fully or partly the bridging tetrahedrons. C-S-H(I) corresponds 1.4 nm - tobermorite -based structures and C-S-H (II) correspond jennite-based structures. According to Taylor's model, both forms C-S-H(I) and C-S-H(II) are formed in the early-age OPC hydration. As the paste matures, these two regions interact, generating intermediate product with jennite-like structures. The regions of 1.4 nm tobermorite and jennite are poorly defined and could even merge at individual layers. [27]

*Cong & Kirkpatrick's model*

Cong and Kirkpatrick questioned the existence of jennite type -structures in hardened OPC.[19] According to their studies, only tobermorite –type structures are present. Higher Ca/Si -ratios are results of missing bridging and paired silicate tetrahedrons. By eliminating whole dreieketten sections from the 1,4nm- tobermorite structure, it is possible to attain higher Ca/Si -ratios which are encountered in the OPC hydration. Total elimination of bridging tetrahedrons corresponds to the Ca/Si -ratio of 1.35 with only dimeric silicate tetrahedrons present. However, experimental observation indicated that the polymerisation greater then pure dimeric silicates were observed in the samples with Ca/Si -ratio greater than 1.35. Therefore it is essential to Cong and Kirkpartick's model to eliminate full dreiketten -chains. In Cong and Kirkpatrick's study, XRD measurements did not show structures similar to jennite with Ca/Si -ratio greater than 1.35. Only 1.4 nm -tobermorite type crystal lattices were observed.

Cong and Kirkpatrick also observed that crystalline portlandite was present in the samples Ca/Si -ratios higher than 1.54 and the polymerisation degree of silicate chains was thus greater than composition studies indicated. According to Cong and Kirkpatrick's model, C-S-H gel is a solid solution of disordered 1.4 nm-tobermorite and portlandite.

*Nonat & Leqoc's model*

Nonat & Leqoc's model is also based on 1.4 nm -tobermorite structure as Cong & Kirkpatrick's model. In Nonat and Leqoc's model, the 1.4 nm -tobermorite is not disordered. High Ca/Si -ratios are explained as additional $Ca(OH)_2$ bound to interlayer sites of silicate tetrahedrons. According to Nonat and Leqoc, each missing bridging tetrahedron provides two sites for $OH^-$ and allows accommodation of one $Ca(OH)_2$ in the structure. According to Nonat and Leqoc, model is capable to explain whole range of the Ca/Si -ratios from 0.66 up to 2. [24]

*Comparison of the models*

All three models describe C-S-H gel as defect 1.4 nm -tobermorite in low Ca/Si -ratios. The differences are in high Ca/Si -ratios which is the C-S-H gel encountered in normal OPC hydration. According to Taylor's model, C-S-H in high Ca/Si -ratios is defect jennite -type, whereas Cong & Kirkpatrick and Nonat & Leqoc explain higher Ca/Si -ratios with modification of 1.4 nm - tobermorite. In Nonat & Leqoc's model, increased calcium content is related to calcium bounding

to C-S-H interlayer. Cong & Kirkpatrick explains the increased Ca -content by eliminating bridging and paired silicon tetrahedrons from the C-S-H structure.

These differences have been recently evaluated in the light of Si-NMR, XRD, solubility - measurements and modelling. Solubility data presented existence of two C-S-H phases in hardened OPC, named as α-C-S-H and β-C-S-H. Alpha C-S-H had solubility product log K = 11.2 and was stable in the Ca/Si -ratios 0.75–1. Beta C-S-H had solubility product log K = 14.2 and was stable in the Ca/Si -ratios 1–1.5. It is now generally considered that both of these C-S-H phases are 1.4 nm - tobermorite-based and fit in the definition of C-S-H(I).[24]

Local environments of Ca and Si in NMR measurements remained unaltered with the evolution of Ca/Si -ratio, supporting that the structure does not change. Also calculated Si- NMR spectra of 1.4 nm -tobermorite is much closer to the experimentally observed and differ greatly of calculated spectrum of jennite.[45] XRD-patterns changes only slightly throughout various Ca/Si -ratios. The d-spacing corresponds to the basal plane of 1.4 nm -tobermorite, even in Ca/Si -ratios close to 2.[20] However, 1.4 nm -tobermorite and jennite have relatively close spacing and it is impossible to exclude jennite by the XRD evidence.

Silicate elimination from the bridging position has been accounted in the all three models and it is consistent with the measured data. Silicate elimination from the paired silicate tetrahedron according to Kong & Kirkpatrick would produce monomeric silicate which was not measured in the Si-NMR.[24] Removal of the whole dimeric tetrahedrons would produce local environments similar to jennite, which is inconsistent with the current evidence. On the other hand, inelastic neutron spectroscopy has presented that in 8-month hydrated $C_3S$ -paste ~23% of Ca was balanced with OH.[18] This results is in-line with the structure of jennite which has ~33% of calcium balanced with OH, indicating corrugated calcium oxide sheets. In crystallline 1.4 nm -tobermorite, calcium oxide sheets do not have Ca-OH bonds and the value is 0%.

The density of C-S-H in OPC hydration is 2.6–2.7 g/cm$^3$ which is considerable higher than density of pristine 1.4 nm -tobermorite (2.2 g/cm$^3$) or jennite (2.32 g/cm$^3$). In order to presents C-S-H gel which forms in OPC hydration, the density and Ca/Si -ratio of the C-S-H must increase. Elimination of the silicates increases the Ca/Si -ratio but lowers the density as the volume of the crystal cell does not alter. Silicate elimination and addition of calcium to the interlayer fulfils both requirements of Ca/Si -ratio and density.

*Conclusions of the C-S-H models*

It seems unlikely that elimination of whole dreiketten segments is the explanation of the C-S-H gel structure as proposed by Cong & Kirkpatrick. Taylor's and Leqoc & Nonat models differ in the explanation of CaOH in the C-S-H gel structure. According to Taylor's model, CaOH -sites are in the central calcium oxide sheet, corresponding to the Jennite -like structures. According to Leqoc & Nonat model Ca-OH sites are related to the interlayer calcium. Indisputable conclusion cannot be made on the basis of current experimental evidence. Circumstantial evidences can be presented for both models. Density measurements of C-S-H gel favour the calcium addition to the C-S-H interlayer whereas amount of measured CaOH sites (23%) is close to value of Jennite (33%), supporting the model of Taylor.

**C-S-H composition in low-pH concretes**

Low pH concretes have large amounts of pozzolanic materials intermixed with OPC. Pozzolanic materials are considered chemically inert in the beginning of the hydration. Pozzolanic materials

can take part of hydration through their physical appearance and provide additional nucleation sites for hydration products.[46][47] However, physical effects do not change the chemical composition of C-S-H gel. Pozzolanic materials become chemically active when calcium hydroxide begins to precipitate in the hydration. Pozzolanic materials begin to react with calcium hydroxide, forming additional C-S-H gel. As long as calcium hydroxide is present, the forming C-S-H gel is in the equilibrium with calcium hydroxide and the hydration products are similar to pristine OPC hydration products, assuming that there are no local variations in the forming C-S-H gel composition. After all crystalline calcium hydroxide is consumed, pozzolanic materials begin to react with the calcium in C-S-H gel. As a consequence, the Ca/Si -ratio of the C-S-H decreases and the silicate chain polymerisation increases (Figure 17).
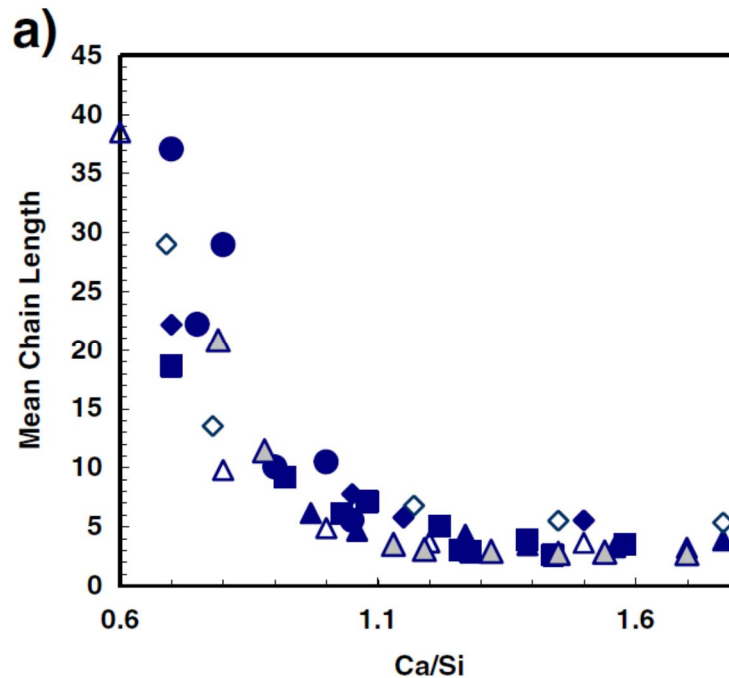


*Figure 5.6.17. Mean chain length and Ca/Si -ratio of C-S-H gel.*[36]

Low Ca/Si -ratio C-S-H can uptake significant amount of alkalis into crystal structure.[35] As a consequence the alkali content of the pore solution also decreases. Lowering of the pore solutions alkali concentration and Ca/Si-ratio of C-S-H gel, the pore solution pH decreases. The pH decrease depends on the amount of pozzolanic materials and also their composition.[20]

*Pozzolans in low-pH concrete*

Pozzolans are defined as materials that can react with crystalline calcium hydroxide and produce hydration products. Various pozzolans have been investigated for low-pH concretes. The most used one is silica fume (SF). Fly ash (FA) is also used commonly. Metakaolin has been also studied.[5] Blast furnace slag (BFS) which is latent hydraulic binder has been also studied in low-pH concretes. BFS has large content of calcium and can provide higher amounts of C-S-H gel than pristine pozzolans. BFS has lower Ca/Si -ratio than pristine OPC hydration products and will therefore also react with calcium hydroxide. Table 5.6.1 presents the chemical compositions of silica fume, fly ash, metakaolin and blast furnace slag.

*Table 5.6.1. Typical composition of low-pH concrete materials.*[13][5]

| | Silica fume | Fly ash (class C) | Fly ash (class F) | Blast furnace slag |
|---|---|---|---|---|
| $SiO_2$ | 94–98% | 30.2–47.9% | 50% | 32–38% |
| $Al_2O_3$ | 0.1–0.4% | 10.7–21.9% | 25% | 10–16% |
| $Fe_2O_3$ | 0.02–0.15% | 4.9–9.9% | 7% | 0.3–9.3% |
| MgO | 0.3–0.9% | 2.9–7.9% | 2% | 3–9% |
| CaO | 0.08–0.3% | 13.3–25% | 6% | 38–44% |
| $K_2O$ | 0.2–0.7% | 0.5–1.0% | 1% | 0.4–1% |
| $Na_2O$ | 0.1–0.4% | 0.2–7.3% | 1% | |
| C | 0.2–1.3% | | | |
| S | 0.1–0.3% | 1.1–12.3% | 0,5% | 1% |
| LOI | 0.8–1.5% | 0.3–1.8% | 4% | 0–1% |

Low-pH concrete binder mix designs are typically classified according to number of the binder components. Binary mix designs have two components, usually OPC and silica fume. Ternary mix designs have three part binder composition, usually OPC, silica fume and fly ash or slag.

*Equilibrium pH*

Pozzolanic material content will determine the final composition of the hydration products and the equilibrium solution composition. The pore solution pH in pozzolanic reaction has schematically similar profile as the leaching process pH development (Figure 5.6.1).[5] At the first stage, solution pH is controlled by the amount of alkalis. In the second stage, pH is controlled by the presence of crystalline calcium hydroxide. When calcium hydroxide is consumed from the mixture and the alkalis are bound into the C-S-H gel structure, the pH is controlled by C-S-H gel. pH is in the equilibrium with the C-S-H gel which Ca/Si -ratio defines the systems pH. As the Ca/Si -ratio of the C-S-H gel decreases, the pH will also decrease. Final pH value of the mixture is attained when all the pozzolanic material has reacted with C-S-H gel or the C-S-H gel becomes to equilibrium with amorphous $SiO_2$.

Cau Dit-Coumes has presented that the $SiO_2$ content of the binder has linear relationship to the equilibrium pH of the solution (Figure 5.6.18). A linear relation seems to be most appropriate at the higher pH -values (> 11). The pH values under 11 are more scattered and ternary, fly ash containing mix designs have higher pH value than binary composition of OPC/silica fume.
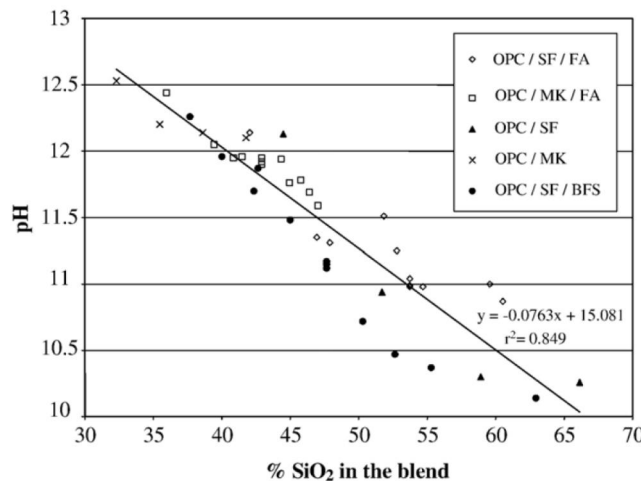


*Figure 5.6.18. The amount of $SiO_2$ in the low-pH binder and the equilibrium pH.*[5]

*Ca/Si -ratio*

Ca/Si-ratio of fully reacted low-pH concretes will be low on the basis of mix designs.[48] In young low-pH concretes, the Ca/Si-ratio of the C-S-H gel will resemble pristine hydrated OPC as the pozzolanic reaction has not yet consumed calcium hydroxide from the matrix. As the concrete ages, lower and lower Ca/Si -ratio C-S-H gel will be formed. The kinetics of the low Ca/Si -ratio C-S-H gel formation is however unclear.

*Kinetics of Ca/Si -ratio development*

Figure 5.6.19 presents pore fluid pH of low-pH concretes in various times.[49] In 91 days, the pore fluid pH lowers rapidly to a certain level which is dependent on the amount of siliceous material. From 91 days forward, the pH remains relatively constant up to two years. The pH in 91 days differs from the equilibrium pH of corresponding Ca/Si -ratio. pH in 91 day samples is significantly higher than corresponding Ca/Si -ratio pH, indicating incomplete reaction degree of siliceous material (Table 5.6.2). Yet, the reaction rate at the beginning is very rapid and is dependent on the amount of pozzolanic material (Figure 5.6.19).
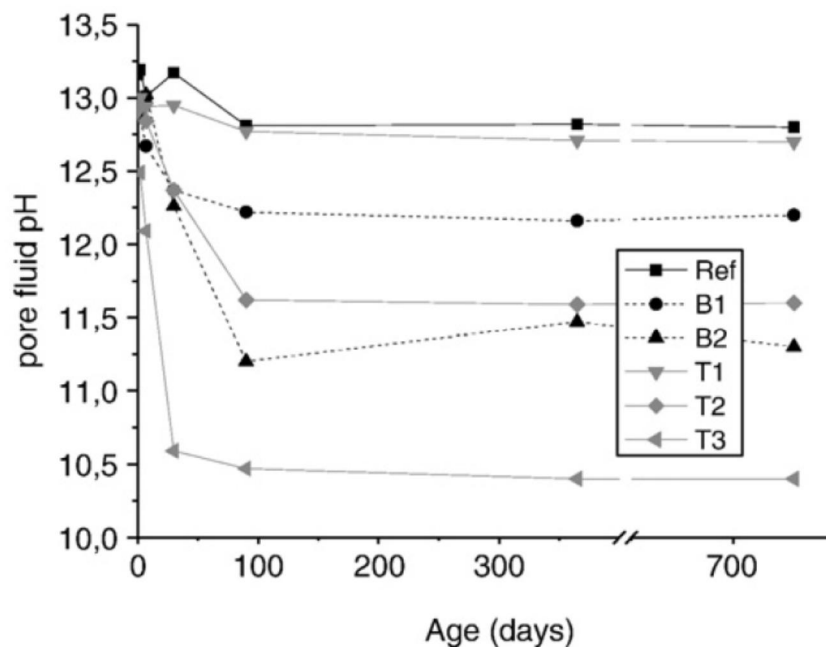


*Figure 5.6.19. Pore fluid pH of various mix designs. Mix design compositions are summarized in Table 5.6.2.*

*Table 5.6.2. Summarized mix designs of low -pH concretes* [49]*, measured pH value after two years and calculated equilibrium pH according to mix designs.*

|      | OPC  | SF  | FA  | Ca/Si | Measured pH | Equilibrium pH according to Ca/Si -ratio |
|------|------|-----|-----|-------|-------------|------------------------------------------|
| ref  | 100% |     |     | 3.71  | 12.9        | >12.5                                    |
| B-1  | 60%  | 40% |     | 0.86  | 12.2        | 10.2–11.5                                |
| B-2  | 50%  | 50% |     | 0.62  | 11.2        | 10                                       |
| T-1  | 80%  | 10% | 10% | 1.87  | 12.6        | 12.5                                     |
| T-2  | 35%  | 35% | 30% | 0.46  | 11.2        | <10                                      |
| T-3  | 20%  | 50% | 30% | 0.24  | 10.5        | <10                                      |

Based on the above described behaviour, it seems that pozzolanic reaction happens through two individual processes which are related to the surface area of pozzolanic materials. Pozzolanic reaction that happens on the surface of siliceous materials is very rapid and enables fast lowering of the pore solution pH within first days. After all available pozzolanic material surfaces become covered with hydration products, the reaction level decreases significantly. Pozzolanic reaction rate in the surfaces is very rapid and changes in pH can be observed on the daily basis. The reaction rate with covered surfaces is very low. Within years perspective changes in pH cannot be observed.

If above presented reaction mechanisms is true, great care must be taken when pozzolanic materials are selected for low-pH concretes as the surface area seems to be the crucial factor in low-pH development.

*Silicate chain*

Experimental research on C-S-H gel nature in low-pH concretes is sparse. Reactive powder concretes have some similarities to low-pH concretes, such as large utilization of pozzolanic materials.[50] Reactive powder concretes have high OPC content and they are usually cured in elevated temperatures which differ from low-pH concretes.

Silicate chains are linear in reactive powder concretes, cured in normal temperatures. Reactive powder concretes, cured at elevated temperatures (200–250 °C) silicate chain branching has been detected. Silicate chain branching in elevated temperatures was related to formation of Xonolite ($Ca_6Si_6O_{17}(OH)_2$), which was confirmed with X-ray diffraction and water loss measurements.[51] However, it is unclear was the formation of Xonolite related high temperature curing or increased level of reactivity of pozzolanic material due the elevated temperature. If latter is the case, then similar silicate chain branching might take also place in low-pH concretes.

The calcium/silicon -ratio of low pH-concretes indicates long silicate chain length in fully reacted low-pH concretes. In fully reacted low-pH concretes, the mean silicate chain length can be up to 10–40 silicate tetrahedrons.[52]

It can be concluded on the basis of reactive powder concretes and Ca/Si -ratio of low-pH concretes that fully reacted low-pH concretes have certainly long silicate chain length and possibly some side branching of the silicate chain.

*Ca-OH Si-OH*

All the described models for C-S-H gel composition and experimental measurements indicate that the C-S-H gel in low Ca/Si -ratios is fully 1.4 nm -tobermorite-like. 1.4 nm -tobermorite-like structures does not have Ca-OH -sites in the structure. On the basis of experimental results, Si-OH sites are present in C-S-H gel with Ca/Si -ratio lower than 1. Depending on the amount of silicate chain branching the amount of SiOH -sites may vary if the branching, will take place from these SiO-sites.

*Effect of other ions*

*Alkali uptake*

C-S-H has varying capability to include alkalis into the structure. In low calcium concentrations and low Ca/Si-ratios alkali uptake is profound. Alkali uptake is related to $SiO^-$ content of C-S-H and the counter ions. In high calcium concentrations, calcium ions dominate the charge balancing sites although the alkali concentrations are significantly higher than calcium concentration. This is due

the bivalent nature of calcium which bonds more firmly into SiO⁻ sites than monovalent alkalis. The Low Ca/Si-ratio C-S-H provides more SiO-sites compared to higher Ca/Si -ratio C-S-H. The maximum Na/Si and K/si ratios reported are in the range of 0.3–0.5.[20][53] Alkali binding to C-S-H is presented in Figure 5.6.20.
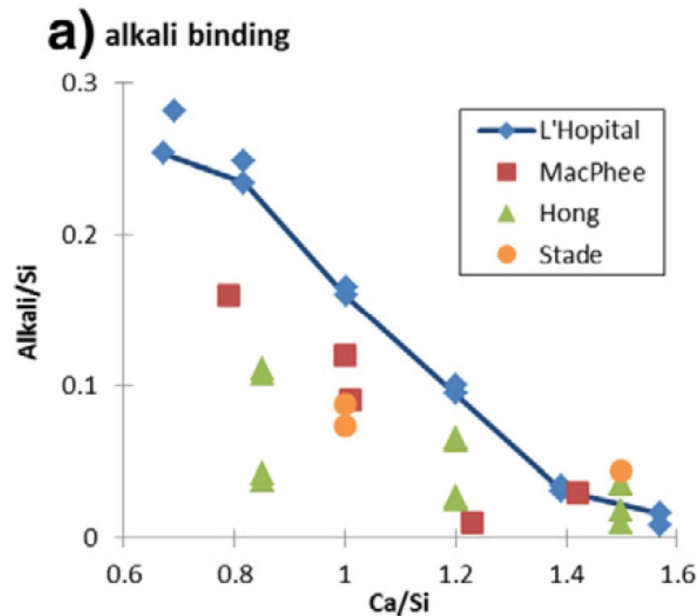


*Figure 5.6.20. Alkali binding of C-S-H with various Ca/Si -ratios.* [20]

Alkali uptake can take place in the interlayer and/or the surface sites of C-S-H. No preferential sites have been reported. However, Na-NMR studies have revealed to two different environments for sodium in C-S-H. First environment is related to broad NMR peak which has been assigned to sodium with low mobility. Another chemical environment is related to sharper NMR-signal which has been assigned to sodium with higher mobility or symmetrically bounded sodium. These are labelled as bound Na and mobile Na, respectively. The fraction of bound sodium is observed to decrease with increasing Ca/Si -ratio in the presence of low sodium concentrations (Figure 5.6.21)[20][54].



*Figure 5.6.21. Sodium population distributions in function of C-S-H Ca/Si-ratio and total Na/Si - ratio.* [20][54]

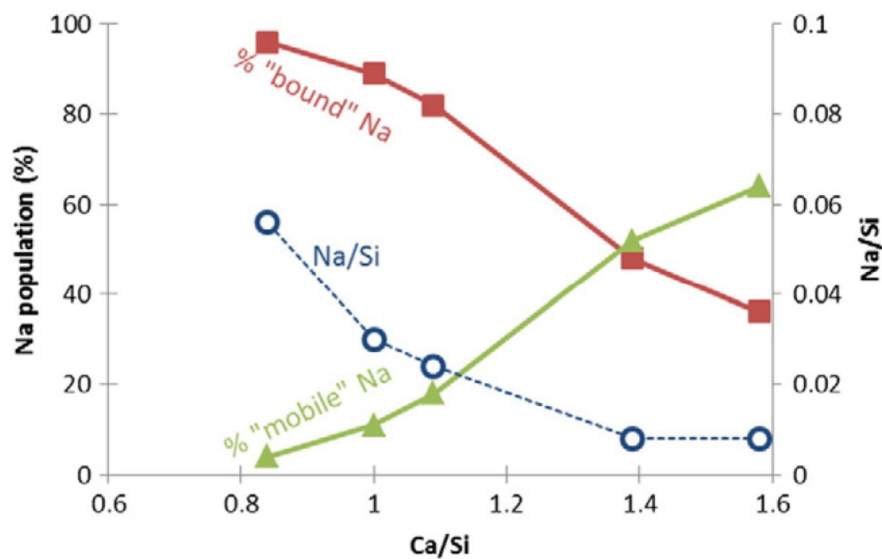Alkali salts are also observed to influence to the silicate chain length. With the presence of alkalis, the silicate chain polymerisation is lower than without alkalis (Figure 5.6.22). It has been suggested that the calcium ions that alkalis replace from charge balancing sites forms additional main calcium oxide layer, increasing the Ca/Si -ratio of the C-S-H main layer although the total Ca/Si -ratio is not altered.
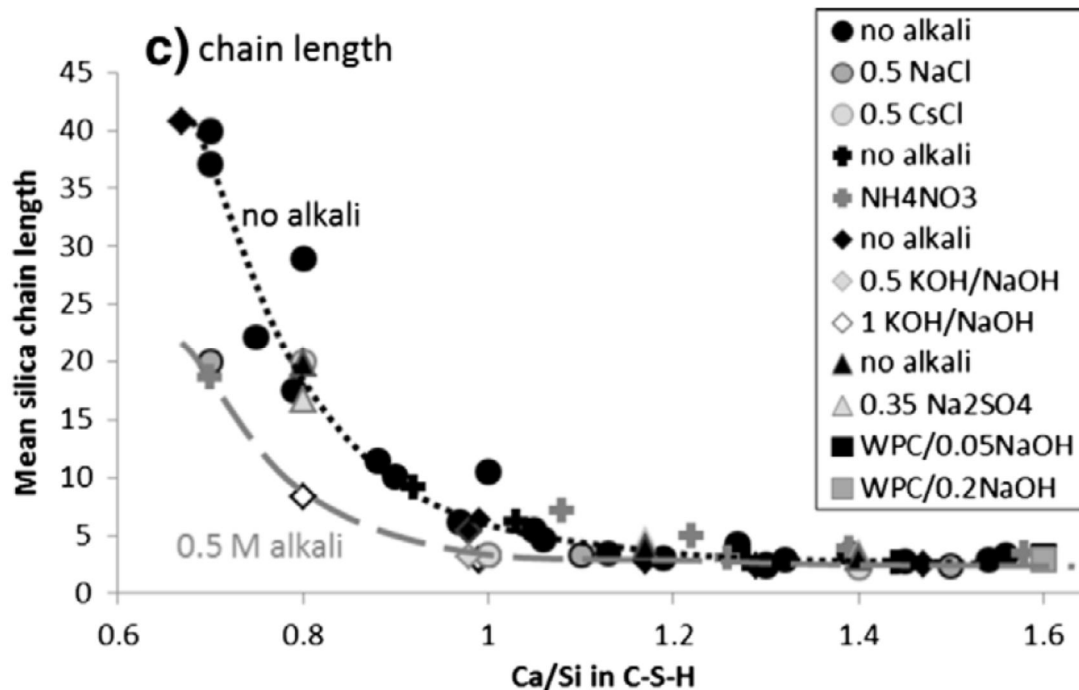


*Figure 5.6.22. Mean silicate chain length in presence of various alkalis.* [20]

The replacement of charge balancing calcium by alkali ions in the C-S-H interlayer, decreases the basal spacing of C-S-H at the lower Ca/Si-ratios.[55][56]

*Aluminium*

C-S-H is able to accommodate substantial amounts of aluminium. Figure 5.6.23 presents the aluminium content of C-S-H and the dissolved aluminium. C-S-H binds the aluminium irreversibly and the lowering of aluminium concentration does not lead automatically to further dissolution of aluminium from the C-S-H structure. This is observation has been also confirmed by ab-initio calculations of the stability of the alumina as the bridging tetrahedron.[57]

*Figure 5.6.23. The amount of dissolved aluminium and the Al/Si -ratio of various C-S-H samples, a) in absence of alkalis and b) in absence and presence of KOH in cements.* [20]

Aluminium can replace silicate tetrahedrons in silicate chain, act as counter-ion in the interlayer (or surface) and replace calcium in the main calcium oxide sheet. Aluminium accommodation is complicated process and depending on the process conditions, the aluminium is found at multiple sites.
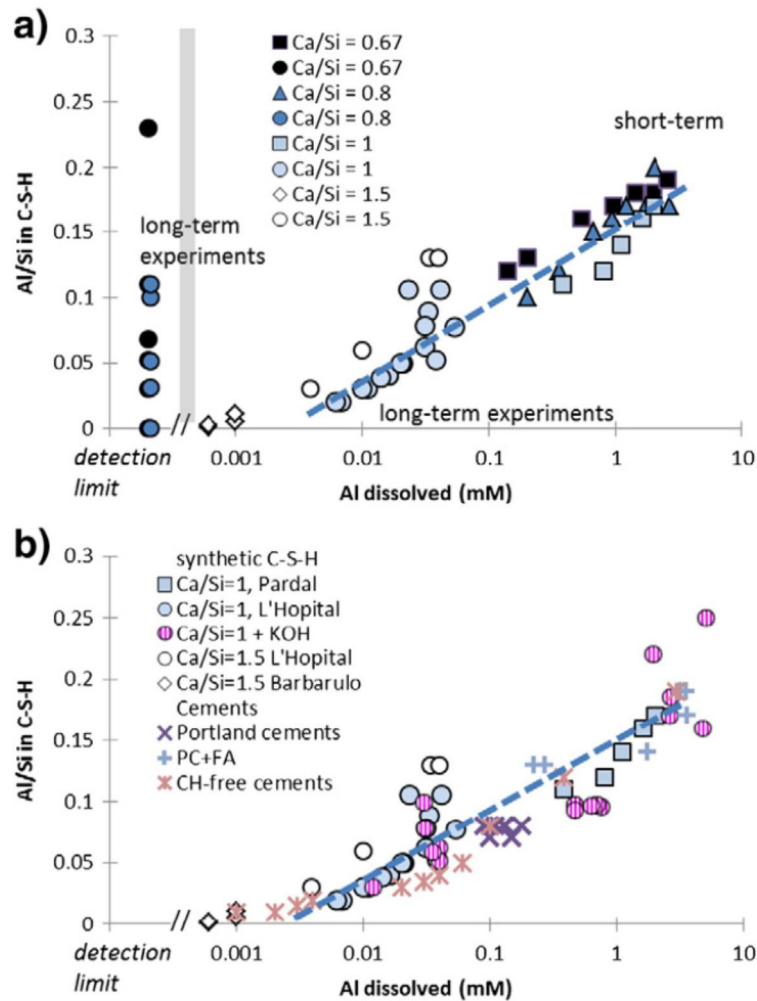
In the low Ca/Si -ratios, C-S-H silicate chains are long providing multiple sites to aluminium to replace silicates in the polymeric chain. In the presence of alkalis as counter-ions, bridging position in aluminium substitution is favoured.[17] In the bridging position, alumina is also able to crosslink the two silicate chains. Crosslinking can take place with two adjacent chains of different layers which structure correspond the structure of Al-tobermorite. Crosslinking can also take place within two adjacent chains of same layer which is more likely in the calcium-aluminate-silicate-hydrates.[55] As Ca/Si -ratio increases, more calcium binding to aluminium is observed. This can take place either by replacement of paired silicate tetrahedrons or bridging position replacement with calcium as counter ion. Exact knowledge of which is more likely is still missing.

In the low Ca/Si -ratio and with low alkali content, lower level of substitution is observed and the replacement of paired silicate tetrahedrons is favoured. Due the electrostatic repulsion, the replacement of two adjacent silicates is not possible, e.g. Al-O-Al -bond in the silicate chain is not stable. Due to this restriction, maximum observed aluminium substitution ratio is 0.22. Higher

replacement ratios are only stable if aluminium replaces bridging tetrahedron and the system is stabilized in the presence of the alkalis.

Aluminium has been also observed to replace silicates in the silica gel which is present in the C-S-H samples with extremely low Ca/Si -ratio. [17]

In the higher Ca/Si -ratios, when C-S-H silicate chains are in dimeric form, aluminium substitution into silicate chains do not take place. Aluminium does not seem to be stable at the end of silicate chain or its immediate neighbourhood. Instead, aluminium incorporation in the central CaO layer has been observed (hexa-coordinated aluminium) with increased basal spacing. Two other hexa-coordinated aluminium phases have been also identified. First one has been observed in the C-S-H samples were AFm-phases has been supersaturated. Second one is attributed to an amorphous alumina hydrate associated with the C-A-S-H. This phase is called third aluminium hydrate (TAH).[20][58]

Aluminium has been also found to exist in the interlayer at the charge balancing ion (penta-coordinated aluminium). The amount of penta-coordinated aluminium is approximately 10% and is independent of Ca/Si -ratio. However, more information on the role of penta- and hexa- coordinated aluminium is still needed. Figure 5.6.24 presents the amount of variously bound aluminium.
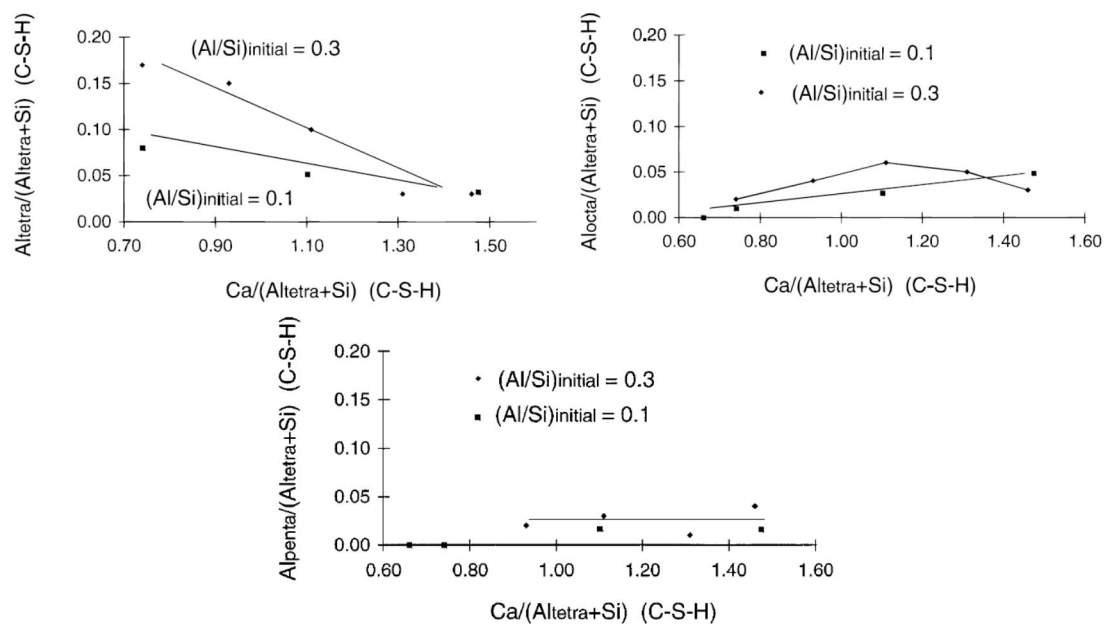


*Figure 5.6.24. The amount of variously coordinated aluminium in C-S-H.* [17]

**Leaching**

In long-term nuclear repository low-pH concretes are exposed to groundwater. As the groundwater constantly flows, the concrete experiences a leaching process. Flow rates of groundwater might not be large but long lifetime of the repository makes the leaching process significant. Hardened Portland cement is a soluble material that equilibrates with the pore solution. Solubility of the hardened Portland cement phases will determine the composition of the pore solution. As pore solution is constantly interacting with the surrounding groundwater, more hardened OPC phases will dissolve to maintain chemical equilibrium. Eventually leaching causes degradation of the hardened Portland cement matrix.[9] [31]

*Leaching of OPC*

Various stages of leaching are known and the schematic dissolution of sulphate resistant OPC is presented in Figure 5.6.1. First phases that will dissolve are the alkalis that causes pH values above saturation pH of portlandite (pH > 12.4). Second step is the dissolution of the portlandite, followed by the incongruent dissolution of calcium-silicate-hydrates. When congruently dissolving calcium-silicate-hydrates are formed, the pH will remain constant as long as calcium-silicate-hydrates are present in the Portland cement matrix.[31][9]

Besides alkalis, calcium hydroxide and C-S-H gel, also other OPC phases will dissolve. Apart from the dominant C-S-H gel and calcium hydroxide, a partly independent minerals containing calcium, iron, aluminium and sulphur will also dissolve. The two dominant groups of alumina ferrites are called Aluminium-Iron-tri (Aft) and Aluminium-Iron-mono (AFm). Tri- and mono- are referring to the single formula unit of $CaX_2$ where X can denote $OH^-$, $\frac{1}{2}SO_4^{2-}$, $Cl^-$ and $\frac{1}{2}CO3_{-2}$. Ettringite $[Ca_3Al(OH)_6*12H_2O]_2*(SO_4)_3*2H_2O$ is dominant phase of AFt and monosulphate $Ca_3Al_2O_6*CaSO_4*12H_2O$ is the dominant phase of AFm in normal hydrated OPC. In non-equilibrium conditions, ettringite is stable in pH above 10.7. In similar conditions monosulphate is stable in pH > 11.7.[59]

As pH lowers below 11.7, the monosuphate will decompose into ettringite and calcium aluminate hydrate (hydrogarnet). At the pH 10.5, Ettringite will decompose to sulphates and metal hydroxides. It has been observed that in dynamic dissolution, decomposed sulphates from ettringite will form additional ettringite in the inner region of the leaching concrete due the higher pH of the inner region. This process creates inward moving boundary of sulphates. Similar inward movement of calcium hydroxide has been also observed. Inward movement of ettringite and calcium hydroxide develops a dense zone inside the leaching concrete. [59]

Ettringite is not a highly stable mineral. High temperature or large alkali concentrations can cause the degradation of the ettringite. High chloride concentrations can cause formation of Friedel's salt which is an AFm phase. Large amount of carbonates in the leaching phase can cause formation of thaumasite $[Ca_3Si(OH)_6*12H_2O](SO_4)(CO_3)$ at a low temperature environment.[59]

*Alteration zone*

Leaching of OPC happens through alteration zone where the chemical processes takes place (Figure 5.6.25). Alteration zone can be defined as the region between intact cement paste and groundwater. In the alteration zone, leached ions transport outwards from intact cement paste but also ions are transported into alteration zone due the charge balance requirement. Transport rate of these ions determines the overall leaching rate.

Transport rate on the ions in alteration zone are controlled by multiple factors. Rate of the pure diffusion of the ions is controlled by the concentration gradient of intact cement paste pore solution and the leaching water, and the ionic mobilities of the ions. The rate of the leaching is dependent on the movement of whole ion ensemble because the electroneutrality must be maintained throughout the leaching process. It has been observed that chlorides in the leaching solution increase the leaching rate. Chloride can charge balance rapidly the outward movement of hydroxide ions enabling higher dissolution rate. [59][60]
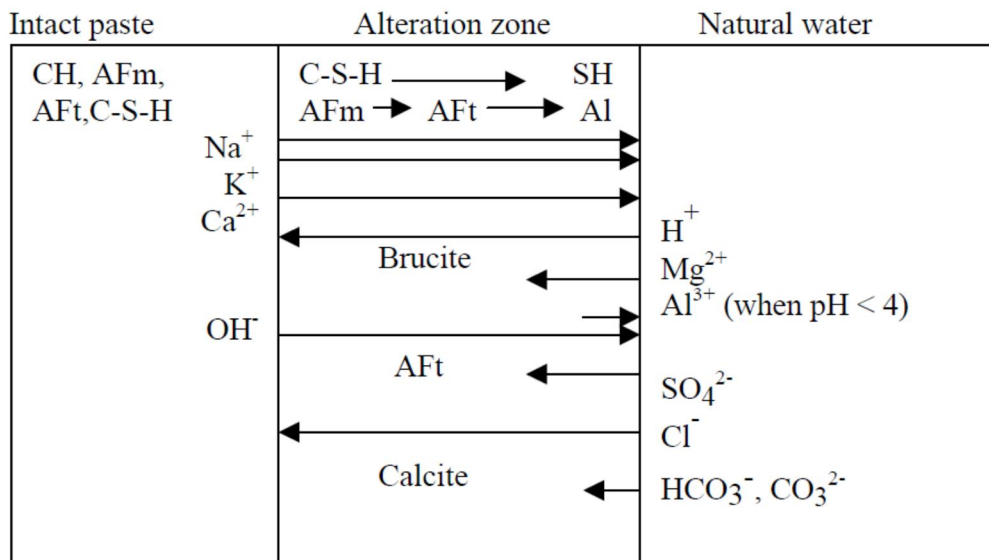
*Figure 5.6.25. Schematic presentation of ion movement and precipitation at the cement paste in the alteration zone.* [59]

Physical structure of the alteration zone affects the leaching rate. The structure of leaching concrete has three types of porosity that is relevant to the ion diffusion. The porosity consist gel porosity, initial porosity and porosity formed by material dissolution. Gel porosity has insignificant effect when compared to latter two porosities. Initial porosity depends on the concrete quality and the degree of hydration. Diffusion mainly occurs throughout the connected capillary pores which amount depends mainly on the water/cement -ratio of the concrete. It has been estimated that capillary porosity becomes connected at the porosity volume 18%. The main formed porosity will consist of dissolved calcium hydroxide volume. It has been estimated that calcium hydroxide induced porosity becomes connected with porosity volume 12–15%.[59]

In dense concretes, very narrow capillary pores exists which make the surface effects significant. Surfaces are covered with oriented water molecules with the electric double layers, reducing further the volume where free diffusion can take place.

Alteration zone is not a homogeneous phase but have large diversity of various zones. These zones are presented schematically in the Table 5.6.3, based on real leached concrete structures.

*Table 5.6.3. Schematic interpretation of zonal patterns in the leached concrete and their chemical characteristics.* [60][59]

| | Zone 1 | Zone 2 | Zone 3 | Zone 4 | Zone 5 | Zone 6 |
|---|---|---|---|---|---|---|
| Phases | Calcite Silica-gel Hydroxides | Silica-gel Calcite Hydroxides | Silica-gel /C-S-H Hydroxides | C-S-H (2) Ettringite | C-S-H (1) Ettringite (Cement) | C-S-H CH Ettringite (Cement) |
| $Al_2O_3$ | High | Medium | low | low | low | low |
| *MgO | High | Medium | Low | None | None | None |
| *$CaO/SiO_2$ | < 0.1 | < 0.5 | 0.5–1.0 | Around 1 | 1.0–1.6 | 1.6–1.7 |
| [Ca] mmol/kg | low | < 2 | < 4 | < 10 | 10–20 | >20 |
| [Si] mmol/kg | 1.5 | 4.2 | 1.5 | 1.5 | <1 | <1 |
| pH | 7 | Around 10 | 10.0–10.5 | > 10.5 | 10.5–12.4 | > 12.4 |
| Porosity | Low | Medium | High | Medium | Low | Very Low |

202

*Shell formation*

Leaching rate is a combination of physical and chemical processes as above has been described. Various studies have been conducted which simulates the leaching process. These studies are performed either in distilled water or the leaching is accelerated by increasing acidity of the leachate. It has been observed that a shell of silica and various metal hydroxides is formed at the leaching boundary. The development of this shell was a controlling factor in the rate of the leaching. The pH of the leachate was not prominent in neutral and basic leachates. At the leachate pH below 4, components of the shell become soluble affecting the total leaching rate. If carbonates are present in the leaching solution, calcite was observed to form similar shell.[59][61][62]

*Silicon transport*

Silicon transportation in the OPC leaching is particularity interesting as it presents the complexity of the leaching process. In pore solution with pH > 10.5, silica is not highly soluble due the high calcium concentration of the pore solution. As the pH lowers < 10.5, silica becomes more soluble due the depletion calcium content. As dissolved silica, in ionic form $HSiO_3^-$, diffuses towards the leaching boundary where it encounters pore solution with pH < 10. The solubility of the silica decreases. As a result, silica gel precipitates on the leaching boundary and will affect the leaching rate as above have been described.[59]

*Leaching rate*

Leaching is dependent on the ion diffusion between bulk leaching solution and intact cement paste. Attempts to calculate the leaching rate has been performed.[63][59] Leaching rate has been estimated on the basis of Fick's second law of diffusion and various parameters to include the solid structure. Equation 1 presents the formula for relative diffusivity through alteration zone.

$$D/D_0 = 0{,}025 - 0{,}07\varphi_i^2 - H(\varphi_i - 0{,}18) * 1{,}8(\varphi_i - 0{,}18)^2 + 0{,}14\varphi_l^2 - H(\varphi_l - 0{,}16) * 3{,}6(\varphi_l - 0{,}16)^2$$
*(Equation 1.)*

Where, $D/D_0$ = relative diffusivity ($D_0$ diffusivity of pure water $0.8*10\text{-}9$ $m^2$/s, $\varphi_i$ = water porosity in initial paste, $\varphi_l$ = water porosity after leaching.

*Leaching of low-pH cement*

Low-pH cement leaching is not widely studied. It can be assumed that leaching of low-pH concrete is similar to normal concrete leaching, with the exception that low-pH cements have lower Ca/Si - ratio of the C-S-H gel in the long-term. The leaching low-pH cement system can be divided to two extreme cases and the actual leaching scenario is something between the two extremes. First extreme is the dissolution at the young ages where the pozzolanic reaction has not yet significantly proceeded. This system consists of hydrated Portland cement mixed with large amount of amorphous silica. Second extreme is the dissolution of the matured low-pH cement where the pozzolanic material has reacted with calcium hydroxide and lowered the Ca/Si-ratio of C-S-H gel. This system consists of low Ca/Si -ratio C-S-H gel and other hydration products that are stable in that environment. Unreacted pozzolans are present, or not in the mixture.

The leaching at the young ages is very similar to normal OPC leaching except the solution remains saturated respect to silicon. The effect of saturated silicon needs to be studied as the calcium leaching in saturated silicon solution might cause formation of secondary C-S-H. Any solid conclusions cannot be made on without experimental studies.

The leaching of the matured low-pH cement has also pending uncertainties. A large difference is the dissolution behaviour of various Ca/Si -ratio C-S-H. The following chapter summarizes the current understanding of the leaching of C-S-H at the various Ca/Si-ratios.

*The Ca/Si-ratio effect on the C-S-H gel leaching*

The Ca/Si -ratio of the C-S-H determines the dissolution behaviour. Incongruent dissolution of C-S-H with the Ca/Si -ratio higher than 0.9 mainly dissolves calcium from the C-S-H structure. Higher the Ca/Si -ratio, more calcium is respectively dissolved (Figure 5.6.26). Incongruent dissolution of C-S-H with Ca/Si -ratio lower than 0.8 will dissolve more silicon compared to congruent dissolution of the C-S-H. The Ca/Si -ratio increases as a result leaching of pristine water in low Ca/Si -ratio C-S-H. Congruent dissolution of the pristine C-S-H takes place in Ca/Si -ratio between 0.8–0.9. The pH of the C-S-H is proportional to the Ca/Si -ratio. Equilibrium pH of congruently dissolving C-S-H is 10.6 in pristine water (Figure 5.6.27). Depending on the low-pH cement Ca/Si -ratio, leaching behaviour will differ and in some cases even pH increase throughout leaching is possible. [31]
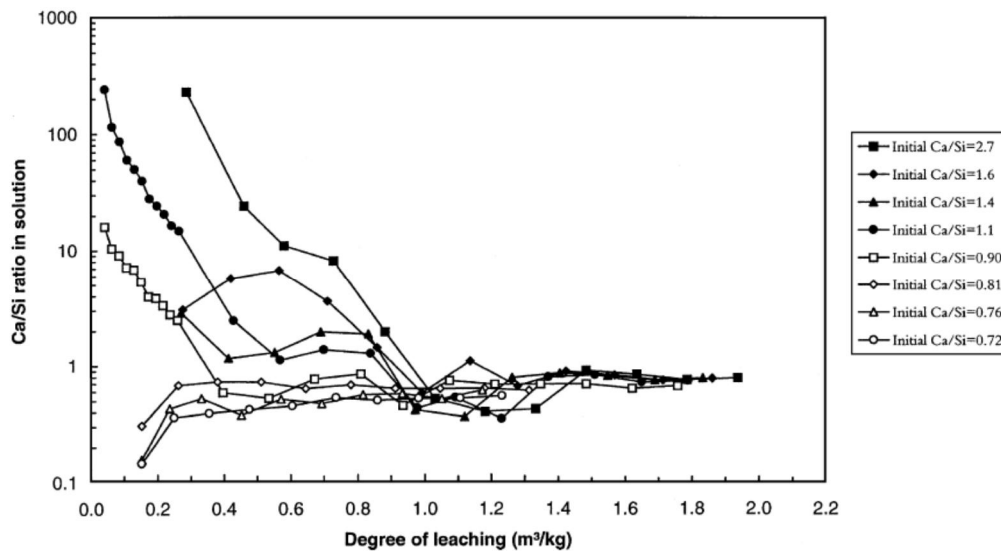


*Figure 5.6.26. The Ca/Si -ratio in the solution and the leachate volume with C-S-H with various initial Ca/Si -ratios.* [31]
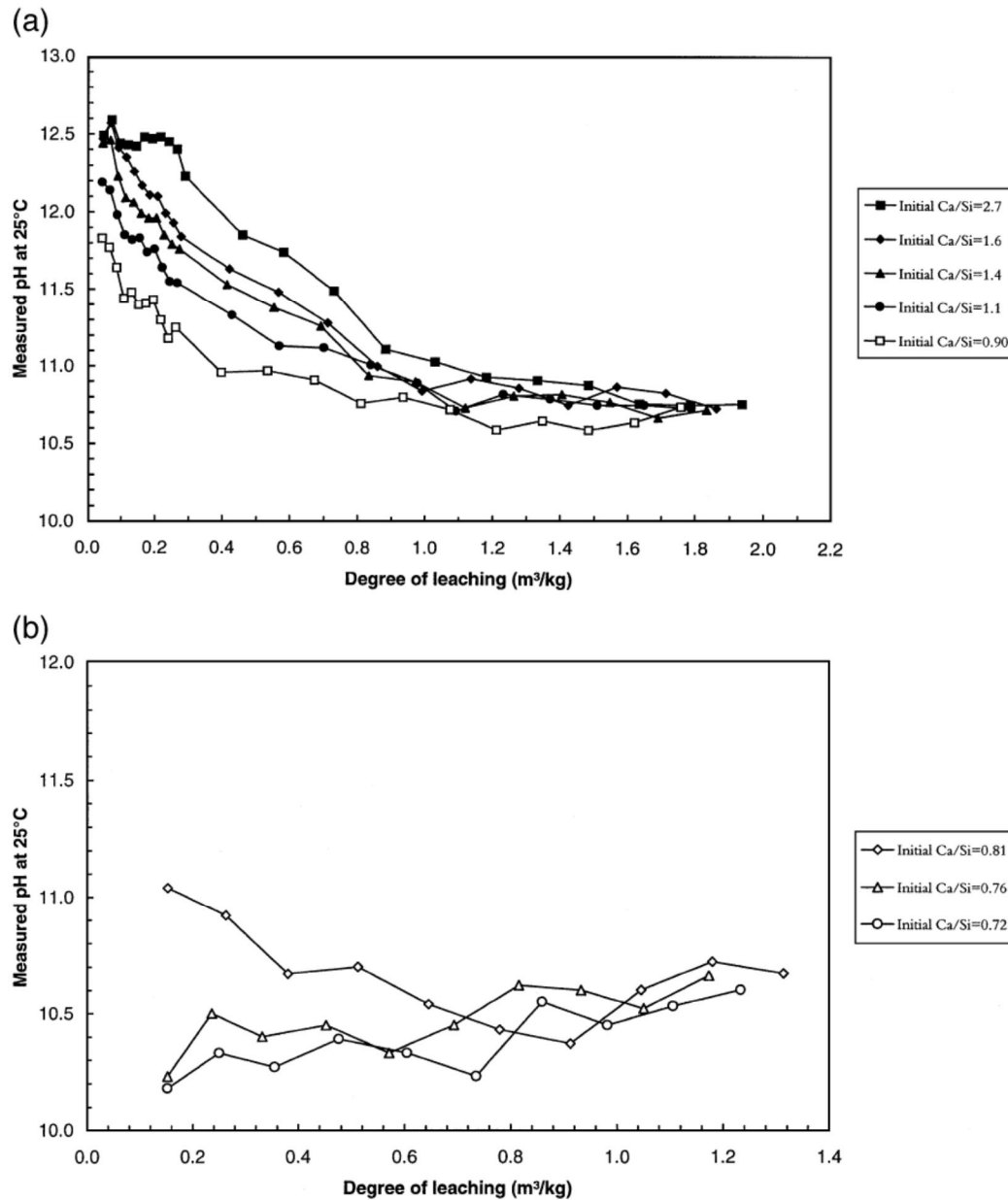
*Figure 5.6.27. pH of the leaching solution and the leachate volume with various Ca/Si -ratio of C-S-H.* [31]

However, information of pristine C-S-H leaching behaviour is not enough to reliably estimate the leaching behaviour of low-pH concrete. Multiple simultaneously affecting factors and potential re-precipitation of hydration products makes the real leaching scenario difficult to predict. One large factor is the effect of non-reacted silicates. Do they act as inert material or do they hinder the dissolution of certain phases due the saturation of silicon in the pore solution is unknown. The solution compositions are affected by the solid phase and vice versa.

**Groundwater effect**

The third factor that will affect the pH of the low-pH cementitious materials is the groundwater composition. If groundwater includes ions that will dissolve from the cementitious phase, the dissolution becomes limited. As the dissolution becomes limited, also the amount of dissolving hydroxyl -ions will lower and the pH will be lower than in pristine water. This effect is usually

described as common ion effect. The common ion effect can have large effect on the solutions pH. Figure 5.6.28 presents the pH of low-pH concrete in ion-exchanged water and in Olkiluoto groundwater. The difference of the solution pH is almost one unit. This effect might be critical when the pH of low-pH concrete system is evaluated in the nuclear waste repository environment. [48]
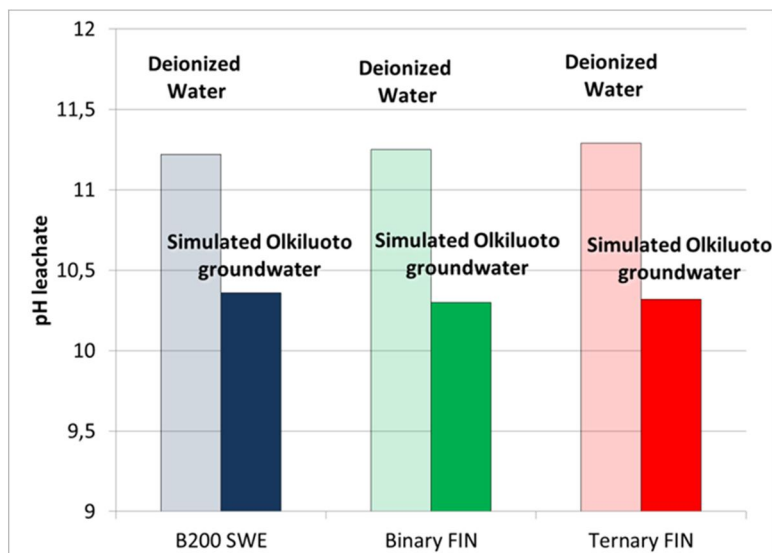


*Figure 5.6.28. pH of the identical solid low-pH concrete sample measured in deionized water and simulated olkiluoto groundwater. [6]*

Groundwater composition can also have an effect on composition of solid phases. Magnesium uptake has been reported in the low Ca/Si -ratio C-S-H gels which were submerged in magnesium containing water. Magnesium was included into C-S-H structure or even forming a new phase of magnesium-silicate-hydrates.[49]

## C-S-H in nuclear waste repositories

The constructed long-term nuclear waste repositories will have extremely long lifetime. The lifetime expands over timeline which none of the current infrastructure materials have encountered. Some indications of concrete stability with the timeline can be gained by studying old structures. Oldest structures that have been constructed with modern cements are over hundred years old whereas similar hydration products have been used since Roman times.

*Long-term stability of OPC and low-pH concretes*

Modern cements have been used for one hundred years. During that time the composition of the OPC has not altered, although today's cements are more finely-graded than the cements used hundred years ago.[59] Hundred year old concrete structures have been studied and the effect of constant leaching has been estimated. Lagerblad et al. has studied old concrete water basins which were cast during years 1910–1960.[59] These studies have been able to improve understanding of leaching process and the significance of precipitation of secondary minerals in the concrete crust. [64] However, the crystalline composition of the concrete was not altered and little new information of long-term behaviour was gained. At the moment, we can reliably estimate the durability and the chemical processes of OPC in hundred year perspective.

Hydraulic binders have been utilized since Roman times and the study of Roman constructions has been performed in order to gain information of the concrete structures durability in two thousand

years perspective.[65][66][67] The composition of Roman hydraulic binders differs from modern OPC but they still have major similarities. Roman binders consist from quicklime, volcanic ashes and various pyroclastic rocks. Modern OPC consist of artificially made calcium silicates with minor various ingredients. Main elements in Roman binders and modern OPC are calcium, alumina and silicates. Studied Roman mortars had calcium content $\leq 10\%$, alumina ~15% and silicates ~50%. In modern OPC, calcium content is typically 60%, silicates 20% and alumina < 5%. Roman binders have significantly lower Ca/(Si+Al) -ratio compared to modern OPC. In that respective, the elemental composition of Roman binders resembles today's low-pH cements rather than pristine OPC. The difference between low-pH cements and Roman binders is the significantly higher alumina content of the Roman binders.[68]

Reaction products of Roman binders were mixture of crystalline of Al-tobermorite and C-A-S-H gel. According to researcher's analysis, the formation of Al-tobermorite was not related aging of the binder but the Al-tobermorite was formed in relatively early-ages. Al-tobermorite was formed in the early-ages were the temperature of the mortar was sufficient to crystallization of Al-tobermorite. C-A-S-H gel seems to be highly stable which enables C-A-S-H presence in two thousand year old samples in aggressive maritime environment. C-A-S-H gel and crystalline Al-tobermorite had same chemical composition. The difference of the C-A-S-H and Al-tobermorite was related to the coordination of aluminium tetrahedrons. Al-tobermorite had a double silicate chain structure where aluminium acted as bridging tetrahedron between two silicate chains. Also the polymerisation degree of the Al-tobermorite was high. C-A-S-H had aluminium in tetrahedral and octahedral coordination with strong heterogeneities in 25 nm scale. [68]

High stability of C-A-S-H was hypothesised to originate from charge balancing stability of the silicate chain interlayer. Al-O -bonds are 8–10% longer than Si-O bonds -which enabled effective accommodation of charge balancing cations in the interlayer. Aluminium substitution also increases the negative charge balance of silicate chains and silanol binding capacity. This increases the irreversible binding of charge balancing cations and causes improved resistance to chemical attacks compared to pure C-S-H gels.

It remains to be seen, is the aluminium role vital in longevity of C-(A)-S-H gels. Studies related to the role of aluminium in polymerisation of silicate chains has demonstrated that aluminium prefers sites of bridging octahedral and increases effectively the polymerisation degree of the silicate chains. In that respective, the role of aluminium in low-pH binder longevity should be studied.

*Pending topics*

According to current research review and the previously done research, some topics needs to be further studied to understand the behaviour of the low-pH concrete in the repository. Although lot of research has been conducted, the kinetics of the pozzolanic reaction is sparsely studied. In order to evaluate the development of the alkaline plume, the kinetics of the pozzolanic reactions must be defined. Also the leaching of low-pH concrete is a subject of limited study and understanding.

The long-term stability of low-pH concrete has not been throughout analysed. There might be processes that have not yet been recognised but have a large influence on the low-pH concrete stability. One of these subjects is the combined effect of alumina ferrite phases and the pH development of the low-pH concrete. It is generally known fact that Aft phases will transform to AFm phases during the concrete maturing process but the pH development favours the Aft stability as it is stable at the lower pH -values. This might lead to similar AFm $\rightarrow$ Aft transformation which is encountered in delayed ettringite formation.

# References

[1] "www.posiva.fi." .

[2] W. Report, "Facility Description 2012 Summary Report of the Encapsulation Plant and Disposal Facility Designs," *Posiva Oy*, no. October 2013, 2012.

[3] K. Koskinen, "Effects of Cementitious Leachates on the EBS," *Posiva Oy*, vol. 31, no. January, 2014.

[4] D. Savage, "SKI Report 2007 : 32 Low pH Cements," *Ski Rep. 200732*, no. May, 2007.

[5] C. Cau Dit Coumes, S. Courtois, D. Nectoux, S. Leclercq, and X. Bourbon, "Formulating a low-alkalinity, high-resistance and low-heat concrete for radioactive waste repositories," *Cem. Concr. Res.*, vol. 36, no. 12, pp. 2152–2163, 2006.

[6] E. Holt, M. Leivo, and T. Vehmas, "Low-pH concrete developed for tunnel end plugs used in nuclear waste containment," in *concrete Innovation Conference (CIC2014)*, 2014.

[7] C. Vogt, B. Lagerblad, K. Wallin, F. Baldy, and J.-E. Johansson, "Low pH self compacting concrete for deposition tunnel plugs," Stockholm, 2009.

[8] J. Martino, D. Dixon, B. Holowick, and C.-S. Kim, "Enhanced sealing project (ESP) Seal Construction and Instrumentation report," 2011.

[9] U.-R. Berner, "Evoliution of pore water chemistry during degradation of cement in a radioactive waste repository environment," *Pergamon Press. Elsevier*, vol. 12, pp. 201–219, 1992.

[10] M. Snelman and T. Vieno, "Long-term safety aspects of the use of cement in a repository for spent nuclear fuel," in *2nd low pH workshop*, 2005, pp. 27–40.

[11] J. J. Chen, J. J. Thomas, H. F. W. Taylor, and H. M. Jennings, "Solubility and structure of calcium silicate hydrate," *Cem. Concr. Res.*, vol. 34, no. 9, pp. 1499–1519, 2004.

[12] I. G. Richardson, "The calcium silicate hydrates," *Cem. Concr. Res.*, vol. 38, no. 2, pp. 137–158, 2008.

[13] H. F. W. Taylor, *Cement Chemistry*, 2nd ed. London: Thomas Telford Publishing, Thomas Telford Services Ltd, 1997.

[14] I. G. Richardson, "The calcium silicate hydrates," *Cem. Concr. Res.*, vol. 38, pp. 137–158, 2007.

[15] "www.mpi.stonybrook.edu/people/LawrieSkinner/index.html." .

[16] L. B. Skinner, S. R. Chae, C. J. Benmore, H. R. Wenk, and P. J. M. Monteiro, "Nanostructure of calcium silicate hydrates in cements," *Phys. Rev. Lett.*, vol. 104, no. 19, pp. 1–4, 2010.

[17] P. Faucon, a Delagrave, J. C. Petit, C. Richet, J. M. Marchand, and H. Zanni, "Aluminum Incorporation in Calcium Silicate Hydrates ( C-S-H ) Depending on Their Ca / Si Ratio," *J. Phys. Chem. B*, vol. 103, pp. 7796–7802, 1999.

[18] J. J. Thomas, J. J. Chen, and H. M. Jennings, "Ca-OH bonding in the C-S-H gel phase of tricalcium silicate and white portland cement pastes measured by inelastic neutron scattering," *Chem. Mater.*, vol. 15, no. 20, pp. 3813–3817, 2003.

[19] X. Cong and R. J. Kirkpatrick, "29Si MAS NMR study of the structure of calcium silicate hydrate," *Adv. Cem. Based Mater.*, vol. 3, no. 3–4, pp. 144–156, 1996.

[20] B. Lothenbach and A. Nonat, "Calcium silicate hydrates: Solid and liquid phase composition," *Cem. Concr. Res.*, vol. 78, pp. 57–70, 2015.

[21] I. G. Richardson, "Nature of the hydration products in hardened cement pastes," *Cem. Concr. Compos.*, vol. 22, no. 2, pp. 97–113, 2000.

[22] L. S. Dent Glasser, E. E. Lachowski, M. Y. Qureshi, H. P. Calhoun, D. J. Embree, W. D. Jamieson, and C. R. Masson, "Identification of some of the polysilicate components of trimethylsilylated cement paste," *Cem. Concr. Res.*, vol. 11, no. 5–6, pp. 775–780, Sep. 1981.

[23] J. Hirljac, Z.-Q. Wu, and J. F. Young, "Silicate polymerization during the hydration of alite," *Cem. Concr. Res.*, vol. 13, no. 6, pp. 877–886, Nov. 1983.

[24] A. Nonat, "The structure and stoichiometry of C-S-H," *Cem. Concr. Res.*, vol. 34, no. 9, pp. 1521–1528, Sep. 2004.

[25] H. F. W. TAYLOR, "Proposed Structure for Calcium Silicate Hydrate Gel," *J. Am. Ceram. Soc.*, vol. 69, no. 6, pp. 464–467, Jun. 1986.

[26] V. Ramachandran, R. Feldman, and J. Beaudoin, "No Title," *Concr. Sci.*, p. 427, 1981.

[27] H. F. W. Taylor, "Nanostructure of C-S-H: current status," *Adv. Cem. Based Mater.*, vol. 1, pp. 38–46, 1993.

[28] A. J. Allen, J. J. Thomas, and H. M. Jennings, "Composition and density of nanoscale calcium-silicate-hydrate in cement." *Nat. Mater.*, vol. 6, no. 4, pp. 311–316, 2007.

[29] H. F. W. Taylor, "Proposed structure for calcium silicate hydrate gel," *J. Am. Ceram. Soc.*, vol. 69, no. 6, pp. 464–467, 1986.

[30] S. Grangeon, F. Claret, Y. Linard, and C. Chiaberge, "X-ray diffraction: A powerful tool to probe and understand the structure of nanocrystalline calcium silicate hydrates," *Acta Crystallogr. Sect. B Struct. Sci. Cryst. Eng. Mater.*, vol. 69, no. 5, pp. 465–473, 2013.

[31] A. . Harris, M. . Manning, W. . Tearle, and C. . Tweed, "Testing of models of the dissolution of cements—

leaching of synthetic CSH gels," *Cem. Concr. Res.*, vol. 32, no. 5, pp. 731–746, May 2002.

[32] D. Heidemann and W. Wieker, "Charaterization of protons in C-S-H phases by means of high-speed 1H MAS NMR investigations," in *Nuclear magnetic resonance spectroscopy of cement-based materials*, Berlin: Springer, 1998, pp. 169–180.

[33] R. Rassem, H. Zanni-Théveneau, D. Heidemann, and A. R. Grimmer, "Proton high resolution solid state NMR study of C3S hydration," *Cem. Concr. Res.*, vol. 23, no. 1, pp. 169–176, Jan. 1993.

[34] I. Klur, B. Pollet, J. Virlet, and A. Nonat, "C-S-H structure evolution with calcium content by multinuclear NMR," in *Nuclear magnetic resonance spectroscopy of cement-based materials*, Berlin: Springer, 1998, pp. 199–141.

[35] S. Hong and F. P. P. Glasser, "Alkali binding in cement pastes Part I. The C-S-H phase," *Cem. Concr. Res.*, vol. 29, no. 12, pp. 1893–1903, 1999.

[36] B. Lothenbach and F. Winnefeld, "Thermodynamic modelling of the hydration of Portland cement," *Cem. Concr. Res.*, vol. 36, no. 2, pp. 209–226, Feb. 2006.

[37] R. Barbarulo, H. Peycelon, and S. Leclercq, "Chemical equilibria between C–S–H and ettringite, at 20 and 85 °C," *Cem. Concr. Res.*, vol. 37, no. 8, pp. 1176–1181, Aug. 2007.

[38] I. . Richardson, "The nature of C-S-H in hardened cements," *Cem. Concr. Res.*, vol. 29, no. 8, pp. 1131–1147, Aug. 1999.

[39] J. E. Rossen, B. Lothenbach, and K. L. Scrivener, "Composition of C-S-H in pastes with increasing levels of silica fume addition," *Cem. Concr. Res.*, vol. 75, pp. 14–22, 2015.

[40] I. G. Richardson and G. W. Groves, "Microstructure and microanalysis of hardened ordinary Portland cement pastes," *J. Mater. Sci.*, vol. 28, no. 1, pp. 265–277.

[41] J. J. Thomas, H. M. Jennings, and A. J. Allen, "Relationships between composition and density of tobermorite, jennite, and nanoscale CaO-SiO2-H2O," *J. Phys. Chem. C*, vol. 114, no. 17, pp. 7594–7601, 2010.

[42] A. C. A. Muller, K. L. Scrivener, A. M. Gajewicz, and P. J. McDonald, "Densification of C-S-H measured by 1H NMR relaxometry," *J. Phys. Chem. C*, vol. 117, no. 1, pp. 403–412, 2013.

[43] Webmineral, "Jennite mineral data." [Online]. Available: http://webmineral.com/data/Jennite.shtml#.VrnzdU1PrDA. [Accessed: 09-Feb-2016].

[44] G. Renaudin, J. Russias, F. Leroux, F. Frizon, and C. Cau-dit-Coumes, "Structural characterization of C-S-H and C-A-S-H samples-Part I: Long-range order investigated by Rietveld analyses," *J. Solid State Chem.*, vol. 182, no. 12, pp. 3312–3319, 2009.

[45] P. Rejmak and J. S. Dolado, "29Si NMR in Cement: A Theoretical Study on Calcium Silicate Hydrates," *J. Phys. Chem.*, vol. 116, no. 17, pp. 9755–9761, 2012.

[46] J. J. Thomas, H. M. Jennings, and J. J. Chen, "Influence of nucleation seeding on the hydration mechanisms of tricalcium silicate and cement," *J. Phys. Chem. C*, vol. 113, no. 11, pp. 4327–4334, 2009.

[47] T. Vehmas and A. Kronlöf, "A study of Early-age ordinary portland cement hydration according to autocatalutic reaction model," in *Norsk betongforeningen*, 2011, pp. 269–272.

[48] E. Holt, M. Leivo, and T. Vehmas, "Low-Ph Concrete Developed for Tunnel End Plugs Used in," 2014.

[49] J. L. Garc??a Calvo, A. Hidalgo, C. Alonso, and L. Fern??ndez Luco, "Development of low-pH cementitious materials for HLRW repositories. Resistance against ground waters aggression," *Cem. Concr. Res.*, vol. 40, no. 8, pp. 1290–1297, 2010.

[50] A. Loukili, A. Khelidj, and P. Richard, "Hydration kinetics, change of relative humidity, and autogenous shrinkage of ultra-high-strength concrete," *Cem. Concr. Res.*, vol. 29, no. 4, pp. 577–584, 1999.

[51] H. Zanni, M. Cheyrezy, V. Maret, S. Philippot, and P. Nieto, "Investigation of hydration and pozzolanic reaction in Reactive Powder Concrete (RPC) using 29Si NMR," *Cem. Concr. Res.*, vol. 26, no. 1, pp. 93–100, Jan. 1996.

[52] J. Haas and A. Nonat, "From C-S-H to C-A-S-H: Experimental study and thermodynamic modelling," *Cem. Concr. Res.*, vol. 68, pp. 124–138, 2015.

[53] H. Stade, "On the reaction of C-S-H(di, poly) with alkali hydroxides," *Cem. Concr. Res.*, vol. 19, no. 5, pp. 802–810, Sep. 1989.

[54] G. Renaudin, J. Russias, F. Leroux, C. Cau-dit-Coumes, and F. Frizon, "Structural characterization of C-S-H and C-A-S-H samples-Part II: Local environment investigated by spectroscopic analyses," *J. Solid State Chem.*, vol. 182, no. 12, pp. 3320–3329, 2009.

[55] E. L'Hôpital, B. Lothenbach, G. Le Saout, D. Kulik, and K. Scrivener, "Incorporation of aluminium in calcium-silicate-hydrates," *Cem. Concr. Res.*, vol. 75, pp. 91–103, 2015.

[56] T. T. H. Bach, E. Chabas, I. Pochard, C. Cau Dit Coumes, J. Haas, F. Frizon, and A. Nonat, "Retention of alkali ions by hydrated low-pH cements: Mechanism and Na +/K+ selectivity," *Cem. Concr. Res.*, vol. 51, pp. 14–21, 2013.

[57] L. Pegado, C. Labbez, and S. V. Churakov, "Supporting Information for: Mechanism of aluminium incorporation into C–S–H from ab initio calculations," *J. Mater. Chem. A*, vol. 2, p. 3477, 2014.

[58] X. Pardal, F. Brunet, T. Charpentier, I. Pochard, and A. Nonat, "27Al and 29Si solid-state NMR

characterization of calcium-aluminosilicate-hydrate," *Inorg. Chem.*, vol. 51, no. 3, pp. 1827–1836, 2012.

[59] B. Lagerblad and S. K. Ab, "Leaching performance of concrete based on studies of samples from old concrete constructions," p. 85, 2001.

[60] J. Trägårdh and B. Lagerblad, "Leaching of 90-year old concrete mortar in contact with stagnant water." 1998.

[61] L. Romben, "Aspects on testing methods for acid attack on concrete," 1978.

[62] L. Romben, "Aspects on testing methods for acid attack on concrete -further experiments," 1979.

[63] R. J. van Eijk and H. J. H. Brouwers, "Study of the relation between hydrated Portland cement composition and leaching resistance," *Cem. Concr. Res.*, vol. 28, no. 6, pp. 815–828, 1998.

[64] B. Lagerblad and J. Trägårdh, "Conceptual model for concrete long time degradation in a deep nuclear waste repository," *Archives of surgery (Chicago, Ill. : 1960).* 1994.

[65] P. Brune and R. Perucchio, "Roman Concrete Vaulting in the Great Hall of Trajan's Markets: Structural evaluation," *J. Archit. Eng.*, vol. 18, no. 4, pp. 332–340, 2012.

[66] M. Jackson, D. Deocampo, F. Marra, and B. Scheetz, "Mid-Pleistocene pozzolanic volcanic ash in ancient Roman concretes," *Geoarchaeology*, vol. 25, no. 1, pp. 36–74, 2010.

[67] M. D. Jackson, J. M. Logan, B. E. Scheetz, D. M. Deocampo, C. G. Cawood, F. Marra, M. Vitti, and L. Ungaro, "Assessment of material characteristics of ancient concretes, Grande Aula, Markets of Trajan, Rome," *J. Archaeol. Sci.*, vol. 36, no. 11, pp. 2481–2492, Nov. 2009.

[68] M. D. Jackson, S. R. Chae, S. R. Mulcahy, C. Meral, R. Taylor, P. Li, A.-H. Emwas, J. Moon, S. Yoon, G. Vola, H.-R. Wenk, and P. J. M. Monteiro, "Unlocking the secrets of Al-tobermorite in Roman seawater concrete," *Am. Mineral.*, vol. 98, no. 10, pp. 1669–1687, Oct. 2013.

## 5.7 Geochemical Interaction of the Groundwater-Concrete-Bentonite system and its impact in the near field and EDZ

*CIEMAT Research Centre for Energy, Environment and Technology, Madrid, Spain*
*CSIC High Research Council of Spain, Madrid, Spain*
*UAM Autonomous University of Madrid, Madrid, Spain*

The Deep Geological Repository (DGR) is currently the most accepted management option for the long-term isolation of high level radioactive wastes [1, 2]. Regardless of the geological options considered for the DGR, they all call for use of a multi-barrier system (Engineered barrier system, EBS) in order to achieve the safety requirements for limiting the eventual release of radionuclides to the biosphere.

The main EBS taking a relevant role in the stability of the repository are:

1) the host rock where the galleries are built,
2) The concrete to hold and close the galleries,
3) The bentonite barrier surrounding the canister containing the radioactive waste, and
4) The metallic canister containing the radioactive waste.

These barriers are in close contact and they interact each other, so that a physical-chemical compatibility between the interfaces of all barriers is a mandatory requirement for construction of the DGR. Besides the engineering barriers are in contact with groundwaters flowing that will affect the long-term safety if degradation processes are developing.

The chemical composition of the groundwaters has a critical function to maintain the integrity and retard degradation phenomena at the interface level of the engineering barriers towards the bulk. Clayey waters and granitic waters will interact both with concrete and bentonite which chemical composition (ionic content) is critical to maintain the stability within each barrier. In addition to, the corresponding waters flowing through each barrier can contribute to the advance of long-term interaction between concrete/bentonite barriers. The different scenarios actuating in a DGR are schematised in Figure 5.7.1 where the main EBS interactions are highlighted.
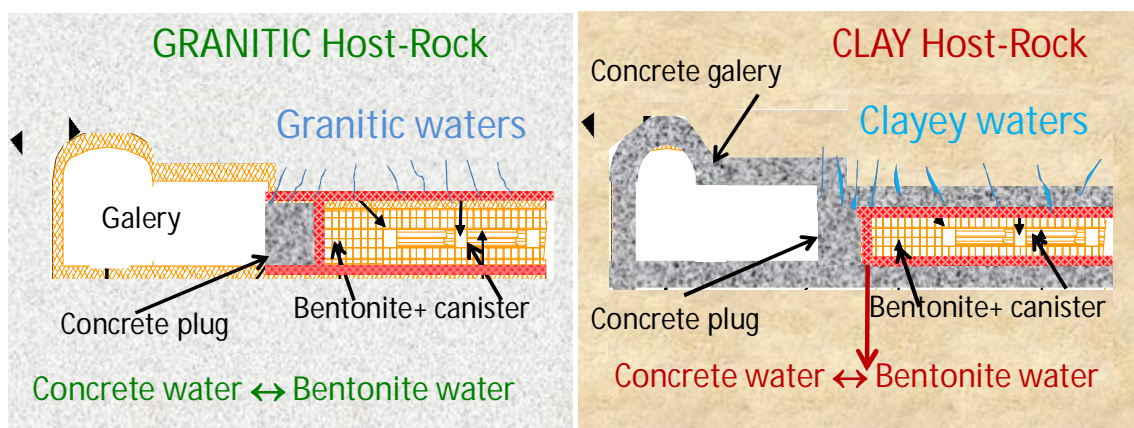


*Figure 5.7.1. Interactions Host-rock/concrete/bentonite in DGR groundwaters.*

The understanding of the phenomenological processes of degradation due to the interaction between the barriers and the waters and the identification of the critical parameters involved are of

fundamental interest to advance in the design of the DGR, being the scope of present analysis of the actual knowledge. The specifics aspects to be addressed are:

1) Role of groundwaters and pore water in the DGR.
2) Concrete groundwaters interactions in EBS.
3) Bentonite-concrete interface reactivity in granitic repository.

**References**

[1]     U.S. DOE. 2014. U.S. Department of Energy. 2014. Evaluation of Options for Permanent Geologic Disposal of Spent Nuclear Fuel and High-Level Radioactive Waste, Volume I. Used Fuel Disposition Campaign. Sandia National Laboratories. FCRD-UFD-2013-000371, Revision 1. SAND2014-0187P. 89 pp.
[2]     NEA-OECD. 2003. NEA-OECD. 2003. Engineered Barrier Systems and the Safety of Deep Geological Repositories. State-of-the art Report. OECD Publications, Paris. 70 pp.

### 5.7.1 Role of groundwater and pore water in the DGR

*M. Jesús Turrero, E. Torres, A. Garralón, P. Gómez*

*CIEMAT Research Centre for Energy, Environment and Technology, Madrid, Spain*

Disposal of radioactive wastes includes cement-based materials and bentonite as materials to tunnel reinforcement, and to buffer, plug and seal main galleries, grouts and wells in the selected repositories. At the time scale of a repository these materials interacts each other and with the surrounding media, namely granite or clay rock plus groundwater and pore water (Figure 5.7.1.1), so its integrity in terms of barrier function isolating the wastes must be assessed.

In this context three levels should be considered for analysis: groundwater/pore water from the host rock, pore water from the Engineered Barrier System (EBS) and the interaction among them. The aim of the analysis is assessing the stability of groundwater and pore water conditions over time, since this is one of the most important safety requirements; the chemical composition of water (groundwater and pore water of the DGR as a whole) influences the reliability of containment in the repository, canister corrosion, dissolution of waste matrix, sorption on mineral surfaces, the mobility of radionuclides, and the rate of their leakage back to the surface [1].

This section refers specifically to hydro-geochemistry in terms of types of water entering/hydrating the system, the initial processes during hydration and hydro-geochemical reaction among the different components of the system.
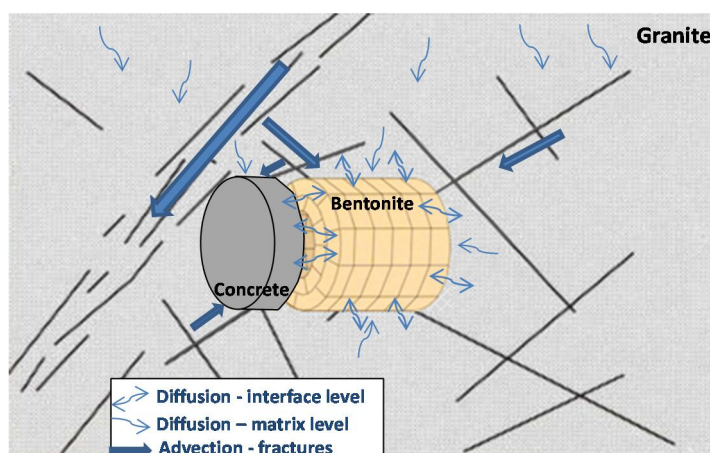


*Figure 5.7.1.1. Water movement and interactions in a granite repository concept.*

### Groundwater from the host rock

The term groundwater refers to that water coming from the host rock (either granite or clay or salt) and hydrating the EBS. In this sense groundwater chemistry influences the function and integrity of each component in the repository, and the system cannot be completely understood if a complete dataset on the composition of the groundwater and its evolution over time is not made. This dataset should help to construct a clear model including the groundwater initial conditions (baseline) and the evolution of the groundwater composition over time before and after interacting with the different components of the EBS. This model will offer the opportunity of assessing processes occurring in the system with performance assessment purposes.

Movement of groundwater through *crystalline rocks* is dependent on the presence of open fractures and connected matrix pores according to two hydraulic regimes (Figure 5.7.1.1): water-conducting zones linked to fracture networks where solute transport occurs by advection, being the faster form of transport in the media ($< 10^{-8}$ m/s), and water stored in the bedrock mass, which cannot flow or flows at very low rates ($< 10^{-11}$ m/s) due to low permeability, where solute transport is dominated by diffusion [2–5]. On the other hand, *clay rocks* mainly contain stored matrix water (pore water), and the pores are usually very small, with pore space connection very poor, so the water cannot move easily (hydraulic conductivities are $< 10^{-12}$ m/s) and there is a solute movement mainly controlled by diffusion [6].

During construction and operation of the DGR the fractures and matrix of the rock mass surrounding the galleries will partially desaturate and atmospheric pressure and oxidizing conditions will prevail [7], causing chemical changes in the groundwater/pore water and creating what is named the excavation disturbed zone (EDZ) [8]; as example, pyrite oxidation in the EDZ may increase sulfate content in the groundwater/pore water [9-11]. Additionally, water evaporation may occur, increasing salt concentration [12]. All this processes may in turn have an impact on the EBS materials and questioning its reliability.

As galleries are getting closed, pre-existing groundwater pressures and conditions will be restored. Groundwater will flow until achieving the re-saturation of both, the rock surrounding the EBS and the EBS itself [8, 13, 14]. This process will take a few years. During the re-saturation stage simultaneous processes occur: (a) the chemical disequilibrium between groundwater hydrating the EBS from the rock and pore water from the EBS will alter the system up to equilibrium is once again achieved, and (b) air in the repository will be slowly replaced by water and the oxygen in the pore space will be consumed by different reaction processes so reduced conditions will be re-established over the repository.

The groundwater/pore water re-saturating the EBS in crystalline rocks can be very variable depending on the location. For example, the deeper granite groundwater in countries considering crystalline rocks in their programs, as Sweden, Finland (Fennoscandian Shield) and Canada (Canadian Shield), is close to neutral, reduced and saline Na-Ca-Cl type water, with total dissolved solids of 1–10 g/L [15–20], and other ions including sulfate and magnesium are also present in relatively high concentrations. However, the deeper granite groundwater in other countries, as Switzerland, Japan or Spain, is close to neutral or slightly alkaline, reduced and dilute Na-HCO3 type water [21–23]. The differences are important since salinity influences the hydration and swelling capacity of bentonite (loss of swelling) [1, 24] or may alter the concrete properties affecting its durability [25–27] ( see section 5.7.2).

On the other hand, some countries are undertaking research programs on consolidated or plastic argillaceous formations: France (Toarcian-Domerian Clay at Tournemire and Callovo-Oxfordian Clay at Bure), Belgium (Boom Clay at Mol), Hungary (Boda Clay at Mecsek) and Switzerland (Opalinus Clay at Mt Terri and Palfris Formation at Wellenberg). All the pore waters that would re-saturate the EBS in these clayey rocks are neutral, reduced and with rather high salinity, being sulfate and chloride the dominant anions, and sodium and magnesium the dominant cations, except for the Boom Clay [28–34]. In Spain, studies on cores from an Oligocene-Miocene argillaceous formation (RAF) at Central-North Spain provided data on clay water composition very similar to the above ones, being the water neutral, reduced and Mg-SO$_4$ type [35]. The main variations in the pore water of the different clay rocks are in the contents of sulfates and bicarbonates, suggesting that processes related to carbonate and redox systems are critical in defining the final composition.

Once established the baseline conditions of the system, one step further may be using natural tracers behaving conservatively, such as Cl, Br, $\delta^{18}O$, $\delta^2H$ and $^4He$, to quantify rates and mechanisms of solute transport in the rock formation [19, 36–39] and also between the different components of the EBS [40–42], main flow paths and also water-rock interaction processes occurring in the system.

In summary, processes as water redistribution during desaturation and re-saturation periods and equilibration of EBS pore water with surrounding groundwater, among others (e.g. temperature gradients), will induce a series of geochemical processes (see sections 5.7.2 and 5.7.3) that will play an important role in the evolution of the whole system. Within this context, baseline composition of groundwater and pore water of the different constituents in the DGR and their evolution during the life time of the repository is a key issue in two aspects: (a) may condition the properties of the EBS materials, and (b) can provide valuable data to understand processes taking place in the repository.

**Bentonite/groundwater interaction**

During re-saturation stage the chemistry of the bentonite pore water varies as a function of the composition of the host rock groundwater (e.g. fresh or saline), besides the interactions with the other components of the EBS. Moreover, during this period the interactions are strongly dependent on the temperature. Once the galleries are closed the re-saturation of the bentonite occurs. The area located near the canister will dry due to water evaporation caused by temperature rise. Vapor generated near the canister will flow towards cooler areas and will condensate. As a result, bentonite pore water near the canister will evaporate in the early stages of the saturation phase, causing the precipitation of some mineral phases and a saline front will develop. Since the thermodynamic equilibrium between the aqueous and solid phases can be altered, minerals could precipitate in pore spaces, leading to clogging of porosity and loss of plasticity, or dissolve, resulting in an increasing of permeability of the material [43]. These processes overlap to those occurring during previous stages and described in previous section. When ionic content in the rock is lower than in the bentonite pore water (e.g. FEBEX bentonite in contact with fresh granite water [21, 44], the slow migration of the species from bentonite to granite by diffusion occurs.

Subsurface repository facilities for low and intermediate level radioactive waste and underground research laboratories (URLs) in different are used for performing generic-type experiments of interest to deep disposal. Between them, the FEBEX experiment, an in situ full-scale experiment in one such underground laboratory at Grimsel Test Site in Switzerland [13] has simulated the thermal evolution of the engineered barriers in a repository for high-level wastes in a granite formation and has served to provide a realistic setting to study the processes influencing barrier evolution that will affect radionuclide migration away from waste packages.

Boreholes drilled in the granite very close to the experiment have provided information on groundwater composition along time. Chloride and sodium were selected as natural tracers of solutes transfer between the bentonite porewater and granite groundwater given the difference in concentration (about two orders of magnitude) of these ions between these two types of water. Therefore, the study of an element such as Cl in the FEBEX experiment has a double application due to its role as a tracer in the mass transfer between the bentonite and the granite, and their chemical analogy with the radionuclide $^{36}Cl$.

The Na and Cl concentration in the granite groundwater increase in a way that evolved from Ca-$HCO_3$ type water to a Na-Cl type water. The lack of flow related to complete saturation, a transmissivity of the bentonite 3 orders of magnitude lower than in the granite and the absence of pressure gradients indicate no water movement; the hydrogeological model based on data recorded in the gallery concludes that there is a unique flow in a direction parallel to the gallery (Martínez

Landa, pers. comm.). Then, there is a bentonite–granite solute transfer occurring via diffusion (Figure 5.7.1.2). This suggests similar changes might occur in other bentonite–granite scenarios [39].
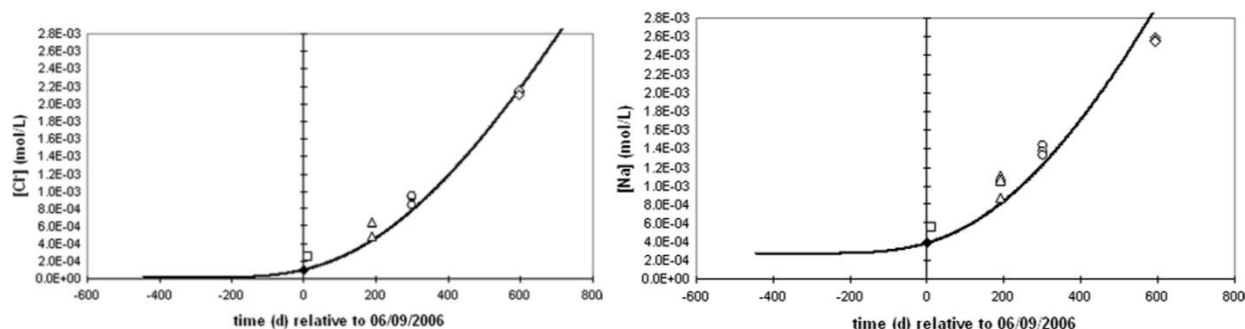


*Figure 5.7.1.2. Diffusive transport of Cl and Na between the bentonite pore water and the granite groundwater in the FEBEX in situ experiment. Circles and squares correspond to analysis of Cl and Na in groundwater along time [39].*

Most predictive models of bentonite porewater evolution take into account of ion-exchange reactions between the bentonite (smectite) and the infiltrating groundwater. The dominant ion-exchange reaction is likely to be between sodium in the bentonite and calcium in the groundwater, although other exchanges are possible depending on the composition of the groundwater. This is important since the concentration of exchangeable cations can influence the swelling [45].

**Concrete/groundwater interaction**

The concrete pore water chemical composition depends on a number of parameters, namely the initial composition of the water in contact with the cement, the components of the material, the degradation of the solid phases in the system, etc. During the re-saturation stage, leaching will be a dominant process in the system, and the pore solution of concrete equilibrates with the surrounding saline (e.g. water from clay rock or granite rock from Fennoscandian and Canadian Shields) or fresh water. The final composition will be controlled by strong alkalis (KOH and NaOH) and their evolution towards equilibrium with portlandite ($Ca(OH)_2$), which confers a high-pH plume to the system, with pH ranging from 12 to 13 or higher [46]. The hyperalkaline solutions may react with the rocks hosting the repositories and change their physical and chemical properties; A number of experiments have been made in situ and in laboratory to investigate the interactions between cementitious materials and clayey [47] or granite deep formation [48, 49]. The results show that the composition of the alkaline water can have an influence on the diffusion of cations in geological media and Soler and Mäder [49] observe a decrease in the permeability of the rock in an experiment of injection of hyperalkaline fluids in the granite Grimsel Tests Site. Furthermore, Baker et al. [50] stated that groundwater that had reacted with cement hydrated phases within a cementitious repository will subsequently react with the surrounding rock to form an alkaline disturbed zone (ADZ) in which the change of the chemistry of the pore solution will provoke subsequent dissolution/precipitation of different mineral phases [51] (see section 5.7.2).

In the Underground Reasearch Laboratory at Manitoba, Canada, geochemical monitoring was made after injecting a sulphate resistant concrete in fractures in a granitic rock [52]. It was demonstrated that the degree of interaction of hydrated cement phases with groundwater will depend on c/w ratio, porosity, permeability and, most of all, the composition of the cement. If OPC is used in freshwater environments, leaching of $Ca(OH)_2$ will occur leading eventually to dissolution of CSH phases and disintegration of the concrete (see section 5.7.2). In saline groundwaters, the dissolution rate is lower due to the higher ionic strength of the water, particularly of Ca.

Cement components as $C_3A$ may also react with sulphate (gypsum) derived from the cement composition used as setting regulator or from environmental sources such as $SO_4^{2-}$ that occurs naturally in pore water in clay rock, and both mechanisms will produce gypsum [53] (see section 5.7.2). Low $SO_4^{2-}$ and $HCO_3^-$ concentrations in the groundwater will stabilize the cement and maintain a high pH [52]. Another reaction that can occur between concrete and groundwater is the chloride attack, also present in the more saline waters, resulting in the conversion of aluminate phases in different kind of complexes (see section 5.7.2). A clear definition of the baseline groundwater is a key issue to anticipate those phenomena that may affect the performance of the system.

**Concrete/bentonite interaction**

Different European Projects such as ECOCLAY I and II, NF-PRO and PEBS have dealt with how the concrete changes both its chemical and physical properties over time and how it interacts with bentonite. These projects comprised batch leaching tests with bentonite mixed with different synthetic solutions of cement pore water as well as in situ experiment on the concrete/bentonite interface and the determination of chemical and microstructural changes by the interaction between both materials [54, 55](further information can be found in section 5.7.3).

Once the concrete is saturated a hyperalkaline fluid starts moving towards the bentonite, reacting with it and affecting its physical and chemical properties [40–42, 56, 57]. This fluid could also enter the host formation, and react with it as seen in previous section. The main reactions described in the literature consist of ion exchange and mineral dissolution/precipitation, which affect the sorption and transport properties of the whole system.

In order to explain the main aspects of soluble ions mobility [58] designed several laboratory column experiments in which bentonite was in contact with a lime mortar on one side and magnetite on the other side, and the system was hydrated with fresh granite type water (Grimsel Test Site water). Magnetite-bentonite–mortar solute transfer was inferred from the Cl and $SO_4^{2-}$ concentration in the system. A selective concentration of chloride in the mortar and the precipitation of sulfate solid phases, both in the mortar and in the magnetite powder were observed. An identical experiment without interfaces showed chloride back-diffusion to the water reservoir. The same processes has been observed from the in situ FEBEX experiment (see previous sections) and from similar experiments considering a saline groundwater for hydration purposes [59, 60]. The phenomenological approach related to this processes is widely explained in section 5.7.3.

**References**

[1]     Sneyers, A., Understanding and Physical and Numerical Modelling of the Key Processes in the Near Field and their Coupling for Different Host Rocks and Repository Strategies (NF-PRO). Final Report. 2008, European Commission. Euratom. p. 217.

[2]     Neretnieks, I., T. Eiksen, and P. Tahtinen, Tracer movement in a single fissure in granitic rock: Some experimental results and their interpretation. Water Resources Research, 1982. 18(4): p. 849–858.

[3]     Bernabé, Y., The transport properties of networks of cracks and pores. Journal of Geophysical Research, 1995. 100(B3): p. 4231–4241.

[4]     Cvetkovic, V. and A. Frampton, Transport and retention from single to multiple fractures in crystalline rock at Äspö (Sweden): 2. Fracture network simulations and generic retention model. Water Resources Research, 2010. 46(5): p. 1–17.

[5]     Mariner, P.E., et al., Granite Disposal of U.S. High-Level Radioactive Waste. 2010, Sandia National Laboratories. p. 114.

[6]     Yong, R.N., R. Pusch, and M. Nakano, Containment of High-Level Radioactive and Hazardous Solid Wastes with Clay Barriers. 2010: Spon Press. 467.

[7]     Bildstein, O. and F. Claret, Stability of barriers under chemical perturbations, in Natural and Engineered Clay Barriers, C. Tournassat, et al., Editors. 2015, Elsevier B.V.: Amsterdam. p. 432.

[8]     Johnson, L. and F. King, The effect of the evolution of environmental conditions on the corrosion evolutionary path in a repository for spent fuel and high-level waste in Opalinus Clay. Journal of Nuclear Materials, 2008. 379: p. 9–15.

[9]     De Craen, M., et al., Extent of oxidation in Boom Clay as a result of excavation and ventilation of the HADES URF: Experimental and modelling assessments. Physics and Chemistry of the Earth, Parts A/B/C, 2008. 33(1): p. S350–S362.

[10]    Lerouge, C., et al., Constraints from sulfur isotopes on the origin of gypsum at concrete/claystone interfaces. Physics and Chemistry of the Earth, 2014. 70-71: p. 84–95.

[11]    Vinsot, A., et al., Oxidation front and oxygen transfer in the fractured zone surrounding the Meuse/Haute-Marne URL drifts in the Callovian-Oxfordian argillaceous rock. Vol. Special Publication 400. 2014, London: Geological Society.

[12]    Vinsot, A., et al., Insights on Desaturation Processes based on the Chemistry of Seepage Water from Boreholes in the Callovo-Oxfordian Argillaceous Rock. Procedia Earth and Planetary Science, 2013. 7: p. 871–874.

[13]    ENRESA, FEBEX Project. Full-scale Engineered Barriers Experiment for a Deep Geological Repository for High Level Radioactive Waste in Crystalline Host Rock. Final Report. 2000, ENRESA: Madrid. p. 374.

[14]    Dessirier, B., J. Jarsjö, and A. Frampton, Modeling two-phase-flow interactions accross a bentonite clay and fractured rock interface Nuclear Technology, 2014. 187(2): p. 147–157.

[15]    Gascoyne, M., et al., Saline groundwaters and brines in plutons in the Canadian Shield, in Saline Water and Gases in Crystalline Rocks, P. Fritz and S.K. Frape, Editors. 1987, Geological Association of Canada: Waterloo. p. Special Paper 33: 53–68.

[16]    Gascoyne, M., Hydrogeochemistry, groundwater ages and sources of salts in a granitic batholith on the Canadian Shield, southeastern Manitoba. Applied Geochemistry, 2004. 19: p. 519–560.

[17]    Laaksoharju, M., et al., Hydrogeochemical conditions and evolution at the Äspö HRL, Sweden. Applied Geochemistry, 1999. 14: p. 835–859.

[18]    Laaksoharju, M., et al., Hydrogeochemical evaluation and modelling performed within the Swedish site investigation programme. Applied Geochemistry, 2008. 23: p. 1761–1795.

[19]    Waber, H.N. and J.A.T. Smellie, Characterization of pore water in crystalline rocks. Applied Geochemistry, 2008. 23: p. 1834–1861.

[20]    Posiva, Models and Data Report 2010. 2010, Posiva Oy: Eurajoki. p. 484.

[21]    Pearson, F.J. and A. Scholtis, Chemistry of reference waters of the Crystalline Basement of Northern Switzerland for Safety Assessment studies. 1993, NAGRA: Wettingen.

[22]    Iwatsuki, T. and H. Yoshida, Groundwater chemistry and fracture mineralogy in the basement granitic rock in the Tono uranium mine area, Gifu Prefecture, Japan- Groundwater composition, Eh evolution analysis by fracture filling minerals. Geochemical Journal, 1999. 33: p. 19–32.

[23]    Gómez, P., et al., Hydrogeochemical characteristics of deep groundwaters of the Hesperian Massif (Spain). Journal of Iberian Geology, 2006. 32(1): p. 113–131.

[24]    Dixon, D.A., Pore water salinity and the development of swelling pressure in bentonite-based buffer and backfill materials. 2000, Posiva Eurajoki. p. 51.

[25]    Chandler, N.A., et al., The five year report on the tunnel sealing experiment: an international project of AECL, JNC, ANDRA and WIPP. 2002, Atomic Energy of Canada Limited: Ontario. p. 443.

[26]    Höglund, L.O., Modelling of long-term concrete degradation processes in the Swedish SFR repository. 2001, SKB: Stockholm. p. 164.

[27]    Adeyemi, O.F. and A.G. Modupola, The Effect of Sea water on Compressive Strength of Concrete. International Journal of Engineering Science Invention 2014. 3(7): p. 23–31.

[28]    Reeder, S., et al., A study of the Boom clay drillcore from Mol in Belgium. Chemical and isotopic characterization of porewater and clay mineralogy. 1993, British Geological Survey.

[29]    Baeyens, B. and M.H. Bradbury, Physico-chemical characterization and calculated in situ porewater chemistries for a low permeability Palfris Marl sample from Wellemberg. 1994, NAGRA: Wettingen. p. 30.

[30]    Pearson, F.J., et al., Geochemistry of water in the Opalinus Clay Formation at the Mont Terri Rock Laboratory. Swiss Federal Office for Water and Geology Series. Vol. 5. 2003. 319.

[31]    De Craen, M., et al., Geochemical analyses of Boom Clay pore water and underlying aquifers in the Essen-1 borehole. 2006, SCK·CEN: Mol. p. 24.

[32]    Beaucaire, C., et al., Groundwater characterisation and modelling of water-rock interaction in an argillaceous formation (Tournemire, France). Applied Geochemistry, 2008. 23: p. 2182–2197.

[33]    Vinsot, A., S. Mettler, and S. Wechner, In situ charaterization of the Callovo-Oxfordian pore water composition. Physics and Chemistry of the Earth, 2008. 33: p. 575–586.

[34]    Gaucher, E.C., et al., A Robust Model for Pore-water Chemistry of Clayrock. Geochimica et Cosmochimica Acta, 2009. 73: p. 6470–6488.

[35]    Turrero, M.J., et al., Pore water chemistry of a Paleogene continental mudrock in Spain and a Jurassic marine mudrock in Switzerland: sampling methods and geochemical interpretation. Journal of Iberian Geology, 2006. 32(2): p. 233–258.

[36]    Gimmi, T., et al., Stable water isotopes in porewater of Jurassic argillaceous rocks as tracers for solute transport over large spatial and temporal scales. Water Resources Research, 2007. 43(4): p. W04410.

[37]    Mazurek, M., et al., CLAYTRAC Project: Natural tracer profiles across argillaceous formations - review and synthesis. 2009, Radioactive Waste Management Nuclear Energy Agency, OECD: Paris. p. 375.

[38]    Marques, J.M., et al., Isotopic and hydrochemical data as indicators of recharge areas, flow paths and water-rock interaction in the Caldas da Rainha-quinta das Janelas thermomineral carbonate rock aquifer (Central Portugal). Journal of Hydrology, 2013. 476: p. 302–313.

[39]    Buil, B., et al., Modeling of bentonite-granite solutes transfer from an in-situ full-scale experiment to simulate a Deep Geological Repository (Grimsel Test Site, Switzerland). Applied Geochemistry, 2010. 25: p. 1797–1804.

[40]    Fernández, R., et al., Alteration of compacted bentonite by diffusion of highly alkaline solucitons. European Journal of Mineralogy, 2009. 21: p. 725–735.

[41]    Fernández, R., A.I. Ruiz, and J. Cuevas, The role of smectite composition on the hyperalkaline alteration of bentonite. Applied Clay Science, 2014. 95: p. 83–94.

[42]    Fernández, R., et al., Precipitation of chlorite-like structures during OPC porewater diffusion through compacted bentonite at 90ºC. Applied Clay Science, 2013. 83-84: p. 357–367.

[43]    Savage, D., D. Noy, and M. Mihara, Modelling the interaction of bentonite with hyperalkaline fluids. Applied Geochemistry, 2002. 17: p. 207–223.

[44]    Fernández, A.M., et al., Analysis of the porewater chemical composition of a Spanish compacted bentonite used in an engineered barrier. Physics and Chemistry of the Earth 2004. 29: p. 105–118.

[45]    Davis, J., et al., Investigation of Reactive Transport and Coupled THMC Processes in the EBS. 2013, Lawrence Berkeley National Laboratory.

[46]    Berner, U.R., Evolution pore water chemistry during degradation of cement in a radioactive waste repository environment. Waste Management, 1992. 12: p. 201–219.

[47]    Bartier, D., et al., In situ investigations and reactive transport modelling of cement paste/argillite interactions in a saturated context and outside an excavated disturbed zone. Applied Geochemistry, 2013. 31: p. 94–108.

[48]    Holgersson, S., Studies on the effect of concrete on the chemistry in a repository for radioactive waste. 2000, Chalmers University of Technology: Goteborg. p. 169.

[49]    Soler, J.M. and U. Mäder, Cement-rock interaction: infiltration of a high-pH solution into a fractured granite core. Geologica Acta 2010. 8(3): p. 221–233.

[50]    Baker, A.J., et al., Research on the alkaline disturbed zoned resulting from cement-water-rock reactions around a cementitious repository in a silicate-rich host rock. 2002, NIREX: Harwell.

[51]    Savage, D., A review of analogues of alkaline alteration with regard to long-term barrier performance. Mineralogical Magazine, 2011. 75(4): p. 2401–2418.

[52]    Gascoyne, M., Influence of grout and cement on grounwater composition. 2002, Posiva Oy: Eurajoki. p. 47.

[53]    Lawrence, C.D., Sulphate attack on concrete. Magazine of Concrete Research, 1990. 42: p. 835–859.

[54]    Cuevas, J., et al., the alkaline reaction of FEBEX bentonite: a contribution to the study of the performance of bentonite7concrete engineered barrier systems. Journal of Iberian Geology, 2006. 32: p. 151–174.

[55]    Dauzères, A., et al., Physico-chemical investigation of clayey/cement-based materials interaction in the context of geological waste disposal: experimental approach and results. Cement and Concrete Research, 2010. 40: p. 1327–1340.

[56]    Gaucher, E.C. and P. Blanc, Cement/clay interactions - A review: Experiment, natural analogues and modeling. Waste Management, 2006. 26: p. 776–788.

[57]    Sánchez, L., et al., Reaction kinetics of FEBEX bentonite in hyperalkaline conditions resembling the cement-bentonite interface. Applied Clay Science, 2006. 33: p. 125–141.

[58]    Cuevas, J., et al., Lime mortar-compacted bentonite-magnetite interfaces: An experimental study focused on the understanding of the EBS long-term performance or high-level nuclear waste isolation DGR concept. Applied Clay Science, 2016. 124-125: p. 79–93.

[59]    Turrero, M.J., et al., Laboratory tests at the interfaces: First results on the dismantling of tests FB3 and HB4. 2011. p. 64.

[60]    Torres, E., et al., Geochemical interaction at the concrete-bentonite interface of column experiments. 2013. p. 75.

### 5.7.2   Concrete groundwaters interactions in EBS

*M.C. Alonso, J.L. Garcia-Calvo*

*CSIC High Research Council of Spain, Madrid, Spain*

This section summarizes the degradation processes expected in cementitious materials in contact with groundwaters according to those described in 5.7.1. First of all, it should be noted that concrete pore waters originating from a Portland cement have high alkalinity and are able to react with and modify the bentonite barrier. These early cement pore waters have alkali ions that will be transported by diffusion and possibly by advection due to bentonite suction if this material is emplaced under unsaturated conditions. However, the transformations promoted in the bentonite barrier are discussed in section 5.7.3. In present section only the most relevant studies related to the use of concretes in radioactive waste repositories have been considered. Most of the related studies published in the literature deal with conventional Portland concretes but there are also some studies concerning low-pH cementitious materials.

Although concrete is stable in high humid environments, the direct contact with water, stagnant, percolation, flowing, produces a diffusion of the pore solution and also alteration of the solid phases. Degradation of concrete due to leaching occurs when the hydrates in cementitious materials dissolve into the surrounding water and the precipitation of new phases takes place. Moreover, carbonation reactions can occur and different aggressive agents dissolved in water can attacked the existing hydrates (e.g., sulphates attack). All these phenomena can cause a loss of strength. Obviously, these processes are difficult to predict since there are many parameters involved that are not easily quantifiable [1]. Although the expected degradation rate is slow, its evaluation is very important for structures near field DGR, where extremely long-term stability is needed.

The leaching processes of materials that contain cement pastes are a combination of chemical reactions and diffusion transport and have to be studied thermodynamically and kinetically. Cement degradation depends on physical factors including the effect of porosity, compressive strength and density as well as on leachant characteristics including the effect of pH, flow rate, temperature and water chemical composition.

In realistic conditions of DGR, concrete durability is based on its interaction with clays and/or granite groundwaters. In general, groundwaters are mineralised solutions; however their exact composition in site must be known for evaluating their interaction with concretes. For example, as indicated in 5.7.1, salinity of groundwater is very variable depending on the emplacement of the repository, while in south of Europe the more expected groundwaters have low salinity, in the North it would be expected water with high saline content, around 50g/l [2].

The presence of cementitious materials may greatly alter the chemistry of water in the DGR. These materials provide a large reservoir of unstable Ca-silicate phases that will dissolve and reprecipitate at the rock-water or concrete-bentonite interfaces. Chemical interactions between water and concrete may well be dominated by the dissolution kinetics of the unstable amorphous and crystalline phases and precipitation kinetics of the meta-stable or stable phases. Therefore, there is an enormous concern on determining the concrete behaviour under the long-term action of water, in representative conditions of the real storage scenario. However, up to now, there are very few published experienced about this subject.

Regarding conventional Portland cement (PC) materials, most of the published results refer to tests made in laboratory conditions. It is well known that the solid hydrates of cement paste are more persistent at pH above 12–13, but at lower pHs the hydrated phases are no longer remain stable and dissolve. The pore solution of a typical Portland cement paste is highly alkaline, so that the leaching process starts by removing alkalis ($Na^+$ and $K^+$), followed by dissolution of portlandite and subsequently by the leaching of calcium from silicates, e.g., C-S-H [3–5]. Aluminate phases are also affected, dissolution/precipitation processes of AFm, ettringite and calcite are observed [6, 7], and aluminium might be incorporated in the C-S-H gel. Silica gel formation has also been detected in the outer layer of cement pastes exposed to leaching in deionized water.

In different leaching tests carried out, decreases in the C/S ratio of C-S-H were observed [8]. In the degraded zone, between surface and unaffected concrete, there is a continuous decrease in calcium concentration. The concentration of silica species in the pore solution remains very low whatever the concentration of Ca [7, 9]. Several experimental studies had been performed to elucidate the leaching mechanism of C-S-H [6, 7, 10–12]. It seems that the leachable calcium is located in the silicates interlayer. Aluminium may substitute Si in regions of low Ca/Si but only in the bridging tetrahedral. When cement paste is put in contact with an aqueous solution two phenomena take place simultaneously:

a)          The transport of mass by diffusion.
b)          Chemical reactions of dissolution and precipitation.

If the kinetics of the chemical reactions are slower than diffusion then the first controls the leaching, but if chemical reactions occur rapidly the leaching flow will be controlled by diffusion [7, 8]. Diffusion takes place across a solid–liquid interface, and a diffusion front appears where local chemical equilibrium is usually assumed to have been achieve [13, 14]. Anyway, leaching may be a slow process; 5 to 10 mm leached depth having been found in PC concretes exposed for 100 years submerged in natural waters [15]. This is in part due to the hydration of anhydrous grains of cement during leaching, which leads to a densification of the material and new portlandite is formed from in-situ hydration [15].

In real conditions, it is expected that the interactions between groundwaters, interstitial cement waters, cement and host rock minerals will progressively use up the pH buffering capacity of the concrete barrier and an alteration front will develop the concrete barrier [16]. Although, as previously mentioned, the alterations promoted in the concrete matrixes depend on the chemical composition of the groundwater, in general, four types of reaction mechanism have been described in the literature [8–36]:

- Leaching due to the pH gradient (groundwater pH is lower than pore solution pH of concrete) that lead to dissolution of hydration products, mainly portlandite. Degradation consists in dissolution of calcium and hydroxide ions out of the matrix, which causes an increase in porosity and transport properties of surface concrete [19, 20]. Leaching is accelerated with neutral and acid solutions/groundwaters [21, 22], and it may be coupled with the ingress of aggressive ions such as chloride, sulphate, magnesium [23]. It is evident that the other major components of the cement paste can also leach out, which during the interaction and equilibration with surrounding groundwater, changes the chemistry of the pore solution resulting in disintegration of cement paste [24]. An example of the leaching processes associated to calcium dissolution in Portland cement pastes is showed in Figure 5.7.2.1.
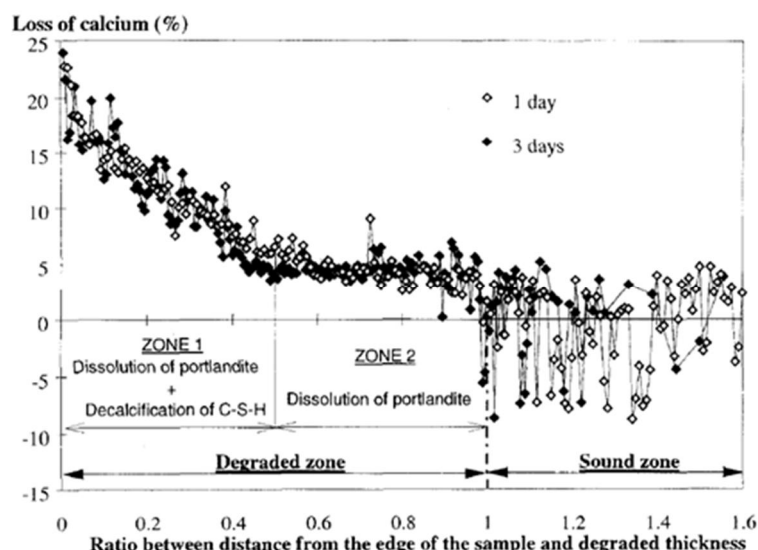
*Figure 5.7.2.1. Profiles of loss of calcium in the solid phase for pure PC pastes present two degraded zones of the same thickness: (1) both dissolution of portlandite and progressive decalcification of C-S-H; (2) only dissolution of portlandite [19].*

- Sulfate attack: this phenomenon has been described when clayey groundwaters/solutions with high sulphate concentrations are considered. In this sense, concrete based on PC with mineral additions has been predicted to be less sensitive than those based on pure PC to sulphate attack [25]. Scenarios involving sulphate attack are shown to potentially alter strongly a concrete engineered barrier based on pure Portland cement. The mechanism of degradation of concrete exposed to external sulphate attack depends on exposure conditions, such as temperature [26, 27], associated cation [28, 29] and sulphate concentration [30–32]. The best known mechanism involves calcium aluminates ($C_3A$) and portlandite in the cement matrix and sulphate ions [28, 33–35]. The first stage of this mechanism is based on a diffusion-reaction based phenomenon. Sulphate ions react with portlandite to form gypsum, which can in turn react with the hydration products of $C_3A$ to form ettringite. The formation of gypsum and ettringite can be expansive.
- Figure 5.7.2.2 shows a SEM image of the gypsum and ettringite crystals in the exposed surface of Portland cement pastes exposed for 3 months to a 50 mmol/l $Na_2SO_4$ solution in unsaturated conditions [35]. During the second stage of degradation the expansive products that have filled the porosity of concrete cause swelling, damage and finally a strength loss of concrete [36].
  Carbonation due to calcium leaching. This aspect is also more relevant when concentration of carbonates in the groundwater is high. The carbonation layer formed can act as protective layer as it makes denser the cement paste matrix thus increasing its resistance against groundwater penetration.
- Magnesium attack: although this degradation process had limited effects in the studies carried out.
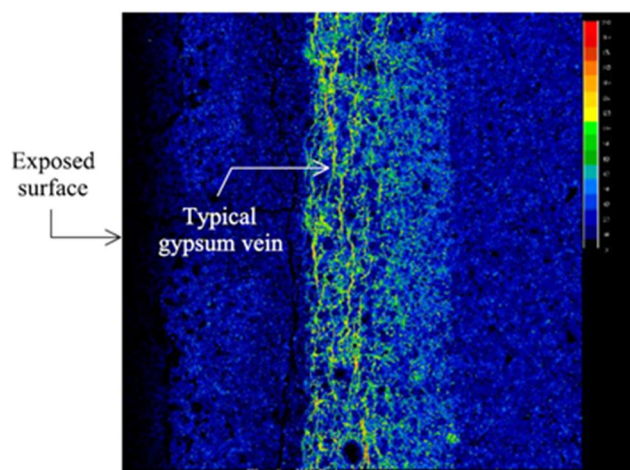
*Figure 5.7.2.2. Sulphur content mapping (2 x 2 mm) for a PC paste exposed for 3 months to a 50 mmol/l Na$_2$SO$_4$ solution in unsaturated conditions [35].*

Obviously, all these interactions are going to promote modifications in the porosity profiles of the used concretes: porosity reduction may occur due to carbonation of the cement paste or due to precipitation of different hydrates but porosity increases will occur due to leaching phenomena [8–36]. However, according to the published studies, the main detrimental reactions of concrete are taking place at small depths from the exposure surface, which is typically relatively small part of the whole structure and, especially, of the total multiple technical barriers[24].
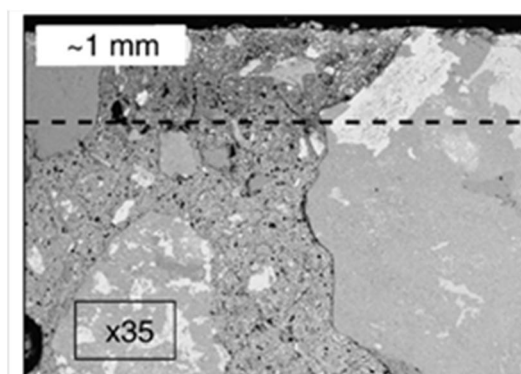


*Figure 5.7.2.3. Degradation front detected in a low-pH shotcreted concrete based on PC plus silica fume after two years in contact with granitic water [39].*

Regarding low-pH cementitous materials, results from the scarce leaching tests made, show, in general, a good resistance of the low-pH cementitious materials against water aggression, although an altered front can be also observed from the surface in all the tested samples, as can be seen in Figure 5.7.2.35.7.2.3. From leaching analyses using deionised water, a Ca$^{2+}$ released in the leaching solution has been described, as well as a decalcification process governed by diffusion being the Ca$^{2+}$ flux not only balanced by the release of OH$^-$ but also by that of sulphate ions [37, 38]. However, in most of the cases the decalcification of the low-pH cement pastes is much slower than that of OPC ones.

Apart from a very low CaO/SiO$_2$ ratio (0.3 to 0.4 for all pastes), a disappearance of ettringite and enrichment in a hydrotalcite-like phase have been reported near the leached surfaces of low-pH cement pastes [38].

In leaching tests made on low-pH concretes using real groundwater (from the Äspö Site) [39] or simulated fresh groundwater [37], leaching of $Ca^{2+}$ is again clearly recognized. After the test periods, low-pH concretes show a small altered front that can be observed from the surface. In this altered front, decalcification of the C-S-H gels followed by the incorporation of magnesium ions from ground water into them (even forming M-S-H phases) and into the anhydrous phases (as "magnesia nodules"). However, after this small zone, the rest of the paste of both types of concretes has a similar composition than those obtained before testing. It is remarkable that when immersed low-pH cementitious materials in saline water, leaching of $Ca^{2+}$ is much higher, but Si leaching was the lowest [37]. The decalcification intensity varies in the different published studies but, in general, it seems that the degradation front is higher when clayey environments are considered and lower when aggressive granitic waters are taken into account [18, 39]. Therefore, it is essential to respect the in-situ conditions for understanding cement paste degradation mechanisms.

Anyway, recent results have demonstrated that Mg-perturbation is systematically observed for low-pH cementitious materials placed in clayey, or granitic environment, or in any kind of environment containing at least 3 mmol/L of magnesium in its pore solution [18, 39–41]. The mineralogical phase associated with such Mg-perturbation was identified as a Mg–Si gel-like phase. A typical example of this Mg-perturbation is showed in Figure 5.7.2.4.
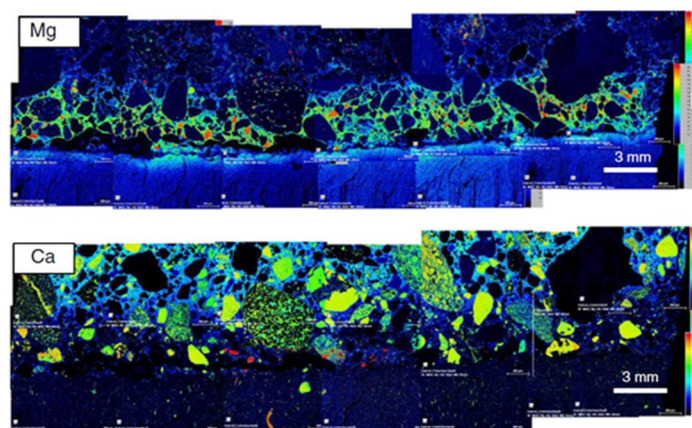


*Figure 5.7.2.4. SEM picture and EDS mappings of Mg and Ca at the interface between low-pH concrete (top) and clay (bottom) after 5 years of interaction [41].*

It has been also observed that for low-pH cement in contact with groundwaters carbonation occurs [18, 39, 40]. This carbonation is linked to the precipitation of calcite and thus the decalcification of C-S-H. Calcite and smectite were shown to form a protective coating at the surface of low-pH cementitious materials in contact with this saline water [37].

All the cases commented above were made in low-pH cementitious materials based on PC with mineral additions but there are a few studies focused on low-pH concretes based on calcium aluminate cement (CAC) plus mineral admixtures (silica fume, SF, and fly ashes, FA). The corresponding obtained results of leaching tests show a good resistance of the low-pH concretes based on CAC+SF against granitic groundwater aggression. Moreover, calcite precipitation observed on the leached surface could be playing a protecting role against the water aggression. In those concretes based on CAC+FA, an altered front can be observed from the surface in the tested samples. In this altered front, a decalcification of the C-A-S-H phases and an incorporation of magnesium ions from groundwater into them are suggested, as it is occurred in low-pH concretes based on PC [42, 43]. Moreover, the formation of calcium sulfoaluminate hydrates (probably

ettringite) in pores has been also reported in low-pH concretes based on CAC+FA even for granitic waters with low sulphate concentration PC [43]. Figure 5.7.2.5 shows this last phenomenon.
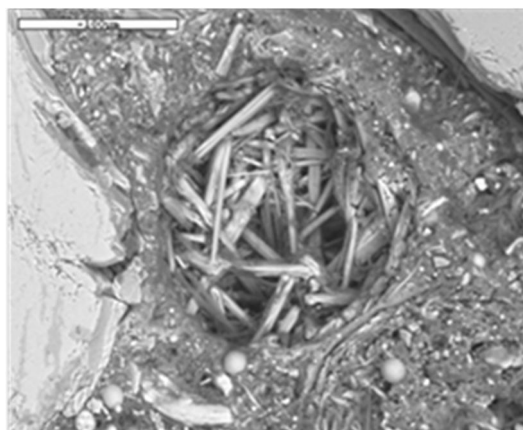


*Figure 5.7.2.5. Sulfoaluminate hydrates formation in low pH concretes based on CAC plus FA after two years in contact with granitic water (BSEM image x350) [43].*

# References

[1]     M. Romer, H. Lorenz. 2003. What triggers concrete deterioration in aqueous underground environments?. Proceedings of the 11th International Congress on the Chemistry of Cement (ICCC) Cement's contribution to the development in the 21st century, Eds. G.Grieve, G. Owens.

[2]     AA.VV. 2010. Geological repository systems for safe disposal of spent nuclear fuels and radioactive waste. Ed. Joonhong Ahn & Michael J. Apted, ISBN: 978-1-84569-542-2, Woodhead Publishing Limited.

[3]     H.F.W. Taylor. 1997. Cement Chemistry. Chap 9, Concrete Chemistry, 380–383.

[4]     A. Hidalgo, C. Andrade, C. Alonso. 2000. An accelerated leaching test to evaluate the long term behaviour of concrete in waste disposal, 5th CANMET/ACI Inter. Conf. on Durability of Concrete, June, 373–381, Barcelona.

[5]     B. Gerard. 2000. Hydrolysis of cement-based materials: a review, 3th Int Bolomey Workshop. Pore solution in hardened cement paste, Aedificati Pub., 271–304.

[6]     P. Faucon, F. Adenot, M. Jordá, R. Cabrilac. 1997. Behaviour of crystallised phases of Portland cement upon water attack, Mat. Struct. 30 (8) 480–485.

[7]     P. Faucon, F. Adenot, J.F. Jaquinot, C. Petit, R. Cabrillac, M. Jorda.  1998. Longterm behaviour of cement pastes used for nuclear waste disposal: review of physico-chemical mechanisms of water degradation, Cem. Conc. Res. 28 (6) 847–857.

[8]     P. Lovera, P. le Bescop, F. Adenot, G. Li, Y. Tanaka, E. Owaki. 1997. Physicochemical transformations of sulphated compounds during the leaching of highly sulphated cement wastes, Cem. Conc. Res. 27 (10) 523–1532.

[9]     S.A. Stronach, F.P. Glasser. 1997. Modelling the impact of abundant geochemical components on phase stability and solubility of CaO–SiO2–H2O system at 25 °C: Na+, K+, SO4 = , Cl- and CO3 = , Adv. Cem. Res. 9 (6) 167–181.

[10]    B. Gerard. 1995. Hydrolysis of cement-based materials: a review. 3th Int Bolomey Workshop. Pore solution in hardened cement paste, Aedificatio Pub., (2000) 271–304.

[11]    S. Chatterji. Concrete durability and CaO/SiO$_2$ mole ratio of CSH, Cem. Conc. Res. 25 (5) 929–932.

[12]    R.J. Van Eijk, H.J.H. Brouwers. 1996. Study of the relation between hydrated Portland cement composition and leaching resistance, Cem. Conc. Res. 28(6) (1998) 815–828.

[13]    F. Adenot, P. Faucon. Modellisation du comportement a long terme des betons utilises dans le stockage des dechets radioactfs, Int. RILEM Conf., Arles, 277–288.

[14]    F. Adenot. 1992. Durabilite du beton: Characterisation et modelisation des processus physiques et chimiques de degradation du cement. Doctoral Thesis, Univ. D'Orleans.

[15]    B. Lagerblad. 1999. Texture and chemistry of historic concrete subjected to prolonged hydration. Workshop on water in cement paste and concrete hydration and pore structure, Nordic Concrete Federation, Skagen, 148–154.

[16]    L. Trotignon, V. Devallois, H. Peycelon, C. Tiffreau, X. Bourbon. 2007. Predicting the long term durability of concrete engineered barriers in a geological repository for radioactive waste, Phys. Chem. Earth. 32 259–274.

[17]    C. Alonso, M. Castellote, I. Llorente, C. Andrade. 2006. Ground water leaching resistance of high and ultra high performance concretes in relation to the testing convection regime, Cem. Conc. Res. 36, 1583–1594.

[18] A. Dauzères, P. Le Bescop, C. Cau-Dit-Coumes, F. Brunet, X. Bourbon, J. Timonen, M. Voutilainen, L. Chomat, P. Sardini. 2014. On the physico-chemical evolution of low-pH and CEM I cement pastes interacting with Callovo-Oxfordian pore water under its in situ CO2 partial pressure, Cem. Conc. Res. 58, 76–88.

[19] C. Carde, R. François. 1999. Modelling the loss of strength and porosity increase due to the leaching of cement pastes, Cem. Conc. Comp. 21, 181–188.

[20] M. Mainguy, C. Tognazzi, J.-M. Torrenti, F. Adenot. 2000. Modelling of leaching in pure cement paste and mortar, Cem. Concr. Res. 30, 83–90.

[21] F. Adenot, M. Buil. 1992. Modelling of the corrosion of the cement paste by deionized water, Cem. Conc. Res. 22, 259–272.

[22] S. Kamali, B. Gérard, M. Moranville. 2003. Modelling the leaching kinetics of cementbased materials – influence of materials and environment, Cem. Conc. Compos. 25, 451–458.

[23] M. Moranville, S. Kamali, E. Guillon.2004. Physicochemical equilibria of cement-based materials in aggressive environments – experiment and modeling, Cem. Concr. Res. 34, 1569–1578.

[24] O.P. Kari, J. Puttonen. 2014. Simulation of concrete deterioration in Finnish rock cavern conditions for final disposal of nuclear waste, Annals of Nucl. Ener. 72, 20–30.

[25] L. Trotignon, H. Peycelon, X. Bourbon. 2002. Comparison of performance of concrete barriers in a clayey geological medium, Phys. Chem. Earth. 31, 610–617.

[26] N.J. Crammond. 2002. The thaumasite form of sulphate attack, Proceedings of the First Int. Conf. on Thaumasite in Cementitious Materials, BRE.

[27] K. Lipus, S. Punkte. 2003. Sulfatwiderstand unterschiedlich zusammengesetzter Betone, Tl.1 – Sulphate Resistance of Concretes with Different Compositions (Part 1), Beton – Dusseldorf, vol. 53, 97–101, Part 2.

[28] R. Duval, H. Hornain. 1992. Chapitre 9: La durabilité du béton vis-à-vis des eaux agressives, dans La durabilité des bétons, sous la direction de J. Baron et J.-P. Ollivier, Presses de l'ENPC.

[29] A. Neville. 2004. The confused world of sulphate attack on concrete, Review, Cem. Conc. Res. 34, 1275–1296.

[30] M. Santhanam, M.D. Cohen, J. Olek. 2001. Sulphate attack research – whither now? Cem. Conc. Res. 31, 845–851.

[31] D.D. Higgins, N.J. Crammond. 2002 Resistance of Concrete Containing ggbs to the Thaumasite Form of Sulphate Attack, paper presented at The First International Conference on Thaumasite in Cementitious Materials, Watford, UK, June.

[32] H.A.F. Dehwah. 2007. Effect of sulphate concentration and associated cation type on concrete deterioration and morphological changes in cement hydrates, Constr. Build. Mater. 21, 29–39.

[33] E.F. Irassar, V.L. Bonavetti, M. González. 2003. Microstructural study of sulphate attack on ordinary and limestone Portland cements at ambient temperature, Cem. Conc. Res. 33, 31–41.

[34] R. Tixier, B. Mobasher.2003. Modeling of damage in cement-based materials subjected to external sulphate attack. I: formulation, J. Mater. Civ. Eng. 15, 4, 305–313.

[35] Y. Maltais, E. Samson, J. Marchand. 2004. Predicting the durability of Portland cement systems in agressive environments – laboratory validation, Cem. Conc. Res. 34, 1579–1589.

[36] E. Roziére, A. Loukili, R. El Hachem, F. Grondin. 2009. Durability of concrete exposed to leaching and external sulphate attacks, Cem. Conc. Res. 39, 1188–1198.

[37] T. Yamamoto, H. Imoto, H. Ueda, M. Hironaga. 2007. Leaching alteration of cementitious materials and release of organic additives – study by Numo and Criperi, R&D on low-pH cement for a geological repository. 3rd Workshop Paris June, 52–61.

[38] M. Codina, C. Cau-dit-Coumes, P. Le Bescop, J. Verdier, J.P. Ollivier. 2008. Design and characterization of low-heat and low-alkalinity cements, Cem. Conc. Res. 38, 437–448.

[39] J.L. García Calvo, A. Hidalgo, C. Alonso, L. Fernández Luco. 2010. Development of low-pH cementitious materials for HLRW repositories. Resistance against ground waters aggression, Cem. Conc. Res. 40, 1290–1297.

[40] A. Jenni, U. Mäder, C. Lerouge, S. Gaboreau, B. Schwyn. 2014. In situ interaction between different concretes and Opalinus Clay, Phys. Chem. Earth A/B/C 70–71, 71–83.

[41] A. Dauzeres, G. Achiedo, D. Nied, E. Bernard, S. Alahrache, B. Lothenbach. 2016. Magnesium perturbation in low-pH concretes placed in clayey environment-solid characterizations and modelling, Cem. Conc. Res. 79, 137–150.

[42] J.L. García Calvo, A. Hidalgo, M.C. Alonso, L. Fernández Luco. 2009. Low pH concretes based on CAC for underground repositories of HLW. Resistance respect to ground water aggression. Long-Term Performance of Cementitious Barriers and Reinforced Concrete in Nuclear Power Plants and Waste Management. EFC Event 314 NUCPERF. Edited by V. L'Hostis, R. Gens and C. Gallé. RILEM Publications S.A.R.L., 99–108.

[43] J.L. García Calvo, M.C. Alonso, A. Hidalgo, L. Fernández Luco, V. Flor-Laguna. 2013. Development of low-pH cementitious materials based on CAC for HLW repositories: long-term hydration and resistance against groundwater aggression, Cem. Conc. Res. 51, 67–77.

### 5.7.3 Concrete-bentonite interface reactivity in granitic repository

*J. Cuevas, R. Fernández, A.I., Ruiz*

*UAM Autonomous University of Madrid, Madrid, Spain*

**Concrete and bentonite in granite repository concepts**

In a generic concept of DGR bentonite clay is commonly used as hydraulic seal and physical-chemical buffer material while concrete is used as a structural support or in the form of plug seals for constructing drifts or isolating galleries, respectively. In any case, concrete will act as a source of alkaline fluids being itself an alkaline barrier in which migrating radionuclides would be eventually precipitated and retained. The interactions between clay and concrete materials generate a complex and evolutionary system whose reaction pathways lead to a varied mineralogy depending on materials considered [1, 2], geological and experimental environment [1, 3], and thermodynamic-kinetic framework in the system predictions at several time-scales [4–7].

Most clay-concrete interactions studies have been found to be relevant under the scope of clay-rock repository concepts for spent nuclear waste isolation. For the geometry (usually horizontal galleries), and geological environment (rock mechanics) of these repositories they use to have a requirement for the presence of a concrete annulus to provide mechanical support for the excavated galleries (e.g. in the Swiss concept: PEBS, 2012 [8]). Temperatures as high as 60 °C are expected to be maintained during several thousand years at the concrete annulus/bentonite interface [9]. Figure 5.7.3.1 shows clay rock (Swiss and French) and crystalline rock (Finland, Sweden, Spain) schematic designs. In crystalline rock [10, 11], in deposition tunnels and horizontal galleries, concrete plugs are used in order to tap the backfill and buffer clay materials. In these cases the thermal impact in the concrete plug- clay should be lower than in the clay rock-concrete annulus-bentonite interaction. Temperatures considered in these cases are within 15–35 °C [12–16] (Boom Clay).
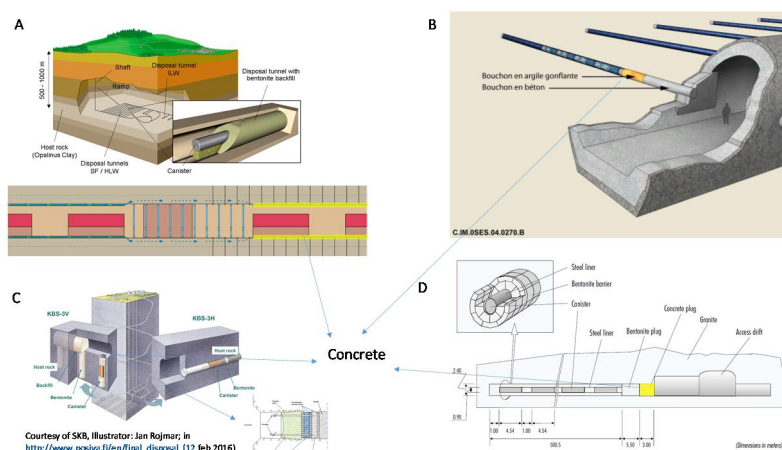


*Figure 5.7.3.1. Repository concepts in clay rock (A and B) and in crystalline rock: concrete location. A: NAGRA: SF/HLW/ILW repository in Opalinus Clay using low pH shotcrete tunnel support [8]. B: ANDRA: DOSSIER 2005 ARGILE -ARCHITECTURE AND MANAGEMENT OF A GEOLOGICAL DISPOSAL SYSTEM [17]. C: POSIVA (Finland) and SKB (Sweden) KBS3 concepts in crystalline rock: [10]; concrete plug at the access drift: [12]); D: ENRESA (Spain) concept in granite [11].*

**Concrete-bentonite interface reactivity under the scope of a granite repository concept**

The environmental conditions of concrete-clay interaction in granite deposits can be restricted to low-moderate temperatures and to the interaction of bentonite and concrete materials. These conditions are met in the above mentioned repositories, some of them supported in large scale underground experiments as FEBEX, ESP, etc. [13, 18, 19]. Besides, concrete/bentonite mass ratio should be very low (5:1000 in the constructing repositories (Onkalo based: [10]) and the interactions may take place just in the concrete plugs/bentonite seals contacts. Then, the study of concrete-bentonite in granite-like repositories focus to local geochemical perturbations of the system which can be significant for describing the long-term evolution of EBS system interfaces.

Local geochemistry in the concrete-bentonite interface surrounded by a granitic environment is driven by:

- Granite groundwater chemistry (see section 5.7.1)
- Concrete chemistry (high pH, low pH, mineralogy, ageing; see section 5.7.2)
- Bentonite chemistry (surface chemistry (exchangeable cations); mineralogy (d-p reactions); porewater chemistry (see section 5.7.1)

The groundwater chemistry in granite-like repositories (i.e. granite-granodioritic gneissic crystalline rocks) varies significantly form very low salinity (TDS < 0.1 g/L at GTS; [20, 21]) to > 10 g/L (~ > 0.2 M, NaCl) , for instance at OLKILUOTO, [22] in the Fennoscandian Shield. NaCl based (Na-Ca-Cl-$SO_4$-$HCO_3$; pH 8-9) compositions are typical, being carbonates more significant at lower depths, although significant Mg ions concentration (in Na-Ca cations predominant groundwaters) can be found in ASPO saline groundwater (see section 5.7.1). These solutions are going to hydrate concrete and bentonite through the surface galleries contact.

In terms of porewater chemistry one of the major chemical gradients in the EBS system are related to concrete interfaces. Granite groundwater affected by concrete has been analyzed in 5.7.1 and here the focus will be bentonite-concrete interaction. In fact, bentonite porewater can be also a saline (~ 0.3 M NaCl; pH ~ 8 type (Na-Mg-Ca-Cl-$SO_4$- $HCO_3$) either in the case of FEBEX [23, 24] or MX-80 [25] bentonites.

Taking in mind the pH gradient (> 13–12 to 11–10 in high pH to low pH concrete) at the concrete-bentonite interface, some of the processes and observed reactions are depicted in Figure 5.7.3.2.
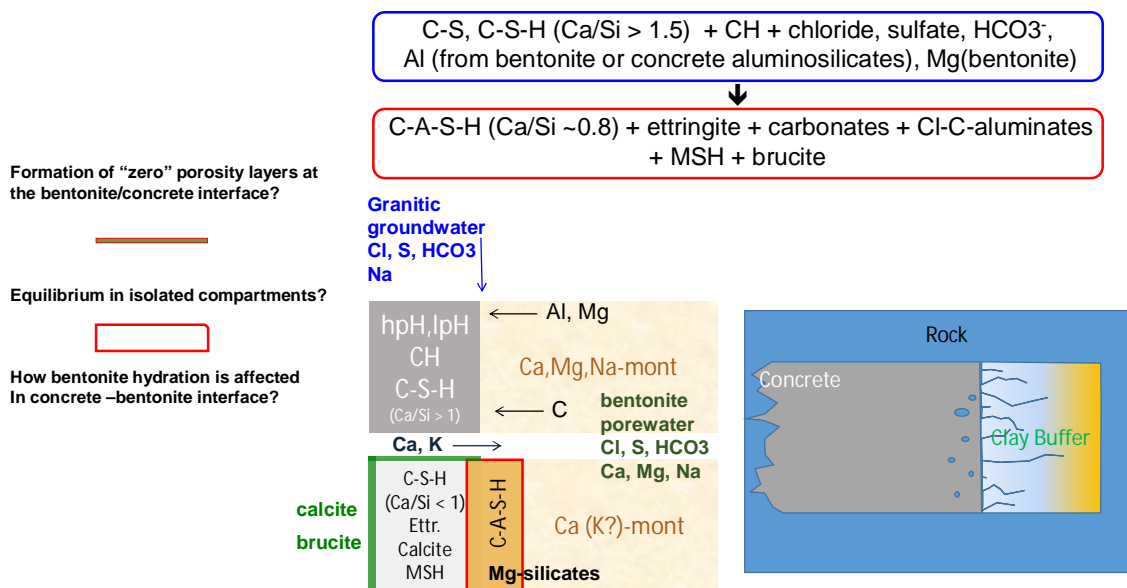
*Figure 5.7.3.2. Scheme of geochemical interactions in a concrete-bentonite interface within a concrete plug in a granite gallery context. hpH, lpH (high pH and low pH concrete).*

The pH gradient produce an alkaline front with the capacity to partially alter both the mineralogy of the bentonite [5, 6, 26] and obviously of the concrete, as has been demonstrated by Dauzères *et al*. [27] and Jenni *et al*. [2] in clay rock contacts. This alteration is expected to be very similar in bentonite contacts [28]. Bildstein and Claret [29] have reviewed the chemical perturbation aspects of concrete/clay interactions recognizing that: "concrete cannot simply be mimicked by a hyperalkaline fluid or a fluid in equilibrium with portlandite". Many experiments have focused on the chemical behavior of clay when it is exposed to an alkaline plume at several temperatures. Most of them introduces Na, K-hyperalkaline fluids at pH > 13, rather than lower pH environments dominated by $Ca(OH)_2$ (pH 12.5) or C-S-H phases (pH < 12) as have been identified by Dauzères *et al*. [1]. These authors outline the relative absence of representative experiments in real clay/concrete interfaces, and their failure to take into account the effects of real volumes and composition of solutions migrating through the porosities of the involved materials. Moreover, even fewer papers have been dedicated to exploration of the clay pore-water impacts on the concrete mineralogy and porosity.

Following Figure 5.7.3.2, a variety of processes can be identified in the overall granitic groundwater bentonite-concrete scenario:

- **Carbonation of concrete and concrete-bentonite interface**: the initial high pH interface will favor the dissolution of CH (portlandite) and the precipitation of calcite rims in hydrated high pH concrete surfaces [27]. Calcite, aragonite and gypsum have been observed to precipitate either in the concrete hydration surface or in the bentonite concrete interface in CEM-I concrete disc – FEBEX compacted bentonite long term experiments [30]. In the case of OPC-clay interface calcite is formed with a net volume increase leading to pore space clogging [2], Can this effect to temporary isolate the concrete system? Dissolution of CH and later high Ca/Si C-S-H compete with calcite formation. Moreover, Ca-Al-sulfates and carboaluminates are predicted to form as intermediates to yield finally calcite, gypsum, gibbsite and silica phases [31].

- **Cation exchange in montomorillonite**: high pH cements are initially a source for K and Ca during the migration of concrete porewater. Montmorillonite selective dissolution and K ion exchange can drive to apparent illitization processes (described in [5, 29, 32]), followed by

229

precipitation of secondary phases as zeolites or C-(A)-S-H phases. Direct contact of compacted bentonite and OPC concrete at long term is characterized by the decrease of Mg and the increase of Ca concentrations both in pore waters ([13], FEBEX experiment after 5 years of operation), and in the exchangeable cations population [30, 33]. Mg is exchanged and transferred to the alkaline media where it is precipitated as brucite (direct contact groundwater-concrete) or M-S-H phases [34] depending on the availability of silica released during montmorillonite or amorphous silica dissolution. Mg-silicate rims have been found elsewhere in clay-concrete contacts (FEBEX bentonite: [35]; Boom clay [36]; Opalinus clay [2]). These exchange reactions coupled with some dissolution and precipitation processes are restricted to < 1mm (precipitation rims) to < 5 cm (cation exchange) scales in the experiments with real interfaces.

- **Dissolution of CH, development of a Ca-rich front, C-S-H evolution and C-A-SH formation:** Concrete evolution, affected by the low pH environment of bentonite, is driven by portlandite and high Ca/Si C-S-H dissolution and the precipitation of low Ca/Si tobermorite type C-S-H. C-A-S-H have been identified in FEBEX bentonite-CEM-I and lime mortar interfaces at different time scales (months to 7 years), [32, 37]; detected at concrete interfaces forming part of a calcium rich rim in the bentonite side (Figure3). C-A-S-H phases found in the experiments are consistent with narrow compositional types 0.2-0.3 Al/(Si+Al), ~0.8 Ca/Si ratios described in the literature. Moreover, ongoing structural analyses revealed a potential intercalation or association of montmorillonite and C-A-S-H phases at the pore scale.

- **Sulfate and chloride reactions in concrete.** Cement minerals can react with chloride in different ways to form chloroaluminates or Friedel's salt as Afm-like phases, or adsorbed in C-S-H minerals [38–40], thus retaining the chloride, which can be diffused from the compacted bentonite. In parallel dissolved sulfates can react during CH dissolution from concrete and Al dissolution from montmorillonite to form ettringite-like (Aft) needle aggregates [32].
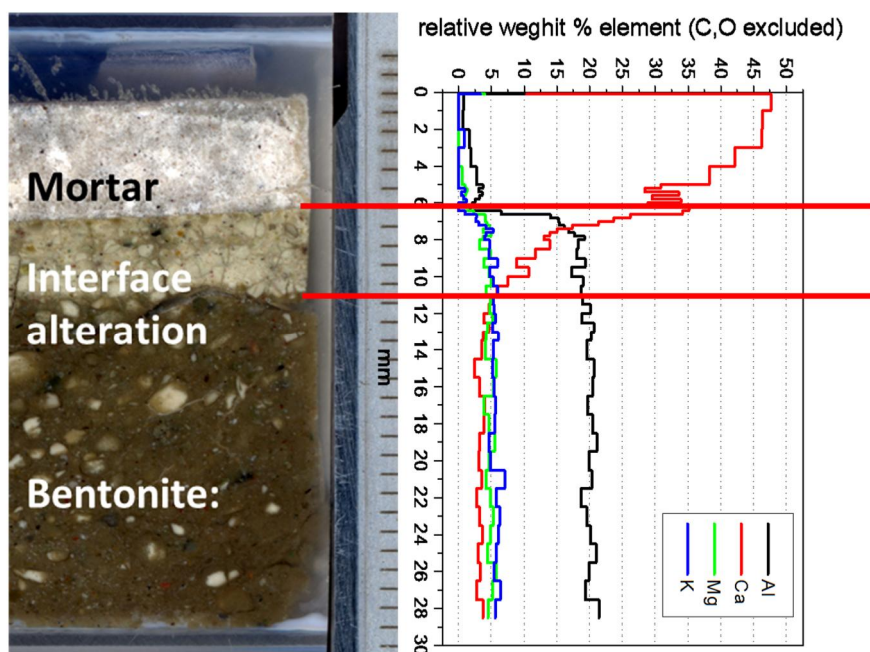


*Figure 5.7.3.3. Cemented calcium rich rim in the contact of a compacted bentonite (Ca-K exchanged).*

All these mentioned processes are basically in agreement with the observations of Dauzères *et al.* [1], regarding realistic conditions of reaction in terms of temperature (low) and transport (mainly diffusive in concrete-clay rock interfaces): carbonation of the interface, CH dissolution, low Ca/Si C-S-H formation, and ettringite precipitation. Dauzères *et al.* [27] and Jenni *et al.* [2] have shown also, in both, low-pH or high-pH concrete interfaces, the role of carbonation and sulfate phases dynamics in producing porosity changes in the concrete when they became in contact with clay pore waters or clay materials. Porosity changes, including volumetric consequences, related to a realistic description of these evolving interfaces, are important in order to study the geochemical evolution of the system in terms of mass transfer and barrier properties. Low pH and high pH concretes exhibited different reactivity, and some of the forming phases are not well known, especially M-S-H or C-A-S-H, [41]. These studies are critical for a complete physical-chemical characterization of the concrete-bentonite interface dynamics.

**Existing scoping models for cement perturbation of bentonite properties**

Numerous models of interaction between the engineered barriers of a repository have been performed over the last 20 years in the context of a DGR. Although not specifically consider barrier systems in a granitic formation, some of these models are focused on the interaction between the concrete (cement paste or alkaline pore fluids as simplistic representations of concrete) and bentonite barriers. In 2002, Savage *et al.* [42] identified several limitations modelling the interaction of bentonite with alkaline fluids using a kinetic approach. These limitations consisted on: 1) uncertainties on the kinetic rates for mineral dissolution at high pH; 2) inability by the geochemical codes to simulate the complexity of the chemical reactions through mineral surfaces, which is eventually solved by mathematical approaches producing dissolution and precipitation of minerals, although is experimentally unreal; 3) limited thermodynamic data for hydrated cement paste minerals, poor crystalline phases and aqueous species relevant at high pH, which in addition exhibited a weak consistency, and 4) transport mechanisms not coupled with respect to mineral transformations that could cause inconsistencies when changing porosity at a certain domain does not affect the fluid flow or diffusion.

A large effort has been performed in the last years to provide accurate and reliable data of chemical species, and cement and clay minerals relevant in the expected reactivity between concrete and bentonite [43, 44]. In this respect, at least two databases have been developed with significant improvement in terms of accuracy, robustness and completeness of data: 1) CEMDATA (latest release on May 07, 2015, version CEMDATA14.01), is a thermodynamic database that include a considerable number of cement phases, e.g. [45, 46], supported from the Swiss Institute of Materials Science and Technology EMPA, and 2) Thermoddem (latest release on December 16, 2014), is a complete set of thermodynamic and kinetic data for a large number of minerals with especial attention for cement and clay minerals [44, 47], supported from the French Geological Survey BRGM.

In addition, geochemical codes have constantly been developed to include new features enabling the simulation of more coupled processes with increasing mechanistic detail [48]. Coupling between changing porosity and transport is now enabled in some codes, as well as multicomponent transport where charged chemical species move independently themselves according to their specific diffusion rates, associated with charged clay surfaces. The later treatment has an important effect in porous materials of low hydraulic conductivity, such as compacted bentonite [49].

Thermodynamic models that have been used either to reproduce laboratory experiments or perform long-term predictions of the geochemical stability of concrete and bentonite as engineered barriers in a conceptual repository assume that the number of secondary minerals available to precipitate

should be large in order to bring the most stable solution to the system [5, 50]. When this case is applied, the thermodynamic data used must be very consistent. Based on this hypothesis, Gaucher and Blanc [50] predicted a limited spatial extension of the alkaline disturbance, below 0.1 m, in a bentonite barrier affected by an evolved cement paste of pH 12.5 after 100,000 years. The most significant effects were a large decrease in porosity at the alkaline interface, accompanied by mineral transformations and ion exchange in montmorillonite (Ca replacing Na). The sequence of partial mineral transformations produces secondary clay minerals like illite, saponite and clinochlore as a consequence of montmorillonite dissolution and formation of zeolites, hydrated cement phases and carbonates near the interface, associated to the porosity decrease. Far from the interface, bentonite does not suffer much alteration except for cation exchange and other mineralogical effects more related with the increase of temperature originated from the radioactive waste than from the concrete degradation, in agreement with de Windt et al. [51]. More recently, Marty et al. [52] performed a comparison of six geochemical codes through a benchmark case of multicomponent reactive transport across a concrete/clay interface. Three scenarios were considered, being the more reliable that using fast reaction rates, which lead to conditions closer to thermodynamic equilibrium. Very limited discrepancies in numerical results were observed between the six codes, and all produced similar results to those by Gaucher et al. [50] considering the reaction evolve to 10,000 years. Porosity clogging is achieved after this time, associated to zeolites and calcite formation, being the alkaline plume diffusion (pH > 9) limited to the first 10 cm from the interface.

Models that include kinetic rates laws in addition to thermodynamics have been also used to reproduce laboratory experiments and to perform long-term predictions using different scenarios [42, 53]. Some of these scenarios lead to very improbable situations at short- and long-term, but they serve to point out the relevance of key parameters such as the kinetic rates and the spatial refinement [4] and how slight modifications in a single parameter may have an important influence on the overall results. Watson et al. [54] showed that the choice of dissolution model for montmorillonite played an important role, while other factors, such as the mineral growth rate, the montmorillonite surface area and the inclusion of trace minerals in the bentonite mineralogy had a smaller impact.

Theoretically, models using kinetics in addition to thermodynamics are more complete and permit more flexibility to the system. Processes can be better captured, especially in systems where temperature and pH increases induce an increase in the mineral dissolution rates. Besides, metastable phases may form consistently. However, kinetic constants are very dependent on the specific experimental conditions used, and wrong values may lead to very implausible scenarios. Modellers who use kinetic models restrict the number of mineral phases involved in the reactivity.

Some processes observed experimentally, like those involving structural changes in a mineral phase are still very difficult to incorporate in the available codes. The simplification used to mimic these structural changes consist on include secondary minerals able to precipitate. Therefore, although not realistic, these processes are modelled through dissolution/precipitation. Fernández et al. [33] found experimentally a chlorite-like phase characterized as a brucite-montmorillonite complex produced by a brucite monolayer intercalation in the montmorillonite interlayer as a consequence of diffusive interaction between a high pH solution representative of an initial pore water from cement (pH 13.5) and a compacted bentonite at 90 °C. A geochemical model of such system introduced Mg-silicates phases (talc and Mg-saponite) to mimic the experimental results [55].

Concrete degradation has been less studied by modelling studies in the system concrete/bentonite, however, a recent model that evaluate the reactive transport of an hyperalkaline solution through a fracture in a limestone rock confirmed the sealing of the fracture by a porosity reduction controlled

by the precipitation of undifferentiated C-S-H/C-A-S-H with gradual decrease of the Ca/Si ratio from the fracture [56]. In addition, ettringite precipitated controlled by diffusion of sulfate and aluminum from the wall rock to the fracture, with aluminum provided by the dissolution of albite. Calcite also precipitated, controlled by diffusion of carbonate from the rock. The processes described in the later study may also be extrapolated to concrete/bentonite systems.

## References

[1]     A. Dauzères, P. Le Bescop, P. Sardini, C. Cau Dit Coumes. 2010. Physico-chemical investigation of clayey/cement-based materials interaction in the context of geological waste disposal: Experimental approach and results. Cement and Concrete Research, 40, 8, 1327–1340.

[2]     A. Jenni, U. Mäder, C. Lerouge, S. Gaboreau, B. Schwyn. 2014. In situ interaction between different concretes and Opalinus Clay, Physics and Chemistry of the Earth, Parts A/B/C, 70–71, 71–83.

[3]     J. L. García Calvo, A. Hidalgo, C. Alonso, L. Fernández Luco. 2010. Development of low-pH cementitious materials for HLRW repositories: Resistance against ground waters aggression, Cement and Concrete Research, 40, 8, 1290–1297.

[4]     N. C. M. Marty, C. Tournassat, A. Burnol, E. Giffaut, E. C. Gaucher. 2009. Influence of reaction kinetics and mesh refinement on the numerical modelling of concrete/clay interactions, Journal of Hydrology 364, 1–2, 58–72.

[5]     E. C. Gaucher, P. Blanc. 2006. Cement/clay interactions - A review: Experiments, natural analogues, and modeling, Waste Management, 26, 7, 776–788.

[6]     D. Savage, C. Walker, S. Benbow. 2010. Analyses of potential changes to barrier components due to interaction with a concrete liner in a repository for SF/HLW in Opalinus Clay. NAB 10-17, Nagra.  Wettingen, Switzerland.

[7]     J. M. Soler. 2013. Reactive transport modeling of concrete-clay interaction during 15 years at the Tournemire Underground Rock Laboratory, European Journal of Mineralogy, 25, 4, 639–654.

[8]     PEBS project D1.1, SKB, ANDRA, NAGRA, ENRESA, GRS, BGR. 2012. The Early Evolution of The EBS in Safety Assessments.

[9]     C. Yang, J. Samper, L. Montenegro. 2008. A coupled non-isothermal reactive transport model for Long-term geochemical evolution of a HLW repository in Clay, Environmental Geology, 53, 1627–1638.

[10]    F. Neall. 2008. Safety assessment of a KBS-3H spent nuclear fuel repository at Olkiluoto Complementary evaluations of safety, SKB Rapport R-08-35.

[11]    ENRESA. 1995. Almacenamiento geológico profundo de residuos radiactivos de alta actividad (AGP). Diseños conceptuales genéricos, Publicación Técnica 11/95, ENRESA. Madrid, Spain, 105 pp.

[12]    B. Fälth, P. Gatter. 2009. Mechanical and thermo-mechanical analyses of the tapered plug for plugging of deposition tunnels. A feasibility study, SKB Rapport R-09-33.

[13]    ENRESA. 2006. FEBEX Project Final Report. Post-mortem bentonite analysis, Enresa publicación técnica 05-1/2006.

[14]    G. W. Lanyon, I. Gaus. 2013. Main outcomes and review of the FEBEX In Situ Test (GTS) and Mock-Up after 15 years of operation, Nagra Arbeitsbericht. NAB 13-096, Nagra, Wettingen.

[15]    U. Mäder, F. Kober, H. Abplanalp, T. Baer, K. Detzner 2015. Shotcrete-Bentonite Interface Sampling. FEBEX-DP Partner Meeting, Stockholm, September 15/16, 2015.

[16]    S. Liu, D. Jacques, J. Govaerts, L. Wang. 2014. Conceptual model analysis of interaction at a concrete-Boom Clay Interface, Physics and Chemistry of the Earth, 70-71, 150–159.

[17]    ANDRA. 2005. Dossier 2005 Argile. Evaluation of the feasibility of a geological repository in an argillaceous formation, Report Series 241.

[18]    S. Norris. 2014. Clays in Natural and Engineered Barriers for Radioactive Waste Confinement: an introduction, In S. Norris, Bruno, J., Cathelineau, M., Delage, P., Fairhurst, C., Gaucher, E. C., Hohn, E. H., Kalinichev, A., Lalieux, P. & Sellin, P. Ed. Geological Society, London, Special Publications, Vol. 400, pp 1–5.

[19]    D. A. Dixon, D. G. Priyanto, J. B. Martino, M. de Combarieu, R. Johansson, P. Korkeakoski, J. Villagran. 2014. Enhanced Sealing Project (ESP): evolution of a full-sized bentonite and concrete shaft seal, In Clays in Natural and Engineered Barriers for Radioactive Waste Confinement, S. Norris, Bruno, J., Cathelineau, M., Delage, P., Fairhurst, C., Gaucher, E. C., Hohn, E. H., Kalinichev, A., Lalieux, P. & Sellin, P. Ed. Geological Society, London, Special Publications.

[20]    M. H. Bradbury, B. Baeyens. 1998. A Physicochemical Characterisation and Geochemical Modelling Approach for Determining Porewater Chemistries in Argillaceous Rocks, Geochimica et Cosmochimica Acta, 62, 5, 783–795.

[21] B. Buil, P. Gómez, J. Peña, A. Garralón, M. J. Turrero, A. Escribano, L. Sánchez, J. M. Durán. 2010. Modelling of bentonite-granite solutes transfer from an in situ full-scale experiment to simulate a deep geological repository (Grimsel Test Site, Switzerland), Applied Geochemistry, 25, 1797–1804.

[22] P. Pitkänen, S. Partamies, A. Luukkonen. 2004. Hydrogeochemical Interpretation of Baseline Groundwater Conditions at the Olkiluoto Site, POSIVA 2003-07.

[23] A. M. Fernández, B. Baeyens, M. Bradbury, P. Rivas. 2004. Analysis of the porewater chemical composition of a Spanish compacted bentonite used in an engineered barrier, Physics and Chemistry of the Earth, 29, 105–118.

[24] L. Zheng, J. Samper, L. Montenegro, A. M. Fernández. 2010. A coupled THMC model of a heating and hydration laboratory experiment in unsaturated compacted FEBEX bentonite, Journal of Hydrology, 386, 1-4, 80–94.

[25] M. H. Bradbury, B. Baeyens. 2002. Porewater chemistry in compacted re-saturated MX-80 bentonite, Nagra NTB 01-08, Wettingen, Switzerland, 42 pp.

[26] D. Savage, C. Walker, R. Arthur, C. Rochelle, C. Oda, H. Takase. 2007. Alteration of bentonite by hyperalkaline fluids: A review of the role of secondary minerals, Physics and Chemistry of the Earth, Parts A/B/C 32, 1-7, 287–297.

[27] A. Dauzères, P. Le Bescop, C. Cau-Dit-Coumes, F. Brunet, X. Bourbon, J. Timonen, M. Voutilainen, L. Chomat, P. Sardini. 2014. On the physico-chemical evolution of low-pH and CEM I cement pastes interacting with Callovo-Oxfordian pore water under its in situ CO2 partial pressure, Cement and Concrete Research, 58, 76–88.

[28] U. Berner, D. A. Kulik, G. Kosakowski. 2013. Geochemical impact of a low-pH cement liner on the near field of a repository for spent fuel and high-level radioactive waste, Physics and Chemistry of the Earth, Parts A/B/C, 64, 46–56.

[29] O. Bildstein, F. Claret. 2015. Chapter 5 - Stability of Clay Barriers Under Chemical Perturbations, In Developments in Clay Science, C. I. S. I. C. B. Christophe Tournassat B. Faqpza Eds. Elsevier, Vol. Volume 6, pp 155–188.

[30] M. J. Turrero, M. V. Villar, E. Torres, A. Escribano, J. Cuevas, R. Fernández, A. I. Ruiz, R. Vigil de la Villa, I. S. de Soto. 2011. Laboratory tests at the interfaces: First results on the dismantling of tests FB3 and HB4, PEBS Deliverable D2.3-3-1, p 64.

[31] F. P. Glasser, T. Matschei. 2007. Interactions between Portland Cement and Carbon Dioxide, In XII International Congress of Chemistry Cement, 8-13 July, Montreal (Canada).

[32] J. Cuevas, A. I. Ruiz, R. Fernández, E. Torres, A. Escribano, M. Regadío, M. J. Turrero. 2016. Lime mortar-compacted bentonite–magnetite interfaces: An experimental study focused on the understanding of the EBS long-term performance for high-level nuclear waste isolation DGR concept, Applied Clay Science, 124–125, 79–93.

[33] R. Fernández, R. Vigil de la Villa, A. I. Ruiz, R. García, J. Cuevas. 2013. Precipitation of chlorite-like structures during OPC porewater diffusion through compacted bentonite at 90 °C, Applied Clay Science, 83–84, 357–367.

[34] J. Cuevas, J. Samper, M. J. Turrero, K. Wieczorek. 2014. Impact of the Geochemical Evolution of Bentonite Barriers on Repository Safety Functions - PEBS Case 4, In Proceedings International Conference on the Performance of Engineered Barriers: Backfill, Plugs and Seals, A. Schäfers S. Fahland Eds. BGR. pp 35–42.

[35] R. Fernández, J. Cuevas, L. Sánchez, R. Vigil de la Villa, S. Leguey. 2006. Reactivity of the cement-bentonite interface with alkaline solutions using transport cells, Applied Geochemistry, 21, 6, 977–992.

[36] D. Read, F. P. Glasser, C. Ayora, M. T. Guardiola, A. Sneyers. 2001. Mineralogical and microstructural changes accompanying the interaction of Boom Clay with ordinary Portland cement, Advances in Cement Research, 13, 4, 175–183.

[37] R. Fernández, A. I. Ruiz, J. Cuevas. 2016. Insight into the formation of C-A-S-H phases as a consequence of the interaction between concrete or cement and bentonite, Clay Minerals, in press.

[38] I. Baur, P. Keller, D. Mavrocordatos, B. Wehrli, C. A. Johnson. 2004. Dissolution-precipitation behaviour of ettringite, monosulfate, and calcium silicate hydrate, Cement and Concrete Research, 34, 341–348.

[39] M. V. A. Florea, H. J. H. Brouwers. 2012. Chloride binding related to hydration products Part I: Ordinary Portland Cement, Cement and Concrete Research, 42, 282–290.

[40] Q. Yuan, C. Shi, G. de Schutter, K. Audenaert, D. Deng. 2012. Chloride binding of cement-based materials subjected to external chloride environment - A review, Construction and Building Materials, 23, 1–13.

[41] B. Lothenbach, D. Nied, E. L'Hôpital, G. Achiedo, A. Dauzères. 2015. Magnesium and calcium silicate hydrates, Cement and Concrete Research, 77, 60–68.

[42] D. Savage, D. Noy, M. Mihara. 2002. Modeling the interaction of bentonite with hyperalkaline fluids, Applied Geochemistry, 17, 3, 207–223.

[43] T. Matschei, B. Lothenbach, F. P. Glasser. 2007. Thermodynamic properties of Portland cement hydrates in the system CaO-Al2O3-SiO2-CaSO4-CaCO3-H2O, Cement and Concrete Research, 37, 10, 1379–1410.

[44]   P. Blanc, A. Lassin, P. Piantone, M. Azaroual, N. Jacquemet, A. Fabbri, E. C. Gaucher. 2012. Thermoddem: A geochemical database focused on low temperature water/rock interactions and waste materials, Applied Geochemistry, 27, 10, 2107–2116.

[45]   B. Lothenbach, L. Pelletier-Chaignat, F. Winnefeld. 2012. Stability in the system CaO–Al2O3–H2O, Cement and Concrete Research, 42, 12, 1621–1634.

[46]   B. Z. Dilnesa, B. Lothenbach, G. Renaudin, A. Wichser, D. Kulik. 2014. Synthesis and characterization of hydrogarnet $Ca_3(Al_xFe_{1-x})_2(SiO_4)y(OH)_4(3-y)$, Cement and Concrete Research, 59, 96–111.

[47]   N. C. M. Marty, F. Claret, A. Lassin, J. Tremosa, P. Blanc, B. Madé, E. Giffaut, B. Cochepin, C. Tournassat. 2015. A database of dissolution and precipitation rates for clay-rocks minerals, Applied Geochemistry, 55, 108–118.

[48]   C. I. Steefel, S. B. Yabusaki, K. U. Mayer. 2015. Reactive transport benchmarks for subsurface environmental simulation, Computational Geoscience, 19, 3, 439–443.

[49]   C. I. Steefel, C. A. J. Appelo, B. Arora, D. Jacques, T. Kalbacher, O. Kolditz, V. Lagneau, P. C. Lichtner, K. U. Mayer, J. C. L. Meeussen, S. Molins, D. Moulton, H. Shao, J. Šimůnek, N. Spycher, S. B. Yabusaki, G. T. Yeh. 2014. Reactive transport codes for subsurface environmental simulation, Computational Geosciences, 19, 3, 445–478.

[50]   E. C. Gaucher, P. Blanc, J.-M. Matray, N. Michau. 2004. Modeling diffusion of an alkaline plume in a clay barrier, Applied Geochemistry, 19, 10, 1505–1515.

[51]   L. De Windt, D. Pellegrini, J. van der Lee. 2004. Coupled modeling of cement/claystone interactions and radionuclide migration, Journal of Contaminant Hydrology, 68, 3-4, 165–182.

[52]   N. C. M. Marty, O. Bildstein, P. Blanc, F. Claret, B. Cochepin, E. C. Gaucher, D. Jacques, J.-E. Lartigue, S. Liu, K. U. Mayer, J. C. L. Meeussen, I. Munier, I. Pointeau, D. Su, C. I. Steefel. 2015. Benchmarks for multicomponent reactive transport across a cement/clay interface, Computational Geosciences, 19, 3, 635–653.

[53]   R. Fernández, J. Cuevas, U. K. Mäder, Modelling concrete interaction with a bentonite barrier, European Journal of Mineralogy, 21, 1, 177–191.

[54]   C. Watson, K. Hane, D. Savage, S. Benbow, J. Cuevas, R. Fernández. 2009. Reaction and diffusion of cementitious water in bentonite: Results of blind' modelling, Applied Clay Science, 45, 1-2, 54–69.

[55]   R. Fernández, J. Cuevas, U. K. Mäder. 2010. Modeling experimental results of diffusion of alkaline solutions through a compacted bentonite barrier, Cement and Concrete Research, 40, 8, 1255–1264.

[56]   J. M. Soler. 2016. Two-dimensional reactive transport modeling of the alteration of a fractured limestone by hyperalkaline solutions at Maqarin (Jordan), Applied Geochemistry, 66, 5.8 systematic approach to describe processes of specie, including radionuclides, into cement material and identification of potential influencing agents and properties.